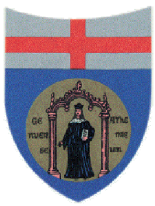

Pricing System Security in Electricity Market Models with Inclusion of Voltage Stability Constraints

by

Federico Milano

A thesis
presented to the University of Genova
in fulfillment of the
thesis requirement for the degree of
Doctor of Philosophy
in
Electrical Engineering

Genova, Italy, April 2003

I hereby declare that I am the sole author of this thesis.
I authorize the University of Genova to lend this thesis to other institutions or individuals for the purpose of scholarly research.

Federico Milano

I authorize the University of Genova to reproduce this thesis by photocopying or other means, in total or in part, at the request of other institutions or individuals for the purpose of scholarly research.

Federico Milano

Acknowledgments

I wish to thank my supervisor, Prof. M. Invernizzi, and Professors G. B. Denegri and B. Delfino for their constant human, technical and financial support. Thanks especially for having made possible the marvelous experience I had in Canada.

Many, many thanks to Prof. C. A. Cañizares, my supervisor when I was a Visiting Scholar at University of Waterloo, Canada. His teachings, help, hospitality and friendship are $\kappa\tau\acute{\eta}\mu\alpha\tau\alpha\ \grave{\varepsilon}\varsigma\ \alpha\grave{\iota}\varepsilon\acute{\iota}$. Thank you so much for everything, Professor.

A special thank to the students of the lab CPH 3373: Claudio, Hassan, Hong, Mithulan, Sameh, Valery and Warren. The long Canadian winters would have been much colder without you guys.

Thanks also to Prof. A. Conejo, from University of Castilla-La Mancha, Spain, for his help about market clearing mechanisms based on mixed integer linear programming.

Finally, thanks to CESI for providing the Italian system data.

Abstract

This thesis proposes novel techniques which allow including voltage stability constraints in competitive electricity markets and pricing system security.

A multi-objective Optimal Power Flow (OPF) approach to account for system security through the use of voltage stability constraints and to provide an estimation of the system congestion, e.g. the system Available Loading Capability (ALC), is proposed and solved by means of an Interior Point Method Nonlinear Programming technique, so that the social benefit and the distance to a maximum loading condition are maximized at the same time.

Two techniques are then proposed to include in the basic voltage stability constrained OPF method first class contingencies, represented here by line outages. The first technique computes an ALC value based on an N-1 contingency criterion for an initial optimal operating condition and then an OPF problem is solved for the worst contingency case. The second approach solves a reduced number of OPF problems associated with the power transfer sensitivity analysis of transmission lines.

Finally, a study of a multi-period market clearing mechanism with inclusion of voltage stability constraints is presented. The daily-ahead market schedule is solved using a Mixed Integer Nonlinear Programming method which allows combining the proposed voltage stability constraints with integer variables, such as unit commitments and ramping limits.

Locational marginal prices and nodal congestion prices resulting from the proposed methods as well as comparisons with results obtained by means of standard techniques currently in use for solving electricity market problems are presented and discussed.

All methods are tested on simple test systems and on a realistic 129-bus Italian network model considering supply and demand side bidding. Simulations were ob-

tained using a self-made MATLAB-based Power System Analysis Toolbox (PSAT), which contains continuation power flow analysis and optimal power flow problems based on an Interior Point method for nonlinear programming and is provided with a GAMS interface for solving complex Mixed Integer Nonlinear Programming problems.

Contents

List of Figures

List of Tables

List of Terms

Acronyms:

ALC	:	Available Loading Capability
ATC	:	Available Transfer Capability
CNS	:	Constrained Nonlinear System
CPF	:	Continuation Power Flow
DAE	:	Differential Algebraic Equation
ESCO	:	Electrical Service Company
ETC	:	Existing Transmission Commitment
GAMS	:	General Algebraic Modeling System
GENCO	:	Generation Company
GME	:	Gestore Mercato Elettrico (Italian IMO)
GRG	:	Generalized Reduced Gradient
GRTN	:	Gestore Rete Trasmissione Nazionale (Italian ISO)
GUI	:	Graphical User Interface
IMO	:	Independent Market Operator
IPM	:	Interior Point Method
ISO	:	Independent System Operator
KKT	:	*Karush-Kuhn-Tucker* (optimality condition)
LIB	:	Limit-Induced Bifurcation
LMP	:	Locational Marginal Price

LP	:	Linear Programming
LR	:	Lagrangian Relaxation
MCP	:	Market Clearing Price
MINLP	:	Mixed-Integer Non-Linear Programming
MIP	:	Mixed-Integer Programming
MLC	:	Maximum Loading Condition
MO	:	Market Operator
NCP	:	Nodal Congestion Price
NERC	:	North American Electric Reliability Council
NLP	:	Non-Linear Programming
OPF	:	Optimal Power Flow
PSAT	:	Power System Analysis Toolbox
SNB	:	Saddle-Node Bifurcation
TRM	:	Transmission Reliability Margin
TSC	:	Transaction Security Cost
TTC	:	Total Transfer Capability
UC	:	Unit Commitment
VSC-OPF	:	Voltage Stability Constrained Optimal Power Flow

Symbols:

f	:	Power flow equations
x	:	Dependent variables
p	:	Independent or control variables
y	:	Decision variables
u, w, z	:	Discrete variables
V	:	Bus voltage magnitudes
θ	:	Bus voltage phases

P_G	:	Generator real powers
Q_G	:	Generator reactive powers
P_L	:	Load real powers
P_S	:	Supply bids
P_D	:	Demand bids
ϕ_D	:	Power factor angle
I_{hk}	:	Transmission line current flows
P_{hk}	:	Transmission line power flows
λ	:	Loading parameter
k_G	:	Distributed slack generator variable
G	:	Objective function
H	:	Generic constraint function
C_S	:	Supply costs
C_D	:	Demand costs
ω	:	Weighting factor
$\mathcal{L}$	:	Lagrangian function
μ	:	Dual Variables (Lagrangian multipliers)
ρ	:	Lagrangian multipliers of power flow equations
s	:	Slack variables (non-negativity conditions)
μ^k	:	Barrier parameter

Chapter 1

Introduction

1.1 Research Motivation

IN recent years, the electricity industry has undergone drastic changes due to a world wide deregulation/privatization process that has significantly affected power system management and energy markets. In a deregulated system, operators' goals are balancing consumer power demand using the available generation and ensuring that economical and technical constraints are respected [1, 2]. The prime economical aspect is the *social benefit*, i.e. power suppliers should obtain maximum prices for their produced energy, while consumers should pay the lowest prices for the purchased electric power. Prices have to be defined in a free market economy and restricted only by power exchange rules. Among the several competitive market models which have been proposed, the following four basic models have been widely accepted and utilized in practice [3]:

Model 1. Wholesale generators provide power supply bids to a single pool; then load-serving companies buy wholesale power from the pool at a regulated price and resell it to retail loads.

Model 2. Wholesale generators and load-serving companies provide power supply and demand bids to a single pool; then load-serving companies resell wholesale power to retail loads.

Model 3. Combinations of models 1 and 2 with bilateral wholesale contracts between generators and load-serving companies.

Model 4. Combinations of all previous plus contracts between all participants and retail loads.

Regardless to the adopted market model, the prime physical constraint is that power supply and demand have to be balanced in real time by scheduling the most economic generation on a fixed time horizon basis (e.g. a day ahead). In a deregulated environment, the balance is obtained by means of a primary electricity market which supplies the scheduled demand.[1]

Furthermore, independent market operators and market participants require a minimum level of quality and system security, i.e. the available power and control systems have to be able to balance the actual load demand in case of first class contingencies (N-1 security criterion), minimize the negative effects of outages and maintain voltages and frequency within their security limits. Thus there is the need of stability studies in order to maintain the desired security level. The latter is generally improved avoiding or limiting as much as possible system congestions caused by transmission system constraints. Observe that congestions affect both security and market transactions. As a matter of fact, several studies propose criteria for pricing congestions and fairly sharing costs among the right market entities [4, 5, 6].

[1]Deviations from scheduled demand are typically adjusted in real time with a frequency-control market. However, frequency control and transient instability issues are beyond the scope of this thesis and will not be discussed any further.

Congestion constraints such as thermal limits on transmission lines, or voltage levels, although should be avoided, do not lead to immediate emergency conditions, and thus optimization methods applied in reality and/or proposed in the literature, generally take advantage from this practical consideration and focus more on computational efficiency than security constraints, in order to be tailored for on-line applications [4, 7, 8]. However, congestions associated with voltage collapse phenomena may have severe and immediate consequences on system stability, but voltage collapse issues are seldom associated with competitive market studies [9, 10, 11].

Voltage collapse has the following characteristics:

1. It is a catastrophic and sudden phenomenon and has typically severe effects on some network areas and, sometimes, even on the entire grid. Thus precise information about the proximity to voltage collapse is needed.

2. It is generally induced by heavy loading conditions and/or outages which limit the power transfer capability. Hence the need for N-1 contingency criteria.

3. A detailed nonlinear analytical model of power system is required to properly study voltage collapse phenomena. This is in contrast with the need of computational efficiency of methods accounting for security and economic dispatch.

With past and current difficulties in building new transmission lines and the significant increase in power transactions associated with competitive electricity markets, maintaining system security, with special regard to voltage instability/collapse issues, is more than ever one of the main concerns for market and system operators.

Hence, there is the need for pricing this security in a simple, unambiguous and transparent way, so that the "right" market signals can be conveyed to all market participants. However, pricing security is not an easy task, since it involves a variety of assumptions as well as complex models and simulations. In the four main market models that have been described above, how to properly include and price system security is still an open question. This thesis tries to address this issue.

1.2 Literature Review

This thesis mainly focuses on competitive electricity markets and on the inclusion of proper security constraints through the use of an Optimal Power Flow (OPF)-based approach, whose ability to solve practical power system problems has been widely recognized [12, 13, 14].

In [15], several strategies were proposed for an OPF with active power dispatch and voltage security, which was represented only by voltage limits. Most of the methods proposed in the literature used a logarithmic barrier Interior Point Methods (IPMs) for solving the OPF problem [16, 17, 18]. IPMs proved to be robust, especially in large networks, as the number of iterations increase slightly with the number of constraints and network size. However, early implementations of IPM for solving market problems, accounting somewhat for system security, were limited to the use of linear programming.

In [19] and [20], the authors present a comprehensive investigation of the use of IPM for nonlinear problems, and describe the application of Merhotra's predictor-corrector to the OPF, which highly reduces the number of iterations to obtain the final solution. Non-linear optimization techniques have also been shown to be adequate for addressing a variety of voltage stability issues, such as the maxi-

mization of the loading parameter in voltage collapse studies, as discussed in [21], [22], [23], [24] and [25]. In [26] and [27], non-linear IPM techniques are applied to the solution of diverse OPF market problems. In this thesis, solutions obtained with the IPM are also tested with other optimization techniques, e.g. Generalized Reduced Gradient (GRG) [28], in order to both double check results and evaluate performances.

In [9], the authors proposed a technique to account for system security through the use of voltage stability based constraints in an OPF-IPM market representation, so that security is not simply modeled through the use of voltage and power transfer limits, typically determined off-line, but it is properly represented in on-line market computations. In the current thesis, a multi-objective approach similar to the one proposed in [25] is used in an OPF-IPM market model, so that the social benefit and the distance to a maximum loading condition are maximized at the same time. In this way, voltage stability concepts and techniques are used to improve power transactions and the representation of system security [29].

Besides the ability of including a variety of security constraints, OPF-based market models allows defining precise price indicators, based on *spot pricing* techniques [6]. Spot pricing was originally defined for active power transactions, considering only congestion alleviations [4, 30], and then extended to account for different price components, such as reactive pricing and ancillary services [5, 31]. The utilization of spot pricing concepts with OPF-based market models is currently a well accepted theory and is based on the decomposition of Lagrangian multipliers associated with power flow equations into the sum of two terms, i.e. costs of generation and losses and costs of system congestions [32]. In this thesis an integrated optimal spot pricing model is mostly based on the technique described in [33] and used to evaluate costs associated with the voltage stability constraints introduced in the OPF problem.

In addition to precise voltage stability constraints and price signals, an OPF-based market model should also be able to take into account first class contingencies, i.e. should include an N-1 contingency criterion. Contingency constrained OPFs have been previously proposed based on linear programming techniques [34, 35] and further developed in [13, 36]. Some studies for contingency planning and voltage security preventive control have also been presented in [37, 38, 39], and the issue of OPF computations with inclusion of voltage stability constraints and contingencies is discussed in [40], based on a heuristic methodology. In this thesis, contingencies are included using methods based on what proposed in [41] and further extended to a multi-objective optimizations as in [29].

Finally, in order to be a complete tool for market computations, the power scheduling process should be able to include integer constraints, such as unit commitment (UC). Several techniques, generally based on mixed linear or quadratic programming and Lagrangian Relaxation (LR) have been proposed in the literature [26, 42, 43, 44]. A UC method combined to nonlinear power flow equations has been presented [45]. In this thesis, integer constraints have been included in the proposed voltage stability constrained OPF method, thus realizing a mixed nonlinear programming model. Furthermore basic UC constraints have been extended to an accurate model of thermal units, including minimum up and down times, ramp up and ramp down limits and ramp up and ramp down ramp rates, as presented [46, 47, 48].

1.3 Research Objectives

The following areas of current interest will be addressed in OPF-based electricity market and pricing electricity studies with inclusion of detailed voltage stability constraints:

1. Development of a Voltage Stability Constrained (VSC) OPF-based electricity market. To be a flexible tool for operators, the VSC-OPF should be able to provide market solutions with a desired level of security.

2. Inclusion in the VSC-OPF of N-1 contingency criteria, in order to provide market solution which are secure also in case of line outages, as required by market operators and participants.

3. Extension of the VSC-OPF to a multi-period horizon, which would allow to provide market operators and participants a valuable tool for daily-ahead market schedule.

Thus, this thesis investigates the effects of voltage stability constraints on competitive market model, and provides a set of techniques able to evaluate the weight of security on the market clearing mechanism and on electricity prices.

1.4 Outline of the Thesis

This thesis is organized as follows: Chapter 2 introduces power electric system equations and test system cases, Chapter 3 presents voltage stability concepts based on the bifurcation theory and the continuation power flow technique and Chapter 4 describes OPF-based market clearing mechanism problems and electricity pricing techniques which have been proposed in the literature and are used as background for the methods developed in this thesis.

Chapter 5 describes the software tools which have been developed for the simulations reported in this thesis. The proposed software is a suite of general routines for static and dynamic power system analysis and is provided with a GAMS interface for solving sophisticated mixed integer nonlinear programming problems. In this chapter a simple three-bus test system is discussed in detail to

illustrate the implemented analysis techniques, with special regards to the Interior Point Method used to solve single period OPF-based markets.

The proposed single-period, multi-objective voltage stability constrained OPF problem is fully described in Chapter 6 paying particular attention to the determination of electricity prices, while Chapter 7 presents two techniques for evaluating efficiently the effects of contingencies (N-1 security criterion) on the proposed VSC-OPF method. Chapter 8 explores the ability of the VSC-OPF to provide security and price signals in a multi-period horizon. In Chapters 6, 7 and 8, a variety of test system examples accompany the theory to properly illustrate the proposed techniques and demonstrate their reliability also for realistic size problems.

Finally, concluding observations along with possible future research directions are presented in Chapter 9, whereas network and market data for all test cases used in this thesis are reported in Appendices A, B and C.

Chapter 2

Power System Models and Test Systems

2.1 Introduction

THIS chapter introduces power electric system models used in this thesis. A discussion on power flow equations with both single and distributed slack bus models is presented in Section 2.2 along with the definition of dependent and control variables relevant to voltage stability and optimal power flow studies. Finally, Section 2.3 presents the three test systems used in the simulations throughout this thesis.

2.2 General System Equations

Equations relevant to the topics under study in this thesis are the well known power flow equations, as follows:

$$0 = f(x, p) = f(V, \theta, P_G, Q_G, P_L, Q_L) \tag{2.1}$$

where, in $f : \mathbb{R}^{n+m} \rightarrow \mathbb{R}^{2N}$ are a set of nonlinear equations, N being the number of network buses, x ($x \in \mathbb{R}^n$) is a vector of *dependent* variables and p ($p \in \mathbb{R}^m$) is a vector of *independent* or *control* variables. In a standard single slack bus power flow formulation, dependent variables are voltage magnitudes V and phases θ at the load buses, generator reactive powers Q_G and voltage phases at the generator buses, while control variables are generator active powers P_G, load powers P_L and Q_L and the slack bus voltage. In optimal power flow computations, dependent and control variables are conveniently collected in a unique vector of *decision* variables, as follows:

$$y \triangleq (x, p) = (V, \theta, P_G, Q_G, P_L, Q_L) \tag{2.2}$$

In distributed slack bus voltage models, y includes also an additional variable, say k_G, which forces all generators to share losses [49].

Since the system is assumed to be steady-state and we make the assumption to ignore special devices (such as FACTS or load tap changers), equations (2.1) reduces to power flows in transmissions lines and transformers, as follows:

$$\begin{aligned} P_h &= V_h^2(g_h + g_{h0}) - V_h \sum_{\ell \neq h}^{n_\ell} V_\ell (g_{h\ell} \cos(\theta_h - \theta_\ell) + b_{h\ell} \sin(\theta_h - \theta_\ell)) \\ Q_h &= -V_h^2(b_h + b_{h0}) - V_h \sum_{\ell \neq h}^{n_\ell} V_\ell (g_{h\ell} \sin(\theta_h - \theta_\ell) - b_{h\ell} \cos(\theta_h - \theta_\ell)) \end{aligned} \tag{2.3}$$

where P_h and Q_h are the real and reactive powers injected at bus h, n_ℓ is the number of connections departing from bus h and g_h, g_{h0}, b_h, b_{h0}, $g_{h\ell}$ and $b_{h\ell}$ are line parameters, namely conductances and susceptances, as commonly defined in the literature.

In the following, power injections are modeled as the sum of generator and load powers connected to the bus h, as follows:

$$P_h = \sum_{i \in \mathcal{I}_h} P_{G_i} - \sum_{j \in \mathcal{J}_h} P_{L_j} \tag{2.4}$$

where $\mathcal{I}_h$ and $\mathcal{J}_h$ are the sub-sets of generators and loads connected to bus h, respectively. P_G and P_L are assumed to be composed of two terms:

$$\begin{aligned} P_G &= P_{G_0} + P_S \\ P_L &= P_{L_0} + P_D \end{aligned} \tag{2.5}$$

where P_{G_0} and P_{L_0} are fixed power amount defining the *base case* condition and P_S and P_D are variable powers, which will be called power *supply* and power *demand* bids, respectively. In all test cases used in this thesis, load reactive powers are assumed to be dependent on the real powers by a constant power factor ($Q_L = P_L \tan \phi_L$), thus leading to:

$$y \triangleq (V, \theta, P_G, Q_G, P_L) \tag{2.6}$$

Equations (2.5) are for single slack bus model, and do not include slack bus real power which is actually a dependent variable, while for the distributed slack bus model, the following expression holds:

$$P_G = (1 + k_G)(P_{G_0} + P_S) \tag{2.7}$$

which is valid for all generators, including the reference phase angle generator. The distributed slack bus model will be used in this thesis in OPF problems since it allows a fair and reasonable distribution of transmission losses among all market suppliers.

2.3 Test Systems

Techniques proposed in this thesis are applied to a variety of test systems which are a three-bus system, a six-bus system and a 129-bus model of the Italian HV transmission system. The three-bus examples is used in Chapter 5 to illustrate

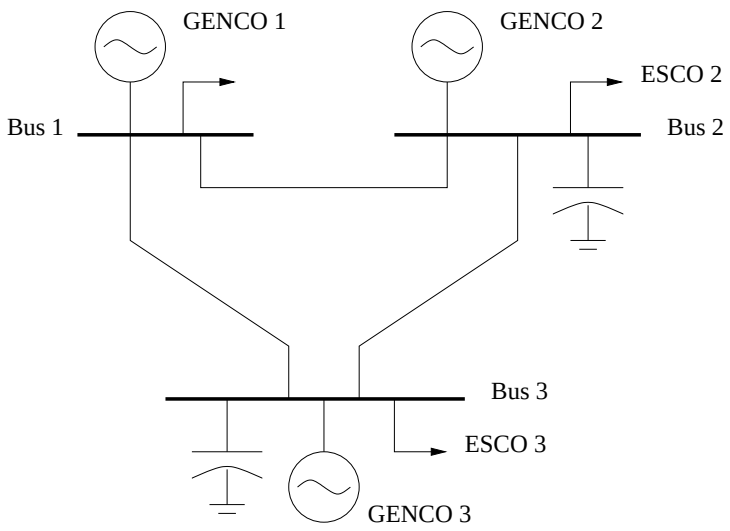

Figure 2.1: Three-bus test system.

the use of a self-made software for power system analysis (PSAT) as well as compare results obtained with third-party optimization methods (GAMS). The six-bus test system is used to test the ideas proposed in this thesis, since its reduced size makes clear results description and comparisons. Finally the 129-bus system allows testing the optimization techniques on a realistic size network, and proves reliability of the proposed methods.

2.3.1 Three-bus Test System

Figure 2.1 depicts the three-bus test case, which is extracted from [11], representing three generation companies (GENCOs) and two energy supply companies (ESCOs) that provide supply and demand bids. The complete data set for this system is provided in Appendix A.

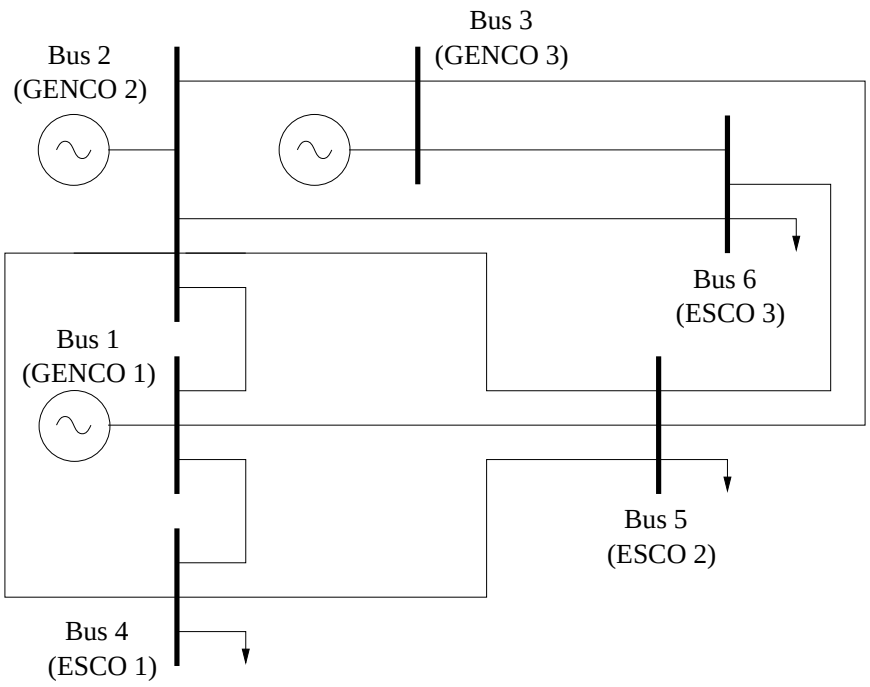

Figure 2.2: Six-bus test system.

2.3.2 Six-bus Test System

Figure 2.2 depicts the six-bus test case, which is extracted from [1], representing three generation companies (GENCOs) and three energy supply companies (ESCOs) that provide supply and demand bids, respectively. The complete data set for this system is provided in Appendix B.

2.3.3 HV Italian System Model

For the last three years, the Italian power system has been subjected to a deregulation process, which has forced ENEL, the main power Italian electricity board, to be divided in three independent companies (generation, transmission, and distribution) and sell part of its generation plants to private firms. In 1999, an Italian independent system operator (Gestore Rete Trasmissione Nazionale, GRTN) was

created to coordinate a competitive electricity market and ensure secure operation of the transmission grid. The Italian electricity market is expected to come on line in 2003 based on a zonal pricing model. The deregulation process and the overall increase in the power consumption forecast for the near future make the Italian system particularly interesting for market and security studies.

Figures 2.3 and 2.4 depicts the complete 129-bus Italian 400 kV transmission grid. In the simulations presented here, it has been assumed that 32 generators and 86 consumers participate in the market auction. Usually, Italy imports about the 15% of its power demand from France and Switzerland, hence power supply bids were assumed at the inter-ties. All bids were based on prices around 30-40 US$/MWh, which are the average prices over the last few years in other European countries where electricity markets are currently in operation, and considering the actual operating costs of thermal plants (66% of the electrical energy offer in Italy is thermal. Figure 2.5 depicts the daily load diagram and energy sources of the Italian system and supplier types). Fixed generation P_{G_0} and fixed loads P_{L_0} were assumed to be about 80% of the average consumption of a typical working day, since only 20% of ENEL's generation has been sold so far. Power bid levels were chosen to be about 40% (30% in case of OPF with inclusion of N-1 contingency criteria) of the average consumption in order to force system congestion. All system data and security constraints, i.e. voltage limits, generation reactive power limits and transmission line thermal limits, were provided by CESI, the Italian electrical research center. For the sake of completeness, data are reported in Appendix C.

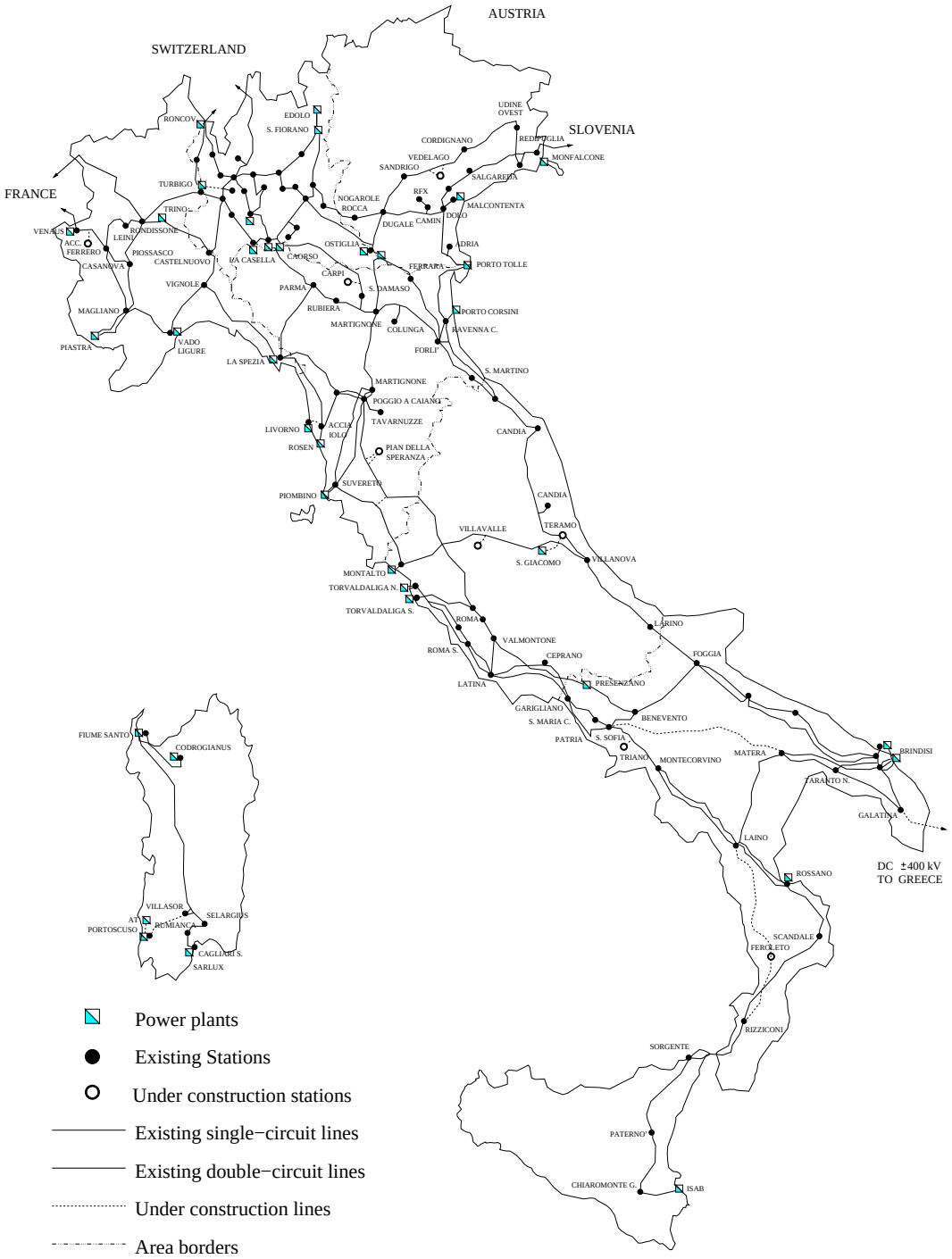

Figure 2.3: Pictorial diagram of the Italian 400 kV transmission system (available at GRTN web site www.grtn.it).

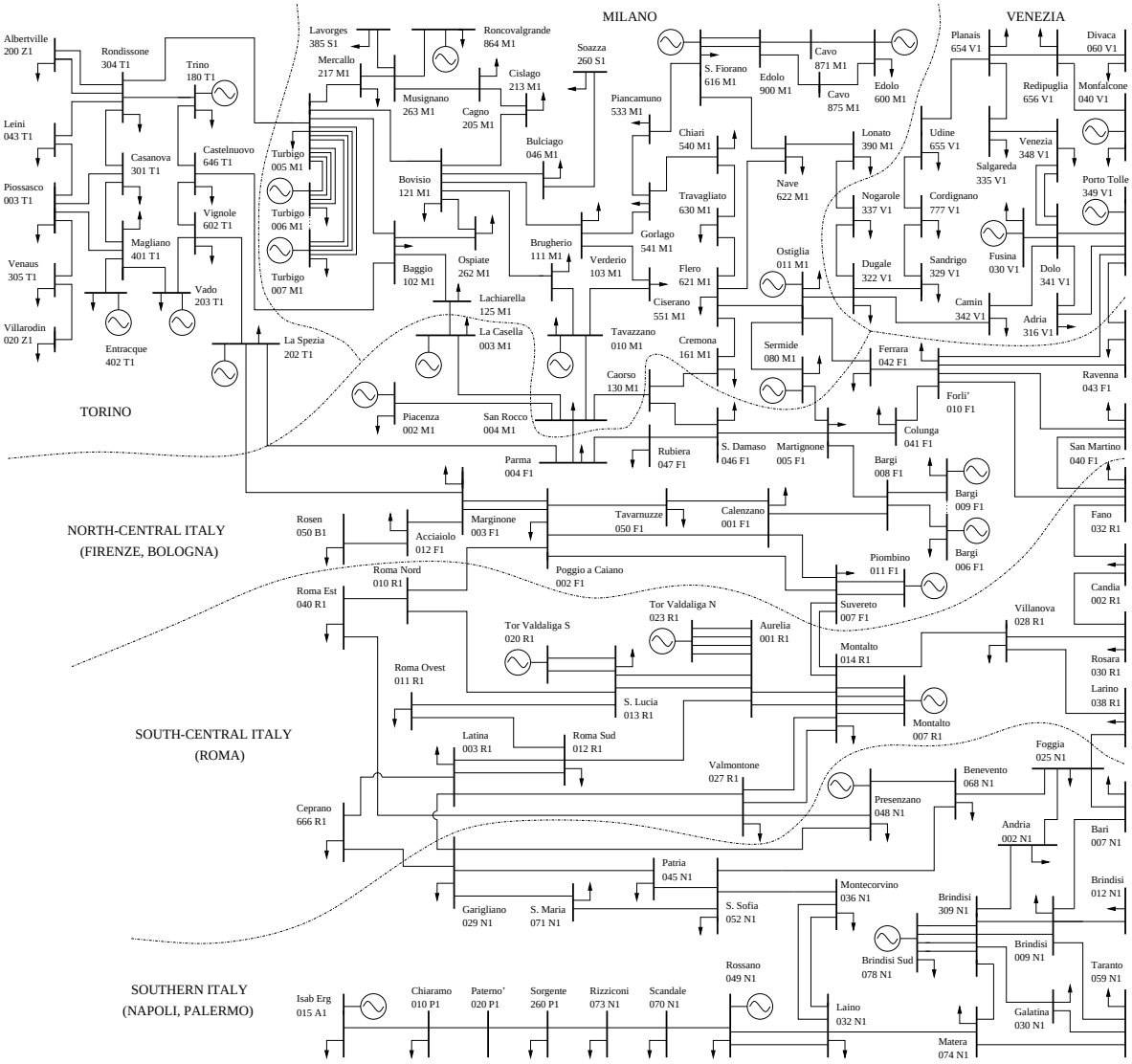

Figure 2.4: One-line diagram of the Italian 400 kV transmission system (most of this information is publicly available at the GRTN web site www.grtn.it).

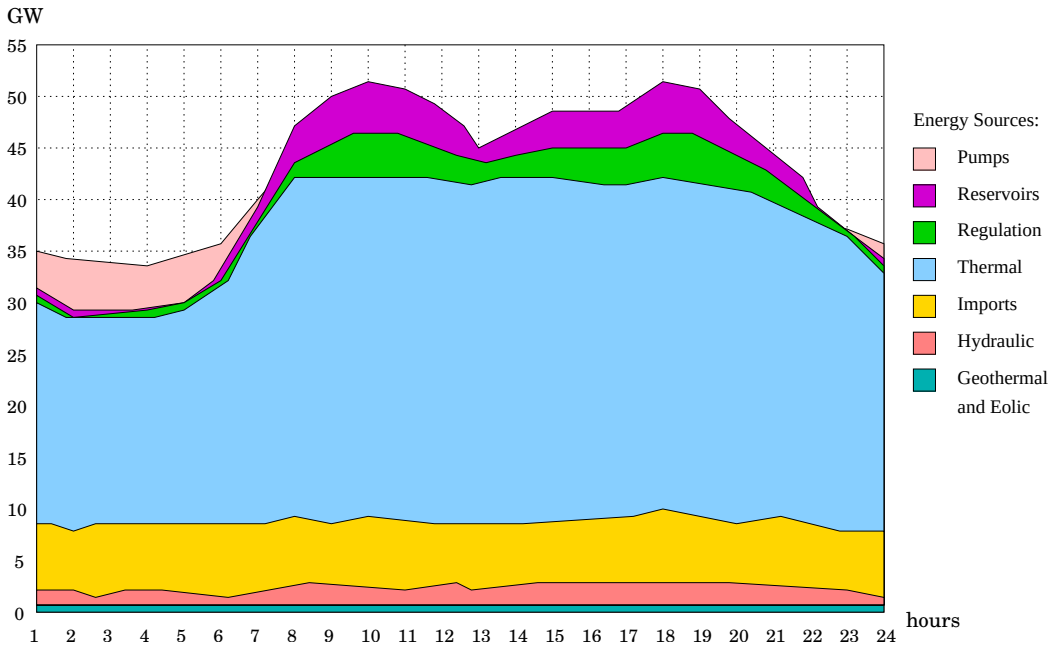

Figure 2.5: Daily load diagram for the Italian system (values refer to the 11 February 2003 and are available at GRTN web site www.grtn.it).

2.4 Summary

This chapter has described the basic equations for electric power systems commonly in use to study static voltage stability and market issues. Test cases used to illustrate the methods proposed in this thesis are also presented.

Chapter 3

Voltage Stability Outlines

3.1 Introduction

IN the last few decades, voltage stability in power systems has become a wide field of research. Voltage instability phenomena range time frames from seconds to hours and have been studied using a variety of static and dynamic models, including regulators and power electronics devices [50].

Topics relevant to the electricity market and optimal power flow techniques are the voltage collapse phenomena resulting from load changes and switching operations. Voltage collapse generally is a consequence of load increase in systems characterized by heavy loading conditions and/or when a change occurs in the system, such as a line outage. The results is typically that the current operating point, which is stable, "disappears" and the following system transient leads to a fast, unrecoverable, voltage decrease.

This chapter gives outlines of bifurcation theory concepts (saddle-node bifurcations and limit-induced bifurcations) and analysis techniques (Continuation Power Flow) which are used in this thesis to include voltage stability constraints in the market clearing mechanism. A discussion on the maximum available loading

condition, N-1 contingency criteria and sensitivity analysis is also presented.

3.2 Loading Parameter and Power Directions

The most accepted analytical tool used to investigate voltage collapse phenomena is the bifurcation theory, which is a general mathematical theory able to classify instabilities, studies the system behavior in the neighborhood of collapse or unstable points and gives a quantitative information on remedial actions to avoid critical conditions [51]. In the bifurcation theory, it is assumed that system equations depend on a set of parameters together with state variables, as follows:

$$0 = f(x, \lambda) \tag{3.1}$$

Then stability/instability properties are assessed varying "slowly" the parameters. In this thesis, the parameter used to investigate system proximity to voltage collapse is the so called *loading parameter* λ ($\lambda \in \mathbb{R}$), which modifies generator and load powers as follows:

$$\begin{aligned} P_{G_1} &= (1+\lambda)(P_{G_0} + P_S) \\ P_{L_1} &= (1+\lambda)(P_{L_0} + P_D) \end{aligned} \tag{3.2}$$

Powers which multiply λ are called *power directions*. Equations (3.2) differ from the model typically used in continuation power flow analysis, i.e.

$$\begin{aligned} P_{G_2} &= P_{G_0} + \lambda P_S \\ P_{L_2} &= P_{L_0} + \lambda P_D \end{aligned} \tag{3.3}$$

where the loading parameter affects only variable powers P_S and P_D. Chapter 6 will discuss the reason for preferring (3.2) in the proposed optimization technique. In typical bifurcations diagrams voltages are plotted as functions of λ, i.e. the measure of the system loadability, thus obtaining the so called P-V or *nose* curves.

3.3 Continuation Power Flow

Continuation Power Flow techniques are widely recognized as a valuable tool to determine nose curves of power systems and allow estimating the maximum loading conditions and "critical" solutions (for instance, saddle-node and limit-induced bifurcation points). Although computationally demanding for large systems [2, 50, 52], CPF is not affected by numerical instabilities (as a matter of fact, it is able to determine the stable and unstable fold of P-V curves) and can provide additional information, such as sensitivity factors of the current solution with respect to relevant parameters [53].

From a mathematical point of view, the CPF is a homotopy technique [2] and allows exploring stability of power system equations when varying a system parameter, which, in typical static and dynamic voltage stability studies, is the loading parameter λ [50, 54, 55]. Generally speaking, CPF consists in a predictor step realized by the computation of the tangent vector and a corrector step that can be obtained either by means of a local parametrization or a perpendicular intersection.

3.3.1 Predictor Step

At a generic equilibrium point p, the following relation applies:

$$f(x_p, \lambda_p) = 0 \quad \Rightarrow \quad \left.\frac{df}{d\lambda}\right|_p = 0 = D_x f|_p \left.\frac{dx}{d\lambda}\right|_p + \left.\frac{\partial f}{\partial \lambda}\right|_p \tag{3.4}$$

and the tangent vector can be approximated by:

$$\tau_p = \left.\frac{dx}{d\lambda}\right|_p \approx \frac{\Delta x_p}{\Delta \lambda_p} \tag{3.5}$$

From (3.4) and (3.5), one has:

$$\begin{aligned} \tau_p &= -D_x f|_p^{-1} \left.\frac{\partial f}{\partial \lambda}\right|_p \\ \Delta x_p &= \tau_p \Delta \lambda_p \end{aligned} \tag{3.6}$$

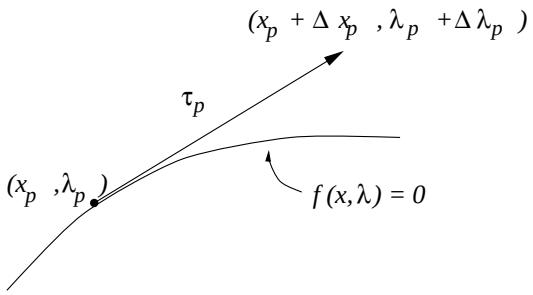

Figure 3.1: Predictor step computed by means of tangent vector.

At this point a step size control k has to be chosen for determining the increment Δx_p and $\Delta\lambda_p$, along with a normalization to avoid large steps when $\|\tau_p\|$ is large:

$$\Delta\lambda_p \triangleq \frac{k}{\|\tau_p\|} \qquad \Delta x_p \triangleq \frac{k\tau_p}{\|\tau_p\|} \tag{3.7}$$

where $\|\cdot\|$ is the Euclidean norm and $k = \pm 1$. The sign of k determines the increase or the decrease of λ. Fig. 3.1 presents a pictorial representation of the predictor step.

3.3.2 Corrector Step

In the corrector step, a set of $n+1$ equations is solved:

$$\begin{aligned} f(x,\lambda) &= 0 \\ \eta(x,\lambda) &= 0 \end{aligned} \tag{3.8}$$

where the solution of f must be in the bifurcation manifold and η is an additional equation to guarantee a non singular set at the bifurcation point. For the choice of η there are two options: the *perpendicular intersection* and the *local parametrization*.

In case of perpendicular intersection, whose pictorial representation is depicted

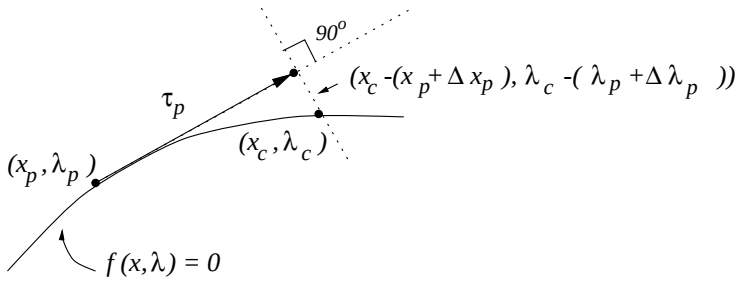

Figure 3.2: Corrector step computed by means of perpendicular intersection.

in Fig. 3.2, the expression of η becomes:

$$\eta(x,\lambda) = \begin{bmatrix} \Delta x_p \\ \Delta\lambda_p \end{bmatrix}^T \begin{bmatrix} x_c - (x_p + \Delta x_p) \\ \lambda_c - (\lambda_p - \Delta\lambda_p) \end{bmatrix} = 0 \tag{3.9}$$

whereas for the local parametrization, either the parameter λ or a variable x_i is forced to be a fixed value:

$$\eta(x,\lambda) = \lambda_c - \lambda_p - \Delta\lambda_p \tag{3.10}$$

or

$$\eta(x,\lambda) = x_{c_i} - x_{p_i} - \Delta x_{p_i} \tag{3.11}$$

The choice of the variable to be fixed depends on the bifurcation manifold of f, as depicted in Fig. 3.3.

3.3.3 Saddle-Node Bifurcations

Figure 3.4 depicts a typical nose curve which presents a Saddle-Node Bifurcation (SNB). SNBs have the following properties [50, 51]:

1. Two equilibria, one stable and one unstable, coalesce.

2. The sensitivity with respect to λ of a "state" variable is infinite.

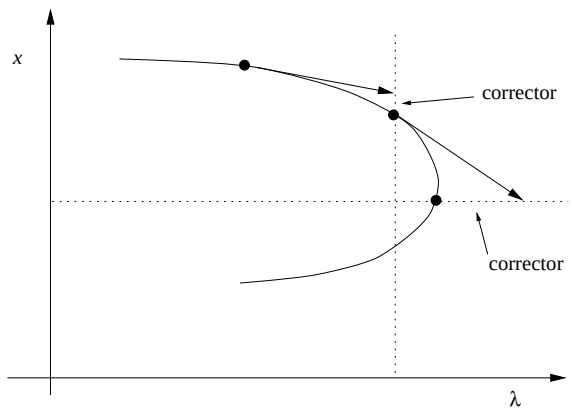

Figure 3.3: Corrector step computed by means of local parametrization.

3. The system Jacobian matrix has a simple zero eigenvalue.

4. The dynamic of the collapse in proximity of the bifurcation point is characterized by a monotonic change of state variables. The change is first slow and then fast and results in a voltage collapse.

In mathematical terms, SNB conditions are as follows:

$$\begin{aligned} f(x_c, \lambda_c) &= 0 \\ D_x f(x, \lambda)|_c \hat{v} &= 0 \\ \|\hat{v}\| &= 1 \end{aligned} \tag{3.12}$$

or

$$\begin{aligned} f(x_c, \lambda_c) &= 0 \\ \hat{w}^T D_x f(x, \lambda)|_c &= 0 \\ \|\hat{w}\| &= 1 \end{aligned} \tag{3.13}$$

where the subscript c stands for the "critical" solution at the bifurcation point, $\hat{v}$ and $\hat{w}$ are the right and the left eigenvectors respectively, and the Euclidean

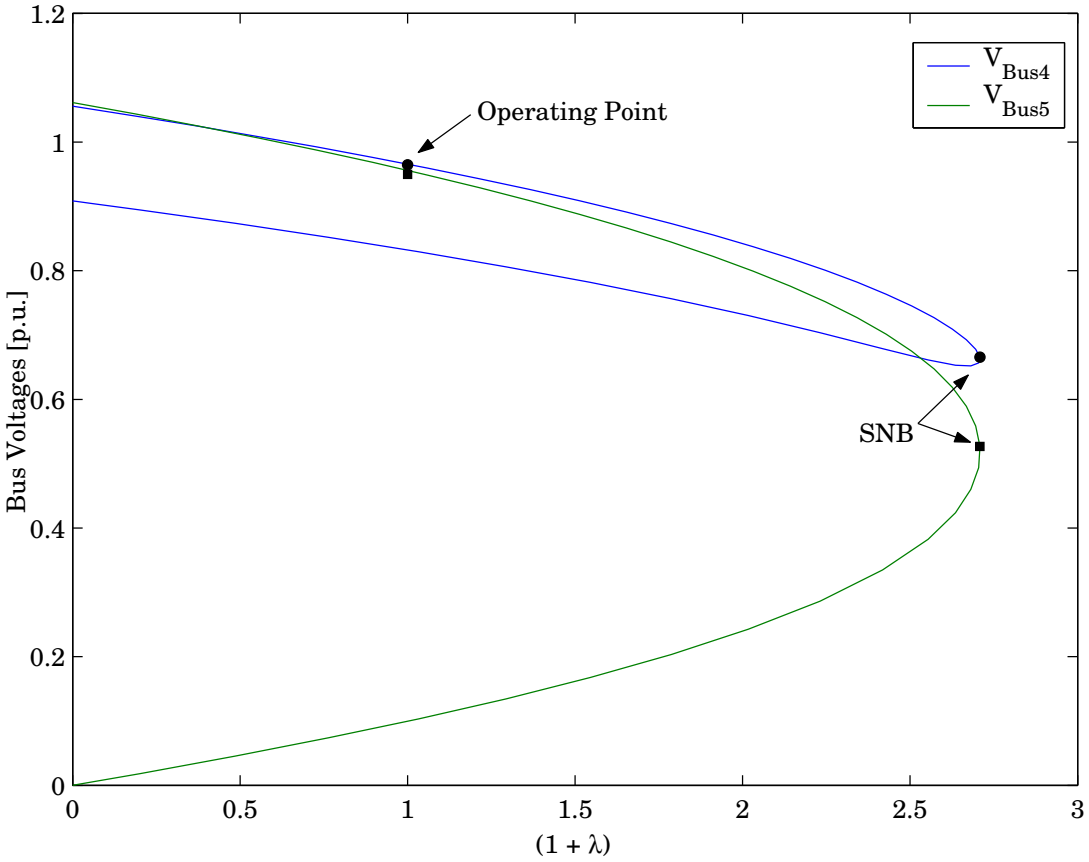

Figure 3.4: Typical nose curve of a power system presenting a saddle-node bifurcation.

Curves refer to voltages at bus 4 and 5 for the 6-bus test system using power directions and $P_S = (0, 25, 20)$ MW and $P_D = (25, 10, 8)$ MW.

norm is used for the $\|\cdot\|$ operator. The Euclidean norm reduce the sparsity of the Jacobian matrix, but allows avoiding refactorizations (which is needed in the case of ∞-norm) and appears to be numerically more stable than the 1-norm. In this thesis "static" SNBs will be considered, i.e. state variables are only the power flow variables x in (2.2).

3.3.4 Limit-Induced Bifurcations

Together with SNBs, also Limit-Induced Bifurcations (LIB) can cause voltage collapse. LIBs are caused by a change in system equations, typically when maximum generator reactive power limits are reached. At a LIB, one generator switches from a PV bus with controlled voltage $V_G = V_{G_0}$ to a PQ bus, where $Q_G = Q_{G_{\max}}$. Figure 3.5 depicts a nose curve with three LIBs. Observe that LIBs might be or not be a catastrophic event, since are not necessarily associated with a maximum loading condition. The LIB can be viewed as the solution of the system:

$$\begin{aligned} 0 &= f(x_c, \lambda_c) \\ 0 &= f^*(x_c, \lambda_c) \end{aligned} \tag{3.14}$$

where f, and f^*, are the initial and the changed system equations and control variables, respectively.

3.3.5 Security Limits

SNBs and LIBs may occur for unacceptable values of some bus voltages, i.e. for voltages below security bounds (typically 0.95 or 0.9 p.u.), or other limits which may lead to unfeasible operating point (e.g. thermal limits on transmission lines). In order to provide realistic results, voltage stability analysis has to take into account all physical constraints. For instance, Table 3.1 depicts the values of the loading parameter λ and the associated security limits and bifurcations

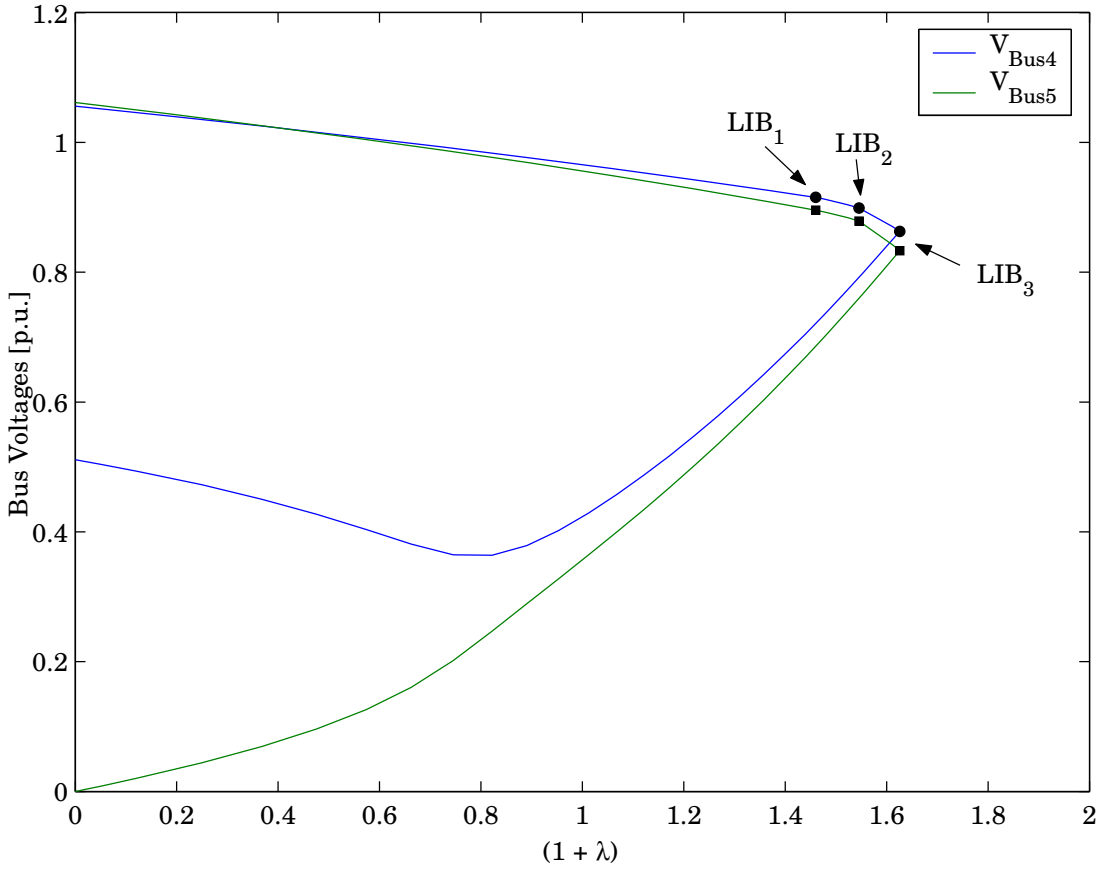

Figure 3.5: Nose curve with several limit-induced bifurcations.
Curves refer to voltages at bus 4 and 5 for the 6-bus test system using power directions $P_S = (0, 25, 20)$ MW and $P_D = (25, 10, 8)$ MW, and enabling reactive power limits for generators.

for the six-bus system. Observe that several thermal and voltage limits occur well before reaching the LIB associated with the maximum loading parameter ($\lambda_{\max} = 0.6261$), thus significantly reducing the feasible loadability of the network ($\lambda_c = 0.4226$).

3.4 Available Loading Capability

Figures 3.4 and 3.5 shows that SNBs and LIBs (and possibly thermal or voltage security limits) may be associated to the system maximum loadability or Maximum Loading Condition (MLC), which can be defined as follows:

$$\text{MLC} = (1 + \lambda_c) \sum_{j \in \mathcal{J}} P_{L_j} = (1 + \lambda_c)(\sum_{j \in \mathcal{J}} P_{L_{0j}} + \sum_{j \in \mathcal{J}} P_{D_j}) \tag{3.15}$$

where λ_c is the "critical" value of the loading parameter at the bifurcation point or security limit. Let us define the concept of Available Loading Capability (ALC) as follows:

$$\text{ALC} = \text{MLC} - \sum_{j \in \mathcal{J}} P_{L_j} = \text{MLC} - \text{TTL} \tag{3.16}$$

where TTL is the Total Transaction Level at the current operating point. Thus, in terms of λ_c, one has:

$$\text{ALC} = \lambda_c \sum_{j \in \mathcal{J}} P_{L_j} = \lambda_c \text{TTL} \tag{3.17}$$

ALC values will be used in this thesis as a measure of the security margin of the current operating point with regard to voltage stability criteria.

3.5 N-1 Contingency Criterion

The definition of ALC given in (3.17) is actually incomplete, since first class emergency contingencies, i.e. an N-1 contingency criterion, are not taken into

Table 3.1: Loading parameter values and associated limits for the six-bus system. Values are obtained for the 6-bus test system using power directions $P_S = (0, 25, 20)$ MW and $P_D = (25, 10, 8)$ MW, enabling generator reactive power limits, and checking for voltage security and thermal limits.

Loading Parameter $1 + \lambda$	Total Loading [MW]	Variable	Limit or Bifurcation
1.4226	459.5	$I_{4-2_{\max}}$	thermal
1.4316	462.4	$V_{5_{\min}}$	voltage security
1.4767	477.0	$Q_{G2_{\max}}$	LIB
1.5457	499.3	$I_{1-4_{\max}}$	thermal
1.5459	499.3	$Q_{G1_{\max}}$	LIB
1.5476	499.9	$V_{4_{\min}}$	voltage security
1.5731	508.1	$I_{3-5_{\max}}$	thermal
1.5811	510.7	$I_{6-3_{\max}}$	thermal
1.6043	518.2	$I_{2-5_{\max}}$	thermal
1.6117	520.6	$I_{5-1_{\max}}$	thermal
1.6117	520.6	$V_{6_{\min}}$	voltage security
1.6261	525.2	$Q_{G3_{\max}}$	LIB

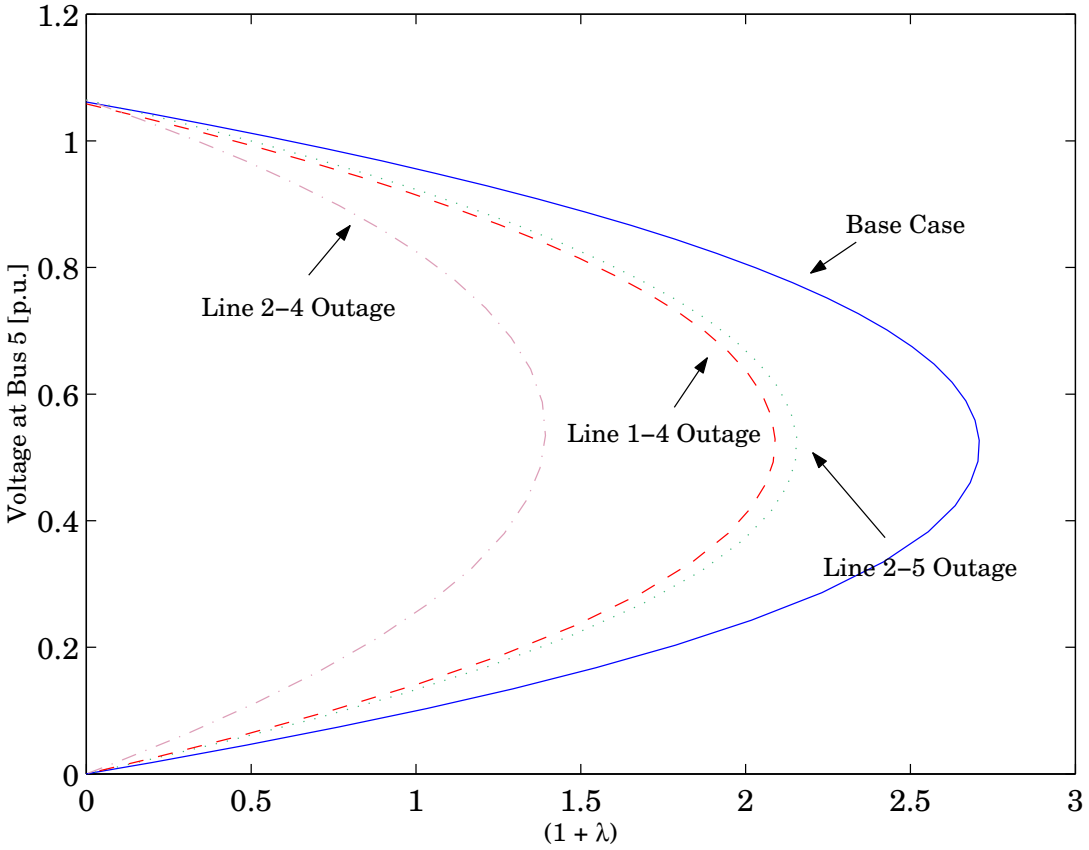

Figure 3.6: Typical nose curves for the base case and for different line outages. Curves refer to voltage at bus 5 for the 6-bus test system using power directions $P_S = (0, 25, 20)$ MW and $P_D = (25, 10, 8)$ MW.

account. As it might be expected, line outages may drastically reduce the values of λ_c and MLC. An example is reported in Fig. 3.6.

In North American power companies, system operators follow the definition of Available Transfer Capability (ATC) as proposed by NERC, which is as follows:

ATC: *"measure of the transfer capability remaining in the physical transmission network for further commercial activity over and above already committed uses"* [56].

The ATC is computed with the following expression:

$$\text{ATC} = \text{TTC} - \text{ETC} - \text{TRM} \tag{3.18}$$

where

$$\text{TTC} = \min(P_{\max_{I_{lim}}}, P_{\max_{V_{lim}}}, P_{\max_{S_{lim}}})$$

represents the Total Transfer Capability, i.e. the maximum power that the system can deliver given the security constraints defined by thermal limits (I_{lim}), voltage limits (V_{lim}) and stability limits (S_{lim}) based on an N-1 contingency criterion, ETC stands for the Existing Transmission Commitments, and TRM is the Transmission Reliability Margin, which is meant to account for uncertainties in system operations. TRM is usually assumed to be a fixed quantity, i.e. TRM = K, where K is a given MW value used to represent contingencies that are not being considered during the ATC computations (e.g. N-2 contingencies). In this thesis, TRM will be ignored without loss of generality, since it would affect the MLCs resulting from the proposed OPF solutions only for an offset value.

The ATC is a basic concept typically associated with "area" interchange limits which are imposed by transmission rights, and is used as a measure of available power which can be further exchanged among different entities [57, 58]. In [11] a "System wide" ATC (SATC), and corresponding "System wide" TTC, ETC and TRM are proposed to extend the ATC concept to a system domain.

In this thesis, we stay away from the debate whether the ATC has to be defined only for area exchange limits or can be extended to a system wide information on the security margin. However, we make use of the structure of the NERC definition of ATC to define an available loading condition which includes N-1 contingency, namely ALC$^{(N-1)}$. Based on (3.16) and (3.18), the following correlations can be stated:

$$\text{ETC} \Rightarrow \text{TTL} \tag{3.19}$$

and

$$\text{TTC} \Rightarrow \text{MLC}^{(N-1)} = (1 + \min_h\{\lambda_{c_h}\})\text{TTL} \tag{3.20}$$

where $\text{MLC}^{(N-1)}$ is the MLC associated with the line outage h which leads to the minimum λ_c. For instance, with regards to nose curves depicted in Fig. 3.6, $\text{MLC}^{(N-1)}$ is the SNB point of the nose curve associated with contingency on line 2-4. Thus, from (3.18), the definition of ALC is as follows:

$$\text{ATC} \Rightarrow \text{ALC}^{(N-1)} = \min_h\{\lambda_{c_h}\} \sum_{j \in \mathcal{J}} P_{L_j} = \min_h\{\lambda_{c_h}\}\text{TTL} \tag{3.21}$$

3.6 Sensitivity Analysis

Continuation power flow analysis may also be used to get a variety of "sensitivity" factors of the current or critical points with respect to the loading parameter [50, 59, 60]. It has been said that, at a SNB point, the sensitivity with respect to λ of a variable is infinite. This actually does not necessarily imply a huge variation of the variable itself [50]. However, sensitivity factors can be used to determine which variable (typically a "control" variable), at the operating point is mostly affected by the parameter variation, and thus varying that variable is likely a good "direction" toward stability improvement. Since the sensitivity analysis is basically a linearization around a current steady state point and power system models are highly nonlinear, variation steps of control variables cannot be huge. It is thus necessary to repeat the computation of sensitivity factors after each step (an example of iterative techniques to optimize transmission congestion in simple auction-based markets with respect to voltage stability criteria is proposed in [11]).

3.7 Summary

This chapter has presented the basic concepts and the main analysis techniques to approach voltage collapse and instability phenomena in electric power system. Continuation power flow technique and bifurcation theory analysis are shown to be able to:

1. investigate equilibrium points close to critical operating conditions (SNB and LIB);

2. estimate stability margins at the current operating point (available loading conditions) both in normal and in first class contingency conditions;

3. provide a variety of indexes (sensitivity factors) which allows estimating remedial actions for avoiding critical conditions.

Voltage stability concepts described here will be used through this thesis for defining voltage stability constraints in competitive electricity markets.

Chapter 4

Optimal Power Flow Outlines

4.1 Introduction

WITH regard to the solution of the electricity auction problem, two main approaches are currently under study in the literature: merit order or single-price auctions and OPF-based power markets. The basic principles of single-price auctions have been implemented by many Independent Market Operators (IMO) all around the world. Market clearing procedures currently in use in competitive pool-based electricity markets differ significantly from one another. However, some common characteristics can be recognized, as follows:

- ◇ merit order market clearing mechanisms are simple, transparent and well accepted by market participants;
- ◇ there is the need of separate procedures to take into account losses, congestions and, in general, nonlinear constraints;
- ◇ Linear Programming (LP) and/or Mixed Integer Programming (MIP) techniques used to solve merit order market problems, have a high computational efficiency, which is needed for on-line applications).

Since in this thesis the main interest is including voltage stability constraints in the market problem, the second point is the main drawback of simple auction techniques. Thus, we will focus only on Optimal Power Flow (OPF) based hybrid markets. Generally speaking, OPF methods are not strictly related to market problems. As a matter of fact, OPF methods have been used in regulated power systems to schedule power generations in order to minimize cost productions and losses in transmission lines. OPF main characteristics are as follows:

- ◇ OPF may include a variety of (nonlinear) constraints, thus allowing for precise power system models;
- ◇ OPF is not very popular among market operators because of its complexity and "obscure" solution process;
- ◇ OPF does not need separate procedures to take into account losses and transmission congestions;
- ◇ low efficiency of solvers for Nonlinear Programming (NLP) and/or Mixed Integer Nonlinear Programming (MINLP) is a critical issue for on-line applications.

This chapter introduces firstly the nomenclature utilized throughout this thesis for the formulations of the OPF problems; then basic models of single-period and multi-period OPF-based market models are presented. The OPF-based approach to maximize the distance to voltage collapse is also discussed since it provides the basic approach to include voltage stability constraints in the OPF-based market mechanisms proposed in this thesis.

4.2 Nomenclature for the OPF-based Market Problem

For the sake of clarity, constants, variables and sets used in the formulation of the single and multi-period OPF-based market problems are reported below. Symbols used here follow mostly the nomenclature given in [47, 48, 61].

Constants:

$P_{S_{\max_i}}$	upper limit of the energy bid offered by unit i [MW];
$P_{S_{\min_i}}$	lower limit of the energy bid offered by unit i [MW];
$Q_{G_{\max_i}}$	upper limit of the reactive power support available at unit i [MVar];
$Q_{G_{\min_i}}$	lower limit of the reactive power support available at unit i [MVar];
T	scheduling time horizon (e.g. 24 hours);
DT_i	minimum down time of unit i [h];
UT_i	minimum up time of unit i [h];
SD_i	shut-down ramp limit of unit i [MW/h];
SU_i	start-up ramp limit of unit i [MW/h];
RD_i	ramp-down limit of unit i [MW/h];
RU_i	ramp-up limit of unit i [MW/h];
Γ_i	number of periods unit i must be on-line at the beginning of market horizon due to its minimum up time constraint [h];
Π_i	number of periods unit i must be off-line at the beginning of market horizon due to its minimum down time constraint [h];
α_i^0	time periods unit i has been on-line at the beginning of the market horizon (end of period 0) [h];
β_i^0	time periods unit i has been off-line at the beginning of the market horizon (end of period 0) [h];
$P_{D_{\max_j}}$	upper limit of the energy bid demanded by consumer j [MW];

$P_{D_{\min_j}}$ lower limit of the energy bid demanded by consumer j [MW];

Variables:

$P_{S_i}(t)$ power output of generation unit i in period t [MW];

$\overline{P}_{S_i}(t)$ maximum power output of generation unit i in period t [MW];

Q_{G_i} reactive power output of unit i [MVar];

$P_{D_j}(t)$ power output of consumer j in period t [MW];

$u_i(t)$ 0/1 variable which is equal to 1 if unit i is on-line in period t;

$w_i(t)$ 0/1 variable which is equal to 1 if unit i is started-up at the beginning of period t;

$z_i(t)$ 0/1 variable which is equal to 1 if unit i is shut-down at the beginning of period t;

Sets:

$\mathcal{I}$ set of indexes of generating units;

$\mathcal{J}$ set of indexes of consumers;

$\mathcal{T}$ set of indexes of periods of the market horizon;

$\mathcal{B}$ set of indexes of network buses;

$\mathcal{N}$ set of indexes of transmission lines;

4.3 Single-Period OPF-based Electricity Market

Single-period OPF-based approach is basically a nonlinear constrained optimization problem, and consists of a scalar objective function and a set of equality and inequality constraints. The objective function is typically maximizing the *social benefit*, i.e. ensuring that generators get the maximum income for their power production and consumers or wholesale retailers pay the cheapest prices for their

power purchase, as follows:

$$\text{Max.} \quad G = \sum_{j \in \mathcal{J}} c_{D_j}(P_{D_j}) - \sum_{i \in \mathcal{I}} c_{S_i}(P_{S_i}) \tag{4.1}$$

where c_S and c_D are generic but monotonic generator and consumer cost functions of power bids P_S and P_D. In this thesis c_S and c_D will be considered linear functions of powers, without losing generality:

$$\text{Max.} \quad G = \sum_{j \in \mathcal{J}} C_{D_j} P_{D_j} - \sum_{i \in \mathcal{I}} C_{S_i} P_{S_i} \tag{4.2}$$

where C_S and C_D are in \$/MWh.

Then power flow equations and "security" constraints are as follows:

Power Flow Equations:

$$\begin{aligned}
P_h &= V_h^2(g_h + g_{h0}) \\
&\quad - V_h \sum_{\ell \neq h}^{n_\ell} V_\ell (g_{h\ell} \cos(\theta_h - \theta_\ell) + b_{h\ell} \sin(\theta_h - \theta_\ell)) \\
&\quad \forall h \in \mathcal{B} \\
Q_h &= -V_h^2(b_h + b_{h0}) \\
&\quad + V_h \sum_{\ell \neq h}^{n_\ell} V_\ell (g_{h\ell} \sin(\theta_h - \theta_\ell) - b_{h\ell} \cos(\theta_h - \theta_\ell)) \\
&\quad \forall h \in \mathcal{B} \\
P_h &= \sum_{i \in \mathcal{I}_h} (P_{G_{i0}} + P_{S_i}) - \sum_{j \in \mathcal{J}_h} (P_{L_{0j}} + P_{D_{0j}}) \\
&\quad \forall h \in \mathcal{B} \\
Q_h &= \sum_{i \in \mathcal{I}_h} Q_{G_i} - \sum_{j \in \mathcal{J}_h} (P_{L_{0j}} + P_{D_{0j}}) \tan(\phi_{D_i}) \\
&\quad \forall h \in \mathcal{B}
\end{aligned} \tag{4.3}$$

where V and θ represent the bus phasor voltages. Load models in power flow equations f are assumed to be (2.5), thus accounting for a fixed amount of powers, i.e. P_{G_0} and P_{L_0}, for must-run generations, non-interruptible loads, etc. The aim of (4.3) is twofold. Firstly, the active and reactive power balance is ensured; then transmission losses are accurately modeled and taken into account.

Supply Bid Blocks:

$$P_{S_{\min_i}} \leq P_{S_i} \leq P_{S_{\max_i}} \quad \forall i \in \mathcal{I} \tag{4.4}$$

Demand Bid Blocks:

$$P_{D_{\min_j}} \leq P_{D_j} \leq P_{D_{\max_j}} \quad \forall j \in \mathcal{J} \tag{4.5}$$

Generator Reactive Power Support:

$$Q_{G_{\min_i}} \leq Q_{G_i} \leq Q_{G_{\max_i}} \quad \forall i \in \mathcal{I} \tag{4.6}$$

Voltage "Security" Limits:

$$V_{\min_h} \leq V_h \leq V_{\max_h} \quad \forall h \in \mathcal{B} \tag{4.7}$$

Thermal Limits:

$$\begin{aligned} I_{hk}(\theta, V) &\leq I_{hk_{\max}} \quad \forall (h,k) \in \mathcal{N} \\ I_{kh}(\theta, V) &\leq I_{kh_{\max}} \end{aligned} \tag{4.8}$$

where I_{hk} and I_{kh} are the line currents and are used to model system security by limiting transmission line flows.

4.3.1 Security Constrained OPF-based Electricity Market

In common practice (e.g. [33]), the inclusion of system congestions in the OPF problem (4.10) is obtained by imposing transmission capacity constraints on the real power flows, as follows:

Transmission Congestion Limits:

$$\begin{aligned} |P_{hk}(\theta, V)| &\leq P_{hk_{\max}} \quad \forall (h,k) \in \mathcal{N} \\ |P_{kh}(\theta, V)| &\leq P_{kh_{\max}} \end{aligned} \tag{4.9}$$

where P_{hk} and P_{hk} limits are obtained by means of off-line angle and/or voltage stability studies. In practice, these limits are usually determined based only on power flow based voltage stability studies [62]. Hence, these limits do not actually represent the actual stability conditions of the resulting OPF problem solution, which may lead in some cases to insecure solutions and/or inadequate price signals, as demonstrated in this thesis. Summarizing and dropping the index notation, the standard *security constrained* single period OPF-based market model can be formulated as follows:

$$\begin{aligned} \text{Max.} \quad & C_D^T P_D - C_S^T P_S && \rightarrow && \text{Social benefit} \\ \text{s.t.} \quad & f(\theta, V, Q_G, P_S, P_D) = 0 && \rightarrow && \text{PF equations} \\ & P_{S_{\min}} \leq P_S \leq P_{S_{\max}} && \rightarrow && \text{Sup. bid blocks} \\ & P_{D_{\min}} \leq P_D \leq P_{D_{\max}} && \rightarrow && \text{Dem. bid blocks} \\ & I_{hk}(\theta, V) \leq I_{hk_{\max}} && \rightarrow && \text{Thermal limits} \\ & I_{kh}(\theta, V) \leq I_{kh_{\max}} \\ & |P_{hk}(\theta, V)| \leq P_{hk_{\max}} && \rightarrow && \text{Congestion limits} \\ & |P_{kh}(\theta, V)| \leq P_{kh_{\max}} \\ & Q_{G_{\min}} \leq Q_G \leq Q_{G_{\max}} && \rightarrow && \text{Gen. } Q \text{ lim.} \\ & V_{\min} \leq V \leq V_{\max} && \rightarrow && V \text{ “security” lim.} \end{aligned} \tag{4.10}$$

4.4 Multi-Period OPF-based Electricity Market

Multi-period OPF-based electricity markets are typically modeled as mixed integer linear programming problems. Equations are kept linear because of the complexity introduced by integer variables. Thus power flow equations (4.3) are generally substituted by a power balance which may or may not include an approximated expression of network losses [47, 48].

In this thesis, we will consider ramping constraints as described in [47], where the authors presents a detailed model of a multi-period auction for pool-based electricity markets. Model presented in [47] is linear, while the multi-period voltage stability constrained OPF proposed in Chapter 8 is a set of nonlinear equations. However, the formulation of ramp rate limits and logical status of commitments do not depends on the modelization of network losses and/or other nonlinear constraints.

The objective function (4.2) as well as constraints (4.4), and (4.6) have to be modified in order to take into account unit commitment of generation units and have to be extended to the scheduling time horizon T. (For instance, for daily-ahead market scheduling, $T = 24$ h.) Furthermore, a set of temporal constraints to account for minimum up and down times, ramp up and down limits and start-up and shut-down ramp rates of generations unit has to be added to properly model thermal plants.

Thus, the objective function becomes:

$$\begin{aligned} \text{Max.} \quad G &= \sum_{t\in\mathcal{T}}\sum_{j\in\mathcal{J}} C_{D_j} P_{D_j}(t) \\ &- \sum_{t\in\mathcal{T}}\sum_{i\in\mathcal{I}} (C_{S_i} P_{S_i}(t) + C_{SU_i} w_i(t) + C_{SD_i} z_i(t)) \end{aligned} \tag{4.11}$$

where C_{SU} and C_{SD} are the start-up and shut-down costs of generating unit.

Supply bid blocks and generator reactive power limits have to take in account

whether the generator is committed at the period t:

$$P_{S_{\min i}} u_i(t) \leq P_{S_i}(t) \leq \overline{P}_{S_i}(t) \qquad \forall i \in \mathcal{I}, \quad \forall t \in \mathcal{T} \tag{4.12}$$

$$Q_{G_{\min i}} u_i(t) \leq Q_{G_i}(t) \leq Q_{G_{\max i}} u_i(t) \quad \forall i \in \mathcal{I}, \quad \forall t \in \mathcal{T} \tag{4.13}$$

where maximum available power output limits $\overline{P}_{S_i}(t)$ are formulated in order to take into account the unit actual capacity, start-up ramp rate limits, shut-down ramp rate limits and rump-up limits, as follows:

$$\begin{aligned} \overline{P}_{S_i}(t) &\leq P_{S_{\max_i}}[u_i(t) - z_i(t+1)] + z_i(t+1) SD_i \quad \forall i \in \mathcal{I}, \quad \forall t \in \mathcal{T} \\ \overline{P}_{S_i}(t) &\leq P_{S_i}(t-1) + RU_i u_i(t-1) + SU_i w_i(t) \quad \forall i \in \mathcal{I}, \quad \forall t \in \mathcal{T} \end{aligned} \tag{4.14}$$

The ramp-down rate limit and the shut-down ramp rate limit are modeled as follows:

$$P_{S_i}(t-1) \leq P_{S_i}(t) + RD_i u_i(t) + SD_i z_i(t) \quad \forall i \in \mathcal{I}, \quad \forall t \in \mathcal{T} \tag{4.15}$$

Equations (4.14) and (4.15) model start-up and shut-down constraints in a more detailed way than the one commonly used in the literature [27, 46], i.e.

$$\begin{aligned} P_{S_i}(t) - P_{S_i}(t-1) &\leq RU_i \quad \forall i \in \mathcal{I}, \quad \forall t \in \mathcal{T} \\ P_{S_i}(t-1) - P_{S_i}(t) &\leq RD_i \quad \forall i \in \mathcal{I}, \quad \forall t \in \mathcal{T} \end{aligned} \tag{4.16}$$

since in (4.16) start-up and shut-down variables are used instead of ramp-up and ramp-down limits as in (4.14) and (4.15). Minimum on-line and off-line time constraints are formulated as presented in [47] and in [61]. These are as follows:

Minimum up time:

$$\begin{aligned}
\sum_{t=1}^{\Gamma_i}(1-u_i(t)) &= 0 \quad \forall i \in \mathcal{I} \\
\sum_{\tau=t}^{k+UT_i-1} u_i(\tau) &\geq UT_i w_i(t) \quad \forall i \in \mathcal{I}, \\
&\quad \forall t = \Gamma_i + 1 \ldots T - UT_i + 1 \\
\sum_{\tau=t}^{T}(u_i(\tau) - w_i(t)) &\geq 0 \quad \forall i \in \mathcal{I}, \\
&\quad \forall t = T - UT_i + 2 \ldots T
\end{aligned} \tag{4.17}$$

Minimum down time:

$$\begin{aligned}
\sum_{t=1}^{\Pi_i} u_i(t) &= 0 \quad \forall i \in \mathcal{I} \\
\sum_{\tau=t}^{t+DT_i-1} (1-u_i(\tau)) &\geq DT_i z_i(t) \quad \forall i \in \mathcal{I}, \\
&\quad \forall t = \Pi_i + 1 \ldots T - DT_i + 1 \\
\sum_{\tau=t}^{T}(1 - u_i(\tau) - z_i(t)) &\geq 0 \quad \forall i \in \mathcal{I}, \\
&\quad \forall t = T - DT_i + 2 \ldots T
\end{aligned} \tag{4.18}$$

where Γ_i and Π_i are the number of periods unit i must be on-line and off-line at the beginning of the time horizon respectively, as follows:

$$\Gamma_i = \min\{T, (UT_i - \alpha_i^0)u_i(0)\} \tag{4.19}$$

$$\Pi_i = \min\{T, (DT_i - \beta_i^0)(1 - u_i(0))\} \tag{4.20}$$

Finally, the start-up and the shut-down status of the units are managed as follows:

$$\begin{aligned}
w_i(t) - z_i(t) &= u_i(t) - u_i(t-1) \quad \forall i \in \mathcal{I}, \forall t \in \mathcal{T} \\
w_i(t) + z_i(t) &\leq 1 \quad \forall i \in \mathcal{I}, \forall t \in \mathcal{T}
\end{aligned} \tag{4.21}$$

Equations (4.21) are necessary to avoid simultaneous commitment and decommitment of a unit. Observe that a single-period market with unit commitment can be directly derived from (4.11)-(4.21) by imposing a scheduling time $T = 1$ h.

4.5 Maximization of the Distance to Voltage Collapse

In [22], it has been demonstrated that the following optimization problem:

$$\begin{aligned} \text{Max.} \quad & \lambda \\ \text{s.t.} \quad & f(x, \lambda) = 0 \end{aligned} \tag{4.22}$$

is formally the same as (3.13), i.e. the solution of (4.22) is the SNB point. In fact, the Lagrangian function associated with (4.22) can be written as:

$$\mathcal{L}(x, \lambda, \rho) = \lambda - \rho^T f(x, \lambda) \tag{4.23}$$

ρ being the Lagrangian multipliers, and the KKT optimality condition gives:

$$\begin{aligned} \frac{\partial \mathcal{L}}{\partial x} &= -\rho^T D_x f(x, \lambda) = 0 \\ \frac{\partial \mathcal{L}}{\partial \rho} &= -f(x, \lambda) = 0 \\ \frac{\partial \mathcal{L}}{\partial \lambda} &= 1 - \rho^T \frac{\partial f}{\partial \lambda} = 0 \end{aligned} \tag{4.24}$$

As it can be noted these conditions are the same as conditions in (3.13), where Lagrangian multipliers ρ correspond to the elements of the left eigenvector $\hat{w}$. Model (4.22) can be extended in two main directions:

1. Adding inequality constraints to take into account voltage limits, generator reactive power limits, thermal limits, etc.

2. Modifying problem (4.22) to maximize the distance to voltage collapse instead of simply determining the collapse point.

The latter issue has been addressed for the first time in [24] and approached by using two sets of power flow equations, one for the current operating point and one for the "critical" solution associated with either a voltage collapse condition (SNB or LIB) or a security limit, as follows:

$$\begin{aligned} \text{Min.} \quad & \lambda_p - \lambda_c \\ \text{s.t.} \quad & f(\theta_p, V_p, Q_{G_p}, P_S, P_D, \lambda_p) = 0 \\ & f(\theta_c, V_c, Q_{G_c}, P_S, P_D, \lambda_c) = 0 \\ & \underline{H}_p \leq H(\theta_p, V_p, Q_{G_p}) \leq \overline{H}_p \\ & \underline{H}_c \leq H(\theta_c, V_c, Q_{G_c}) \leq \overline{H}_c \end{aligned} \tag{4.25}$$

where H are constraint functions of the dependent variables and $\underline{H}$ and $\overline{H}$ their lower and upper limits respectively and load models are assumed to be (3.2) or (3.3). Suffixes p and c indicate the current and the critical operating points, respectively, which solve the two sets of power flow equations. In (4.25) the distance to the maximum loading condition is certainly maximized because of the use of the two loading parameters λ_p and λ_c. The approach of doubling power flow equations and including the dependence on a loading parameter will be used in this thesis to formulate a voltage security constrained OPF.

4.6 Optimization Methods

There is a plethora of optimization methods used in power system analysis [15]. In this thesis, we are interested in methods able to solve nonlinear programming and mixed integer nonlinear programming problems, since voltage stability constraints are best modeled with a set of (highly) nonlinear equations, while market

and physical constraints are both continuous (power flow equations, transmission line flow limits, etc.) and discrete (unit commitment, start-up and shut-down limits of generators, etc.). Approaches and techniques presented in the following subsections are chosen with the aim of both robustness and reliability for large problems.

4.6.1 Nonlinear Programming Problem

Nonlinear programming problems, which are typical in power-engineering and are suitable for solving optimal power flows such as (4.10) and (4.25), can be formulated, in general terms, as follows:

$$\begin{aligned} \text{Min.} \quad & G(y) \\ \text{s.t.} \quad & f(y) = 0 \\ & \underline{H} \leq H(y) \leq \overline{H} \\ & \underline{y} \leq y \leq \overline{y} \end{aligned} \tag{4.26}$$

where

- $y \in \mathbb{R}^n$ is a vector of decision variables, including the control and nonfunctional dependent variables.
- $G : \mathbb{R}^n \to \mathbb{R}$ is a scalar function that represents the power system's operation optimization goal.
- $f : \mathbb{R}^n \to \mathbb{R}^m$ is a vector function with conventional power flow equations and other equality constraints.
- $H : \mathbb{R}^n \to \mathbb{R}^p$ is a vector of functional variables, with lower bound $\underline{H}$ and upper bound $\overline{H}$, corresponding to operating limits on the system.

Functions $G(y)$, $f(y)$ and $H(y)$ are assumed to be twice continuously differentiable. A point $\hat{y}$ is said to *feasible* if it satisfies all constraints in (4.26). The set of all feasible points defines a *feasible region* and a feasible point y^* that attains the desired minimum is called a *local optimum*.

In this thesis, the problem (4.26) is approached by means of two different techniques, namely the primal-dual Interior Point (IP) method, which proved to be a reliable technique for solving OPF problems [16, 18, 19, 20] and the Generalized Reduced Gradient (GRG) technique [28, 63]. The reason for using two methods is twofold: firstly to double-check results which is recommended whenever an optimization of highly nonlinear systems is involved, secondly because the GRG method is then integrated in a MINLP technique used for taking in account unit commitment and discrete ramping constraints in the OPF problem.

4.6.2 Solution of the NLP via Interior Point Method

This section gives a brief outline of the IP method for nonlinear programming. A complete treatise can be found in [20]. The following description is meant only to provide a nomenclature for variables introduced in nonlinear programming techniques and which will be used in this thesis when defining marginal costs.

Firstly, all inequalities in problem (4.26) are transformed into equalities by defining a vector of non-negative slack variables s, and adding to the objective function a logarithmic barrier term, which ensures the non negativity condition $s \geq 0$:

$$\begin{aligned} \text{Min.} \quad & G(y) - \mu^k \sum_{i=1}^{p} (\ln s_{1_i} + \ln s_{2_i}) \\ \text{s.t.} \quad & f(y) = 0 \\ & -s_1 + \overline{H} - H(y) = 0, \quad s_1 > 0 \\ & -s_2 - \underline{H} + H(y) = 0, \quad s_2 > 0 \end{aligned} \tag{4.27}$$

where for sake of simplicity, $\underline{y} \leq y \leq \overline{y}$ are included in $\underline{H} \leq H(y) \leq \overline{H}$, and $s = (s_1, s_2)$. The Lagrangian function $\mathcal{L}$ associated with (4.27) is as follows:

$$\begin{aligned} \mathcal{L}_\mu(z) \triangleq\ & G(y) - \mu^k \sum_{i=1}^{p} (\ln s_{1_i} + \ln s_{2_i}) - \rho^T f(y) \\ & -\mu_1^T(-s_1 + \overline{H} - H(y)) - \mu_2^T(-s_2 - \underline{H} + H(y)) \end{aligned} \tag{4.28}$$

where ρ ($\rho \in \mathbb{R}^m$), μ_1 ($\mu_1 \in \mathbb{R}^p$) and μ_2 ($\mu_2 \in \mathbb{R}^p$) are the Lagrangian multipliers (or dual variables), μ^k ($\mu^k \neq 0$) is the barrier parameter, and $z \triangleq (s, \mu, y, \rho)$, being $\mu = (\mu_1, \mu_2)$. The local minimization of (4.28) is satisfied by the KKT optimality condition:

$$\nabla_z \mathcal{L}_\mu(z) = 0 \tag{4.29}$$

Then, the IP method works as follows:

Step 0 define an initial point ($k = 0$), i.e. μ^0 and z^0;

Step 1 compute Newton direction, i.e. $[\nabla_z^2 \mathcal{L}_\mu(z)|_k]^{-1} \nabla_z \mathcal{L}_\mu(z^k)$, of the current point;

Step 2 compute the step direction Δz^k length in the Newton direction and update $z^k \rightarrow z^{k+1}$;

Step 3 if convergence criteria are satisfied, stop; otherwise update $\mu^k \rightarrow \mu^{k+1}$ and return to *Step 1*.

4.6.3 Mixed Integer Linear Programming

In general terms, the Mixed Integer Linear Programming (MILP) Problem can be formulated as follows:

$$\begin{aligned} \text{Min.} \quad & G = cy + du \\ \text{s.t.} \quad & Ay + Bu > b \\ & \underline{y} < y < \overline{y} \\ & u = 0, 1, 2, \ldots \end{aligned} \tag{4.30}$$

where y is a vector of variables that are continuous real numbers, and u is a vector of variables that can only take integer values. $cy + du$ is the objective function, and $Ay + Bu > b$ represents the set of constraints. $\underline{y}$ and $\overline{y}$ are vectors of lower and upper bounds on the continuous variables, and $u = 0, 1, 2, \ldots$ is the integrality requirement on the integer variables u. In typical optimal power flow problems such as the one presented in Section 4.4, integer variables reduce to *binary* variables, i.e. $u \in \{0, 1\}$.

The solution of a MILP problem is typically $\mathcal{NP}$-hard, thus methods which attempts to find all possible solution alternatives are unpractical, even for tiny problems. Deterministic techniques which attempts to find an exact solution are typically based on multiple solutions of the Lagrangian Relaxation (LR) of (4.30), which consists in removing from (4.30) the integer constraints $u = 0, 1, 2, \ldots$. Most used methods are Cutting Plane Method, Dynamic Programming, Branch & Bound and Branch & Cut [64].

To illustrate the $\mathcal{NP}$-hardness of MIP problems, observe Fig. 4.1, which is taken from [65]. In this example of dynamic programming graph, it is considered a thermal plant characterized by $t_{\text{on}} = 2$ hours and $t_{\text{off}} = 3$ hours for the minimum up and down times respectively and which has been committed for 1 hour before period 1 as indicated in the graph. Each of the 32 points represents a possible *state* of the plant. Observe that the number of subproblems (associated which each state) is significantly lower of the total number of all possible combinations (i.e. 84), yet the graph complexity is growing quickly.

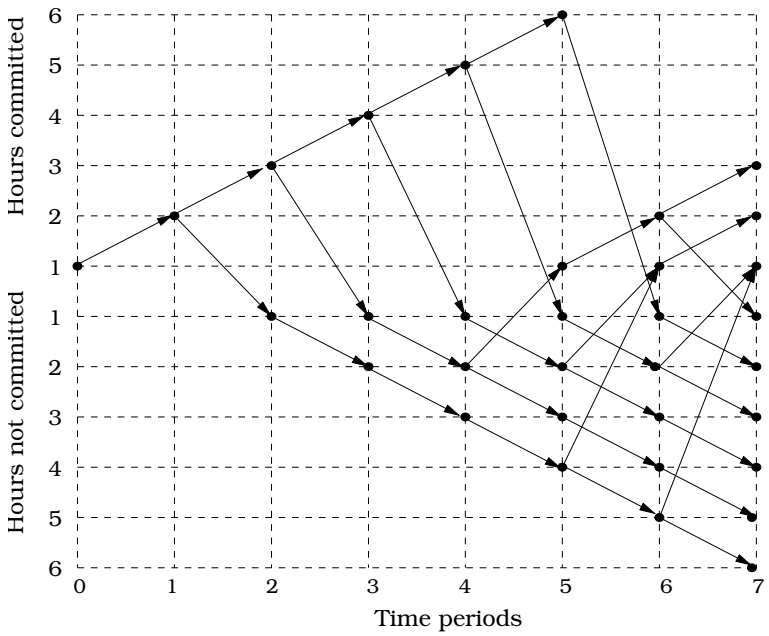

Figure 4.1: Example of dynamic programming graph.

4.6.4 Mixed Integer Nonlinear Programming

Mathematically, the Mixed Integer Nonlinear Programming (MINLP) Problem looks like:

$$\begin{aligned} \text{Min.} \quad & G = c(y) + du \\ \text{s.t.} \quad & g(y) + bu < 0 \\ & \underline{H} < H(y) < \overline{H} \\ & u = 0, 1, 2, \ldots \end{aligned} \tag{4.31}$$

where y is a vector of variables that are continuous real numbers, $c(y) + du$ is the objective function, and $g(y) + bu$ represents the set of constraints. $H : \mathbb{R}^n \rightarrow \mathbb{R}^p$ is a vector of functional variables, with lower bound $\underline{H}$ and upper bound $\overline{H}$, corresponding to operating limits on the system.

As it might be expected, solving MINLP problems is generally highly computa-

tionally demanding since both NLP and MIP issues have to be handled. Typically, MINLP solvers are able to find solutions which are only *locally optimal*. The solver used in this thesis to approach MINLP problems is GAMS/DICOPT [66], which has specifically designed for large-scale problems with smooth nonlinearities. DICOPT works as follows:

Step 1 solve the NLP relaxation of (4.31). If $u^0 = u$ is integer, stop: the optimum integer solution has been found.

Step 2 find an integer point u^1 with a MIP problem which find the minimum over the convex hull determined by (y^0, u^0).

Step 3 Set $u = u^1$ and solve the resulting NLP whose solution is (y^1, u^1).

Step 4 find an integer solution u^2 with a MIP problem which minimizes the intersection of the convex hulls defined by the KKT points u^0 and u^1.

Step 5 repeat steps 3 and 4 until there is an increase in the value of the NLP objective function.

Theoretic and computational aspects of DICOPT are presented in [67] and are not discussed here any further.

4.7 Pricing Electricity and Security

Besides generation and load power scheduling, market clearing mechanism have to provide prices associated with power production and consumption. Two main approaches have been proposed in competitive markets, namely the spot pricing model which gives Locational Marginal Prices (LMP) and the single-price model based on Market Clearing Price (MCP). The latter is currently widely utilized, since it is "transparent" and "easy" to be computed. However, spot pricing through marginal costs can provide reliable pricing indicators for both generation

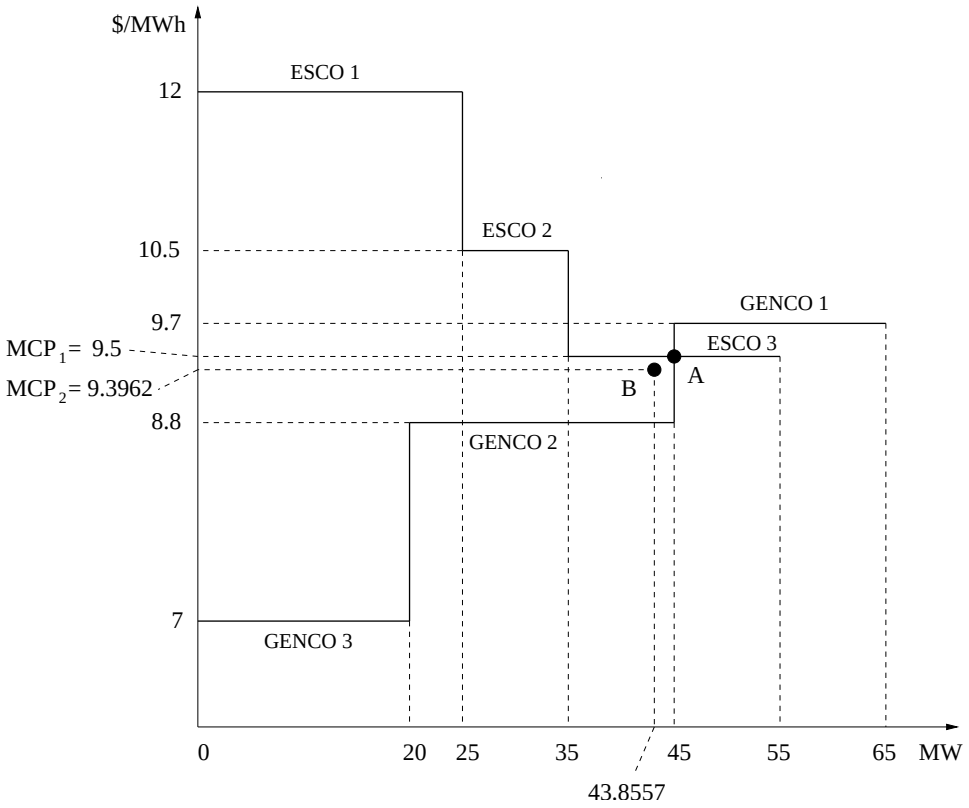

Figure 4.2: Market Clearing Price for the six-bus test system, determined by means of a simple auction technique assuming demand-side bidding.

and congestions [33] and will be utilized in this thesis. Following sections describe both single price and marginal cost approaches for the sake of comparison.

4.7.1 Market Clearing Price (MCP)

Figure 4.2 depicts the results for a simple auction technique with demand side bidding for the six-bus test system. In the figure, point A has been determined assuming the simple power balance:

$$\sum_{i \in \mathcal{I}} P_{S_i} - \sum_{j \in \mathcal{J}} P_{D_j} = 0 \tag{4.32}$$

while point B was obtained with a power balance accounting for a simplified formula of transmission losses:

$$\sum_{i\in\mathcal{I}} P_{S_i} - \sum_{j\in\mathcal{J}} P_{D_j} - P_{\text{loss}} = 0 \tag{4.33}$$

where P_{loss} is an approximated expression which depend on bus voltages and the network admittance matrix [68]. Observe that $\text{MCP}_2 < \text{MCP}_1$ as losses reduce the power delivered to consumers.

Regardless to the power balance model, single price approach appears unfair since it does not take into account congestions caused by each market participant.

4.7.2 Locational Marginal Prices (LMPs)

It is widely recognized that spot pricing through marginal costs can provide reliable pricing indicators [33]. OPF-based market models have the advantage of producing not only the optimal operating point solutions, but also a variety of sensitivity variables through the Lagrangian multipliers, which can be associated with Locational Marginal Prices (LMPs) at each node.

LMPs are basically the Lagrangian multipliers ρ of power flow equations associated with real power injections, i.e. $\text{LMP}_h = \rho_{P_h}$. However, a more detailed information can be deduced from the KKT optimality condition applied to the OPF problem. With regard to (4.10), the Lagrangian function is as follows:

$$\begin{aligned}\text{Min.}\quad \mathcal{L} = {} & G - \rho^T f(\delta, V, Q_G, P_S, P_D) \\ & - \mu^T_{P_{S\,\max}}(P_{S_{\max}} - P_S - s_{P_{S\,\max}}) \\ & - \mu^T_{P_{S\,\min}}(P_S - s_{P_{S\,\min}}) \\ & - \mu^T_{P_{D\,\max}}(P_{D_{\max}} - P_D - s_{P_{D\,\max}}) \\ & - \mu^T_{P_{D\,\min}}(P_D - s_{P_{D\,\min}}) \\ & - \mu^T_{I_{hk\,\max}}(I_{\max} - I_{hk} - s_{I_{hk\,\max}})\end{aligned} \tag{4.34}$$

$$
\begin{aligned}
&- \mu^T_{I_{kh\,\max}}(I_{\max} - I_{kh} - s_{I_{kh\,\max}}) \\
&- \mu^T_{P_{hk\,\max}}(I_{\max} - |P_{hk}| - s_{P_{hk\,\max}}) \\
&- \mu^T_{P_{kh\,\max}}(I_{\max} - |P_{kh}| - s_{P_{kh\,\max}}) \\
&- \mu^T_{Q_{G\,\max}}(Q_{G_{\max}} - Q_G - s_{Q_{G\,\max}}) \\
&- \mu^T_{Q_{G\,\min}}(Q_G - Q_{G\,\min} - s_{Q_{G\,\max}}) \\
&- \mu^T_{V_{\max}}(V_{\max} - V - s_{V_{\max}}) \\
&- \mu^T_{V_{\min}}(V - V_{\min} - s_{V_{\min}}) \\
&- \mu_s(\sum_i \ln s_i)
\end{aligned}
$$

Then, applying (4.29), one has:

$$
\begin{aligned}
\partial\mathcal{L}/\partial P_{S_i} = 0 &= C_{S_i} - \rho_{P_{S_i}} + \mu_{P_{S_{\max_i}}} - \mu_{P_{S_{\min_i}}} \\
\partial\mathcal{L}/\partial P_{D_i} = 0 &= -C_{D_i} + \rho_{P_{D_i}} + \rho_{Q_{D_i}} \tan(\phi_{D_i}) + \mu_{P_{D_{\max_i}}} - \mu_{P_{D_{\min_i}}}
\end{aligned}
\tag{4.35}
$$

Thus, the LMPs can be defined as

$$
\begin{aligned}
\mathrm{LMP}_{S_i} &= \rho_{P_{S_i}} = C_{S_i} + \mu_{P_{S_{\max_i}}} - \mu_{P_{S_{\min_i}}} \\
\mathrm{LMP}_{D_i} &= \rho_{P_{D_i}} = C_{D_i} + \mu_{P_{D_{\min_i}}} - \mu_{P_{D_{\max_i}}} - \rho_{Q_{D_i}} \tan(\phi_{D_i})
\end{aligned}
\tag{4.36}
$$

Table 4.1 depicts the LMPs and power bids of all market participants for the six-bus system example obtained using the standard security constrained OPF (4.10). As it can be noticed, each bus is characterized by a different price, i.e. market participants pay for their consumptions or get paid for their productions according to bids as well as congestions they cause in the network. Furthermore, comparing LMPs in Table 4.1 with MCPs depicted in Fig. 4.2 allows concluding that system congestions do significantly affect market bids and associated costs, hence the need of a precise model for taking in account security constraints.

Table 4.1: LMPs, NCPs and bids for the standard security constrained OPF.

Participant	LMP [$/MWh]	NCP [$/MWh]	P_{BID} [MW]
GENCO 1	9.70	1.33	14.4
GENCO 2	8.80	0.00	2.4
GENCO 3	8.28	-0.04	20.0
ESCO 1	11.64	3.32	15.6
ESCO 2	10.83	1.57	0.0
ESCO 3	9.13	0.40	20.0

4.7.3 Nodal Congestion Prices (NCPs)

Using the decomposition formula for Locational Marginal Prices which has been proposed in [33], [32], one can define a vector of active and reactive Nodal Congestion Prices (NCPs) as follows:

$$\text{NCP} = \left(\frac{\partial f^T}{\partial x}\right)^{-1} \frac{\partial H^T}{\partial x}(\mu_{\max} - \mu_{\min}) \tag{4.37}$$

where $x = (\theta, V)$ are voltage phases and magnitudes, H represents the inequality constraint functions (e.g. transmission line powers and currents), and $\mu_{\max}$ and $\mu_{\min}$ are the dual variables or shadow prices associated to inequality constraints. Equation (4.37) for the standard security constrained OPF (4.10) becomes:

$$\begin{aligned} \text{NCP} &= [D_x f]^{-1} \left[\frac{\partial I_{hk}}{\partial x}(\mu_{I_{hk\,\max}} - \mu_{I_{hk\,\min}}) \right. \\ &\quad \left. + \frac{\partial P_{hk}}{\partial x}(\mu_{P_{hk\,\max}} - \mu_{P_{hk\,\min}}) + \begin{bmatrix} 0 \\ \mu_{V_{\max}} - \mu_{V_{\min}} \end{bmatrix} \right] \end{aligned} \tag{4.38}$$

which for each real power injection h, can be conveniently rewritten as follows:

$$\begin{aligned} \mathrm{NCP}_h &= \sum_{k=1}^{l_k} (\mu_{I_{hk\,\max}} - \mu_{I_{hk\,\min}}) \frac{\partial I_{hk}}{\partial P_h} \\ &+ \sum_{k=1}^{l_k} (\mu_{P_{hk\,\max}} - \mu_{P_{hk\,\min}}) \frac{\partial P_{hk}}{\partial P_h} \end{aligned} \tag{4.39}$$

where l_k is the number of lines departing from bus h. Observe that in (4.38) dual variables or shadow prices $\mu_{P_{hk\,\max}}$ and $\mu_{P_{hk\,\min}}$ directly affect NCPs, which is the main drawback of transmission congestion limits $P_{hk\,\max}$ computed off-line, as demonstrated in Chapter 6. For the sake of completeness, Table 4.1 depicts also NCPs for the six-bus system example obtained using the standard security constrained OPF (4.10). Observe that high NCP values correspond to high LMP values, as expected, since LMPs increase when local congestion increases.

4.8 Summary

This chapter has presented OPF-based models for single and multi-period electricity market clearing mechanisms and for the maximization of the distance to voltage collapse. Analysis techniques to solve optimization problems have also been discussed along with decomposition formulae which allow pricing electricity (LMPs) and security (NCPs). With regard to electricity pricing, the six-bus test system example is used to illustrate the discussed techniques. Models and techniques presented here are the basis for voltage security constrained OPF models proposed in this thesis.

Chapter 5

Software Tools

5.1 Introduction

THIS chapter describes software tools used to obtain simulations presented and discussed in this thesis. Power flow, continuation power flow and IPM-based optimal power flow techniques were computed using a MATLAB-based Power System Analysis Toolbox (PSAT) [69], entirely written by the candidate, whereas relaxed mixed-integer nonlinear programming optimization techniques have been solved using GAMS [70] and linked to MATLAB by means of a PSAT-GAMS interface. The latter is based on an existing MATLAB-GAMS interface [71] which has been improved and adapted to the PSAT environment.

The chapter is organized as follows: Section 5.2 describes briefly some PSAT features, namely input and output of data, SIMULINK library for network design, supported models, data format conversion and user defined models. Sections 5.3 and 5.4 present the features of GAMS and the bridge to PSAT. Finally, Section 5.5 illustrates PSAT usage and compares PSAT and PSAT-GAMS optimization solvers through a three-bus test system example.

5.2 Matlab-based Power System Analysis Toolbox (PSAT)

PSAT is a MATLAB toolbox for electric power system analysis and control. It includes power flow, continuation power flow, optimal power flow, small signal stability analysis and time domain integration. All operations can be assessed by means of graphical user interfaces (GUIs) and a SIMULINK-based library provides an user friendly tool for network design.

This chapter provides a very brief description of PSAT, while the complete documentation of the program is available at [69]. The structure of the toolbox and outlines of its main features follow.

PSAT can be downloaded at:

`http://thunderbox.uwaterloo.ca/~fmilano`

or following the link available at:

`http://www.power.uwaterloo.ca`

The link and the web page are kindly provided by Prof. Claudio A. Cañizares, Professor and Deputy Chair at the Electrical & Computer Engineering Department of the University of Waterloo, ON, Canada.

PSAT has been developed using mainly MATLAB version 6.1.0.450 (R12.1) on a Unix workstation (Sun Ultra Enterprise 450) and has also been tested on Linux, Irix64 and Windows (NT, 2000, XP) platforms.

5.2.1 Launch PSAT

After setting the PSAT folder in the MATLAB path, the program can be launched by typing at the MATLAB prompt:

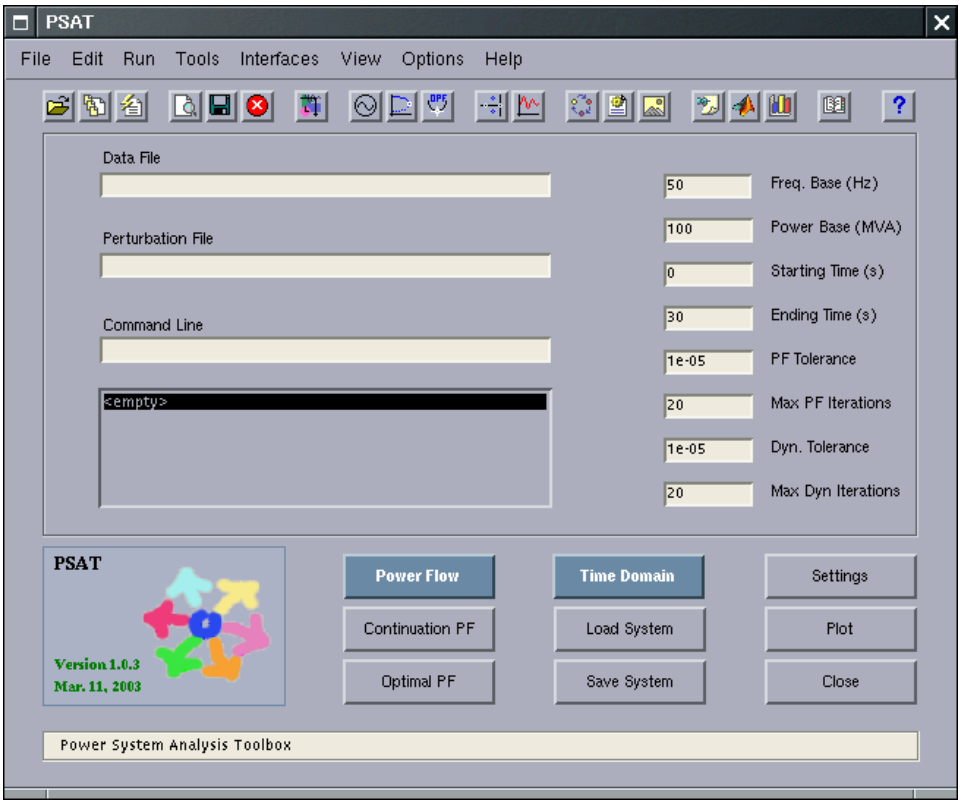

Figure 5.1: Main graphical user interface of PSAT.

```
>> psat
```

This will create all global structures and variables required by the toolbox and will open the main user interface window which is depicted in Fig. 5.1. All modules and procedures can be launched from this window by means of menus, push buttons and/or short cuts. Figure 5.2 depicts the structure of PSAT.

5.2.2 Input Data

Almost all operations require that a data file is loaded. The name of this file is always displayed in the edit text *Data File* of the main window. Data files can be either a *.m* file in PSAT format or a SIMULINK model created with the PSAT

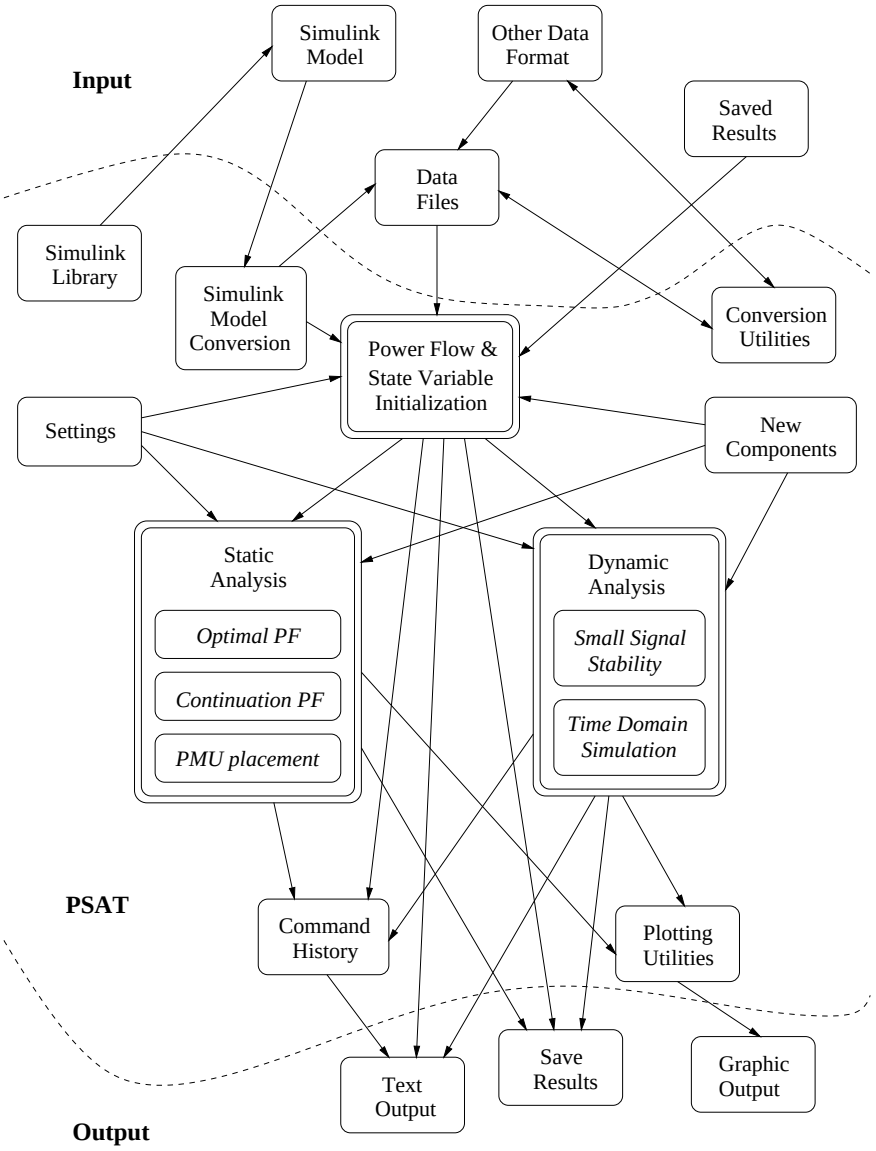

Figure 5.2: Synoptic scheme of the program.

library.

Input data are stored in an internal format, which can handle a variety of static and dynamic component models, as follows:

◇ *Power Flow Data*: Bus bars, transmission lines and transformers, slack buses, PV generators, constant power loads and shunt admittances.

◇ *CPF and OPF Data*: Power supply bids and limits, generator power reserves, generator ramping data, power demand bids and limits.

◇ *Switching Operations*: Transmission line faults and transmission line breakers.

◇ *Loads*: Voltage dependent loads, frequency dependent loads, ZIP (polynomial) loads, linear recovery loads [72] and thermostatically controlled loads [73].

◇ *Machines*: Synchronous machines (dynamic order from 2 to 8) and induction motors (dynamic order from 1 to 5).

◇ *Controls*: Turbine Governors, Automatic Voltage Regulators, Power System Stabilizer, Over-excitation limiters, Secondary Voltage Regulation (Central Area Controllers and Cluster Controllers).

◇ *Under Load Tap Changers*: Load tap changer with voltage or reactive power regulators.

◇ *FACTS*: Static Var Compensators, Thyristor Controlled Series Capacitors, Static Synchronous Source Series Compensators, Unified Power Flow Controllers and High Voltage DC transmission systems.

◇ *Other Models*: Synchronous machine dynamic shaft, dynamic phasor RLC series circuit, sub-synchronous resonance model, Solid Oxide Fuel Cell and sub-transmission area equivalents.

Once a data file is loaded, one can run the power flow routine, which will update all data structures and set up the "base case" solution. Thus, after solving the first power flow, the program is ready for further studies, such as continuation power flow, optimal power flow, PMU placement, small signal stability analysis, and time domain simulation.

5.2.3 Output Data

Results can be generally displayed in more than one way, either by means of a graphical user interface in MATLAB or as a plain text file. Results requiring a graphical output, such as continuation power flow results, multi-objective power flow computations or time domain simulations, can be depicted and saved in *.eps* files with the plotting utilities.

Some computations and several user actions result also in messages stored in the `History` structure. These messages/results are displayed one at the time in the static text banner at the bottom of the main window.

At any time, results contained in global structures can be stored in a output file and, to ensure portability across different computers, also the data file is saved. Furthermore, all static computations allow to create a report in a text file that can be opened and used later. All results presented in these thesis where obtained using text and graphical output produced by PSAT.

5.2.4 Settings

The main settings of the system are directly included in the main window an they can be modified at any time. These settings are frequency and power bases, initial and final simulation times, static and dynamic tolerance and maximum number of iterations. Other general settings, such as the fixed time step used for time domain simulations or the setting to force the conversion of PQ loads into

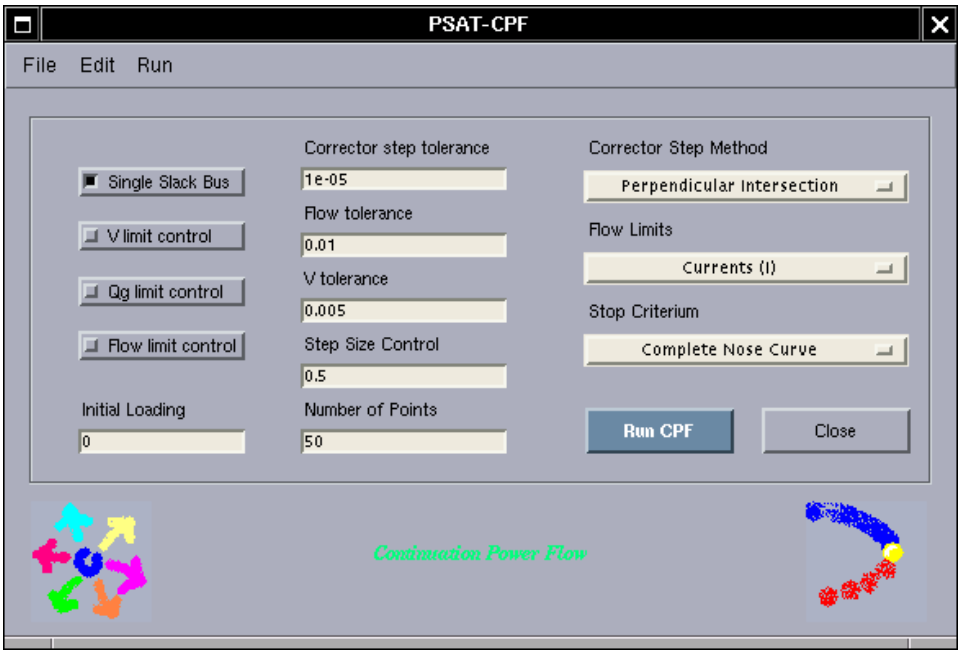

Figure 5.3: PSAT GUI for continuation power flow analysis.

constant impedances after power flow computations, can be modified in specific windows.

Computations requiring additional settings have their own structures and GUIs for modifying and customizing structure fields. For instance, continuation power flow and optimal power flow settings are stored in the structures `CPF` and `OPF` respectively, which can be inspected and set up by means of the GUIs depicted in Figs. 5.3 and 5.4.

5.2.5 Network Design

The SIMULINK environment and its graphical CAD features are used in PSAT to create and design power networks, visualize system topology and easily input and change data, without the need of directly dealing with formatted text data files. For instance, Figure 5.5 depicts a selection of PSAT-SIMULINK library windows.

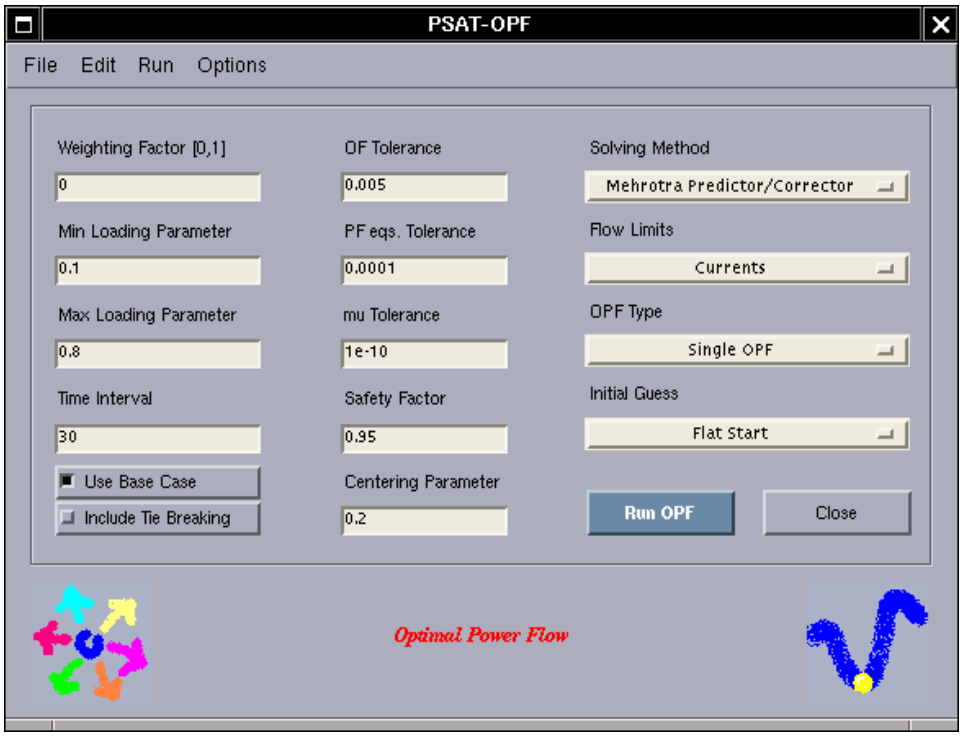

Figure 5.4: PSAT GUI for optimal power flow analysis.

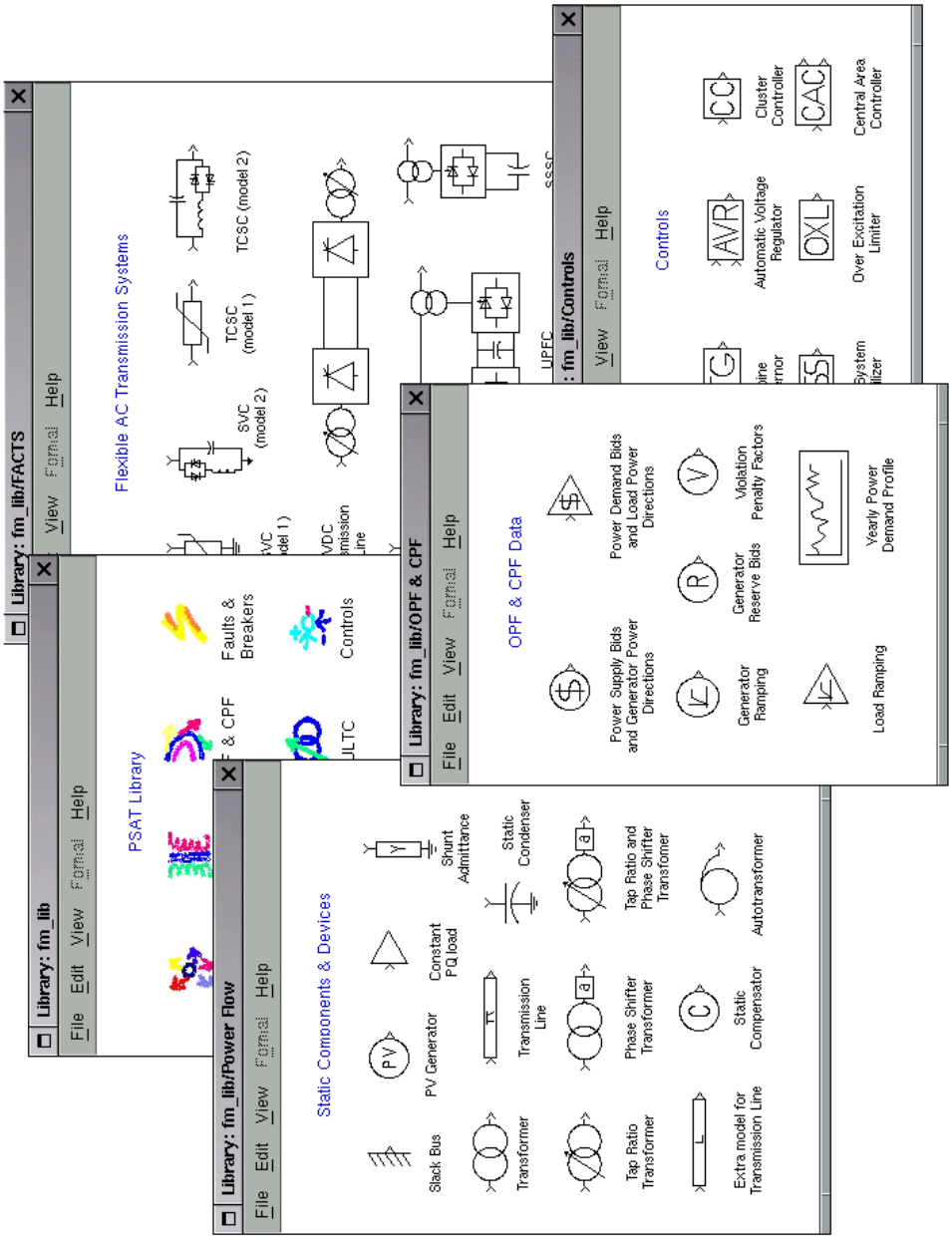

Figure 5.5: PSAT-Simulink library windows.

5.2.6 Data Format Conversion

The data format conversion routines allow importing data written for other power system softwares, namely IEEE Common Data Format, EPRI WSCC, MATPOWER, PST and VST. However, in some cases, the conversion cannot be exact since data formats may have different features than the ones implemented in PSAT. Finally, PSAT static data files can be converted in the IEEE Common Data Format.

5.2.7 User Defined Models

User defined model routines provide a simple way for extending the capabilities of PSAT and, hopefully, facilitating contributions. The construction of a user defined model can be yielded in few steps, as follows:

1. Define parameters and differential-algebraic equations by means of a GUI;
2. Create the MATLAB function of the model;
3. Save the model in a "model" file, which allows model portability and exchange;
4. Install the model in the program, by means of an automatic procedure.

If the component is not needed any longer it can also be "uninstalled" with an automatic procedure as well. Thus, user defined models can be shared easily by simply providing the component function and the component structure stored in a "model" file. However, the routine which compiles model functions is not complete so far, and it is intended only for creating a first draft of the component function.

Table 5.1: MATLAB-based packages for power system analysis

Toolbox	PF	CPF-VS	OPF	SSSA	TDS	GUI	CAD
Matpower	✓		✓				
PSAT	✓	✓	✓	✓	✓	✓	✓
PSB	✓			✓	✓	✓	✓
PST	✓	✓		✓	✓		
VST	✓	✓		✓	✓	✓	

5.2.8 Comparison with Other Matlab Toolboxes

Table 5.1 depicts a rough comparison of the currently available MATLAB-based packages for power electric system analysis. These are MATPOWER [74], Power System Blockset (PSB) toolbox,[1] Power System Toolbox (PST) [75, 76] and Voltage Stability Toolbox (VST) [77, 78]. The features illustrated in the table are standard power flow (PF), continuation power flow and/or voltage stability analysis (CPF-VS), optimal power flow (OPF), small signal stability analysis (SSSA) and time domain simulation (TDS) along with some "aesthetic" features such as graphical user interface (GUI) and graphical network construction (CAD).

5.3 GAMS

The General Algebraic Modeling System (GAMS) is a high-level modeling system for mathematical programming problems. It consists of a language compiler and a variety of integrated high-performance solvers. GAMS is specifically designed for large and complex scale problems, and allows creating and maintaining models for a wide variety of applications and disciplines [70].

[1] See `http://www.matpower.html`

GAMS is able to formulate models in many different types of problem classes, such as linear programming (LP), nonlinear programming (NLP), mixed-integer linear programming (MILP) and (relaxed) mixed-integer nonlinear programming (MINLP).

Single-period VSC-OPF models described in the current thesis are basically a set of non-linear equations, and the inclusion of the "critical" set of power flow equations leads to the need of retaining a detailed model of transmission line losses. This forces the use of NLP solvers (e.g. CONOPT [79]) whose performances and results have been compared, when possible, to the ones obtained by means of the IPM implemented in PSAT. Furthermore, the solution of multi-period VSC-OPF needs a MINLP solver (e.g. DICOPT [66]), which basically works combining "relaxed" NLP with MIP master problem solutions. In large scale MINLP problems, the maximum number of integer iterations turns out to be the only possible stopping criterion. However, from the analysis of several multi-period VSC-OPF test cases, a maximum limit of 50000 integer iterations always led to reasonable results.

5.4 PSAT-GAMS Interface

A bridge between GAMS and MATLAB would allow using a sophisticated nonlinear optimization tools with the visualization capabilities provided by MATLAB. The existing GAMS-MATLAB interface [71] has been improved in collaboration with the master author M. C. Ferris, from University of Wisconsin-Madison. Main contributions are as follows:

1. Improvement of the portability of the interface function (`gams.m`) which can substitute the original *mex*-files and be platform independent. A few minor bugs of the master release were also fixed.

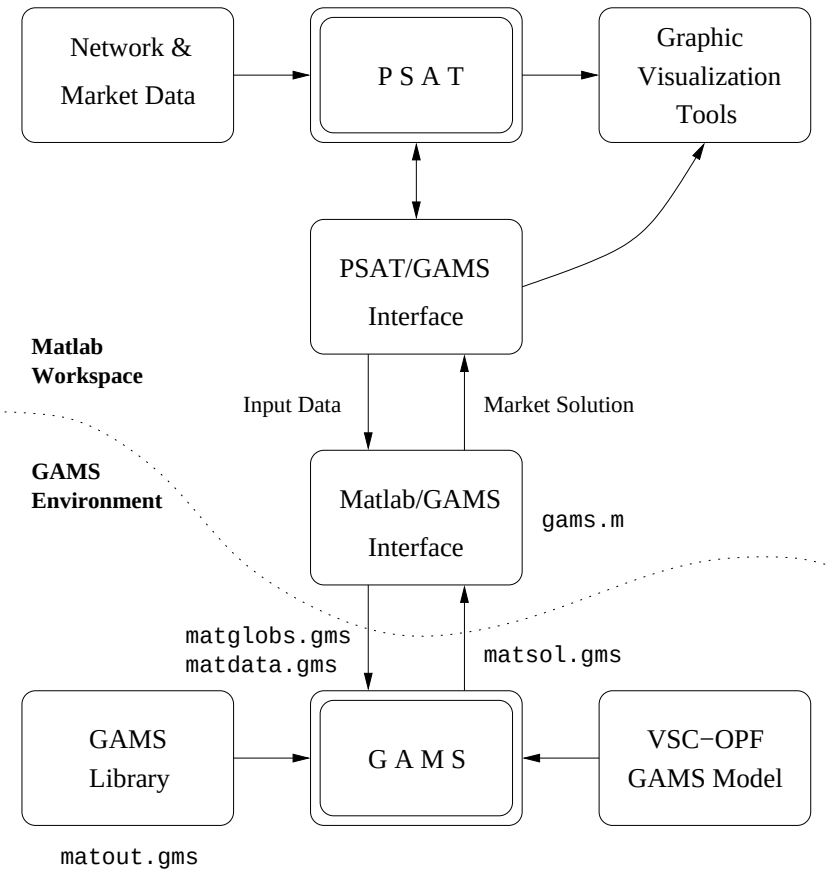

Figure 5.6: Structure of the PSAT-GAMS interface.

2. Enhancement of the features of the GAMS library (`matout.gms`) in order to support tables of any dimension.

The GAMS-MATLAB interface has been used to create a link between PSAT and GAMS, whose scheme is depicted in Figure 5.6. The resulting software is a rather innovative tool able to set up large scale power system test cases, solve complex OPF problems and finally visualize results by means of an user-friendly GUI. Figure 5.7 depicts the PSAT-GAMS interface main window.

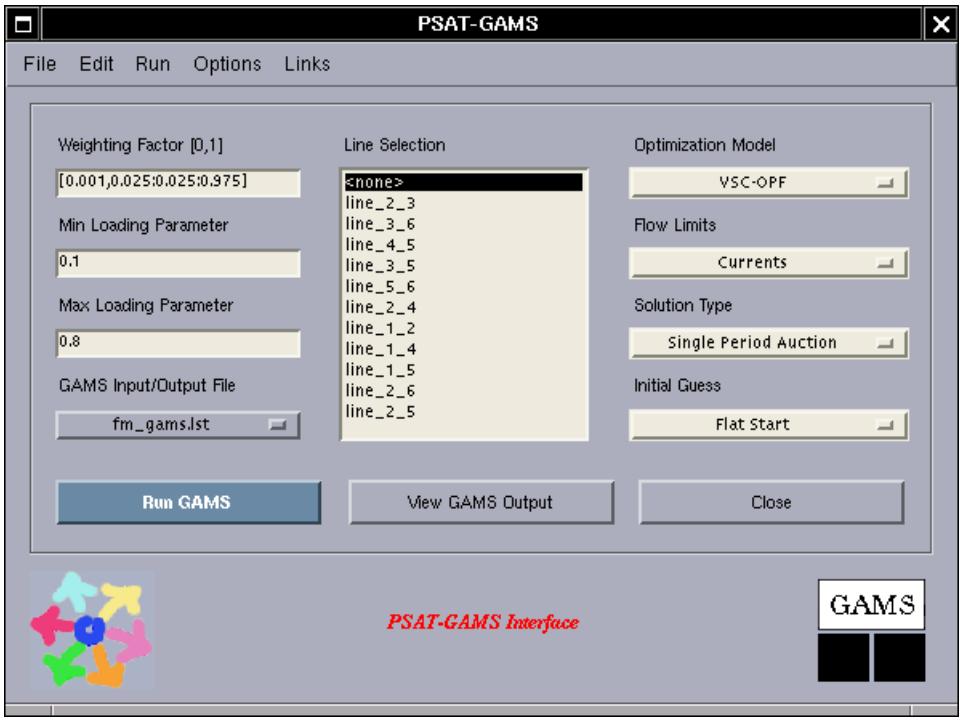

Figure 5.7: GUI of the PSAT-GAMS interface.

5.5 Example

In this section one simple example will be used to illustrate how PSAT and the PSAT-GAMS interface work. At this aim, let us consider the three-bus test system described in Section 2.3.

Firstly the user has to set up data in the PSAT format. This can be done by writing a MATLAB script file or, better, using the PSAT-SIMULINK library. Figure 5.8 depicts the resulting SIMULINK model which represent the three-bus test system. Each block of the diagram hides a mask where the user can set up data associated with the correspondent component. For instance, Fig. 5.9 depicts the mask for the `Supply` data of the generator company connected at bus 1.

Once the model is completed, it has to be loaded in the MATLAB workspace. To load a file simply double click on this edit text, or use the first button of the tool bar, the menu *File/Open/Data File* or the short cut <Ctrl-d> when the main window is active. The name of this file is always displayed in the edit text *Data File* of the main window.

Now, it is possible to solve the power flow, which can be launched by clicking on the "Power Flow" button in the main window. Power flow results can be visualized for a first inspection in the Static Report GUI (which can be launched by <Ctrl-v> from the main window) and saved in a report file, as illustrated in Table 5.2.

After solving the base case power flow, PSAT is ready for further analysis. Observe that all variables, data and results are stored as global structures in the MATLAB workspace so that they are available for other routines and can be inspected at any time by the user.

For the sake of comparison, Tables 5.3 and 5.4 depict the solution of the OPF problem obtained with the IPM MATLAB routine and the PSAT-GAMS interface respectively.

Table 5.2: PSAT power flow report for the three-bus test system.

```
POWER FLOW REPORT

                  File:  ~/psat/tests/d_003.mdl

                  Date:  06-Apr-2003 18:41:57

                  Number of Iterations:  3
--------------------------------------------------------------------------------------------


SYSTEM PROPERTIES
--------------------------------------------------------------------------------------------

Bus:          3
Lines:        3
Generators:   3
Loads:        3
--------------------------------------------------------------------------------------------


POWER FLOW RESULTS
--------------------------------------------------------------------------------------------

              Voltages                    Power Generations           Power Absorptions
              -------------------------   -------------------------   ----------------------

Bus           V (p.u.)      phase (rad)   P (p.u.)      Q (p.u.)      P (p.u.)      Q (p.u.)

Bus1          1.02           0            1.5022         1.1432       1.5           0.8
Bus2          1             -0.01846      1             -0.21688      1.5           0.7
Bus3          1              0.02156      1             -0.39969      0.5           0.3


LINE FLOWS
--------------------------------------------------------------------------------------------

Line    From Bus        To Bus           P Flow        Q Flow        P Loss        Q Loss

1       Bus1            Bus3            -0.16776       0.18596       0.0006        0.49277
2       Bus1            Bus2             0.16998       0.15728       0.00052       0.79381
3       Bus2            Bus3            -0.33054      -0.76578       0.0011        1.2868


Line    From Bus        To Bus           P Flow        Q Flow        P Loss        Q Loss

1       Bus3            Bus1             0.16836      -0.67872       0.0006        0.49277
2       Bus2            Bus1            -0.16946      -0.9511        0.00052       0.79381
3       Bus3            Bus2             0.33164      -0.52097       0.0011        1.2868


--------------------------------------------------------------------------------------------

TOTAL REAL POWER LOSSES:         0.00222
TOTAL REACTIVE POWER LOSSES:     2.5733
```

Table 5.3: PSAT IPM-based OPF report for the three-bus test system.

```
Interior Point Method for OPF Computation
Spot Price of Security (including loading parameter)
Social Benefit Objective Function
Data file "~/psat/tests/d_003(mdl)"
Iter. =  1     mu =  0.00204     |dy| =  777.946     |F(y)| =  0.5         |dG(y)| =  0.2379
Iter. =  2     mu =  0.00219     |dy| =  690.6972    |F(y)| =  0.4998      |dG(y)| =  0.24974
Iter. =  3     mu =  0.00736     |dy| =  196.56      |F(y)| =  0.49944     |dG(y)| =  2.2465
Iter. =  4     mu =  0.03368     |dy| =  29.0175     |F(y)| =  0.4987      |dG(y)| =  0.74374
Iter. =  5     mu =  0.04217     |dy| =  4.8342      |F(y)| =  0.49768     |dG(y)| =  3.3855
Iter. =  6     mu =  0.04181     |dy| =  13.4591     |F(y)| =  0.14664     |dG(y)| =  0.77633
Iter. =  7     mu =  0.02654     |dy| =  2.6056      |F(y)| =  0.12414     |dG(y)| =  0.57051
Iter. =  8     mu =  0.03359     |dy| =  1.4792      |F(y)| =  0.14788     |dG(y)| =  0.34142
Iter. =  9     mu =  0.01346     |dy| =  1.1384      |F(y)| =  0.00953     |dG(y)| =  0.34836
Iter. =  10    mu =  0.00086     |dy| =  0.18377     |F(y)| =  0.01131     |dG(y)| =  0.03732
Iter. =  11    mu =  9e-005      |dy| =  0.0301      |F(y)| =  0.00488     |dG(y)| =  0.0031
Iter. =  12    mu =  0           |dy| =  0.02388     |F(y)| =  0.00071     |dG(y)| =  0.00056
Iter. =  13    mu =  0           |dy| =  0.00374     |F(y)| =  4e-005      |dG(y)| =  2e-005
Iter. =  14    mu =  0           |dy| =  0.00021     |F(y)| =  0           |dG(y)| =  0
Iter. =  15    mu =  0           |dy| =  1e-005      |F(y)| =  0           |dG(y)| =  0

 Bus           Qg            Qg max        Qg min
 <i>           [MVar]        [MVar]        [MVar]
 1.0000        79.7251       150.0000      -150.0000
 2.0000        4.0671        150.0000      -150.0000
 3.0000        34.5459       150.0000      -150.0000

 Power Supplies
 Bus           Ps            Ps max        Ps min        Cs
 <i>           [MW]          [MW]          [MW]          [$/h]
 1.0000        150.0000      150.0000      0.0000        25.0000
 3.0000        0.0000        100.0000      0.0000        32.0000
 2.0000        0.0000        100.0000      0.0000        33.0000

 Power Demands
 Bus           Pd            Pd max        Pd min        Cd
 <i>           [MW]          [MW]          [MW]          [$/h]
 3.0000        100.0000      100.0000      0.0000        35.0000
 2.0000        49.2559       100.0000      0.0000        30.0000

 Bus       V         theta      P          Q          LMP       NCP       Pay
 <i>       [p.u.]    [rad]      [MW]       [MW]       [$/MWh]   [$/MWh]   [$/h]
 1.0000    1.1000    0.0000     150.2223   -0.2749    29.5868   0.0000    -4444.5898
 2.0000    1.0959    -0.0831    -99.2559   -88.9190   30.0000   0.0292    2977.6758
 3.0000    1.0970    -0.0666    -50.0000   -55.4542   29.9176   0.0231    1495.8778

 From Bus  To Bus    Iij        Iijmax     Iij margin  Iji       Ijimax    Iji margin
 <i>       <j>       [p.u.]     [p.u.]      [p.u.]     [p.u.]    [p.u.]    [p.u.]
 1.0000    3.0000    0.6078     999.0000   998.3922    0.6078    999.0000  998.3922
 1.0000    2.0000    0.7579     999.0000   998.2421    0.7579    999.0000  998.2421
 2.0000    3.0000    0.1503     999.0000   998.8497    0.1503    999.0000  998.8497

Losses = 0.744
Total demand = 149.2559
TTL =  499.255
ISO Pay =  28.9638
Interior Point Method for OPF computation successfully completed in 1.001 s
```

Table 5.4: PSAT-GAMS OPF report for the three-bus test system.

```
----------------------------------------------------------------
 PSAT-GAMS Interface
----------------------------------------------------------------

 Standard OPF
 Single-Period Auction

 Power Supplies
  Bus            Ps             Ps max         Ps min
 <i>            [MW]           [MW]           [MW]
 1.0000         150.0000       150.0000       0.0000
 3.0000         0.0000         100.0000       0.0000
 2.0000         0.0000         100.0000       0.0000

 Power Demands
 Bus            Pd             Pd max         Pd min
 <i>            [MW]           [MW]           [MW]
 3.0000         100.0000       100.0000       0.0000
 2.0000         49.2559        100.0000       0.0000

 Generator Reactive Powers
 Bus            Qg             Qg max         Qg min
 <i>            [MVar]         [MVar]         [MVar]
 1.0000         79.7251        150.0000       -150.0000
 2.0000         4.0672         150.0000       -150.0000
 3.0000         34.5459        150.0000       -150.0000

 Power Flow Solution
 Bus          V            theta        PG             PL           QG           QL
 <i>          [p.u.]       [rad]        [MW]           [MW]         [MVar]       [MVar]
 1.0000       1.1000       0.0000       300.2223       150.0000     79.7251      80.0000
 2.0000       1.0959       -0.0831      100.0000       199.2559     4.0672       92.9861
 3.0000       1.0970       -0.0666      100.0000       150.0000     34.5459      90.0000

 Prices and Pays
  Bus            LMP            NCP            Pay S          Pay D
 <i>            [$/MWh]        [$/MWh]        [$/h]          [$/h]
 1.0000         29.5868        0.0000         -8882.6037     4438.0139
 2.0000         30.0000        0.0292         -3000.0000     5977.6770
 3.0000         29.9176        0.0231         -2991.7556     4487.6335

 Flows on Transmission Lines
 From Bus   To Bus     Iij       Iijmax       Iij margin     Iji       Ijimax       Iji margin
 <i>        <j>        [p.u.]    [p.u.]       [p.u.]         [p.u.]    [p.u.]       [p.u.]
 1.0000     3.0000     0.6078    999.0000     998.3922       0.6078    999.0000     998.3922
 1.0000     2.0000     0.7579    999.0000     998.2421       0.7579    999.0000     998.2421
 2.0000     3.0000     0.1503    999.0000     998.8497       0.1503    999.0000     998.8497

 Totals
 ---------------------------------------------------------------
 Total Losses = 0.966 [MW]
 Bid Losses = 0.744 [MW]
 Total demand = 149.2559 [MW]
 Total Transaction Level =  499.255 [MW]
 ISO Pay = 28.9638 [$/h]

 ---------------------------------------------------------------
 Check file C:\Documents and Settings\fmilano\psat\fm_gams.lst for GAMS report.
 PSAT-GAMS Optimization Routine completed in 1.292 s
```

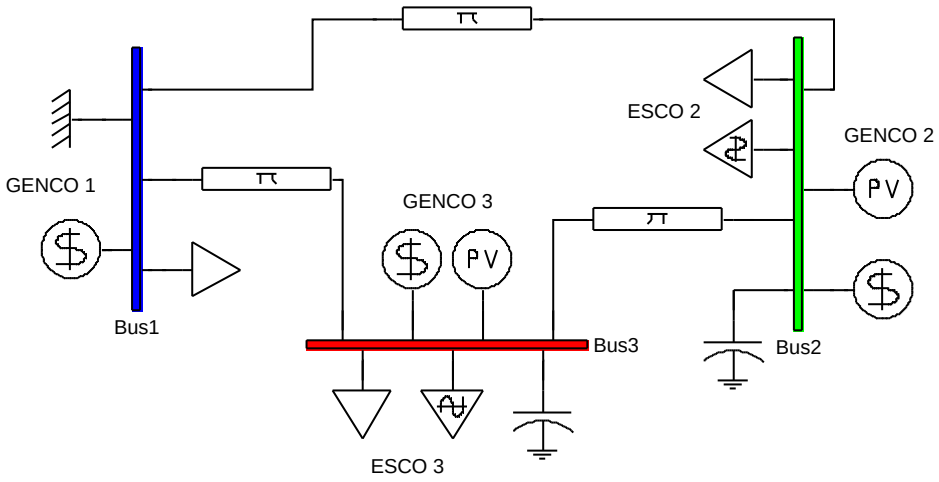

Figure 5.8: PSAT-Simulink model of the three-bus example.

5.6 Summary

This chapter has described the software tools used to run simulations and plot results presented in this thesis, i.e. a home-made MATLAB-based Power System Analysis Toolbox (PSAT), GAMS and the PSAT-GAMS interface, used to double check results obtained by the MATLAB-based IPM and to gain the ability of running MINLP problems.

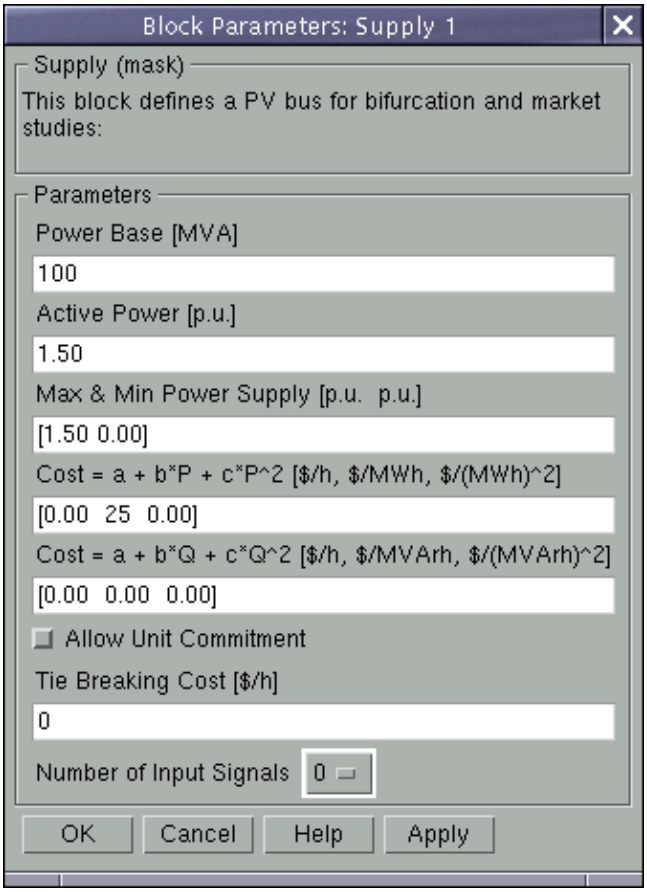

Figure 5.9: Mask of the supply data for the GENCO at bus 1.

Chapter 6

Voltage Stability Constrained OPF

6.1 Introduction

THIS chapter describes a novel technique for representing system security in the operations of decentralized electricity markets, with special emphasis on voltage stability. The Interior Point and GRG methods are used to solve the Optimal Power Flow problem with a multi-objective function for maximizing both social benefit and the distance to maximum loading conditions. The six-bus system with both supply and demand-side bidding is used to illustrate the proposed technique for both elastic and inelastic demand, whereas a 129-bus test system that models the Italian HV transmission network is used for testing the practical reliability of the proposed method. The results obtained show that the proposed technique is able to improve system security while yielding better market conditions through increased transaction levels and improved locational marginal prices throughout the system.

6.2 Multi-Objective VSC-OPF

The following optimization problem is proposed to represent an OPF market model, based on what has been proposed in [9, 24, 25], so that system security is modeled through the use of voltage stability conditions:

$$
\begin{aligned}
\text{Min.} \quad & G = -\omega_1(C_D^T P_D - C_S^T P_S) - \omega_2 \lambda_c && (6.1)\\
\text{s.t.} \quad & f(\delta, V, Q_G, P_S, P_D) = 0 && \rightarrow \text{PF equations}\\
& f(\delta_c, V_c, Q_{G_c}, \lambda_c, P_S, P_D) = 0 && \rightarrow \text{Max load PF eqs.}\\
& \lambda_{c_{\min}} \leq \lambda_c \leq \lambda_{c_{\max}} && \rightarrow \text{loading margin}\\
& 0 \leq P_S \leq P_{S_{\max}} && \rightarrow \text{Sup. bid blocks}\\
& 0 \leq P_D \leq P_{D_{\max}} && \rightarrow \text{Dem. bid blocks}\\
& I_{hk}(\delta, V) \leq I_{hk_{\max}} && \rightarrow \text{Thermal limits}\\
& I_{kh}(\delta, V) \leq I_{kh_{\max}}\\
& I_{hk}(\delta_c, V_c) \leq I_{hk_{\max}}\\
& I_{kh}(\delta_c, V_c) \leq I_{kh_{\max}}\\
& Q_{G_{\min}} \leq Q_G \leq Q_{G_{\max}} && \rightarrow \text{Gen. } Q \text{ limits}\\
& Q_{G_{\min}} \leq Q_{G_c} \leq Q_{G_{\max}}\\
& V_{\min} \leq V \leq V_{\max} && \rightarrow V \text{ ``security'' lim.}\\
& V_{\min} \leq V_c \leq V_{\max}
\end{aligned}
$$

A second set of power flow equations and constraints with a subscript c is introduced to represent the system at the limit or "critical" conditions associated with the maximum loading margin λ_c in p.u., where λ is the parameter that drives the system to its maximum loading condition. The maximum or critical loading point could be either associated with a thermal or bus voltage limit or a voltage stability limit (collapse point) corresponding to a system singularity (saddle-node bifurca-

tion) or system controller limits like generator reactive power limits (limit-induced bifurcation) [50, 23].

In the multi-objective function G, two terms are present, with their influence on the final solution being determined by the value of the weighting factors ω_1 and ω_2 ($\omega_1 > 0$, $\omega_2 > 0$). The first term represents the social benefit, whereas the second term guarantees that the "distance" between the market solution and the critical point is maximized [24]. Observe that $\omega_1 > 0$, since for $\omega_1 = 0$ there would be no representation of the market in the proposed OPF formulation, rendering it useless. Furthermore, $\omega_2 > 0$, otherwise λ_c will not necessarily correspond to a maximum loading condition of the system. Notice that the two terms of the objective function are expressed in different units, since the social benefit would be typically in \$/h, whereas the "security" term would be in p.u., which will basically affect the chosen values of ω_1 and ω_2 (typically, $\omega_1 \gg \omega_2$). However, it is possible to assume that $\omega_1 = (1 - \omega)$ and $\omega_2 = \omega$, with proper scaled values of ω for each system under study ($0 < \omega < 1$), as this simplifies the optimization problem without losing generality.

Boundaries for the loading margin λ_c have been included in (6.1) based on practical considerations. Thus, the minimum limit $\lambda_{c_{\min}}$ is introduced in order to ensure a minimum level of security in any operating condition and for any value of ω, where the maximum value $\lambda_{c_{\max}}$ imposes a maximum required security level. These conditions ensure that the loading parameter remains within certain limits to avoid solutions of (6.1) characterized by either low security levels ($\lambda_c < \lambda_{c_{\min}}$) or low supply and demand levels ($\lambda_c > \lambda_{c_{\max}}$), which would be unacceptable.

Equations (6.1) and (6.2) are for elastic demand. In the case of a pure inelastic demand, P_D is known, and this can be represented in these equations by setting $C_{D_i} = 0$ and $P_{D_i} = P_{D_{i\max}}$; hence the problem basically becomes the same as the one analyzed in [9]. In this case, one must be aware that the associated

OPF problem may have no solution, as the system may not be able to supply the required demand.

6.2.1 Power Directions

For the current and maximum loading conditions of (6.1), the generator and load powers are defined as follows:

$$\begin{aligned} P_G &= P_{G_0} + P_S \\ P_L &= P_{L_0} + P_D \\ P_{G_c} &= (1 + \lambda_c + k_{G_c}) P_G \\ P_{L_c} &= (1 + \lambda_c) P_L \end{aligned} \tag{6.2}$$

where P_{G_0} and P_{L_0} stand for generator and load powers which are not part of the market bidding (e.g. must-run generators, inelastic loads), and k_{G_c} represents a scalar variable used to distribute the system losses associated *only* with the solution of the critical power flow equations in proportion to the power injections obtained in the solution process, i.e. a standard distributed slack bus model is used. It is assumed that the losses corresponding to the maximum loading level defined by λ_c in (6.1) are distributed among all generators; other possible mechanisms to handle increased losses could be implemented, but they are beyond the main interest of the present thesis.

Observe that the loading parameter multiplies both base case powers and bids, as in (3.2). The reason for preferring (3.2) to (3.3) is twofold:

1. Using (3.3) would mean that load directions depend only on the participants to the auction. If the goal were to determine the impact of the auction on the security and to minimize that impact, this approach could be acceptable; however if the goal is to optimize the auction results to improve the system

security, it is more appropriate to determine λ_c considering an increase of load and generation that takes into account also the initial loading and generation pattern.

2. Model (3.3) can lead to numerical issues when power bids P_S and P_D have low values. To better understand this point, let us consider the case $\omega_2 \gg \omega_1$, which leads to mostly maximize the security (λ_c). In this case, the most secure solution is the closest to the base case condition, thus P_S and P_D are low; consequently λ_c gets high values. As $\omega_1 \to 0$, one has $P_S \to 0$, $P_D \to 0$ and, consequently, $\lambda_c \to \infty$, which is clearly a numerical unstable condition.

6.2.2 Maximum Loading Condition and Available Loading Capability

In the proposed OPF-based approach, λ_c represents the maximum loadability of the network and, hence, this value can be viewed as a measure of the congestion of the network. Observe that the maximum loading condition (MLC) and the available loading capability (ALC) can be obtained as a byproduct of the solution of (6.1), as defined in Section 3.4:

$$\begin{aligned} \text{MLC} &= (1+\lambda_c)\sum_{j\in\mathcal{J}} P_{L_j} \\ \text{ALC} &= \lambda_c \sum_{j\in\mathcal{J}} P_{L_j} = \lambda_c \text{TTL} \end{aligned} \tag{6.3}$$

For now, contingencies are not considered when computing λ_c, MLC and ALC. The following Chapter 7 will discuss this issue.

6.2.3 Locational Marginal Prices

The Lagrangian multipliers associated with (6.1) correspond to the standard definition of LMPs only when $\omega = 0$, i.e. for a pure market model. Lagrangian

multipliers for $\omega > 0$ would lead to unrealistic results, since they decrease almost linearly with respect to increases in ω. Hence, LMPs which are not dependent of ω are needed.

Consider the following vector objective function:

$$\overline{G} = \begin{bmatrix} -(C_D^T P_D - C_S^T P_S) \\ -\lambda_c \end{bmatrix} \tag{6.4}$$

From a fundamental theorem of multi-objective optimization [80], an optimal solution of (6.1) is also a Pareto optimal point for the minimization problem constituted by the objective function (6.4) plus the constraints defined in (6.1). Thus, an optimal solution point of (6.1) has the property of independently minimizing both terms of the objective function (6.4). Based on this premise, for a given value of the weighting factor, say ω^*, an IPM is first used to minimize the following Lagrangian function of (6.1):

$$\begin{aligned} \text{Min.} \quad \mathcal{L} = {} & G - \rho^T f(\delta, V, Q_G, P_S, P_D) \\ & - \rho_c^T f(\delta_c, V_c, Q_{G_c}, \lambda_c, P_S, P_D) \\ & - \mu_{\lambda_c \max}(\lambda_{c_{\max}} - \lambda_c - s_{\lambda_c \max}) \\ & - \mu_{\lambda_c \min}(\lambda_c - s_{\lambda_c \min}) \\ & - \mu_{P_S \max}^T(P_{S_{\max}} - P_S - s_{P_S \max}) \\ & - \mu_{P_S \min}^T(P_S - s_{P_S \min}) \\ & - \mu_{P_D \max}^T(P_{D_{\max}} - P_D - s_{P_D \max}) \\ & - \mu_{P_D \min}^T(P_D - s_{P_D \min}) \\ & - \mu_{I_{hk} \max}^T(I_{\max} - I_{hk} - s_{I_{hk} \max}) \\ & - \mu_{I_{kh} \max}^T(I_{\max} - I_{kh} - s_{I_{kh} \max}) \\ & - \mu_{I_{hkc} \max}^T(I_{\max} - I_{hkc} - s_{I_{hkc} \max}) \\ & - \mu_{I_{khc} \max}^T(I_{\max} - I_{khc} - s_{I_{khc} \max}) \end{aligned} \tag{6.5}$$

$$
\begin{aligned}
&- \mu^T_{Q_{G\max}}(Q_{G_{\max}} - Q_G - s_{Q_{G\max}}) \\
&- \mu^T_{Q_{G\min}}(Q_G - Q_{G\min} - s_{Q_{G\max}}) \\
&- \mu^T_{Q_{Gc\max}}(Q_{G_{\max}} - Q_{G_c} - s_{Q_{Gc\max}}) \\
&- \mu^T_{Q_{Gc\min}}(Q_{G_c} - Q_{G\min} - s_{Q_{Gc\max}}) \\
&- \mu^T_{V_{\max}}(V_{\max} - V - s_{V_{\max}}) \\
&- \mu^T_{V_{\min}}(V - V_{\min} - s_{V_{\min}}) \\
&- \mu^T_{V_{c\max}}(V_{\max} - V_c - s_{V_{c\max}}) \\
&- \mu^T_{V_{c\min}}(V_c - V_{\min} - s_{V_{c\min}}) - \mu^k(\sum_h^{2p} \ln s_h)
\end{aligned}
$$

where $\mu^k \in \mathbb{R}$, $\mu_s > 0$, is the barrier parameter, and ρ and $\rho_c \in \mathbb{R}^n$, and all the other μ ($\mu_h > 0$, $\forall h$) correspond to the Lagrangian multipliers. The s variables form the slack vector whose non-negativity condition ($s_h > 0$, $\forall h$) is ensured by including the logarithmic barrier terms $\sum_h^{2p} \ln s_h$, as described in Chapter 4. The solution of (6.5) provides the value of λ_c^* associated with ω^*, along with all other system variables and market bids.

For the following OPF:

$$\text{Min.} \quad \widehat{G} = -(C_D^T P_D - C_S^T P_S) \tag{6.6}$$

with the same constraints as in (6.1), and loading parameter fixed at $\lambda_c = \lambda_c^*$, the solution of (6.1) is also a solution of (6.6), i.e. the vector of voltage phases and magnitudes (θ, V, θ_c and V_c), generator reactive powers (Q_G and Q_{G_c}), power bids (P_S and P_D), the loss distribution factor (k_{G_c}) and the loading parameter (λ_c) are identical for both (6.1) and (6.6). Observe that the value of λ_c cannot be obtained by the mere solution of (6.6), as its value is basically defined by the value of ω in the multi-objective problem (6.1). As a result, the weighting factor ω, although it affects the solution and the dual variables of (6.6), it does not explicitly appear in the equations; thus, the Lagrangian multipliers of the power flow equations in

(6.6) can be associated with the system LMPs, and can be derived from applying the corresponding KKT optimality conditions as follows:

$$\begin{aligned}
\partial\widehat{\mathcal{L}}/\partial P_{S_i} &= C_{S_i} - \rho_{P_{S_i}} + \mu_{P_{S_{\max_i}}} - \mu_{P_{S_{\min_i}}} \\
&\quad - \rho_{cP_{S_i}}(1 + \lambda_c^* + k_{G_c}^*) = 0 \\
\partial\widehat{\mathcal{L}}/\partial P_{D_i} &= -C_{D_i} + \rho_{P_{D_i}} + \rho_{Q_{D_i}} \tan(\phi_{L_i}) \\
&\quad + \mu_{P_{D_{\max_i}}} - \mu_{P_{D_{\min_i}}} + \rho_{cP_{D_i}}(1 + \lambda_c^*) \\
&\quad + \rho_{cQ_{D_i}}(1 + \lambda_c^*) \tan(\phi_{L_i}) = 0
\end{aligned} \tag{6.7}$$

where $\widehat{\mathcal{L}}$ is the Lagrangian of (6.6) and ϕ_{D_i} represents a constant load power factor angle. Thus, the LMPs can be defined as

$$\begin{aligned}
\text{LMP}_{S_i} &= \rho_{P_{S_i}} = C_{S_i} + \mu_{P_{S_{\max_i}}} - \mu_{P_{S_{\min_i}}} \\
&\quad - \rho_{cP_{S_i}}(1 + \lambda_c^* + k_{G_c}^*) \\
\text{LMP}_{D_i} &= \rho_{P_{D_i}} = C_{D_i} + \mu_{P_{D_{\min_i}}} - \mu_{P_{D_{\max_i}}} \\
&\quad - \rho_{cP_{D_i}}(1 + \lambda_c^*) - \rho_{cQ_{D_i}}(1 + \lambda_c^*) \tan(\phi_{L_i}) \\
&\quad - \rho_{Q_{D_i}} \tan(\phi_{L_i})
\end{aligned} \tag{6.8}$$

From this definition, the LMPs are directly related to the costs C_S and C_D, and do not directly depend on the weighting factor ω. These LMPs have additional terms associated with λ_c^* which represent the added value of the proposed OPF technique. If a maximum value $\lambda_{c_{\max}}$ is imposed on the loading parameter, when the weighting factor ω reaches a value, say ω_0, at which $\lambda_c = \lambda_{c_{\max}}$, there is no need to solve other OPFs for $\omega > \omega_0$, since the security level cannot increase any further.

Observe that the computation of these LMPs is quite inexpensive, since the optimal point is already known from the solution of (6.1), thus the determination of the Lagrangian multipliers ρ is basically reduced to solving a set of linear equations.

6.2.4 Nodal Congestion Prices

Using the decomposition formula presented in Section 4.7.3, the real power congestion price at each bus can be rewritten as follows:

$$\text{NCP} = [D_x f]^{-1}\left[\frac{\partial I_{hk}}{\partial x}(\mu_{I_{hk\,\max}} - \mu_{I_{hk\,\min}}) + \begin{bmatrix} 0 \\ \mu_{V_{\max}} - \mu_{V_{\min}} \end{bmatrix}\right] \tag{6.9}$$

Observe that NCPs in (6.9) depends only on shadow prices of dual variables $\mu_{I_{hk\,\max}}$ and $\mu_{I_{hk\,\min}}$ associated with current thermal limits, since the proposed OPF model 6.1 does not include real power flow limits as in (4.10). However, dependence on voltage security constraints given by the inclusion of the "critical" system f_c and on the loading parameter λ_c are implicit in (6.9).

6.3 Test System Examples

In the following subsections, the OPF problem (6.1) and the proposed technique for computing LMPs are applied to a six-bus test system and to a 129-bus model of the Italian HV transmission system. The results of optimization technique (4.10) are also discussed to observe the effect of the proposed method in the LMPs and system security, which is represented here through the ALC. The power flow limits needed in (4.10) were obtained "off-line" by means of a continuation power flow technique [50]. For both test systems, bid load and generator powers were used as the direction needed to obtain a maximum loading point and the associated power flows in the lines, ignoring contingencies, so that proper comparisons can be made.

For both test cases, the limits of the loading parameter were assumed to be $\lambda_{c_{\min}} = 0.1$ and $\lambda_{c_{\max}} = 0.8$, i.e. for any value of ω, it is assumed that the system can be securely loaded to an ALC between 10% and 80% of the total transaction level of the given solution. To allow for adequate comparisons, the actual power

flow limits used in (4.10) were reduced by 10% with respect to the values obtained from the off-line continuation power flow analysis to emulate the $\lambda_c = 0.1$ limit.

6.3.1 Six-bus Test Case with Elastic Demand Model

Results for the OPF formulation (4.10) are reported in Table 6.1; the ALC value in this table was computed off-line using the generator voltages and load and generation power directions obtained from the OPF solution. Table 6.2, on the other hand, shows the solution obtained for the proposed multi-objective OPF (6.1) for $\omega = 10^{-3}$, which is referred to here as Voltage Stability Constrained-OPF (VSC-OPF), since the distance to the maximum loading point is not being really "optimized", with mostly the social benefit being considered in the objective function. For both solutions, generator voltages are at their maximum limits, as expected, since this condition generally provides higher transactions levels. However, in comparison with the standard OPF approach based on "security" limits determined off-line, the solution of the proposed method provides better LMPs, a higher total transaction level TTL (TTL $= \sum_i P_{L_i}$) and higher ALC, which demonstrates that off-line power flow limits are not adequate constraints for representing the actual system congestion. The improved LMPs result also in a lower total price paid to the Independent Market Operator (Pay_{IMO})which is computed as the difference between demand and supply payments, as follows:

$$\text{Pay}_{\text{IMO}} = \sum_{i \in \mathcal{I}} C_{S_i} P_{G_i} - \sum_{j \in \mathcal{J}} C_{D_j} P_{L_j} \tag{6.10}$$

and the network congestion prices are lower, even though the system losses are higher (which is to be expected, as T is higher).

Figures 6.1 and 6.2 show the effect of the weighting factor ω in the total transaction level TTL, the loading margin λ_c and the available loading condition ALC. Observe that, as expected, the more the weight of security, the higher the security

Table 6.1: Six-bus Test System: OPF with Off-Line Power Flow Limits

Participant	V [p.u.]	LMP [$/MWh]	NCP [$/MWh]	P_{BID} [MW]	P_0 [MW]	Pay [$/h]
GENCO 1	1.100	9.70	1.33	14.4	90	-1013
GENCO 2	1.100	8.80	0.00	2.4	140	-1252
GENCO 3	1.084	8.28	-0.04	20.0	60	-663
ESCO 1	1.028	11.64	3.32	15.6	90	1230
ESCO 2	1.013	10.83	1.57	0.0	100	1083
ESCO 3	1.023	9.13	0.40	20.0	90	1005
TOTALS	TTL = 315.6 MW Losses = 11.1 MW			Pay_{IMO} = 389.8 $/h ALC = 127.7 MW		

Table 6.2: Six-bus Test System: VSC-OPF

Participant	V [p.u.]	LMP [$/MWh]	NCP [$/MWh]	P_{BID} [MW]	P_0 [MW]	Pay [$/h]
GENCO 1	1.100	8.94	-0.04	0.0	90	-804
GENCO 2	1.100	8.90	0.00	25.0	140	-1467
GENCO 3	1.100	9.06	0.07	20.0	60	-725
ESCO 1	1.021	9.48	0.19	25.0	90	1090
ESCO 2	1.013	9.57	0.27	10.0	100	1052
ESCO 3	1.039	9.34	0.22	8.0	90	916
TOTALS	TTL = 323 MW Losses = 12.0 MW			Pay_{IMO} = 61 $/h ALC = 166 MW		

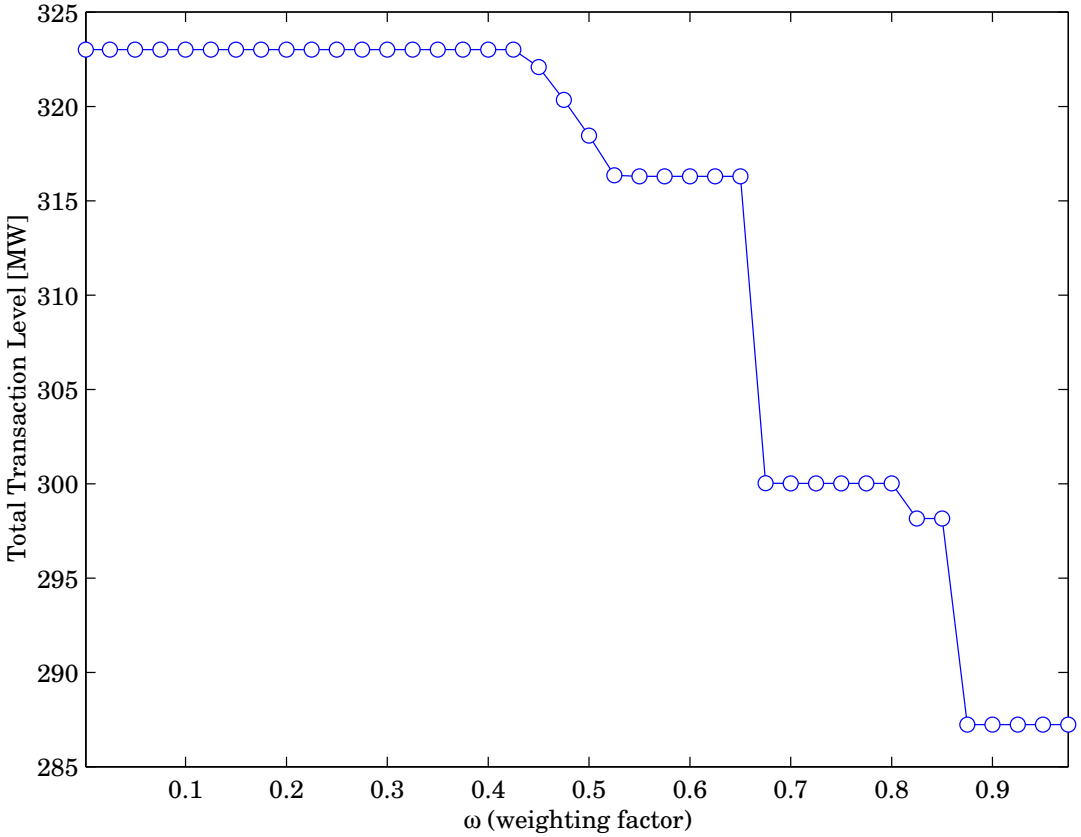

Figure 6.1: Total transaction level for the six-bus test system with elastic demand.

level λ_c (and consequently ALC), but, at the same time, the lower the TTL. This is due to the power bids being free to vary so that, as ω increases, congestion is minimized (security is maximized) by both increasing λ_c and reducing TTL.

Figures 6.3 and 6.4 depict supply and demand power bids and LMPs and NCPs as ω varies, illustrating the transition from an OPF market problem to an OPF security problem as λ_c approaches its maximum imposed value of $\lambda_{c_{\max}} = 0.8$. Observe how the LMPs and NCPs generally decrease in this example as the security levels increase, since the auction solutions move away from the security limits, i.e. the system is less congested. Furthermore, even though the LMPs and the overall total transaction level decrease, local bids may increase or decrease,

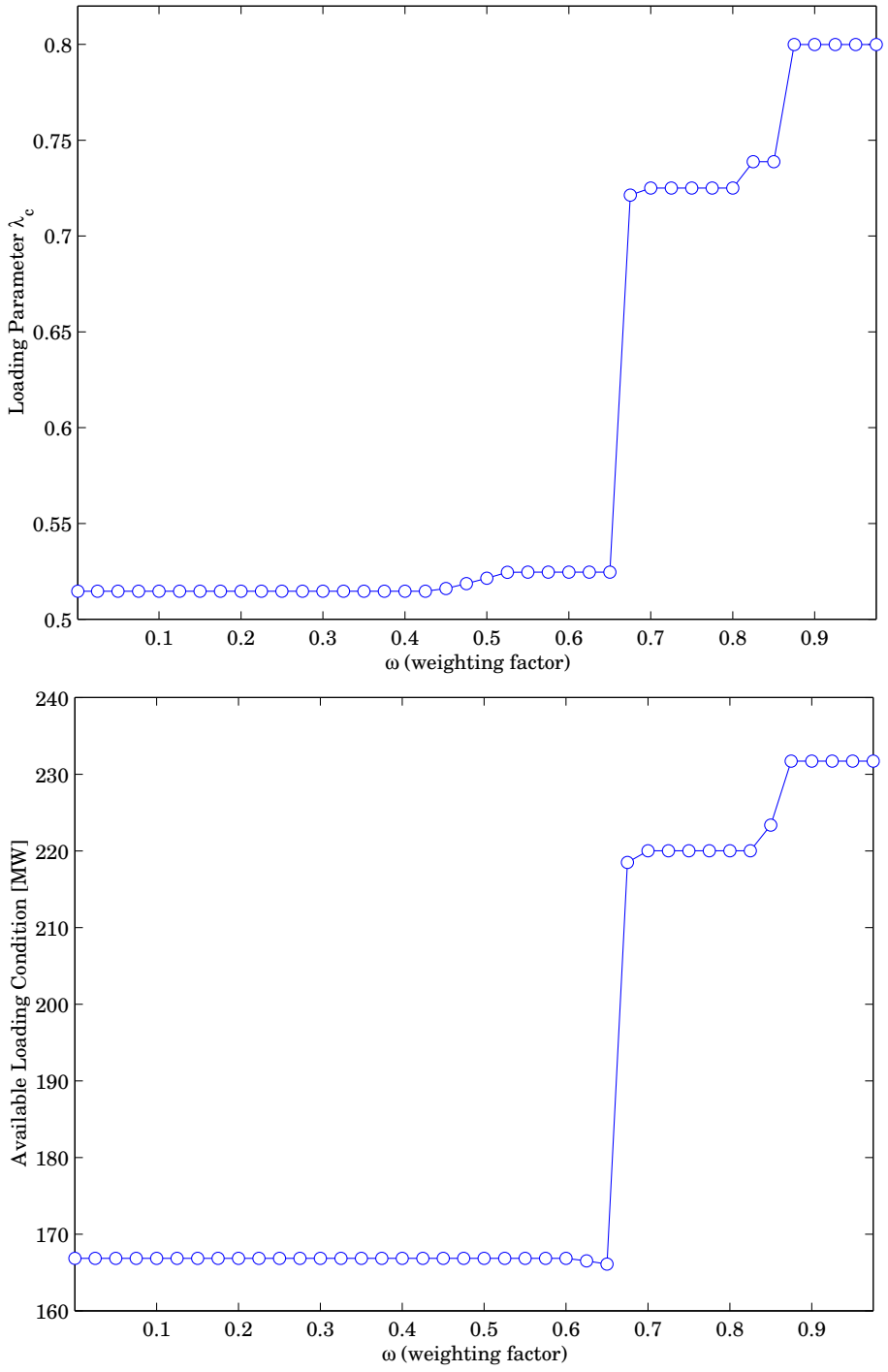

Figure 6.2: Loading margin λ_c and ALC for the six-bus test system with elastic demand.

accordingly to the power schedule which better matches the obtained loading margin.

For example, Fig. 6.5 depicts the LMP at Bus 6 as a function of the power demand of ESCO 3 at that bus with respect to the value of the weighting factor ω, illustrating that the relationship between system security and bids is not obvious and very much depends on the chosen security limits; in other words, as ω increases, i.e. as system security becomes more significant in the optimization problem, the price-power pair does not show any obvious relationship with respect to the system security level.

When the loading parameter λ_c reaches its maximum limit, which in Fig. 6.4 corresponds to $\omega > 0.85$, LMPs decrease below the minimum power supply price bid of 7 \$/MWh (see Table B.1 in Appendix B). The reason for this behavior is that the OPF VS constraints force the system to the power levels needed to maintain the required maximum loading margin, regardless of the social benefit (notice that only the cheapest supplier, i.e. GENCO 3, provides for the required losses and power demands, as expected). Solutions characterized by $\lambda_c = \lambda_{c_{\max}}$ would likely be unacceptable for the market participants, since the total transaction level as well as LMPs are too low. However, not imposing any maximum limit on λ_c would lead to market solutions with zero power bids ($P_S = P_D = 0$), which basically correspond to the base case operating condition associated with the given fixed generation P_{G_0} and load P_{L_0}. Observe that the proposed methodology is designed to give operators and market participants a series of solutions to allow them to analyze the effect of system security on power bids and vice versa, so that proper operating and bidding decisions can be made.

For the sake of completeness, Figs. 6.6, 6.7 and 6.8 depicts voltages, generator reactive powers and line currents for both the actual and the critical system. Observe that the actual system variables move toward a less congested condition

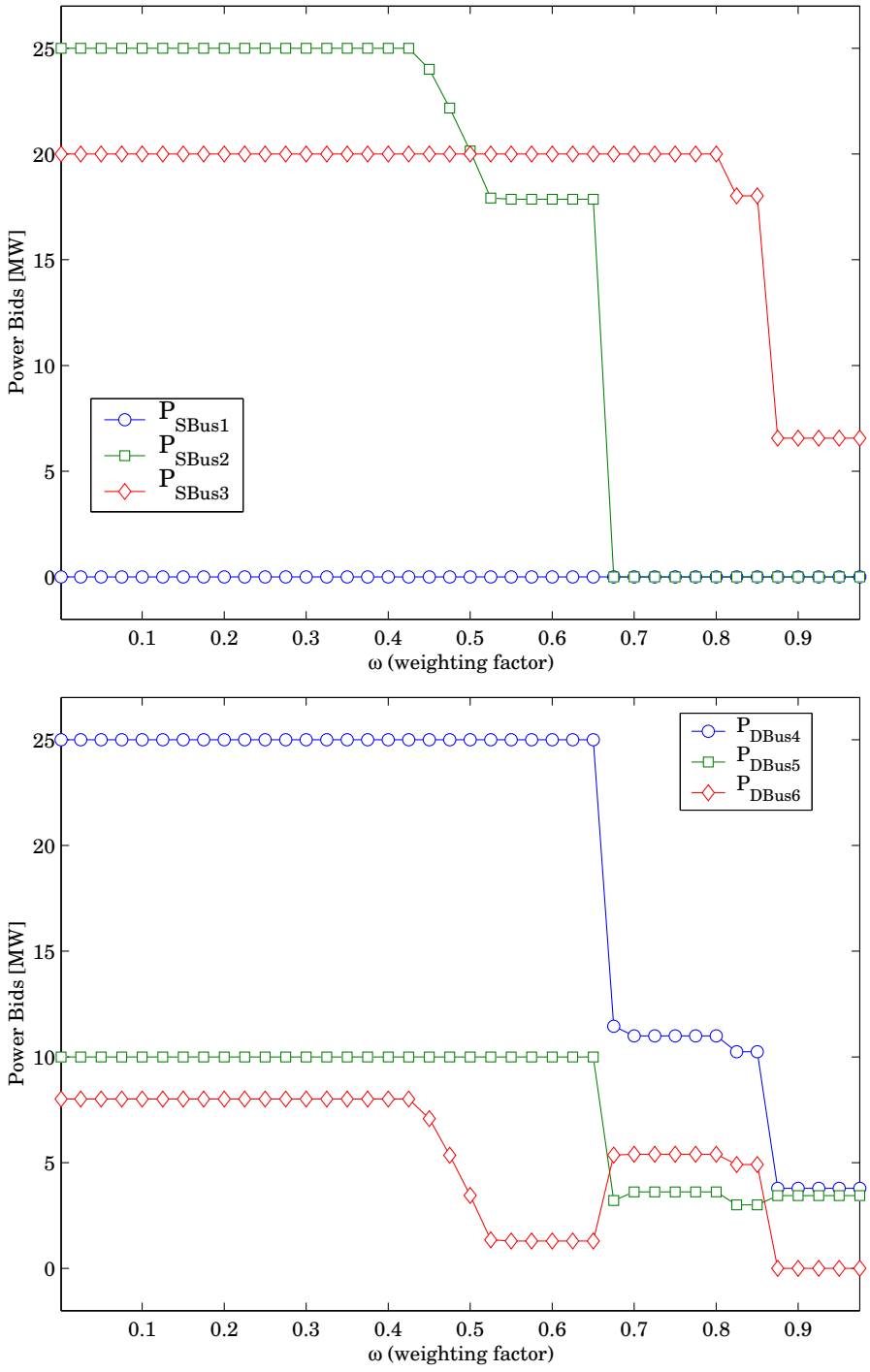

Figure 6.3: Power bids P_S and P_D for the six-bus test system with elastic demand.

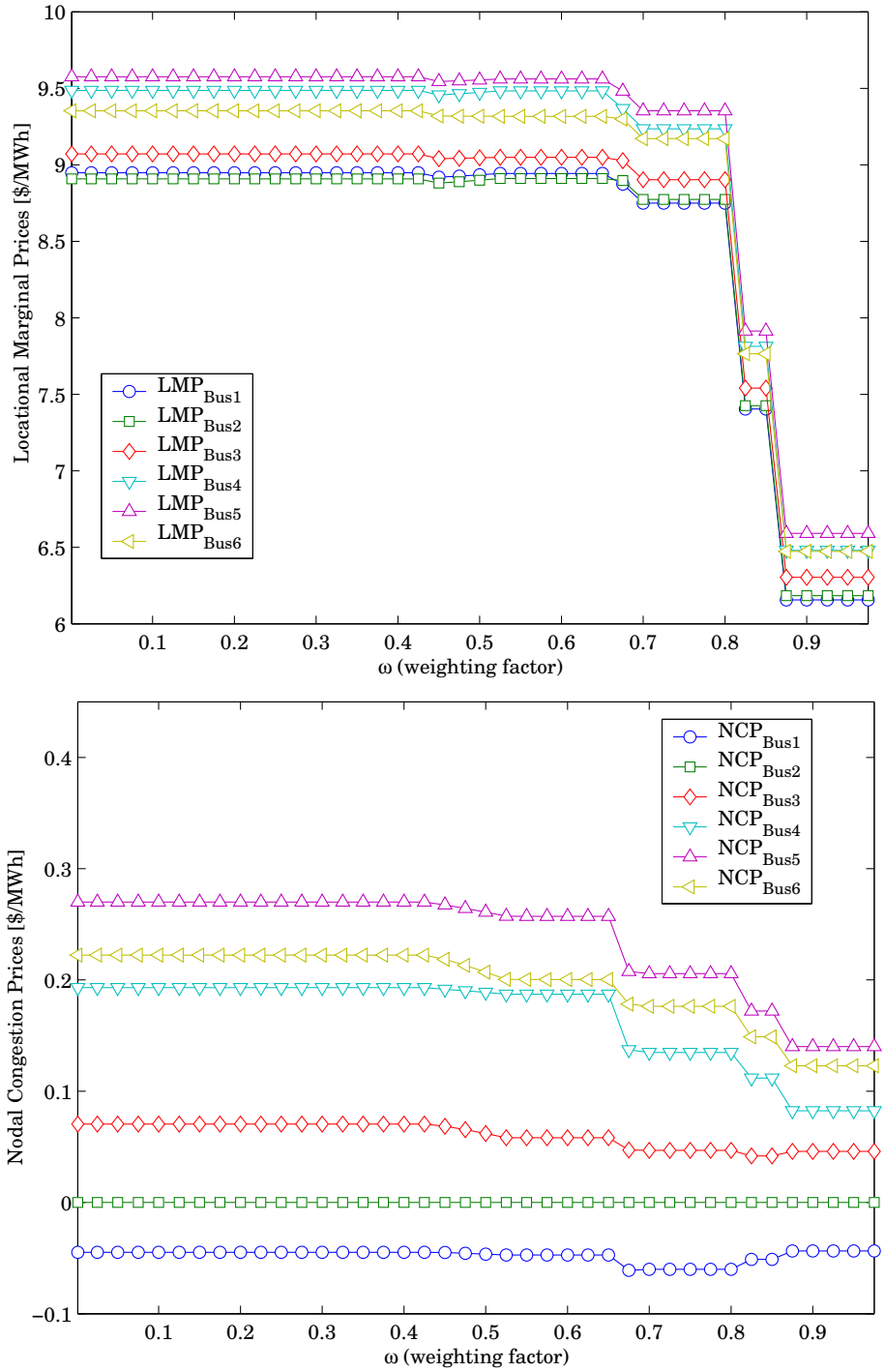

Figure 6.4: Local Marginal Prices and Nodal Congestion Prices for the six-bus test system with elastic demand.

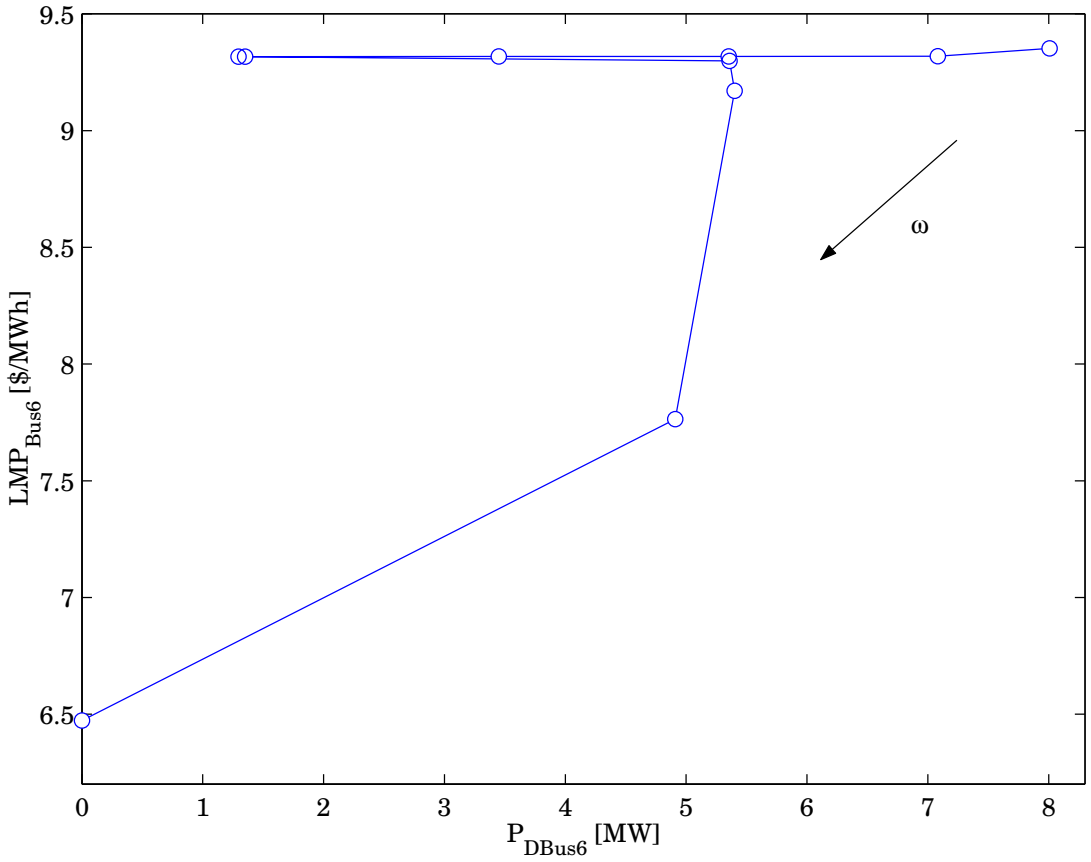

Figure 6.5: LMP at Bus 6 as a function of its power demand (ESCO 3) for the six-bus test system with elastic demand.

(load voltages increase while generator reactive powers and line currents decrease), whereas "critical" variables show a complex behavior which is not predictable *a priori*.

Finally, Figs. 6.9 and 6.10 depicts the total pays for each market participants and the the pay for the IMO. As it can be noted, as the level of security increases, electricity and congestion costs decrease, since the TTL decrease. Thus, in case of elastic demand bidding, competitive consumers can chose among different scenarios:

1. purchasing a high quantity of "expensive" power at a low security level;
2. purchasing a low quantity of "cheap" power at a high security level;
3. purchasing with conditions in between cases 1 and 2.

6.3.2 Six-bus Test Case with Inelastic Demand Model

When the transaction level is fixed, as in the case of inelastic demand, imposing a higher security level would result in price increases [24]. This is illustrated in Figs. 6.11 and 6.12 for the six-bus test system assuming inelastic loads; load demands are assumed to have the same values as those depicted in Table 6.2, so that these figures can be compared to the corresponding Figs. 6.2 and 6.3.

Figures 6.13, 6.14 and 6.15 show LMPs, NCPs, supply and demand pays and the pay due to the IMO respectively. Observe that as ω increases, the security level λ_c and associated LMPs and NCPs increase, as expected, leading to higher electricity and congestion prices.

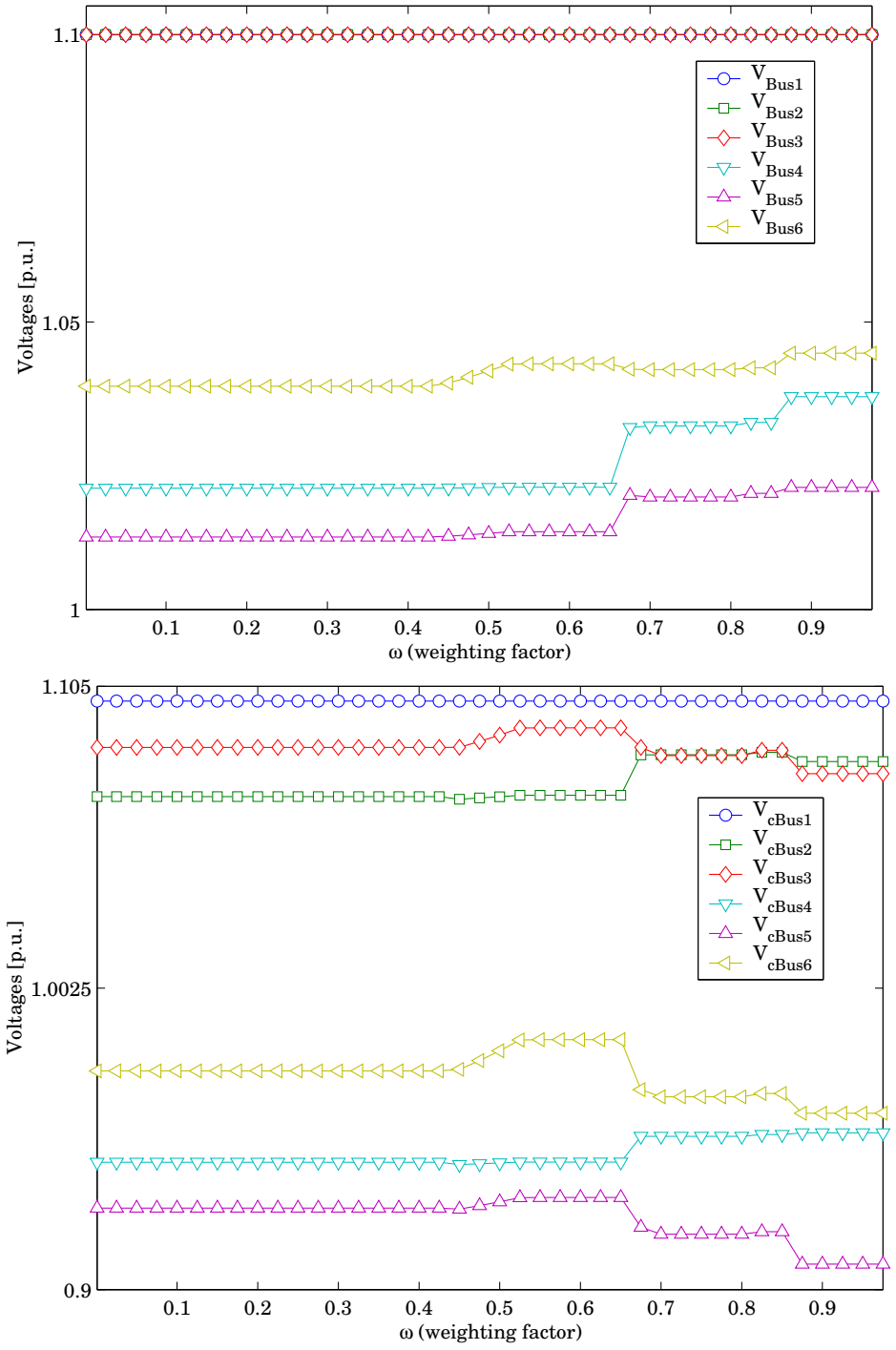

Figure 6.6: Actual and critical bus voltages V and V_c for the six-bus test system with elastic demand.

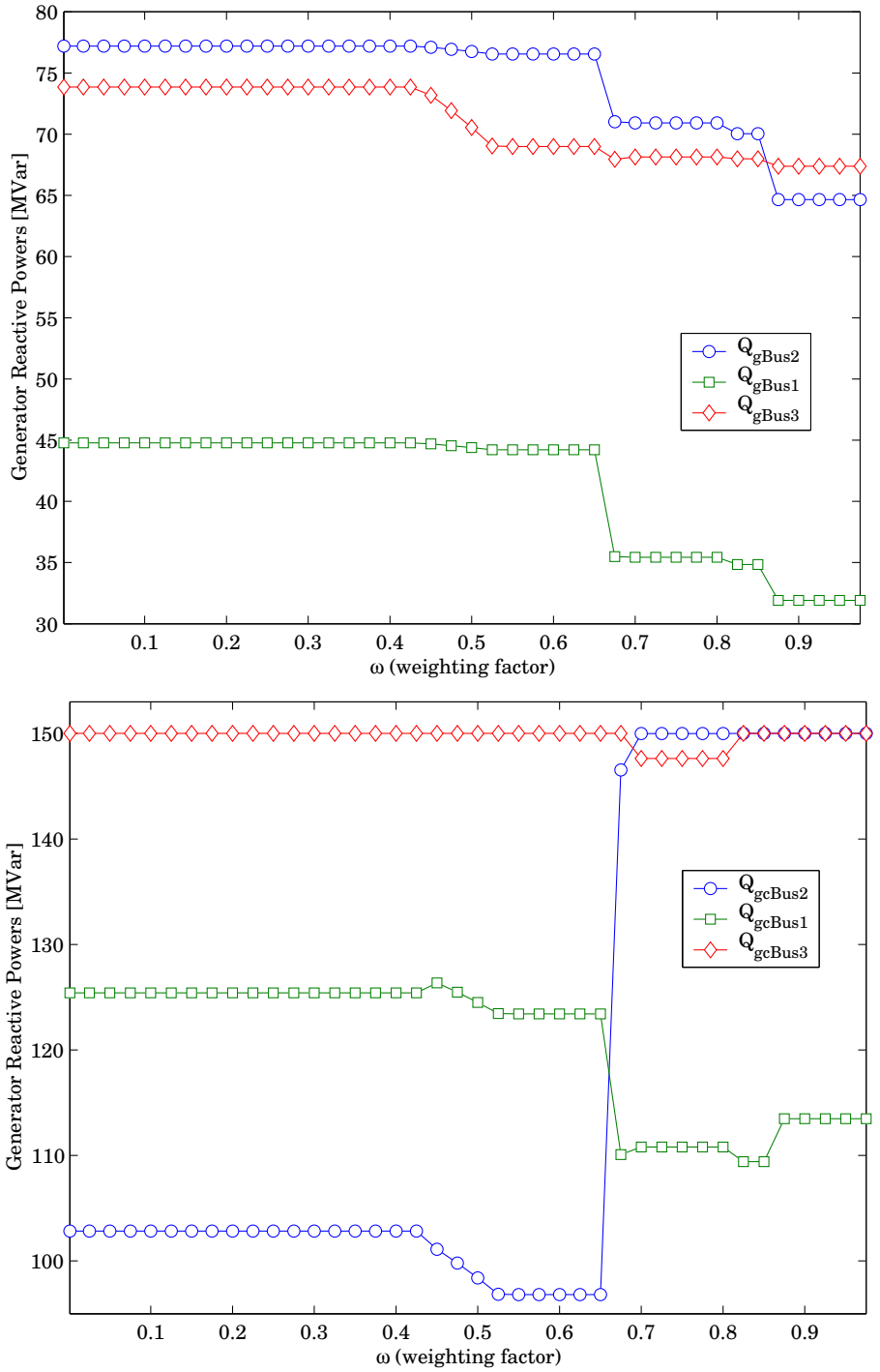

Figure 6.7: Actual and critical generator reactive powers Q_G and Q_{G_c} for the six-bus test system with elastic demand.

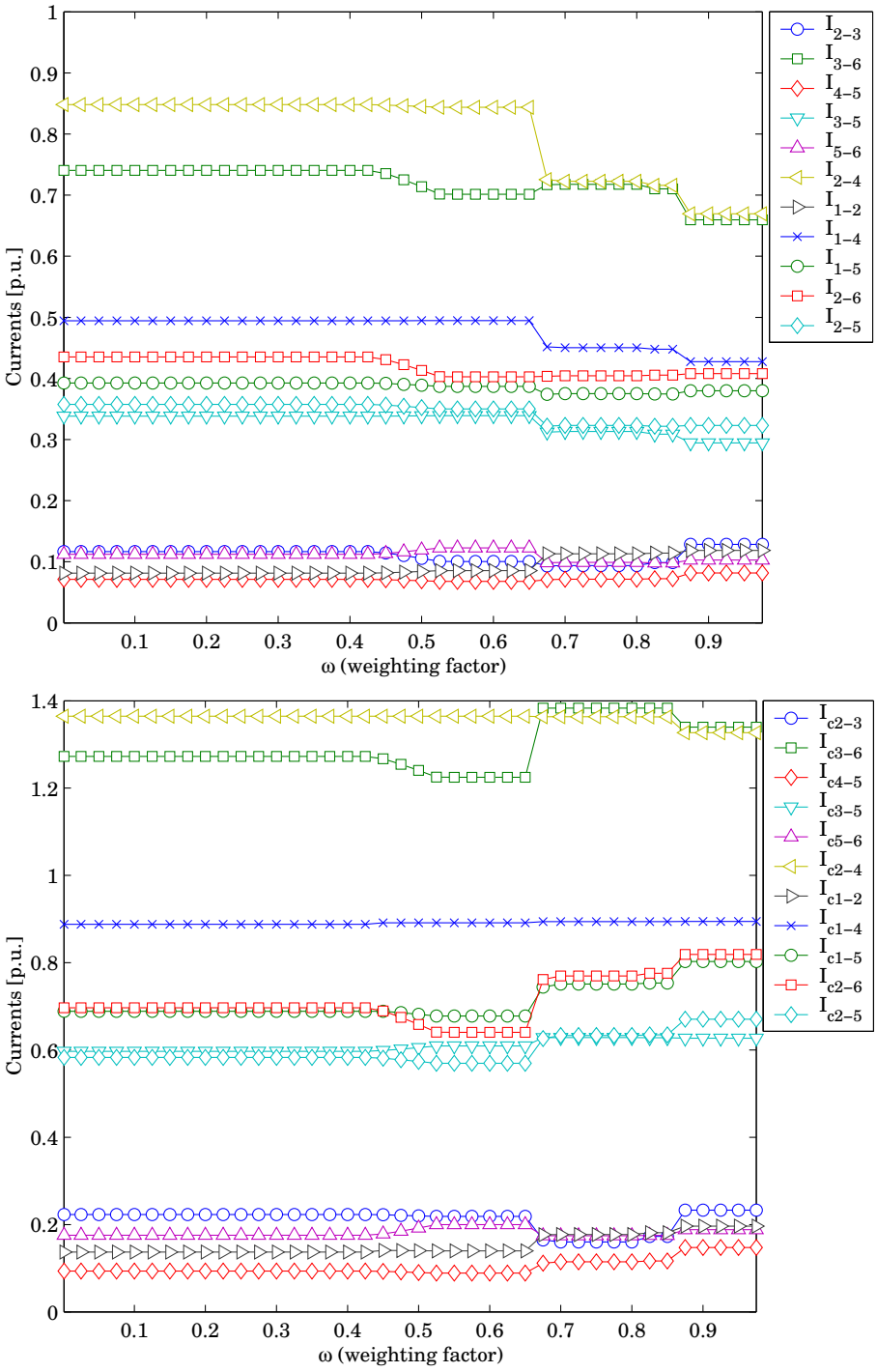

Figure 6.8: Actual and critical transmission line currents I_{hk} and I_{hk_c} for the six-bus test system with elastic demand.

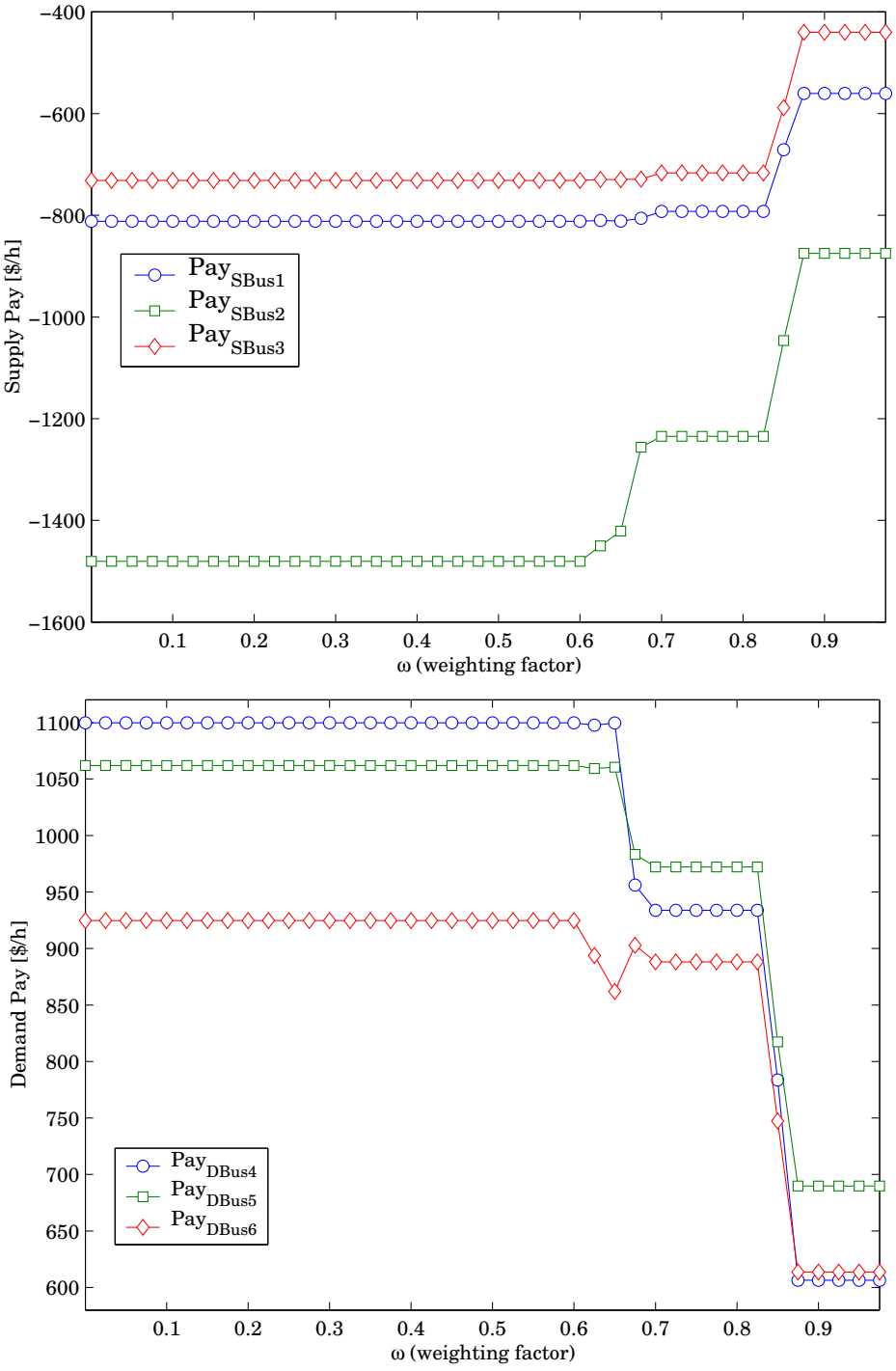

Figure 6.9: Supply and demand pays for the six-bus test system with elastic demand.

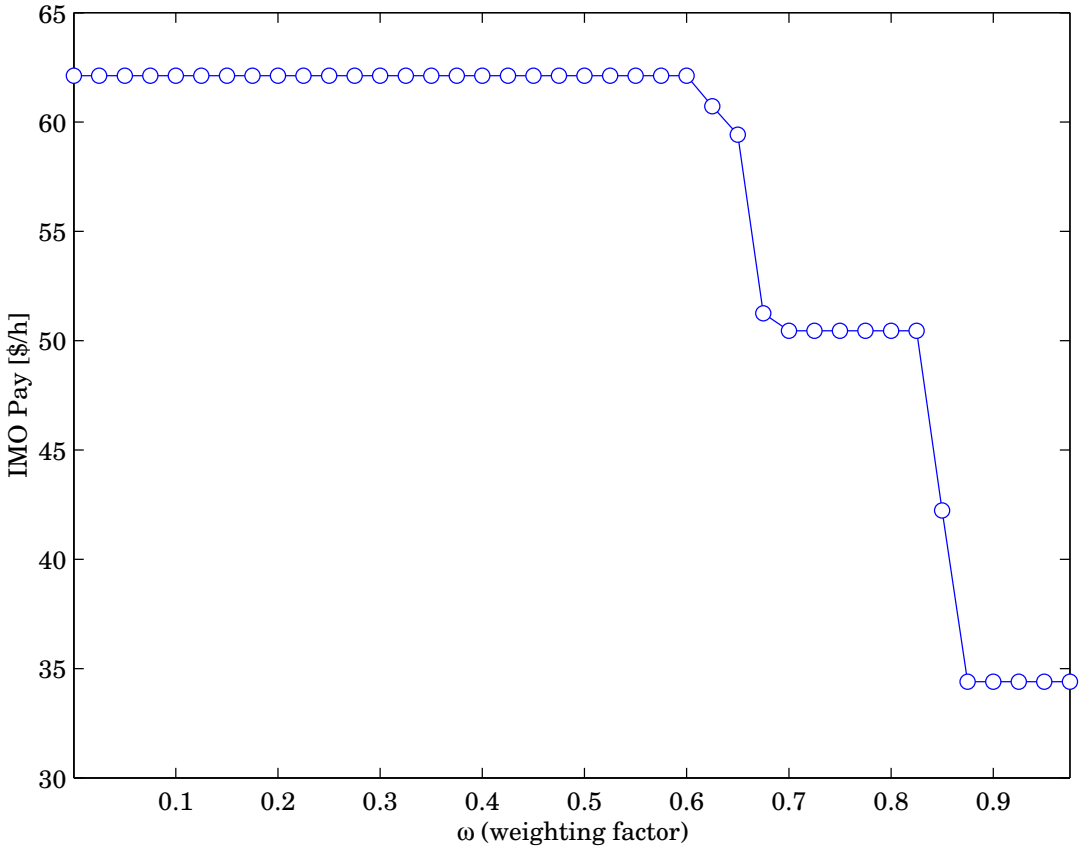

Figure 6.10: IMO pay for the six-bus test system with elastic demand.

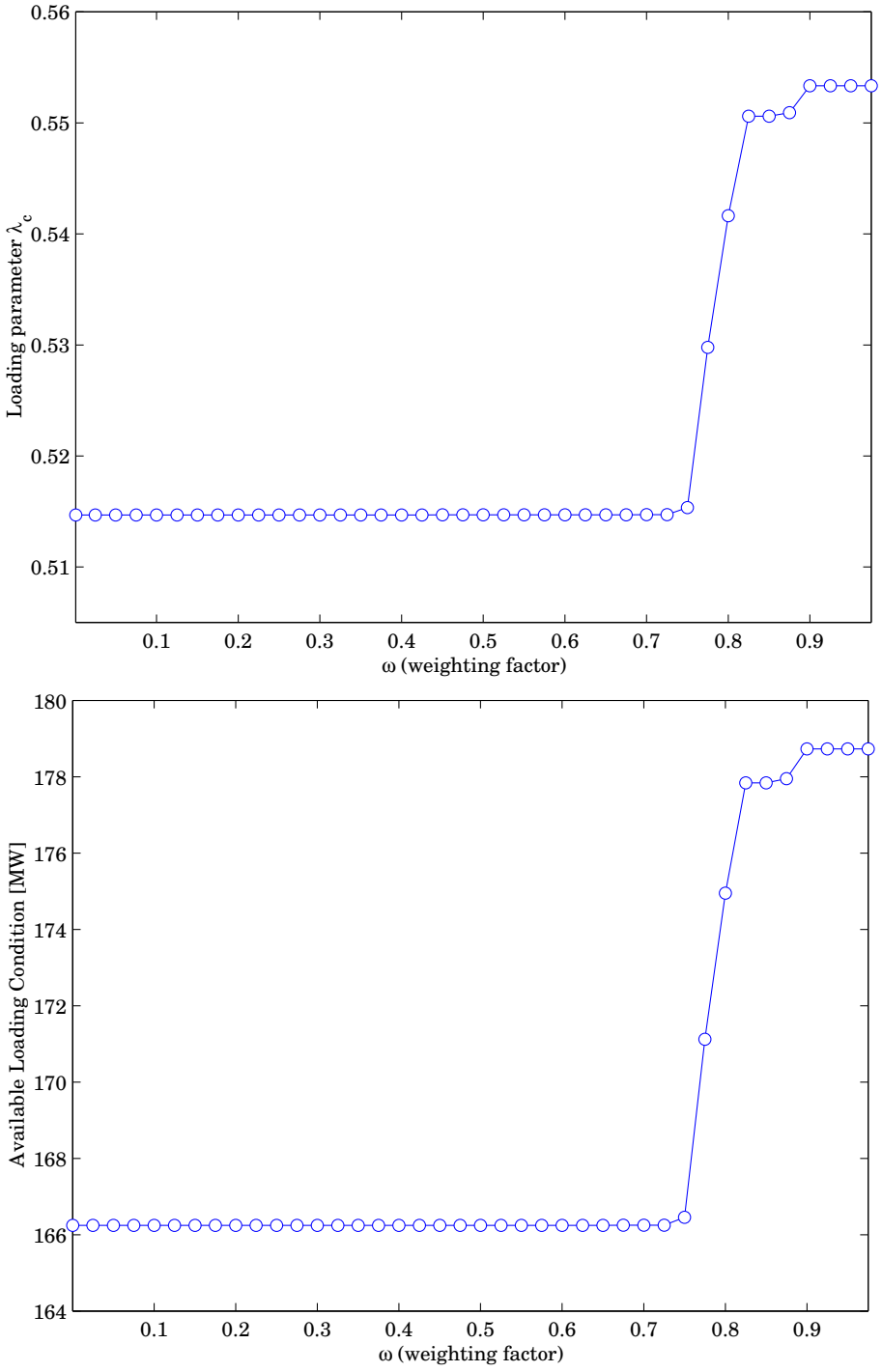

Figure 6.11: Loading parameter λ_c and ALC for the six-bus test system with inelastic demand.

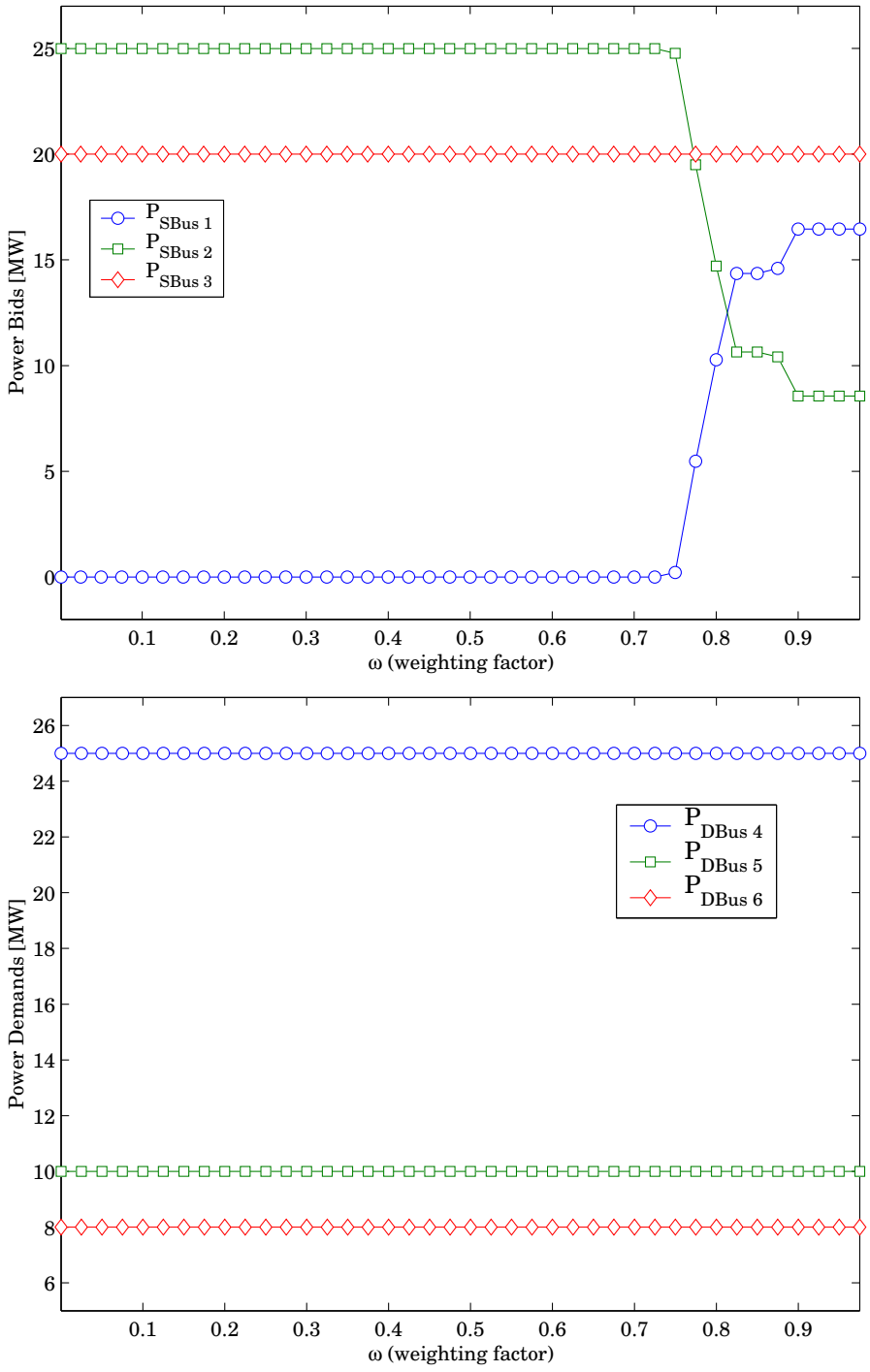

Figure 6.12: Supply power bids P_S and P_D for the six-bus test system with inelastic demand.

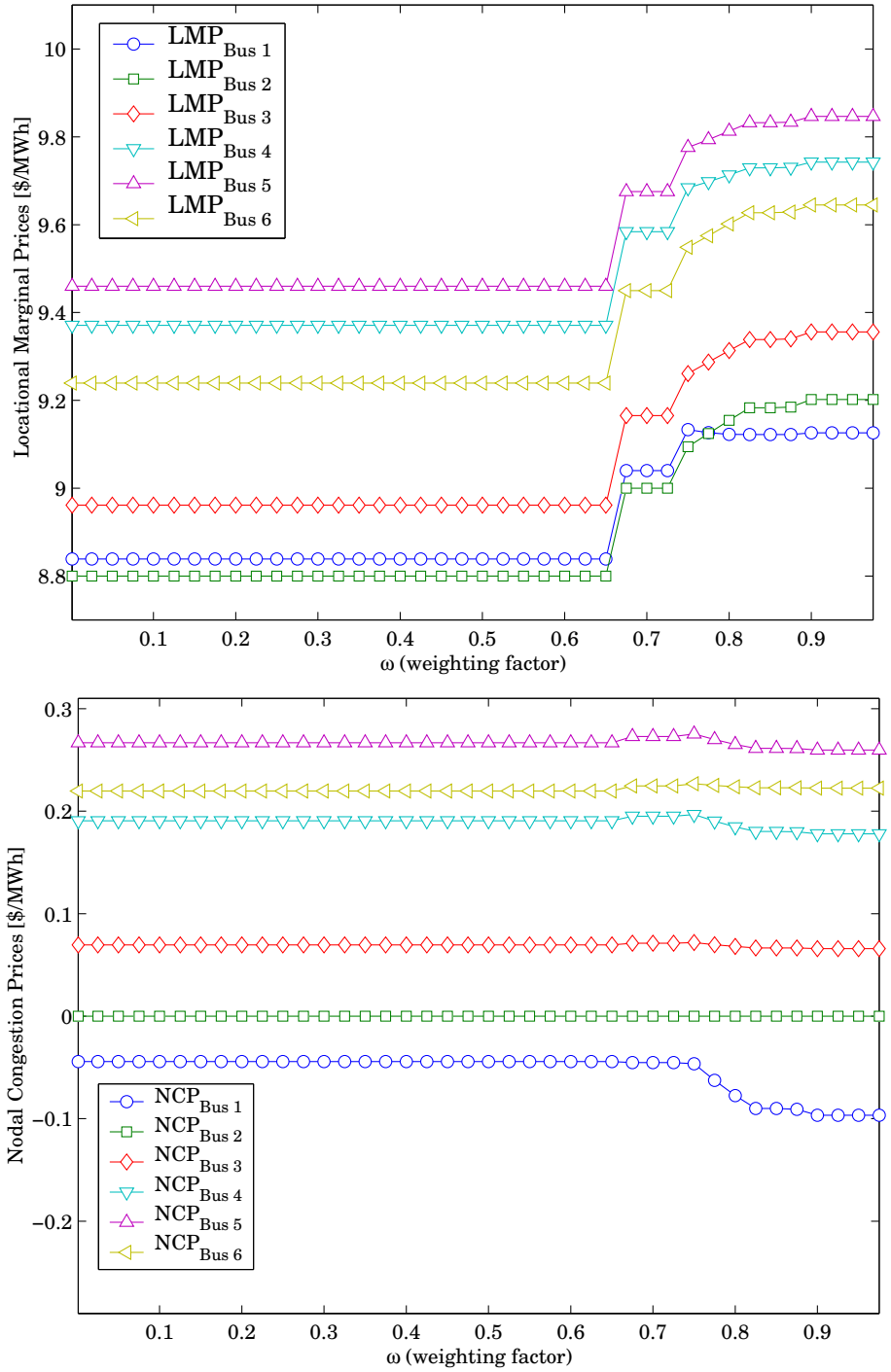

Figure 6.13: Local Marginal Prices and Nodal Congestion Prices for the six-bus test system with inelastic demand.

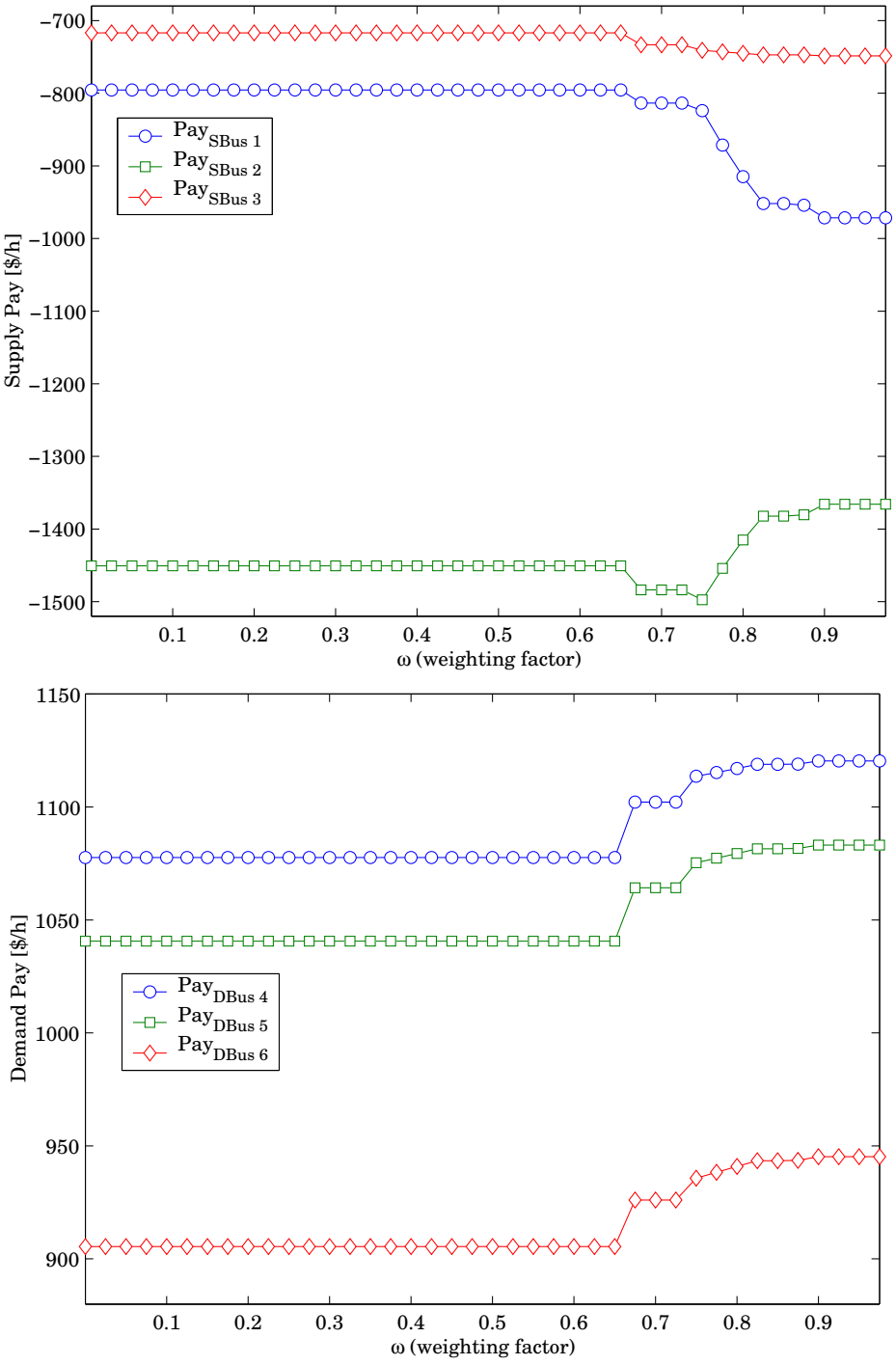

Figure 6.14: Loading parameter λ_c and ALC for the six-bus test system with inelastic demand.

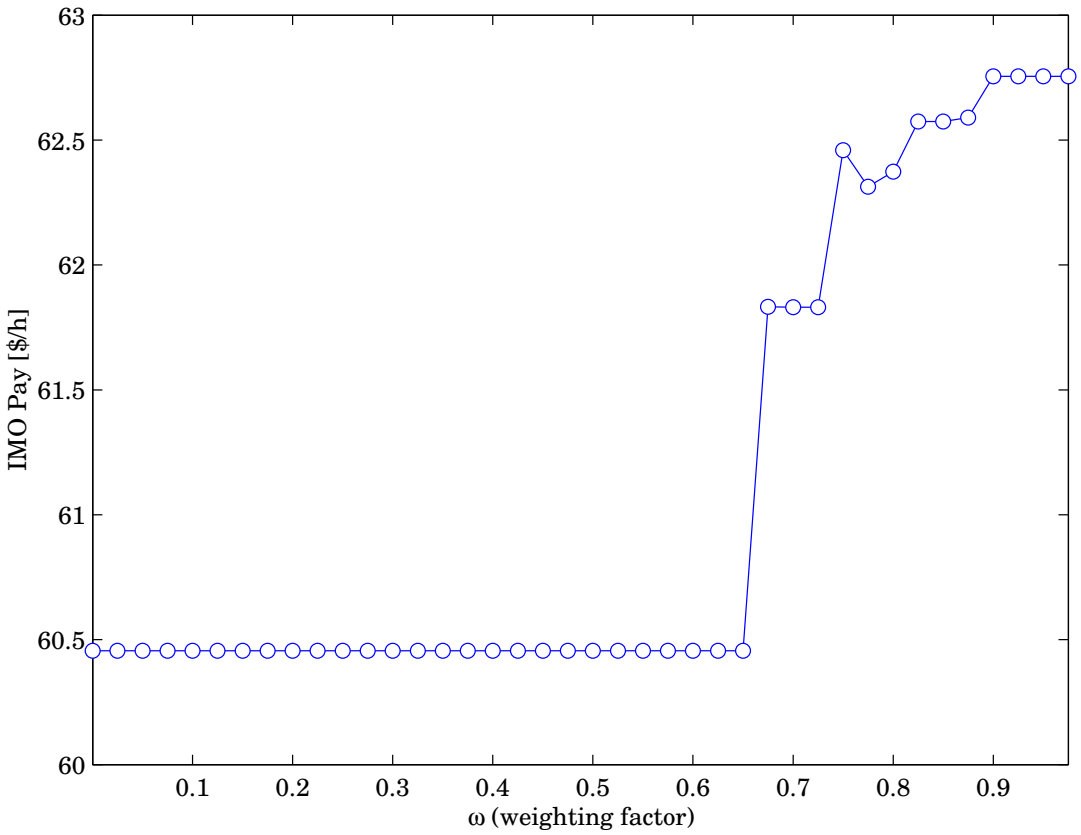

Figure 6.15: IMO pay for the six-bus test system with inelastic demand.

6.3.3 129-bus Italian HV Transmission System

Tables 6.3 and 6.4 show the results of both OPF solutions (4.10) and (6.1) with $\omega = 10^{-3}$ (VSC-OPF) for some market participants that are representative of all the areas in which the Italian system is geographically subdivided. As in the case of the six-bus test system, the proposed method provides a higher TTL, a better distribution of LMPs, and a lower total payment to the system operator (Pay_{GRTN}). Observe that the increased transaction level results also on higher power imports from the inter-ties in Table 6.3 and 6.4 (e.g. Villarodin and Lavorges), as expected, since neighboring countries typically generate electricity at lower prices (nuclear plants).

Figures 6.16 and 6.17 shows the TTL and the loading margin λ_c and the associated ALC as a function of the weighting factor ω. As it can be observed, only for $\omega > 0.75$, the security component of the objective function has an influence in the OPF solutions, due to the multi-objective function scaling. As expected, the transaction level is higher for lower values of security, and it decreases as ω increases to yield a larger loading margin (reduce congestion).

Figures 6.18, 6.19 and 6.20 depict some significant power supplies and demands together with their corresponding LMPs and NCPs, showing a similar behavior as in the case of the simple six-bus test system. Once again, increasing the security level of the overall system does not necessarily imply that all power bids decrease. In this example, the LMPs and NCPs may also increase for higher values of the weighting factor, confirming the results obtained for the six-bus test system, as some generators and/or loads may be penalized whereas others may benefit as a result of increasing security levels (reduce transmission congestion).

Figure 6.21 depicts the behavior of the LMP at the Galatina bus as a function of the correspondent local power demand, showing once again the unpredictable behavior of the quantity-price pair as the security level varies.

Table 6.3: Italian System Example: OPF with Off-Line Power Flow Limits

Participant	V [p.u.]	LMP [$/MWh]	NCP [$/MWh]	P_{BID} [MW]	P_0 [MW]	Pay [$10^3$$/h]
Trino	1.1316	33.6	0.6254	221	266	-16.4
Tavazzano	1.1297	34.3	1.0449	0	879	-30.1
Turbigo	1.1289	34.1	0.9662	413	764	-40.1
Fusina	1.1316	34.6	0.6192	756	77	-28.8
Villarodin	1.1316	32.0	-0.7304	127	541	-21.4
Lavorges	1.1316	32.0	-1.1264	133	451	-18.7
S. Sofia	1.0685	35.2	1.8410	39	307	12.2
Galatina	1.1203	35.2	1.1852	119	191	10.9
Colunga	1.1111	31.4	-1.8674	131	210	10.7
Roma O.	1.0839	34.8	1.3786	207	330	18.7
TOTALS	TTL = 24.8 GW Losses = 135 MW			Pay_{GRTN} = 13.8 k$/h ALC = 3.0 GW		

Table 6.4: Italian System Example: VS-Constrained OPF

Participant	V [p.u.]	LMP [\$/MWh]	NCP [\$/MWh]	P_{BID} [MW]	P_0 [MW]	Pay [10^3\$/h]
Trino	1.1316	33.3	-0.0210	280	266	-18.2
Tavazzano	1.1316	34.5	0.1636	0	879	-30.3
Turbigo	1.1316	34.2	0.0830	753	764	-51.9
Fusina	1.1316	34.1	0.0412	884	77	-32.8
Villarodin	1.1316	33.4	-0.1450	223	541	-25.5
Lavorges	1.1316	34.1	0.0683	186	451	-21.7
S. Sofia	1.1005	35.1	0.4085	192	307	17.5
Galatina	1.1268	34.2	0.2604	83	191	93.7
Colunga	1.1096	34.7	0.2366	132	210	11.9
Roma O.	1.1026	34.7	0.2448	204	330	18.5
TOTALS	TTL = 26.1 GW Losses = 164 MW			Pay_{GRTN} = 13.2 k\$/h ALC = 2.6 GW		

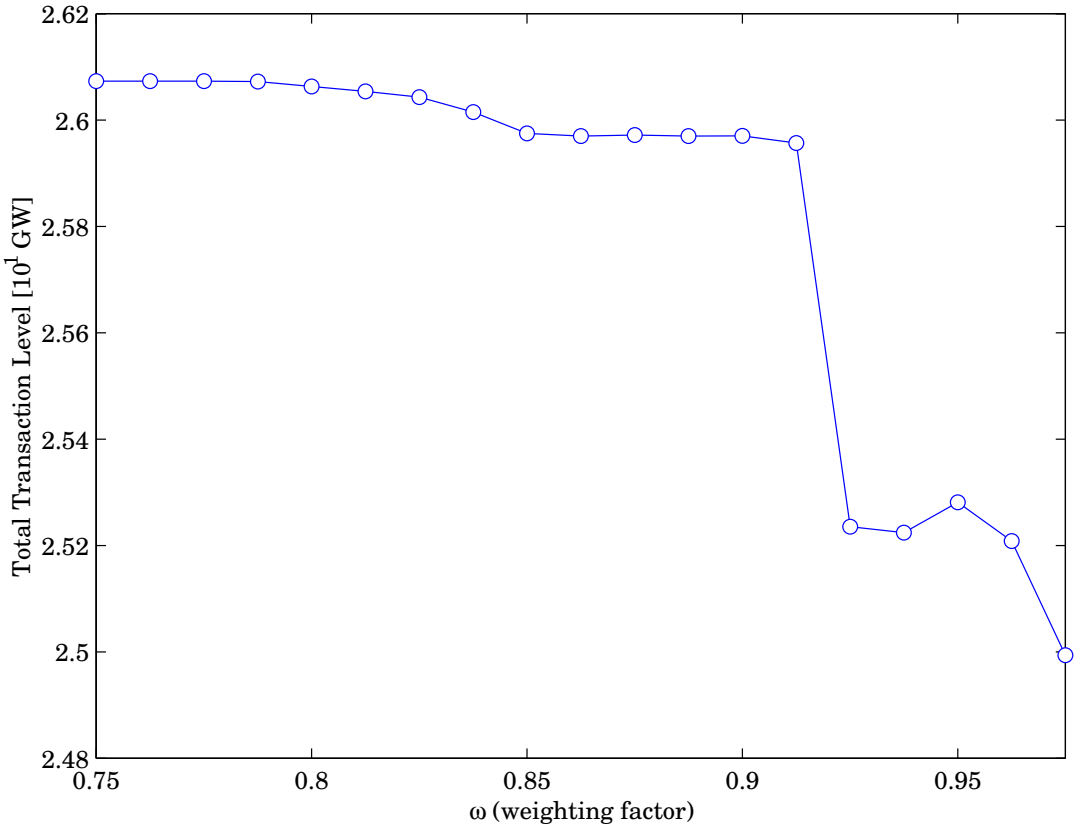

Figure 6.16: Total transaction level for the Italian system example.

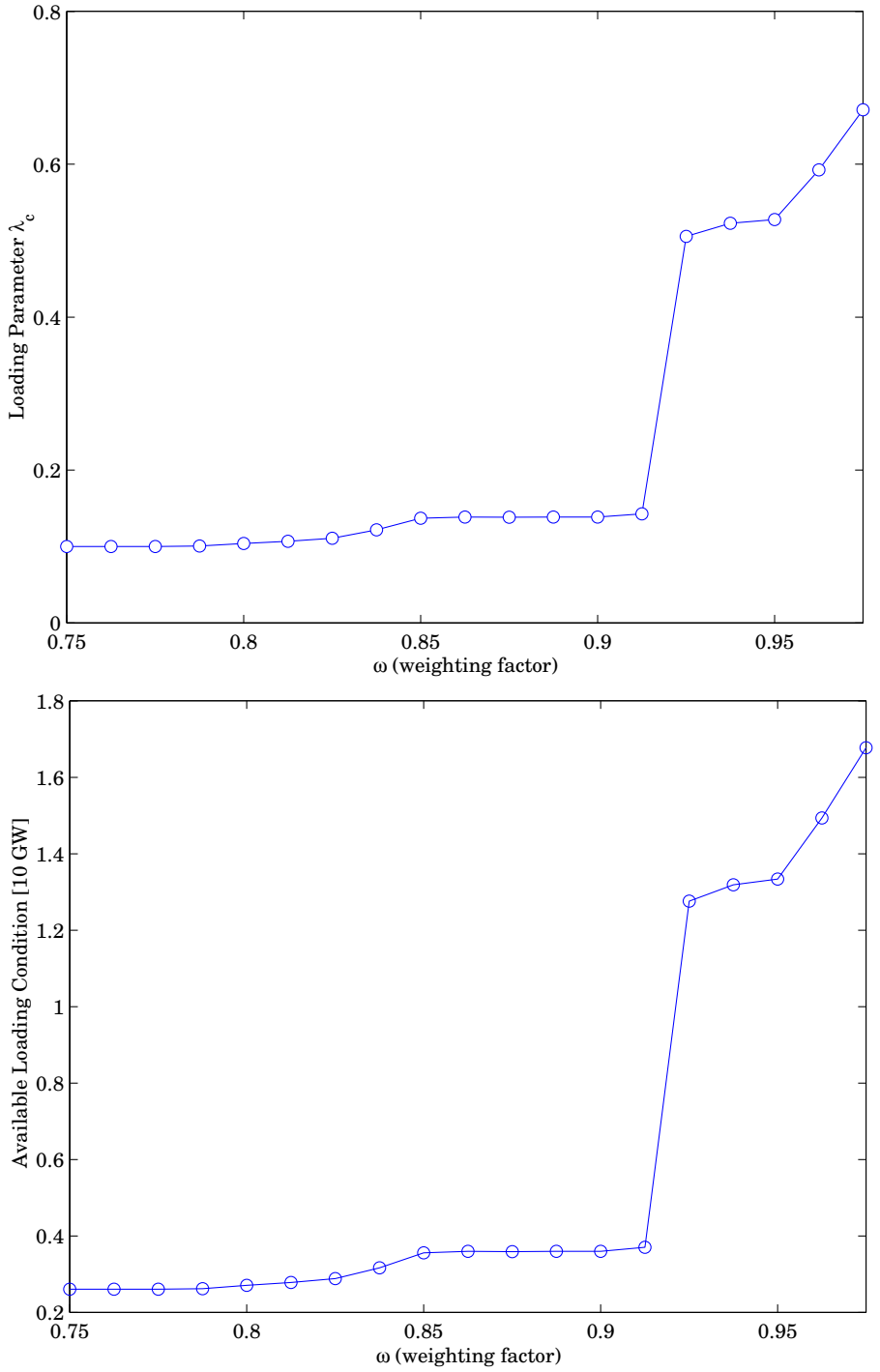

Figure 6.17: Loading parameter λ_c and ALC for the Italian system example.

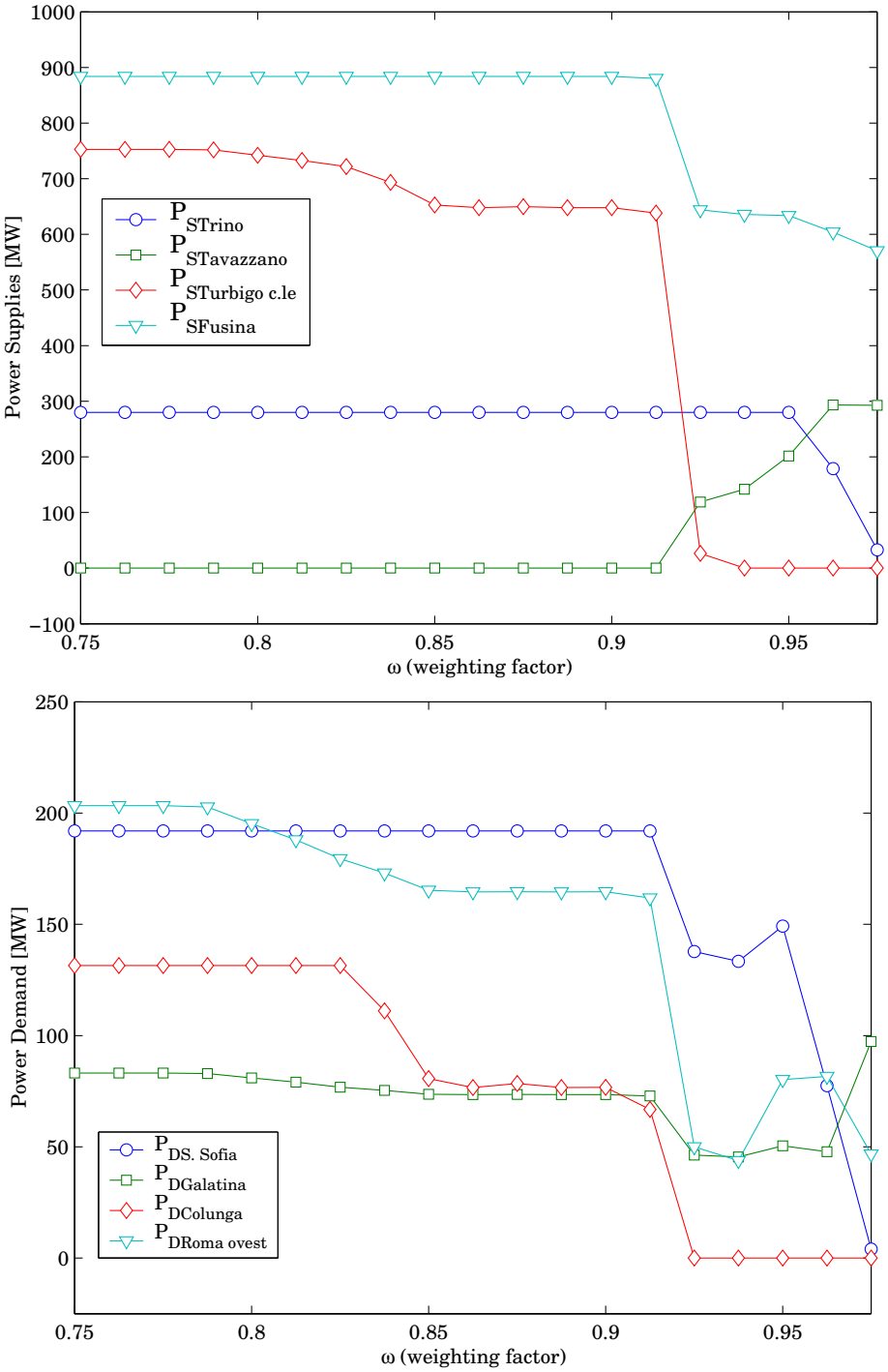

Figure 6.18: Most significant power supplies P_S and demands P_D for the Italian system example.

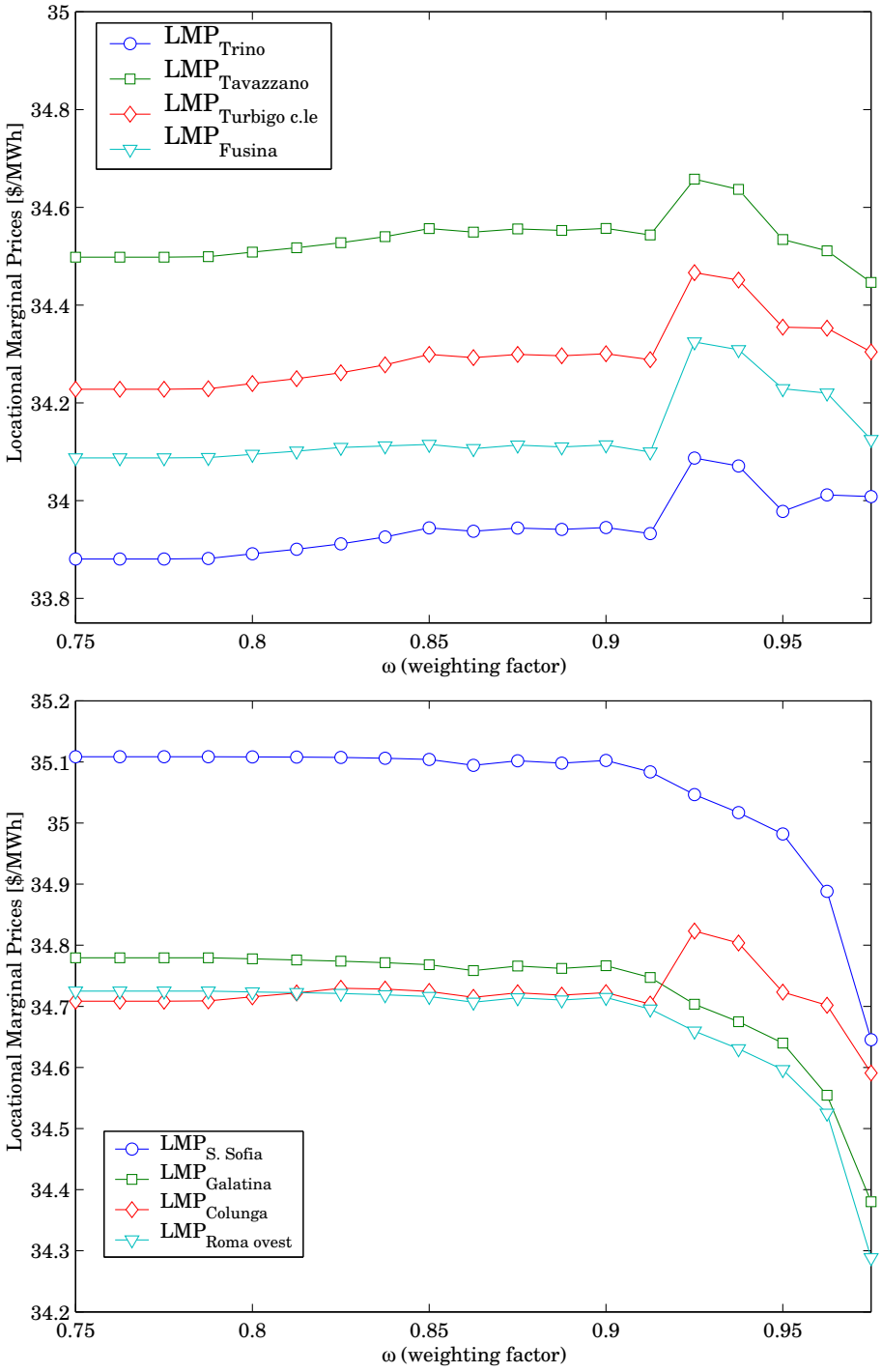

Figure 6.19: LMPs of the most significant market participants for the Italian system example.

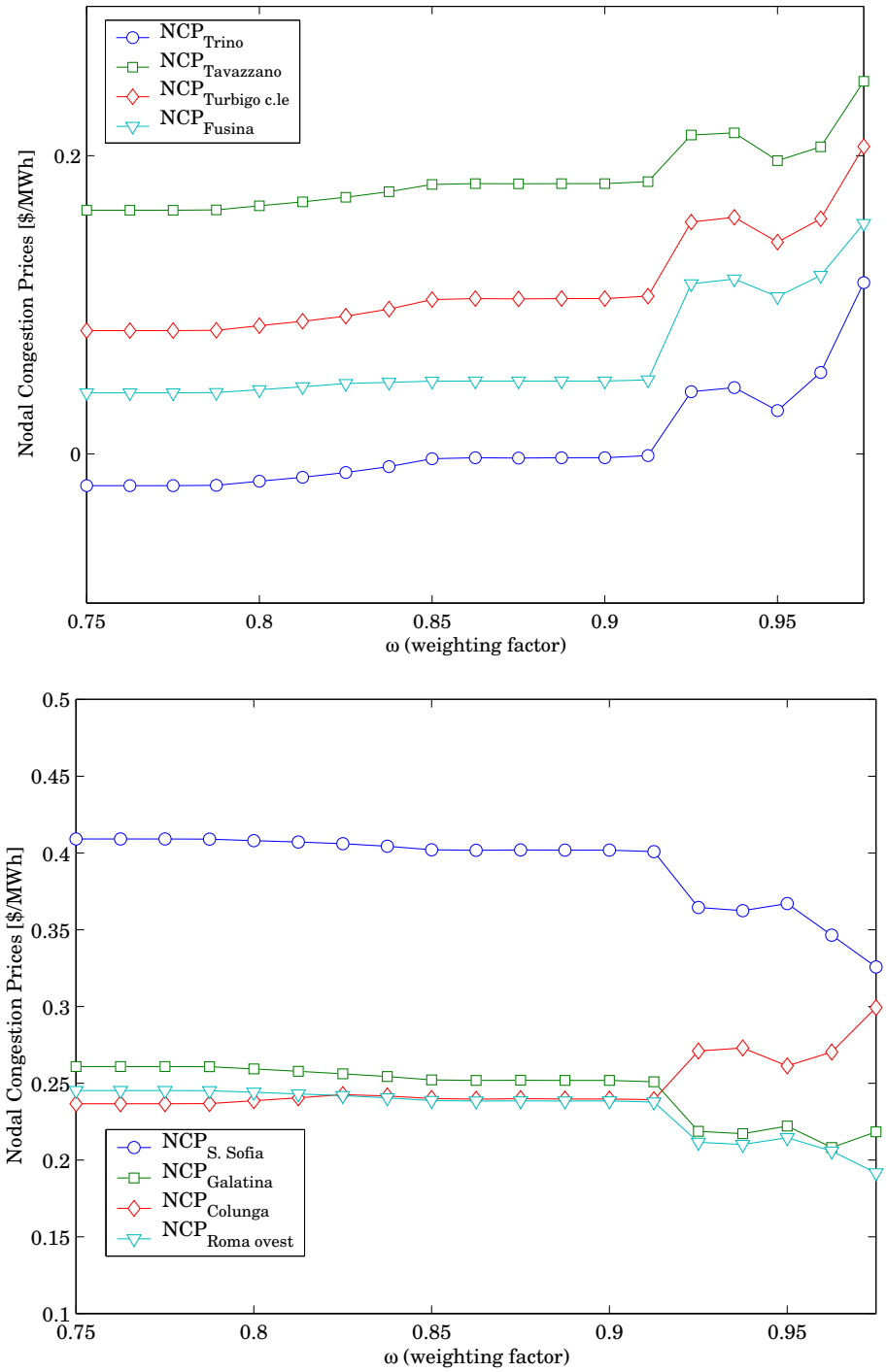

Figure 6.20: NCPs of the most significant market participants for the Italian system example.

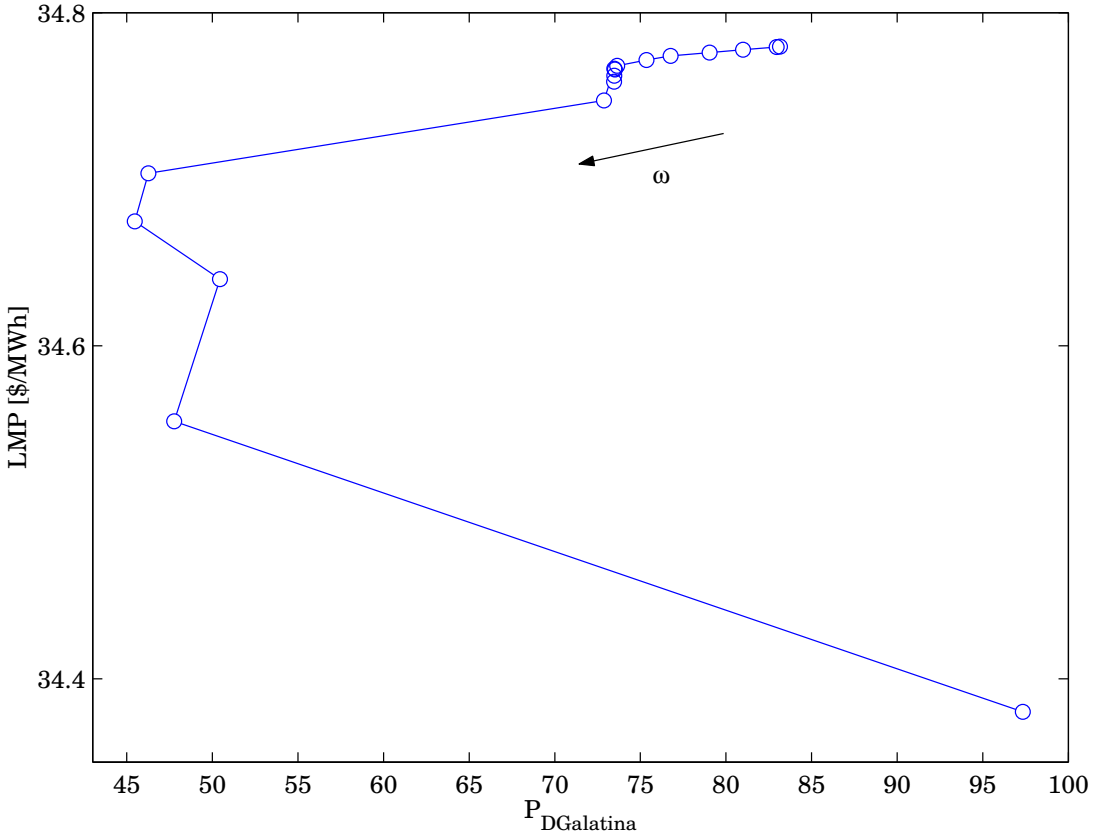

Figure 6.21: LMP as a function of power demand P_D at the Galatina bus.

Finally, Fig. 6.22 illustrates the pays for the most significant power supplies and demands whose bids are depicted in Fig. 6.18, whereas Fig. 6.23 shows the GRTN pay. Although the trend is an overall decrease of market participant pays and congestion costs, some participant may see a pay increase due to local congestions of the current power flow solution. Thus, the proposed VSC-OPF can also be useful to identify market participants which are mostly affected by security issues.

6.4 Summary

In this chapter, a multi-objective optimization for managing and pricing voltage stability is proposed and tested on a simple test system as well as on a realistic network. The results obtained with the proposed technique, when compared to those obtained by means of a typical OPF-based market model, show that proper representation of system security actually results in more secure and overall better transactions, since security margins and transaction levels increase, while locational marginal prices improve.

The proposed multi-objective OPF method allows market operators and participants to directly control the desired level of system security by controlling the weighting factors of the different objective functions, which is not possible in typical security constrained OPF-based market implementations.

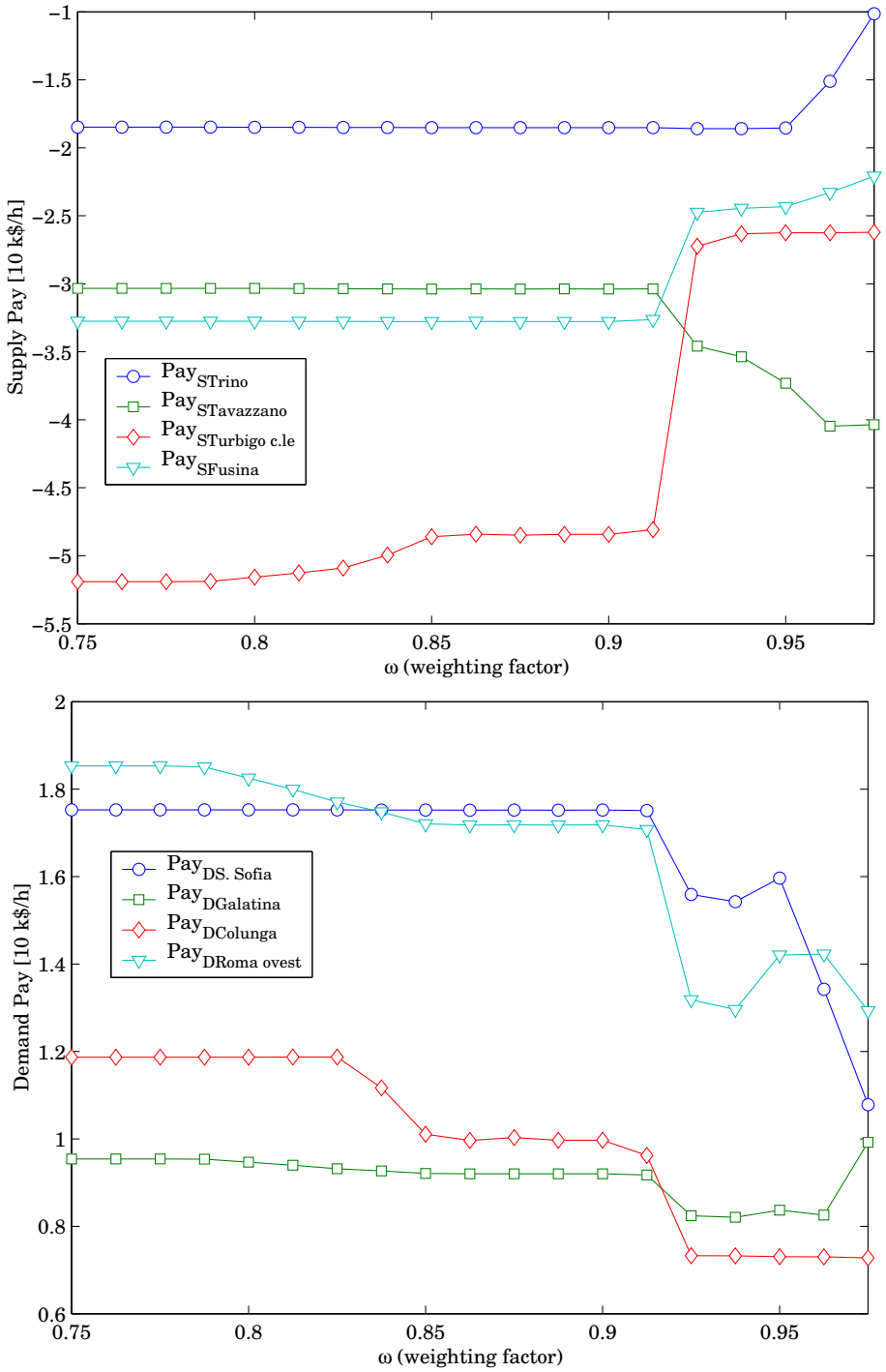

Figure 6.22: Supply and demand pays of the most significant market participants for the Italian system example.

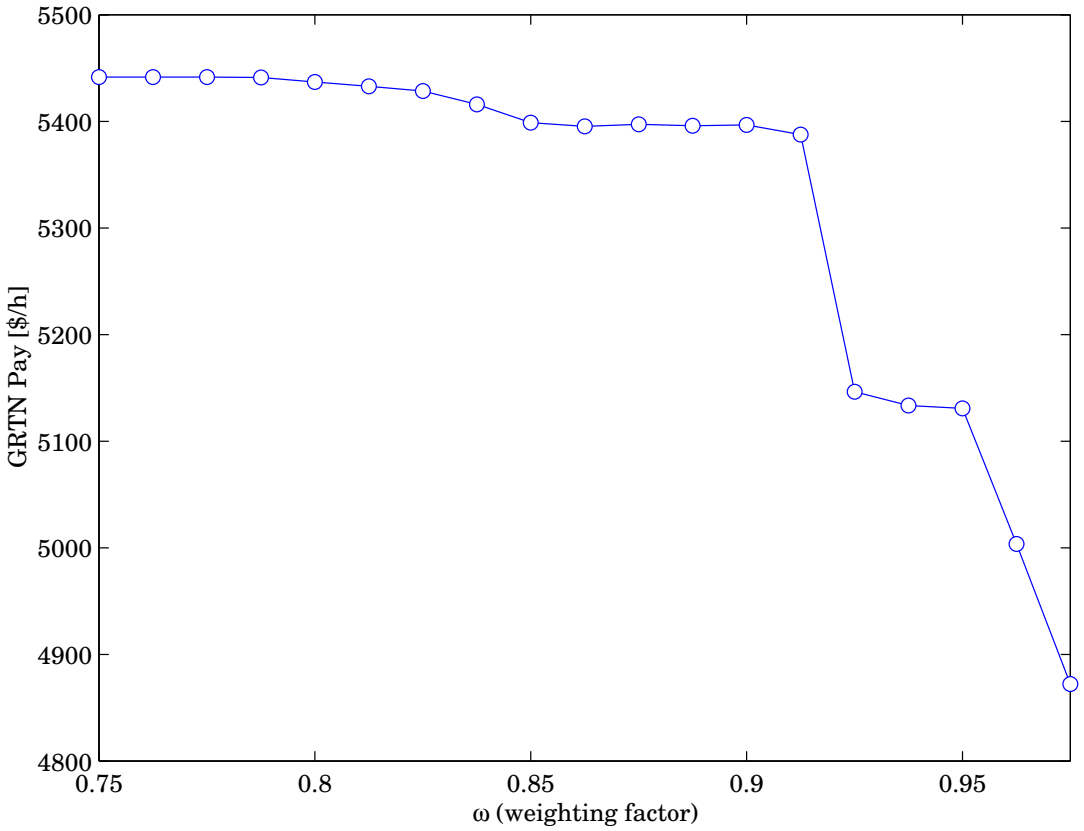

Figure 6.23: GRTN pay for the Italian system example.

Chapter 7

VSC-OPF with N-1 Security Criterion

7.1 Introduction

THIS chapter describes two techniques for including in the Voltage Stability Constrained OPF presented in Chapter 6 a N-1 contingency criterion. The first proposed technique is an iterative method which combines solutions obtained by means of the VSC-OPF with a continuation power flow analysis, while the latter is based on a sensitivity analysis of power flows in transmission lines. Both techniques are tested on a six-bus test system, as well as on a 129-bus model of the HV Italian transmission network, which provides a large scale example for testing the reliability of the proposed methods. The available loading capability, local marginal prices and nodal congestion prices resulting from the proposed solutions as well as comparisons with results obtained by means of a standard OPF technique are also presented and discussed.

7.2 VSC-OPF with N-1 Contingency Analysis

The solution of the VSC-OPF problem (6.1) provides the initial condition for the proposed techniques, which are an iterative method with N-1 contingency criterion (described in Section 7.2.1) and a multiple VSC-OPF with contingency ranking (described in Section 7.2.2). Contingencies are included in (6.1) by taking out the selected lines when formulating the "critical" power flow equations f_c, thus ensuring that the current solution of the VSC-OPF problem is feasible also for the given contingency. Thus, the VSC-OPF problem with N-1 contingency criterion is based on what has been proposed in [9, 25, 29, 41] and formulated as follows:

$$
\begin{aligned}
\text{Min.} \quad & G = -(\omega-1)(C_D^T P_D - C_S^T P_S) - \omega\lambda_c && (7.1)\\
\text{s.t.} \quad & f(\delta, V, Q_G, P_S, P_D) = 0 && \rightarrow \text{PF equations}\\
& f_c^{(N-1)}(\delta_c, V_c, Q_{G_c}, \lambda_c, P_S, P_D) = 0 && \rightarrow \text{Max load (N-1) PF eqs.}\\
& \lambda_{c_{\min}} \leq \lambda_c \leq \lambda_{c_{\max}} && \rightarrow \text{loading margin}\\
& 0 \leq P_S \leq P_{S_{\max}} && \rightarrow \text{Sup. bid blocks}\\
& 0 \leq P_D \leq P_{D_{\max}} && \rightarrow \text{Dem. bid blocks}\\
& I_{hk}(\delta, V) \leq I_{hk_{\max}} && \rightarrow \text{Thermal limits}\\
& I_{kh}(\delta, V) \leq I_{kh_{\max}}\\
& I_{hk}(\delta_c, V_c) \leq I_{hk_{\max}}\\
& I_{kh}(\delta_c, V_c) \leq I_{kh_{\max}}\\
& Q_{G_{\min}} \leq Q_G \leq Q_{G_{\max}} && \rightarrow \text{Gen. } Q \text{ limits}\\
& Q_{G_{\min}} \leq Q_{G_c} \leq Q_{G_{\max}}\\
& V_{\min} \leq V \leq V_{\max} && \rightarrow V \text{ "security" lim.}\\
& V_{\min} \leq V_c \leq V_{\max}
\end{aligned}
$$

where $f_c^{(N-1)}$ represent power flow equations for the system with under study with one line outage. Although one could solve one VSC-OPF problem (7.1) for the outage of each line of the system, this would result in a lengthy process for realistic size networks. The techniques proposed in this thesis address the problem of determining efficiently the contingencies which cause the worst effects on the system, i.e. the lowest loading margin λ_c and $\text{ALC}^{(N-1)}$. The latter is assumed to be defined using loading directions (3.3), as follows:

$$\text{ALC}^{(N-1)} = \min_h \{(\lambda_{c_h} - 1)\text{TTL}_h\} \tag{7.2}$$

where h indicates the line outage. Observe that (7.2) differs from (3.21), where the search for the minimum was limited only to the loading parameters. In (7.2) the minimum ALC is computed for the product of both λ_c and the TTL since power bids P_D are not fixed and the optimization process adjusts both λ_c and P_D in order to minimize the objective function. Finally, LMPs and NCPs are defined as described in Chapter 6.

7.2.1 Iterative Method with N-1 Contingency Criterion

Figure 7.1 depicts the flow chart of the proposed method for combining an N-1 contingency criterion based on the continuation power flow analysis and VSC-OPF-based market solutions. This method is basically composed of two steps. First, an N-1 contingency criterion is performed for determining the most critical line outage based on a continuation power flow analysis and using as generator and loading direction the supply and demand bids P_S and P_D determined from the last VSC-OPF solution. For the continuation power flow computations [50], system controls and limits are all considered to properly determine limit conditions due to voltage stability, thermal and/or bus voltage limits.

Once the N-1 contingency computations are completed, the line outage that

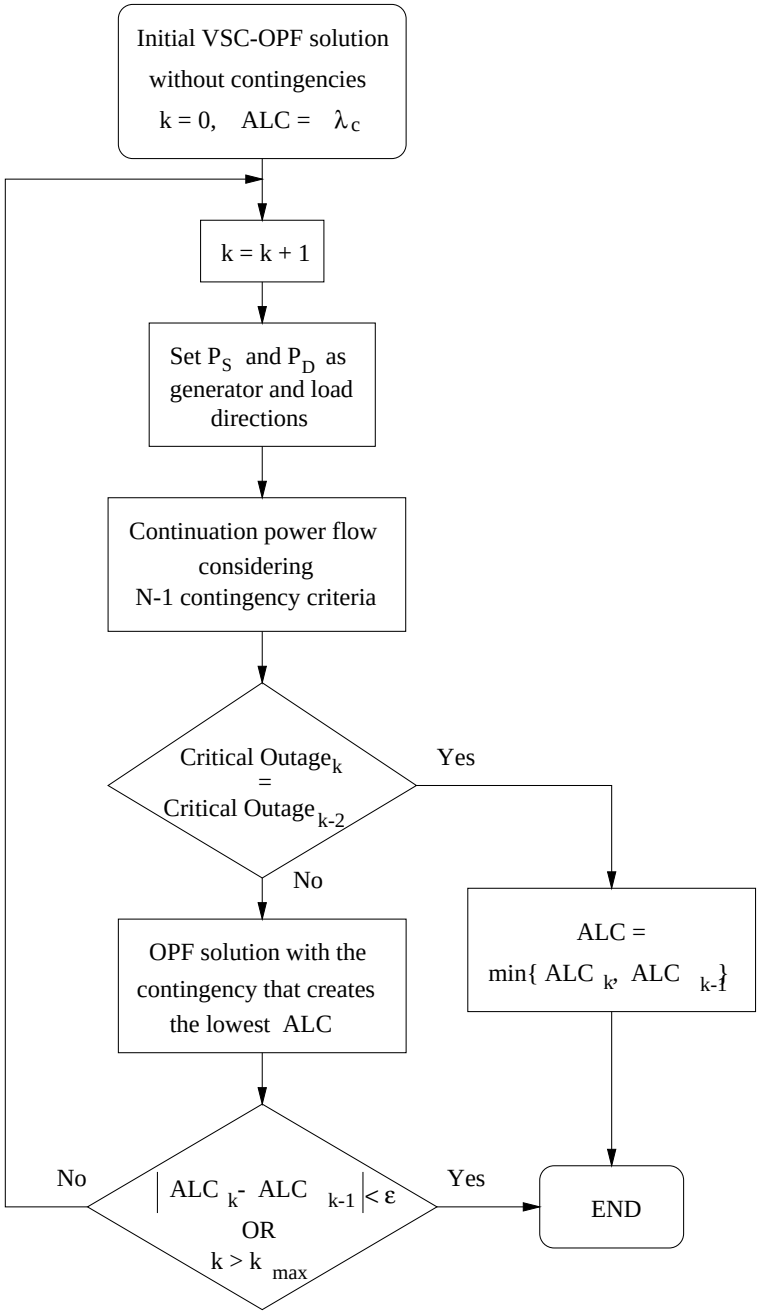

Figure 7.1: Flow chart of the iterative method with N-1 contingency criterion.

causes the minimum $\text{ALC}^{(N-1)}$ is selected and the power flow equations f_c are modified accordingly by taking out this critical line for the solution of the next VSC-OPF problem (6.1). The procedure stops when no "better" solution can be found, i.e. the $\text{ALC}^{(N-1)}$ of the last two iterations is below certain tolerance, or when the continuation power flow yields the same line outage as the most severe one in the last two iterations; the latter criterion is used to avoid "cycling" problems. Observe that the OPF-based solution of the power flow equations f_c and its associated $\text{ALC}^{(N-1)}$ generally differ from the corresponding values obtained with the continuation power flow, since in the VSC-OPF problem control variables such as generator voltages and reactive powers are modified in order to minimize costs and maximize the loading margin λ_c for the given contingency; hence the need for an iterative process.

When evaluating the result of applying the N-1 contingency criterion, it is necessary to consider the "system" effects of a line outage in order to avoid unfeasible conditions. For example, a line loss may cause the original grid to separate into two subsystems, i.e. islanding; in this case, the smallest island may be discarded, or just consider the associated contingency as "unfeasible" for the given operating condition.

7.2.2 Multiple VSC-OPF with Contingency Ranking

First, a basic VSC-OPF solution that does not consider contingencies is used for determining the sensitivity of power flows with respect to the loading parameter λ_c. Then, based on this solution and assuming a small variation ϵ of the loading parameter and recomputing the power flows by solving f_c, normalized sensitivity factors can be approximately computed as follows:

$$p_{hk} = P_{hk}\frac{\partial P_{hk}}{\partial \lambda_c} \approx P_{hk}(\lambda_c)\frac{P_{hk}(\lambda_c) - P_{hk}(\lambda_c - \epsilon)}{\epsilon} \tag{7.3}$$

where p_{hk} and P_{hk} are are the sensitivity factor and the power flows of line h-k respectively. The scaling is introduced for properly evaluating the "weight" of each line in the system, and thus for considering only those lines characterized by both "significant" power transfers and the high sensitivities [60, 81].

The first lines with the biggest sensitivity factors p_{hk} are selected (from multiple tests, 5 lines appear to be a sufficient number), and a VSC-OPF for each one of these contingencies is solved (may be done in parallel). The VSC-OPF solution that presents the lowest $\text{ALC}^{(N-1)}$ is chosen as the final solution. Observe that not necessarily the outage of the line with the highest sensitivity factor will always produce the lowest $\text{ALC}^{(N-1)}$, because of the non-linear nature of the voltage stability constraints in (6.1); hence the need of solving more than one VSC-OPF problem. However, ranking the sensitivity factors leads generally to determine a reduced number of critical areas; $\text{ALC}^{(N-1)}$s associated with outages of high sensitivity lines within a certain area generally show only small differences. Thus, in practice, one needs to evaluate only one contingency constrained VSC-OPF for each critical area that was determined by the sensitivity analysis.

Observe that line outages that cause a separation in islands of the original grid have to be treated in a special way, since the VSC-OPF (6.1) may not converge. In order to solve this problem, the islanded market participants are not committed and the fixed power productions and/or absorptions eliminated. This solution appears to be reasonable especially for realistic transmission grids, which are typically well interconnected, as generally only very few buses result islanded as the consequence of a line outage.

As a final remark, it should be noted that the sensitivity analysis technique discussed here can also be associated with a continuation power flow analysis, thus avoiding the need of running a CPF routine for each line outage as it was stated in the previous section.

7.2.3 Multi-objective VSC-OPF with N-1 Contingency Criterion

Techniques described in the previous Sections 7.2.1 and 7.2.2 assume a fixed value of the weighting factor ω, thus leading to one market solution. However, the multi-objective optimization process which allows defining a Pareto set of the optimization variables as a function of the weighting factor can be obtained simply repeating the proposed techniques for each value of ω.

From a computational point of view, computing the complete Pareto set would be quite expensive, especially for realistic size systems. Nevertheless, in typical systems, a very reduced number of line outages generally leads to find the lowest available loading conditions, as it will be illustrated in the test case discussed in Section 7.3.3.

7.3 Test System Examples

In this section, the VSC-OPF problem (6.1) and the proposed techniques to account for contingencies are applied to a six-bus test system and to a 129-bus model of the Italian HV transmission system. The results of the optimization technique (4.10) are also discussed to observe the effect of the proposed method on LMPs, NCPs and system security, which is represented here through the $\text{ALC}^{(N-1)}$. The power flow limits needed in (4.10) were obtained "off-line", as explained in Section 6.2, by means of a continuation power flow technique [50]. For both test systems, bid load and generator powers were used as the direction needed to obtain a maximum loading point and the associated power flows in the lines, so that proper comparisons with the proposed techniques can be made.

Test cases are organized as follows:

1. Section 7.3.1 and 7.3.2 presents a single-objective VSC-OPF for the six-bus and the 129-bus Italian systems respectively. For both test cases, the limits of the loading parameter were assumed to be $\lambda_{c_{\min}} = 0.1$ and $\lambda_{c_{\max}} = 0.8$, i.e. it is assumed that the system can be securely loaded to an $\text{ALC}^{(N-1)}$ between 110% and 180% of the total transaction level of the given solution. The weighting factor ω in the objective function G of (6.1), used for maximizing the loading parameter, was set to $\omega = 10^{-4}$, as this was determined to be a value that does not significantly affect the market solution.

2. Section 7.3.3 illustrates a Pareto set for the six-bus test system for the multi-objective VSC-OPF with N-1 contingency criterion. In this case loading parameter limits were assumed to be $\lambda_{c_{\min}} = 0.001$ and $\lambda_{c_{\max}} = 0.8$ to better illustrate the effect of security on market solutions. Observe that setting a low value for $\lambda_{c_{\min}}$ does not implies that the current solution has no stability margin, since the worst case contingency is taken in account in the loading parameter computations.

7.3.1 Six-bus Test Case

Table 7.1 depicts the solution of (4.10), which shows a low total transaction level with respect to the max power limits of all bids, and not homogeneous LMPs and NCPs, indicating that system constraints, and, in particular, active power flow limits, are negatively affecting the market solution. The $\text{ALC}^{(N-1)}$ value, which was computed with the continuation power flow, seems to be consistent with the chosen power flow limits and the OPF market solution obtained. Table 7.1 shows also the total losses and the payment given to the Independent Market Operator (referred to as Pay_{IMO}), which is computed as in (6.10).

Table 7.2 illustrates the initial solution of the VSC-OPF problem (6.1). Ob-

Table 7.1: Six-bus test system: OPF with off-line power flow limits

Participant	V p.u.	LMP ($/MWh)	NCP ($/MWh)	P_{BID} (MW)	$P_0^{(N-1)}$ (MW)	Pay ($/h)
GENCO 1	1.1000	9.70	1.26	13.99	67.5	-790
GENCO 2	1.1000	8.45	0.00	0.00	103	-867
GENCO 3	1.1000	7.00	-1.50	20.55	45.0	-459
ESCO 1	1.0415	11.71	2.96	24.56	67.5	1078
ESCO 2	1.0431	10.36	1.60	2.31	75.0	799
ESCO 3	1.0575	9.51	0.88	6.60	67.5	704
TOTALS	TTL = 243.5 MW Losses = 6.2 MW			Pay_{IMO} = 464 $/h $\text{ALC}^{(N-1)}$ = 0.3 MW		

serve that, as expected, the absence of active power flow limits makes possible a higher total transaction level and more homogeneous LMPs and lower NCPs. For the sake of comparison, this table also depicts the value of the $\text{ALC}^{(N-1)}$ obtained "off-line" for this particular operating conditions. Observe that this value is higher than the corresponding TTL as well as the corresponding value in Table 7.1, which is to be expected, as "off-line" power flow limits on lines are not a very good representation of stability. This solution is used as the initial condition for the contingency analysis.

Table 7.3 shows the coefficients p_{hk} used for the sensitivity analysis as well as the $\text{ALC}^{(N-1)}$s computed by means of the continuation power flows technique for the two steps required by the iterative method described in Section 7.2.1 when applying an N-1 contingency criterion. Observe that both methods lead to similar conclusions, i.e. the sensitivity analysis indicates that the line 2-4 has the highest impact in the system power flows, while the N-1 contingency criteria show that

Table 7.2: Six-bus test system: VSC-OPF without contingencies ($\lambda_{c_{\min}} = 0.1$)

Participant	V p.u.	LMP ($/MWh)	NCP ($/MWh)	P_{BID} (MW)	$P_0^{(N-1)}$ (MW)	Pay ($/h)
GENCO 1	1.1000	9.16	-0.012	0.0	67.5	-618
GENCO 2	1.1000	9.06	0.00	37.5	103	-1270
GENCO 3	1.1000	9.15	0.029	30.0	45.0	-686
ESCO 1	1.0302	9.60	0.143	37.5	67.5	1008
ESCO 2	1.0313	9.60	0.172	15.0	75.0	864
ESCO 3	1.0526	9.39	0.131	11.9	67.5	745
TOTALS	TTL = 274.4 MW Losses = 8.25 MW			Pay_{IMO} = 43.9 $/h $\text{ALC}^{(N-1)}$ = 19.1 MW		

the outage of line 2-4 leads to the lowest loadability margin.

Table 7.4 depicts the final VSC-OPF results for the critical line 2-4 outage. This solution presents practically the same total transaction level as provided by the solution without contingencies in Table 7.3, but with different demand side bidding, and, as expected, a higher $\text{ALC}^{(N-1)}$, since the system is now optimized for the given critical contingency. Observe that the rescheduling of demand bids results also in slightly lower LMPs and NCPs, as a consequence of including more precise security constraints, which results in a lower Pay_{IMO} value with respect to the one obtained with the standard OPF problem (4.10) in Table 7.1, but higher losses, since the transaction level is higher.

The $\text{ALC}^{(N-1)}$ in Table 7.4 corresponds to a $\lambda_{c_{\min}} = 0.1$, i.e. 110% of the total transaction level, indicating that the current solution has the minimum required security level ($\lambda_c = \lambda_{c_{\min}} = 0.1$). For the sake of comparison, Table 7.5 depicts the final solution obtained with a different inferior limit for the loading parameter,

Table 7.3: Six-bus test system: Sensitivity coefficients p_{hk} and $\mathrm{ALC}^{(N-1)}$ determined applying an N-1 contingency criterion for two iterations ($\lambda_{c_{\min}} = 0.1$)

Line h-k	$\lvert P_{hk}\rvert$ (p.u.)	p_{hk}	$\mathrm{ALC}_{(1)}^{(N-1)}$ (MW)	$\mathrm{ALC}_{(2)}^{(N-1)}$ (MW)
1-2	0.0463	-0.0219	194.9	200.4
1-4	0.6768	0.3957	110.8	116.2
1-5	0.5263	0.3023	202.9	210.9
2-3	0.1208	0.1114	205.5	210.6
2-4	**1.3872**	**0.8649**	**83.5**	**86.4**
2-5	0.5100	0.3226	184.4	189.8
2-6	0.6211	0.4014	194.4	202.6
3-5	0.5487	0.3258	185.0	190.5
3-6	0.9591	0.5331	165.6	160.4
4-5	0.0351	0.0357	192.4	200.6
5-6	0.1031	0.0656	197.9	206.2

Table 7.4: Six-bus test system: VSC-OPF with contingency on line 2-4 ($\lambda_{c_{\min}} = 0.1$)

Participant	V p.u.	LMP ($/MWh)	NCP ($/MWh)	P_{BID} (MW)	$P_0^{(N-1)}$ (MW)	Pay ($/h)
GENCO 1	1.1000	9.11	-0.013	0.0	67.5	-615
GENCO 2	1.1000	9.02	0.00	37.5	103	-1263
GENCO 3	1.1000	9.12	0.030	30.0	45.0	-684
ESCO 1	1.0312	9.55	0.139	36.0	67.5	989
ESCO 2	1.0313	9.56	0.170	15.0	75.0	860
ESCO 3	1.0518	9.35	0.133	13.3	67.5	756
TOTALS	TTL = 274.3 MW Losses = 8.31 MW			Pay_{IMO} = 43.4 $/h $\text{ALC}^{(N-1)}$ = 27.4 MW		

Table 7.5: Six-bus test system: VSC-OPF with contingency on line 1-4 ($\lambda_{c_{\min}} = 0.125$)

Participant	V p.u.	LMP ($/MWh)	NCP ($/MWh)	P_{BID} (MW)	$P_0^{(N-1)}$ (MW)	Pay ($/h)
GENCO 1	1.1000	8.78	-0.046	0.0	67.5	-671
GENCO 2	1.1000	8.81	0.00	0.0	103	-1045
GENCO 3	1.1000	8.91	0.029	30.0	45.0	-722
ESCO 1	1.0490	9.15	0.082	0.0	67.5	670
ESCO 2	1.0276	9.33	0.152	11.3	75.0	898
ESCO 3	1.0431	9.18	0.137	19.3	67.5	880
TOTALS	TTL = 268.6 MW Losses = 4.52 MW			$\text{Pay}_{\text{IMO}} = 38.9$ $/h $\text{ALC}^{(N-1)} = 33.6$ MW		

i.e. $\lambda_{c_{\min}} = 0.125$. In this case, the line outage that creates the worst congestion problem is determined to be line 1-4. As expected, the higher minimum security margin leads to a lower TTL and, with respect to results reported in Table 7.4, also LMPs and NCPs are generally lower, which is due to the lower level of congestion of the current solution. Observe that a more secure solution leads to lower costs, because the demand model is assumed to be elastic; hence, higher stability margins lead to less congested and "cheaper" optimal solutions.

In this example, the OPF technique does not reach a solution for $\lambda_{c_{\min}} > 0.15$, which means that a solution with at least 15% of security margin is not feasible when taking in account an N-1 contingency criterion. However, it is not reasonable to set high values for $\lambda_{c_{\min}}$, since the resulting security margin takes already in account the most severe contingency, and is thus a conservative estimation of the

system stability level.

7.3.2 129-bus Italian HV Transmission System

Table 7.6 depicts the total results for different OPF problem solutions, i.e. the standard OPF with "off-line" power transfer limits, the VSC-OPF without contingencies and the final results obtained with the proposed techniques for including the worst contingency, which was determined to be the outage of lines in the Milano area (buses Turbigo, Bovisio and Baggio) by both the N-1 contingency criterion and the sensitivity analysis. Conclusions similar to what observed for the six-bus example can be drawn, i.e. the proposed techniques yield a higher TTL and a better $\text{ALC}^{(N-1)}$ value, while reducing the payment to the Italian independent market operator GRTN (Gestore Rete Trasmissione Nazionale). Furthermore, the security constrained OPF solutions of (6.1) show a total loss increase, since the transaction level also increases. Observe that the iterative method and the sensitivity-based technique yield two different critical lines, but provide practically identical results, as the two lines are in the same critical area, i.e. Milano.

Figure 7.2 depicts the comparison of LMPs and NCPs obtained with the standard and the VSC-OPF for an outage of the Turbigo-Baggio line, confirming that a proper representation of voltage stability constraints and worst case contingency result in a better distribution of costs (LMPs) and in a reduced impact of system congestion on electricity prices (NCPs).

7.3.3 Six-bus Test Case with Multi-objective Function and N-1 Contingency Criterion

Figures 7.3, 7.4 and 7.5 depicts the total transaction levels, the critical loading margins λ_c and the available loading capabilities, respectively, for the six-bus test

Table 7.6: Comparison of different OPF-based methods for the Italian system example.

OPF method	Contingency	TTL (GW)	ALC^{N-1} (GW)	Losses (MW)	Pay_{GRTN} (k$/MWh)
OPF (4.10)	"off-line" power flows	19.8	0.04	85.6	21.9
VSC-OPF (6.1)	none	20.8	1.6	96.2	3.21
Iterative VSC-OPF	Turbigo-Bovisio	20.6	2.1	95.2	3.18
VSC-OPF with Sensitivity Analysis	Turbigo-Baggio	20.6	2.4	95.2	3.18

system as functions of the weighting factor ω. Each line in the figures corresponds to the solution of (7.1) assuming in $f_c^{(N-1)}$ a fixed line outage, as indicated in the legends. Observe that the line outages which lead to the lowest λ_c and ALC values are the ones for line 2-4 and line 1-4. Observe that results depicted in Table 7.3, namely sensitivity indexes and ALC obtained with the CPF analysis are consistent with results shown in Figs. 7.4 and 7.5. Thus, even in case of Pareto set computations, one may use results of the sensitivity analysis obtained for the base case solution to determine a reduced number of critical line outages which has to be considered for the multi-objective optimization process. Furthermore, notice that the lowest TTL is not necessarily associated with the line outages which leads to the lowest ALC (observe for example TTLs for line outages on lines 2-6 and 3-6), hence the need of determining the right line outage to avoid erroneous market signals.

7.4 Summary

In this chapter, two methods for including contingencies in a VSC-OPF-based market are proposed and tested on a simple six-bus system as well as on a realistic network. Comparisons between the results obtained with the proposed techniques and those obtained by means of a "standard" OPF-based market model indicate that a proper representation of system security and a proper inclusion of contingencies result in improved transactions, higher security margins and better costs.

The two proposed techniques lead to similar solutions using different strategies. The first method tries to define the worst case contingency by determining the lowest loading condition, while the second approach computes sensitivity factors whose magnitude indicate which line outage is most likely to affect the total transaction level and system security.

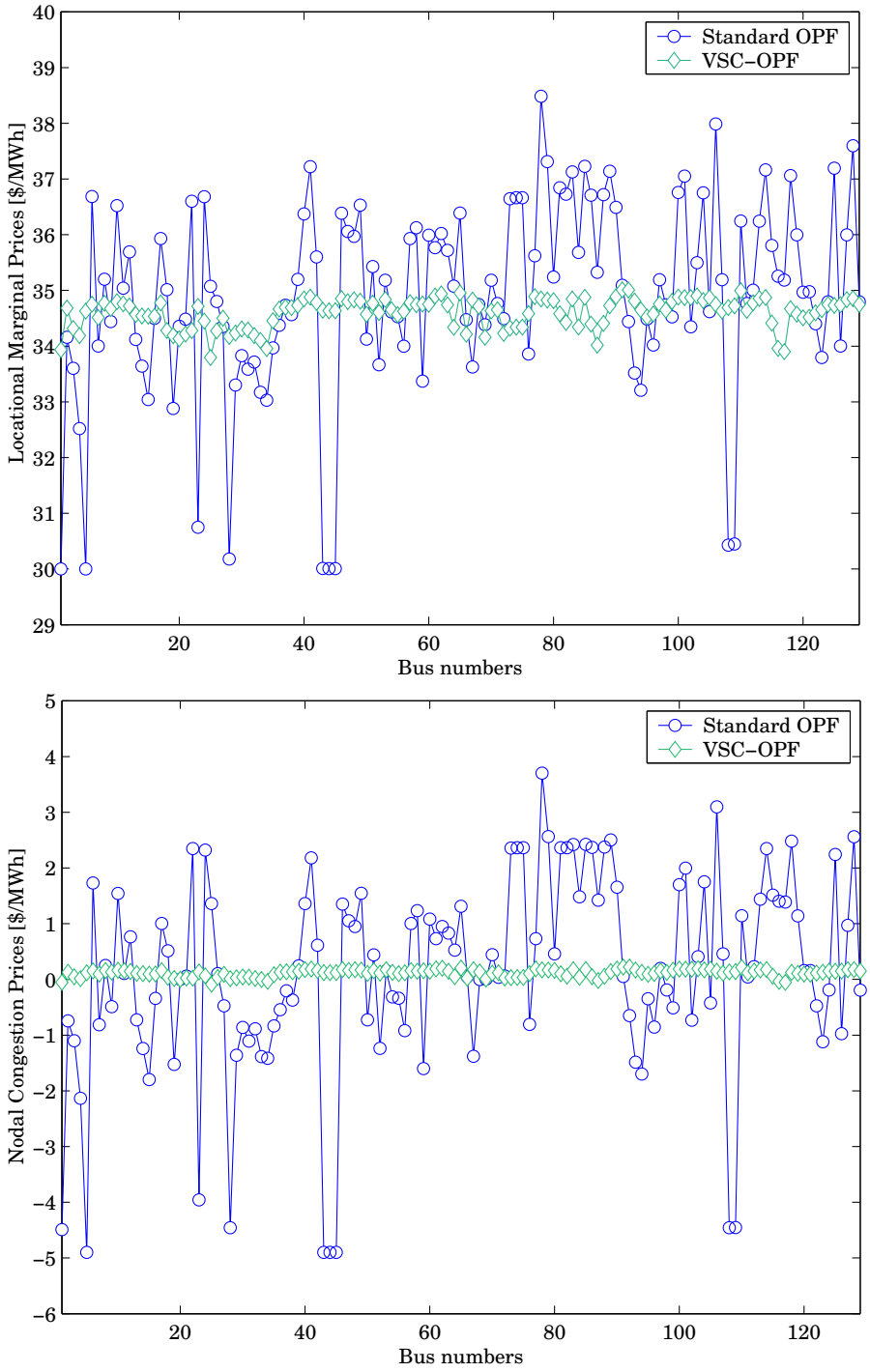

Figure 7.2: Comparison between LMPs and NCPs obtained with the standard and the VSC-OPF with contingency on line Turbigo-Baggio.

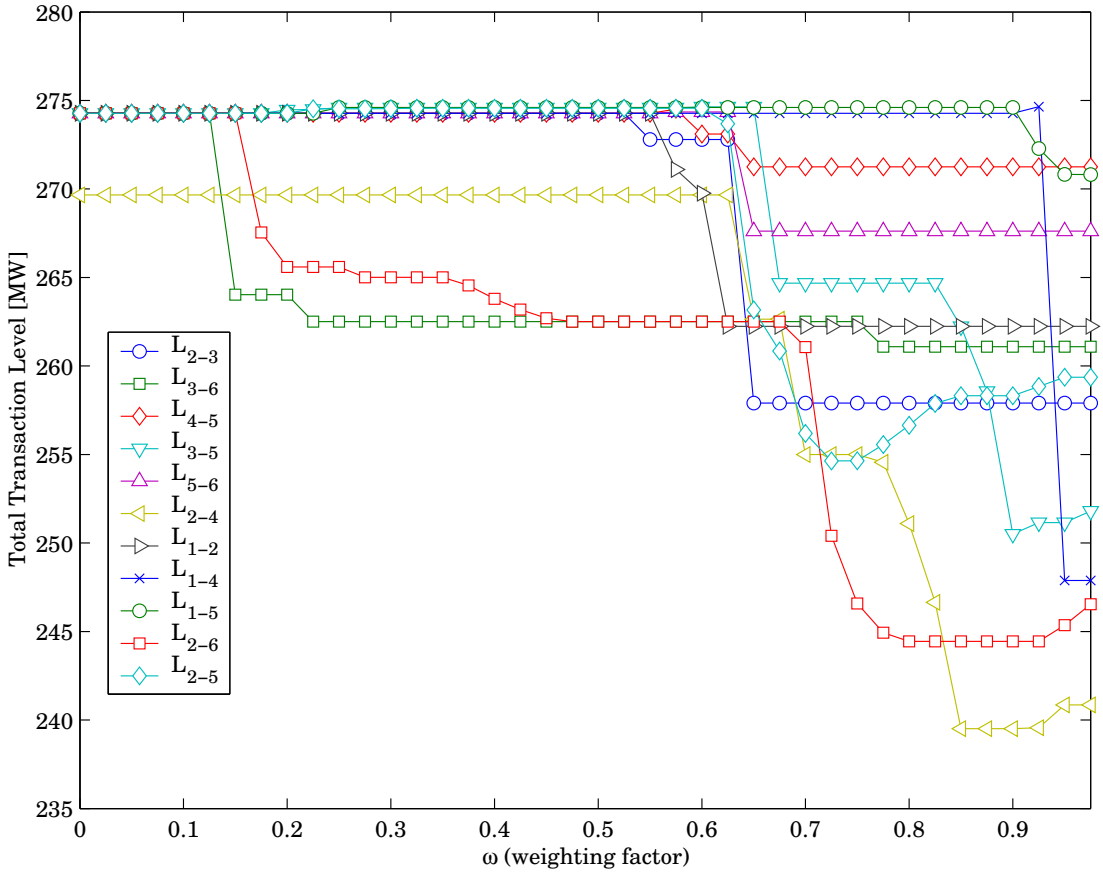

Figure 7.3: TTLs corresponding to line outages (L_{h-k}) for the six-bus system as functions of the weighting factor ω.

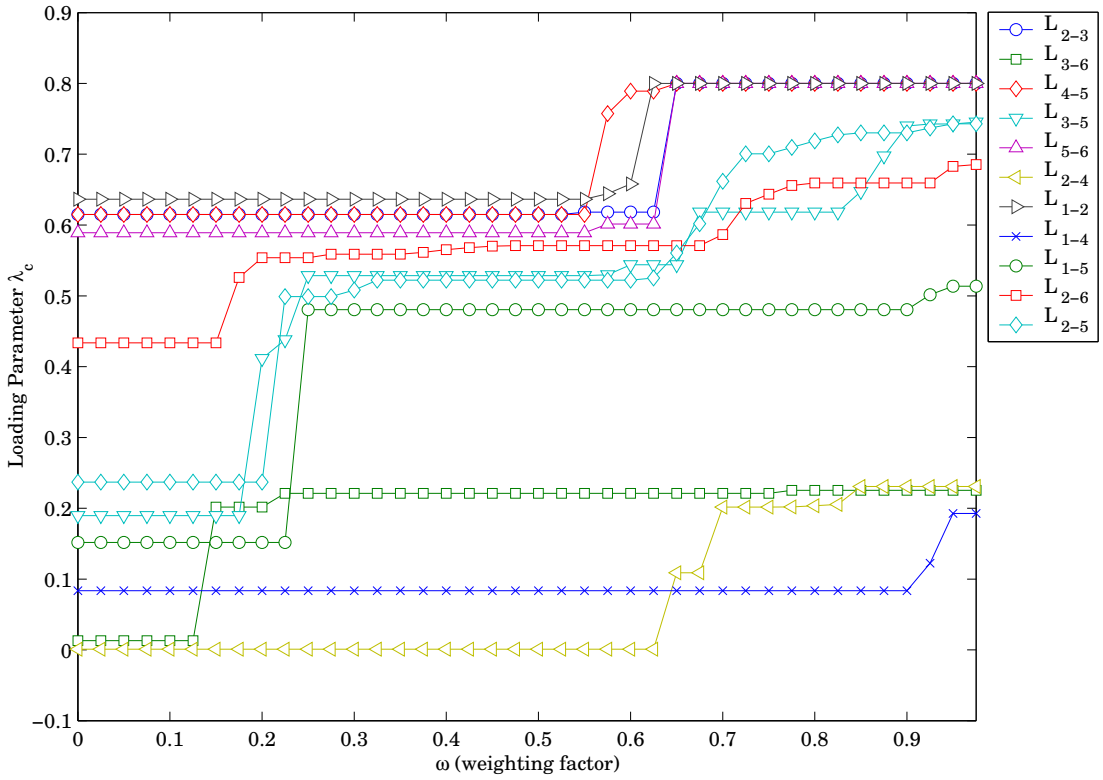

Figure 7.4: Loading parameter λ_c corresponding to line outages (L_{h-k}) for the six-bus system as functions of the weighting factor ω.

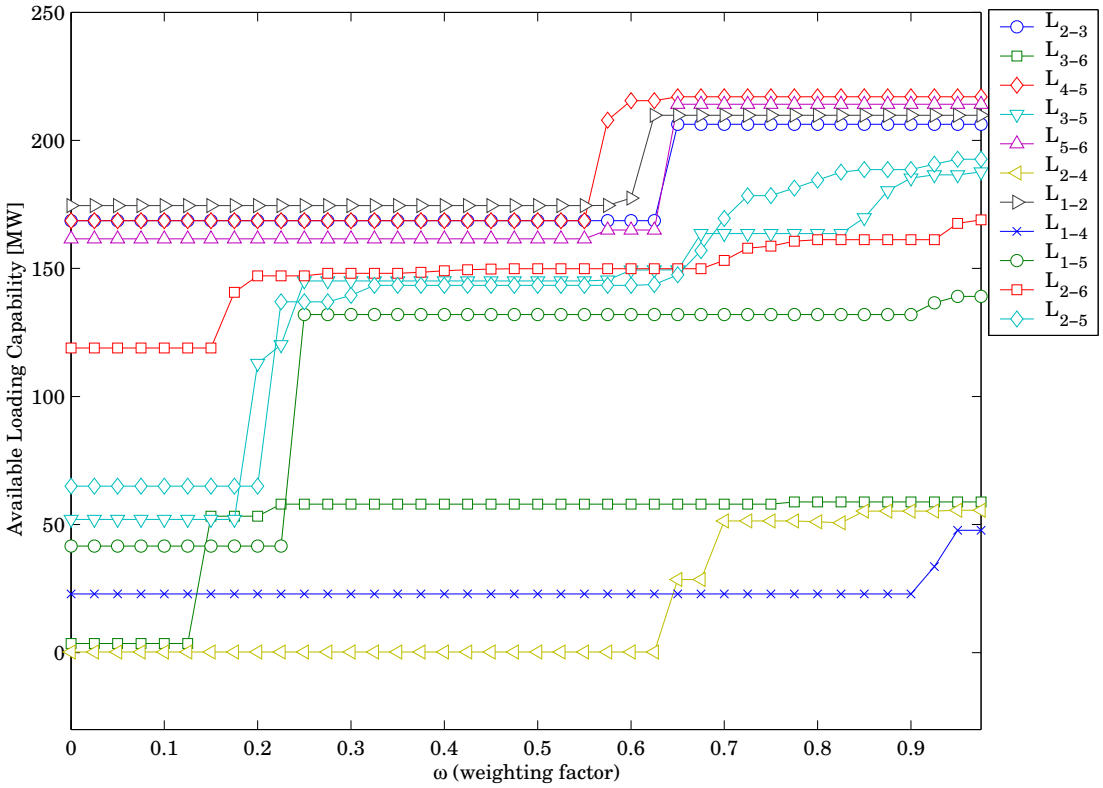

Figure 7.5: ALCs corresponding to line outages (L_{h-k}) for the six-bus system as functions of the weighting factor ω.

Chapter 8

Multi-period Voltage Stability Constrained OPF

8.1 Introduction

THIS chapter presents a Multi-Period Voltage Stability Constrained Optimal Power Flow (MPVSC-OPF), which solves the daily-ahead market taking in account precise security constraints. At this aim, the multi-period OPF model is formulated using time constraints of generator units (i.e. ramp-up and ramp-down limits, minimum up and minimum down times and start-up and shut-down ramp rates) while voltage stability constraints are modeled by means of a loading parameter, as proposed in Chapter 6. N-1 contingency criteria are also discussed and modeled as single line outages in critical equations as presented in Chapter 7. The proposed multi-period OPF-based market technique is tested by means of a six-bus system as well as a 129-bus system which realistically represents the HV Italian network.

8.2 Multi-period Voltage Stability Constrained OPF

The following mixed integer nonlinear programming problem is proposed to represent an OPF market model, based on what has been proposed in [9, 25, 29, 47, 48], so that system security is modeled through the use of voltage stability conditions:

Objective function:

$$\begin{aligned} \text{Max.} \quad G &= \omega \sum_{t\in\mathcal{T}} \lambda_c(t) + (1-\omega)\Bigg(\sum_{t\in\mathcal{T}}\sum_{j\in\mathcal{J}} C_{D_j} P_{D_j}(t) \\ &- \sum_{t\in\mathcal{T}}\sum_{i\in\mathcal{I}} (C_{S_i} P_{S_i}(t) + C_{SU_i} w_i(t) + C_{SD_i} z_i(t))\Bigg) \end{aligned} \tag{8.1}$$

Power Flow Equations:

$$\begin{aligned} P_h(t) &= V_h^2(t)(g_h + g_{h0}) \\ &- V_h(t) \sum_{\ell\neq h}^{n_\ell} V_\ell (g_{h\ell}\cos(\theta_h(t) - \theta_\ell(t)) + b_{h\ell}\sin(\theta_h(t) - \theta_\ell(t))) \\ &\forall h \in \mathcal{B}, \quad \forall t \in \mathcal{T} \end{aligned} \tag{8.2}$$

$$\begin{aligned} Q_h(t) &= -V_h^2(t)(b_h + b_{h0}) \\ &+ V_h(t) \sum_{\ell\neq h}^{n_\ell} V_\ell (g_{h\ell}\sin(\theta_h(t) - \theta_\ell(t)) - b_{h\ell}\cos(\theta_h(t) - \theta_\ell(t))) \\ &\forall h \in \mathcal{B}, \quad \forall t \in \mathcal{T} \end{aligned}$$

$$\begin{aligned} P_h(t) &= \sum_{i\in\mathcal{I}_h} (P_{G_{i0}}(t) + P_{S_i}(t)) - \sum_{j\in\mathcal{J}_h} (P_{L_{0j}} + P_{D_{0j}}) \\ &\forall h \in \mathcal{B}, \quad \forall t \in \mathcal{T} \end{aligned}$$

$$\begin{aligned} Q_h(t) &= \sum_{i\in\mathcal{I}_h} Q_{G_i}(t) - \sum_{j\in\mathcal{J}_h} (P_{L_{0j}} + P_{D_{0j}})\tan(\phi_{D_i}) \\ &\forall h \in \mathcal{B}, \quad \forall t \in \mathcal{T} \end{aligned}$$

"Critical" Power Flow Equations:

$$
\begin{aligned}
P_{c_h}(t) &= V_{c_h}^2(t)(g_h + g_{h0}) \\
&\quad - V_{c_h}(t)\sum_{\ell \neq h}^{n_\ell} V_{c_\ell}(g_{h\ell}\cos(\theta_{c_h}(t) - \theta_{c_\ell}(t)) + b_{h\ell}\sin(\theta_{c_h}(t) - \theta_{c_\ell}(t))) \\
&\quad \forall h \in \mathcal{B}_c, \quad \forall t \in \mathcal{T} \\
Q_{c_h}(t) &= -V_{c_h}^2(t)(b_h + b_{h0}) \\
&\quad + V_{c_h}(t)\sum_{\ell \neq h}^{n_\ell} V_{c_\ell}(g_{h\ell}\sin(\theta_{c_h}(t) - \theta_{c_\ell}(t)) - b_{h\ell}\cos(\theta_{c_h}(t) - \theta_{c_\ell}(t))) \\
&\quad \forall h \in \mathcal{B}_c, \quad \forall t \in \mathcal{T} \\
P_{c_h}(t) &= \sum_{i \in \mathcal{I}_h}(1 + \lambda_c(t) + k_{G_c}(t))(P_{G_{i0}}(t) + P_{S_i}(t)) \\
&\quad - \sum_{j \in \mathcal{J}_h}(1 + \lambda_c(t))(P_{L_{0j}} + P_{D_{0j}}) \\
&\quad \forall h \in \mathcal{B}_c, \quad \forall t \in \mathcal{T} \\
Q_{c_h}(t) &= \sum_{i \in \mathcal{I}_h} Q_{G_{c_i}}(t) - \sum_{j \in \mathcal{J}_h}(1 + \lambda_c(t))(P_{L_{0j}} + P_{D_{0j}})\tan(\phi_{D_i}) \\
&\quad \forall h \in \mathcal{B}_c, \quad \forall t \in \mathcal{T}
\end{aligned}
\tag{8.3}
$$

Supply Bid Blocks:

$$
\begin{aligned}
P_{S_{\min i}}(t)u_i(t) &\leq P_{S_i}(t) \leq \overline{P}_{S_i}(t) \quad \forall i \in \mathcal{I}, \quad \forall t \in \mathcal{T} \\
\overline{P}_{S_i}(t) &\leq P_{S_{\max_i}}[u_i(t) - z_i(t+1)] + z_i(t+1)SD_i \quad \forall i \in \mathcal{I}, \ \forall t \in \mathcal{T} \\
\overline{P}_{S_i}(t) &\leq P_{S_i}(t-1) + RU_i u_i(t-1) + SU_i w_i(t) \quad \forall i \in \mathcal{I}, \quad \forall t \in \mathcal{T} \\
P_{S_i}(t-1) &\leq P_{S_i}(t) + RD_i u_i(t) + SD_i z_i(t) \quad \forall i \in \mathcal{I}, \quad \forall t \in \mathcal{T}
\end{aligned}
\tag{8.4}
$$

Minimum Up Time:

$$\begin{aligned}
\sum_{t=1}^{\Gamma_i}(1-u_i(t)) &= 0 \quad \forall i \in \mathcal{I} \\
\sum_{\tau=t}^{k+UT_i-1} u_i(\tau) &\geq UT_i w_i(t) \quad \forall i \in \mathcal{I}, \\
&\quad \forall t = \Gamma_i + 1 \ldots T - UT_i + 1 \\
\sum_{\tau=t}^{T}(u_i(\tau) - w_i(t)) &\geq 0 \quad \forall i \in \mathcal{I}, \\
&\quad \forall t = T - UT_i + 2 \ldots T
\end{aligned} \tag{8.5}$$

$$\Gamma_i = \min\{T, (UT_i - \alpha_i^0)u_i(0)\} \quad \forall i \in \mathcal{I} \tag{8.6}$$

Minimum Down Time:

$$\begin{aligned}
\sum_{t=1}^{\Pi_i} u_i(t) &= 0 \quad \forall i \in \mathcal{I} \\
\sum_{\tau=t}^{t+DT_i-1} (1-u_i(\tau)) &\geq DT_i z_i(t) \quad \forall i \in \mathcal{I}, \\
&\quad \forall t = \Pi_i + 1 \ldots T - DT_i + 1 \\
\sum_{\tau=t}^{T}(1 - u_i(\tau) - z_i(t)) &\geq 0 \quad \forall i \in \mathcal{I}, \\
&\quad \forall t = T - DT_i + 2 \ldots T
\end{aligned} \tag{8.7}$$

$$\Pi_i = \min\{T, (DT_i - \beta_i^0)(1 - u_i(0))\} \quad \forall i \in \mathcal{I} \tag{8.8}$$

Unit Commitment Blocks:

$$\begin{aligned}
w_i(t) - z_i(t) &= u_i(t) - u_i(t-1) \quad \forall i \in \mathcal{I}, \forall t \in \mathcal{T} \\
w_i(t) + z_i(t) &\leq 1 \quad \forall i \in \mathcal{I}, \forall t \in \mathcal{T}
\end{aligned} \tag{8.9}$$

Demand Bid Blocks:

$$P_{D_{\min j}}(t) \leq P_{D_j}(t) \leq P_{D_{\max j}}(t) \quad \forall j \in \mathcal{J}, \quad \forall t \in \mathcal{T} \tag{8.10}$$

Loading Parameter Blocks:

$$\lambda_{c_{\min}} \leq \lambda_c(t) \leq \lambda_{c_{\max}} \quad \forall t \in \mathcal{T} \tag{8.11}$$

Thermal Limits:

$$\begin{aligned} I_{hk}(t) &\leq I_{hk_{\max}} \qquad \forall (h,k) \in \mathcal{N}, \quad \forall t \in \mathcal{T} \\ I_{kh}(t) &\leq I_{kh_{\max}} \qquad \forall (k,h) \in \mathcal{N}, \quad \forall t \in \mathcal{T} \\ I_{c_{hk}}(t) &\leq I_{hk_{c\max}} \qquad \forall (h,k) \in \mathcal{N}_c, \quad \forall t \in \mathcal{T} \\ I_{c_{kh}}(t) &\leq I_{kh_{c\max}} \qquad \forall (k,h) \in \mathcal{N}_c, \quad \forall t \in \mathcal{T} \end{aligned} \tag{8.12}$$

Generator Reactive Power Blocks:

$$\begin{aligned} Q_{G_i}(t) \;&\leq\; Q_{G_{\max i}} u_i(t) \quad \forall i \in \mathcal{I}, \quad \forall t \in \mathcal{T} \\ Q_{G_{c\min_i}} u_i(t) \;&\leq\; Q_{G_{c_i}}(t) \;\leq\; Q_{G_{c\max_i}} u_i(t) \quad \forall i \in \mathcal{I}, \quad \forall t \in \mathcal{T} \end{aligned} \tag{8.13}$$

Voltage "Security" Limits:

$$\begin{aligned} V_{h_{\min}} \;&\leq\; V_h(t) \;\leq V_{h_{\max}} \qquad \forall h \in \mathcal{B}, \quad \forall t \in \mathcal{T} \\ V_{c_{h_{\min}}} \;&\leq\; V_{c_h}(t) \leq V_{c_{h_{\max}}} \quad \forall h \in \mathcal{B}_c, \quad \forall t \in \mathcal{T} \end{aligned} \tag{8.14}$$

where most of the variables are defined in Chapter 4 and $\mathcal{I}_h$ and $\mathcal{J}_h$ are subsets of generator units and power consumer blocks connected to bus h. The subscript c indicates variables and sets of "critical" power flow equations. Observe that unit commitment variables u as well as power supplies P_S and power demands P_D are shared by the actual and the critical power flow equations, thus ensuring that

the critical power flow solution for each time period t represents the maximum loading condition for the associated actual solution.

Equations (8.10) are for the inelastic demand model and $P_{D_{\min j}}(t)$ and $P_{D_{\max j}}(t)$ are the consumer demand limits for each time periods. $P_{D_{\min j}}(t)$, $P_{D_{\max j}}(t)$ and the fixed power consumptions $P_{L_{0j}}(t)$ define the lower and the upper bounds for the daily-ahead power demand. Figure 8.1 depicts the lower and the upper demand curves for the six-bus system example. The total power demand is covered by must-run and fixed generations $P_{G_{0j}}(t)$ and supply bids $P_{S_j}(t)$, the latter being regulated by minimum up and minimum down times and start-up and shut-down ramp rates (8.4), minimum ramp-up (8.5) and ramp-down (8.7) constraints and unit commitment (8.9). Constraints (8.4), (8.5), (8.7) and (8.9) are for thermal plants. Reservoirs and/or regulated hydro plants logics are neglected, although used in practice for balancing daily load peaks; however hydro plant bids have been considered in the market auction (see the Italian system example discussed in Section 8.3.2). Future researchs may improve the proposed model by including detailed hydro plant logics.

In the literature, multi-period market clearing mechanisms are typically formulated as linear or quadratic programming techniques (e.g. [27, 47, 65]) which can be solved by robust MIP techniques. As discussed in Chapter 4, these techniques do not allow including system congestions or voltage stability constraints. (An iterative technique for coupling voltage stability constraints through continuation power flow analysis with simple auction-based competitive market has been proposed in [11].) Thus, the proposed multi-period VSC-OPF will be compared to a multi-period security constrained OPF similar to (4.10), which includes power

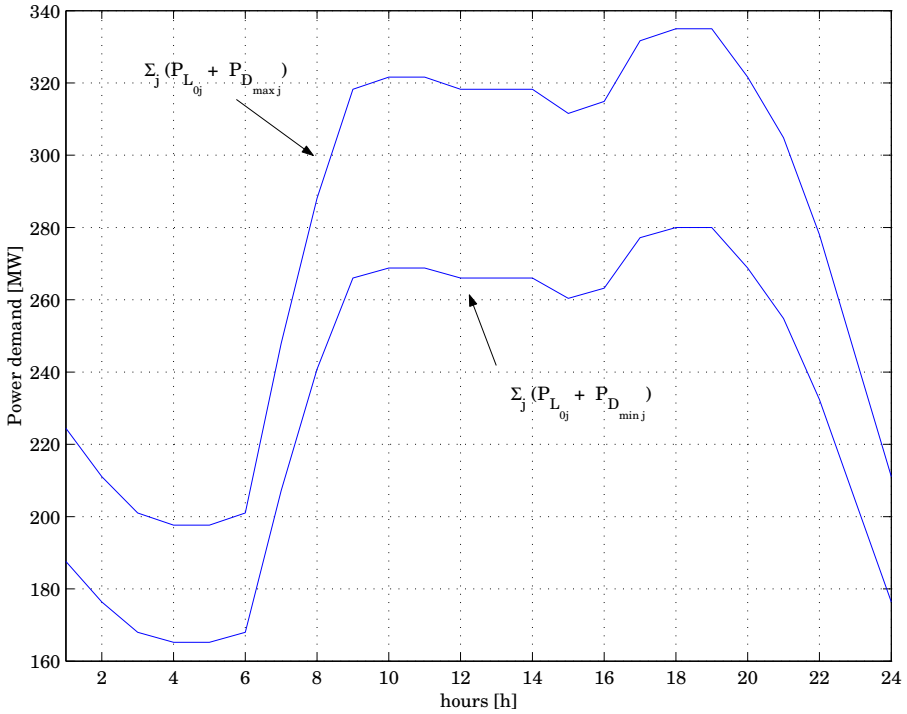

Figure 8.1: Consumer bid limits for the daily-ahead market schedule with inelastic demand model (curves refer to the 6-bus test system).

flow transfer limits computed off-line and extended to a time horizon T:

$$\begin{aligned} |P_{hk}(t)| \leq & P_{hk_{\max}} \qquad \forall (h,k) \in \mathcal{N}, \quad \forall t \in \mathcal{T} \\ |P_{kh}(t)| \leq & P_{kh_{\max}} \qquad \forall (k,h) \in \mathcal{N}, \quad \forall t \in \mathcal{T} \end{aligned} \tag{8.15}$$

For the sake of comparison with the VSC-OPF, in the multi-period security constrained OPF minimum up and minimum down times and start-up and shut-down ramp rates (8.4), minimum ramp-up (8.5) and ramp-down (8.7) constraints and unit commitment (8.9) will be included as well.

Observe that the proposed multi-period VSC-OPF can be quickly modified to take into account contingencies as discussed in Chapter 7, by imposing a line outage in "critical" power flow equations (8.3). However, since the iterative technique which make use of a continuation power flow analysis for including the N-1 contin-

gency criterion would result computational demanding for the daily-ahead market problem, only the solution of a reduced number of VSC-OPF problems based on sensitivity ranking of transmission line currents will be used in the six-bus system example presented in Section 8.3.1.

As a final remark, locational marginal prices and nodal congestion prices are formulated as in (6.8) and (6.9), respectively, for each scheduled hour. Note that LMP values are affected by the weighting factor ω and in order to correctly compute LMPs the procedure described in Section 6.2.3 is needed.

8.3 Test System Examples

In this section the proposed multi-period VSC-OPF is tested on a six-bus system as well as on a 129-bus model of the HV Italian network. The six-bus system is used first to compare results of the proposed VSC-OPF with the ones obtained by means of a standard security constrained OPF. Then results obtained varying the weighting factor ω are presented and discussed for both elastic and inelastic demand models. Finally, a multi-period VSC-OPF with inclusion of N-1 contingency criteria is illustrated for the sake of completeness. The 129-bus model of the HV Italian system is also used to compare results of the proposed VSC-OPF with the ones obtained by means of a standard security constrained OPF and to demonstrate the reliability of the proposed technique for realistic size networks. Test system data are reported in Appendices B and C for the six-bus and the 129-bus systems, respectively.

8.3.1 Six-bus Test Case

Comparison between the Multi-period VSC-OPF and the Standard Security Constrained OPF

Figure 8.2 depicts the total transaction levels for the six-bus example obtained by means of the proposed multi-period VSC-OPF and the standard security constrained OPF with power flow limits computed off-line. For the sake of comparison, it has been assumed a $\omega = 0.0001$ in (8.1), so that the social benefit is mostly maximized. Observe that the proposed VSC-OPF gives a higher TTL for the more congested hours, as expected, since this result is in accordance with the results obtained for the single-period VSC-OPF described in Chapter 6.

Figure 8.3 illustrates the loading parameter λ_c and the associated ALC for the multi-period VSC-OPF. Note that the upper loading parameter limit $\lambda_{c_{\max}}$ has not been fixed, in order to better show the actual maximum loading margins for the daily-ahead market. As expected, the higher the power demand, the lower the λ_c and ALC. Following Figs. 8.4, 8.5, 8.6 and 8.7 are shown to compare power supplies, power demands, LMPs and NCPs for the standard OPF and the VSC-OPF. These figures confirm that the more the power demand, the higher the electricity prices since as the power demand increases, more and more expensive generators are needed and included in the market. However, the VSC-OPF leads to smoother power profiles, lower locational marginal prices and lower congestion costs, which is the added value of the proposed technique.

Pareto Set of the Multi-period VSC-OPF with Elastic and Inelastic Demand Model

Figures 8.8 and 8.9 depict the TTL, ALC, the Total Demand Pay (TDP = $\sum_{j\in\mathcal{J}} \mathrm{LMP}_j P_{L_j}$) and the IMO pay for the six-bus test system obtained solving

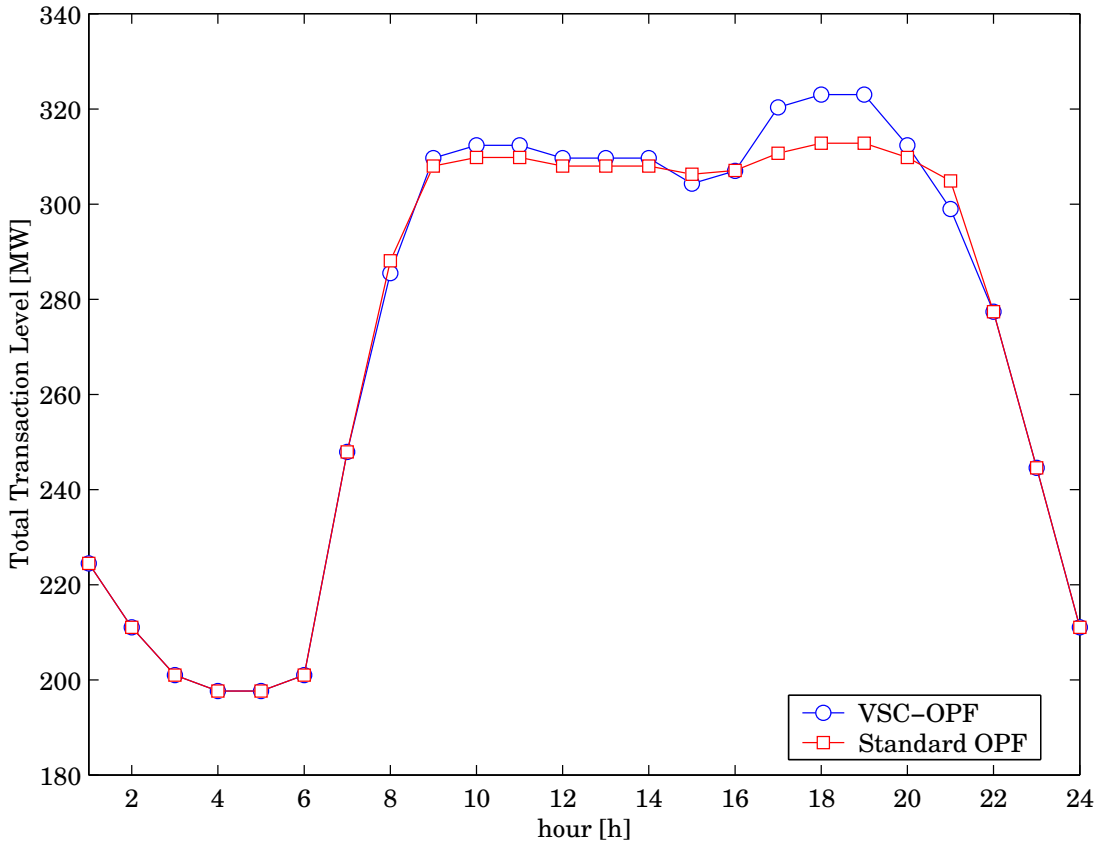

Figure 8.2: Comparison of daily-ahead total transaction level for the six-bus test system obtained with the standard OPF with off-line power flow limits on transmission lines and the VSC-OPF.

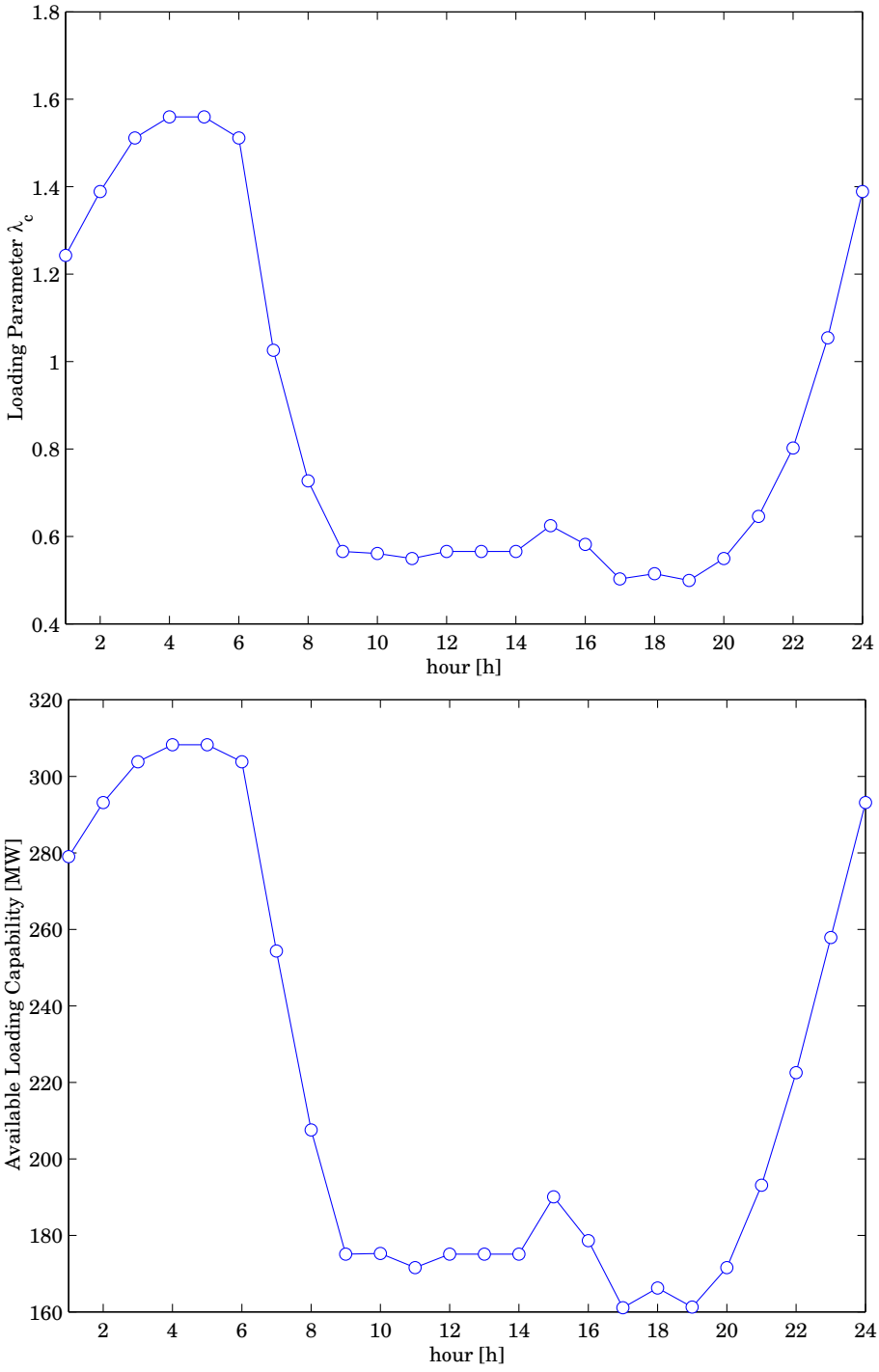

Figure 8.3: Daily-ahead power loading parameter and ALC for the six-bus test system obtained with the VSC-OPF.

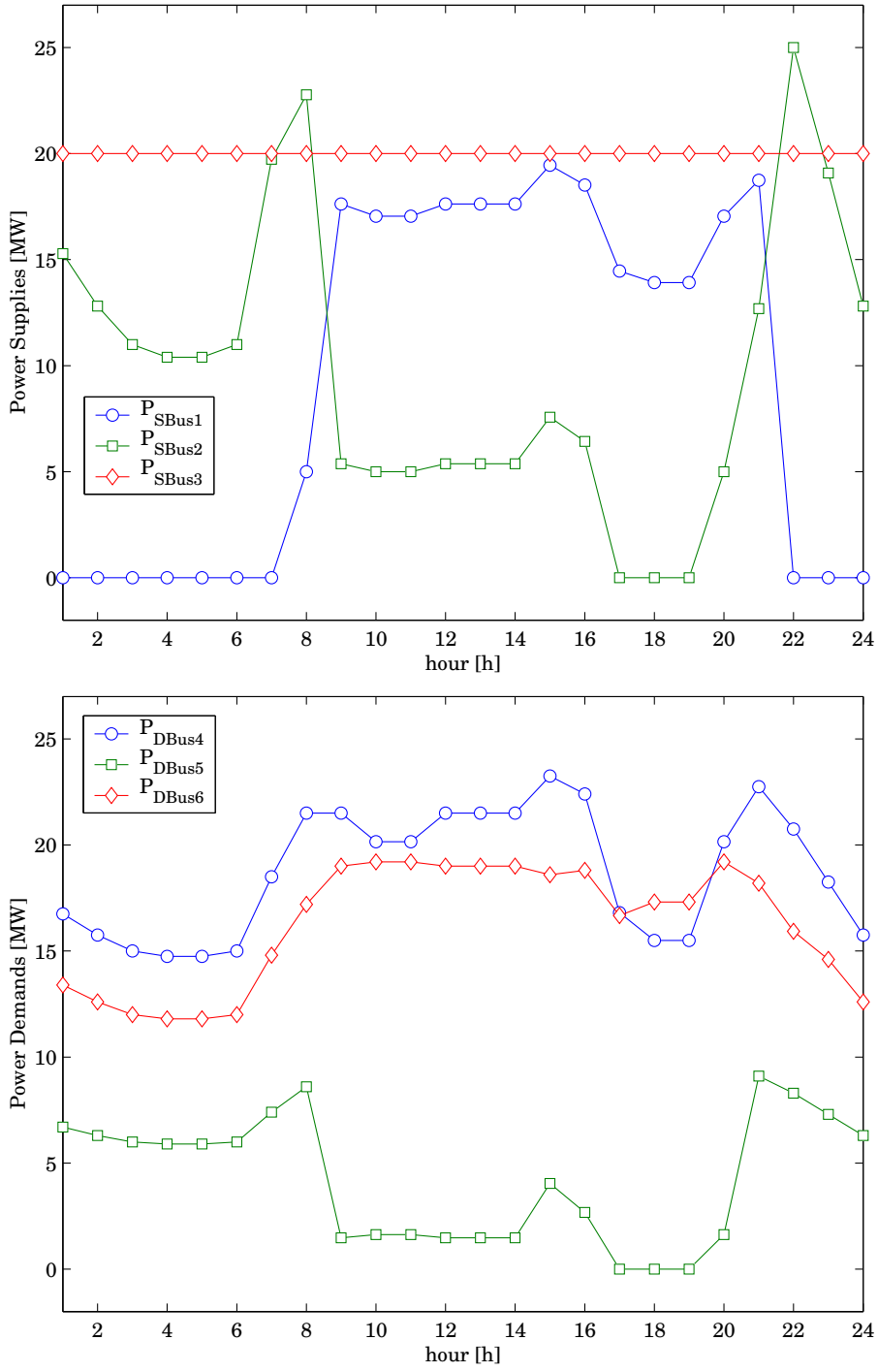

Figure 8.4: Daily-ahead power supplies P_S and demands P_D for the six-bus test system with off-line power flow limits on transmission lines.

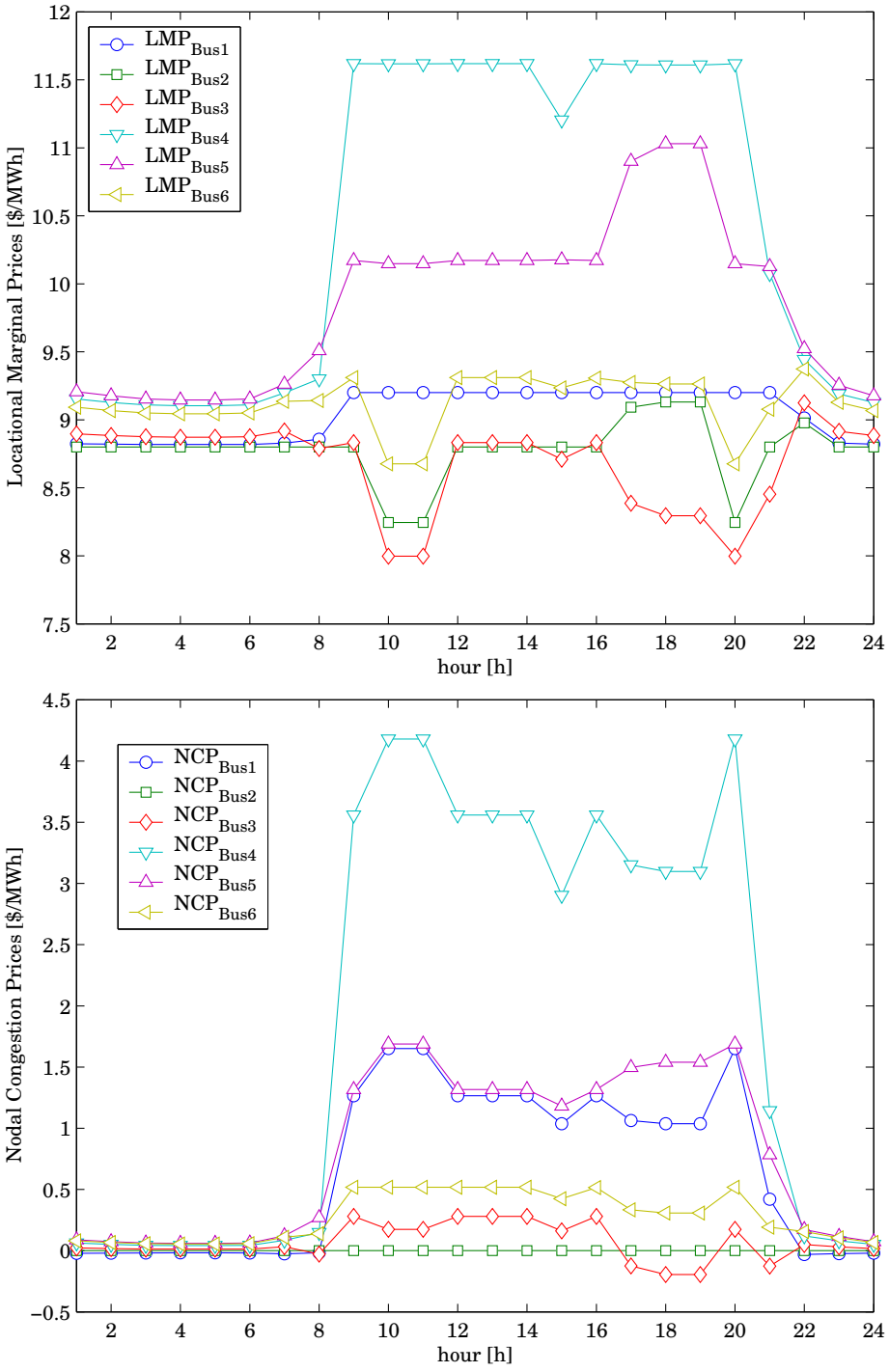

Figure 8.5: Daily-ahead LMPs and NCPs for the six-bus test system with off-line power flow limits on transmission lines.

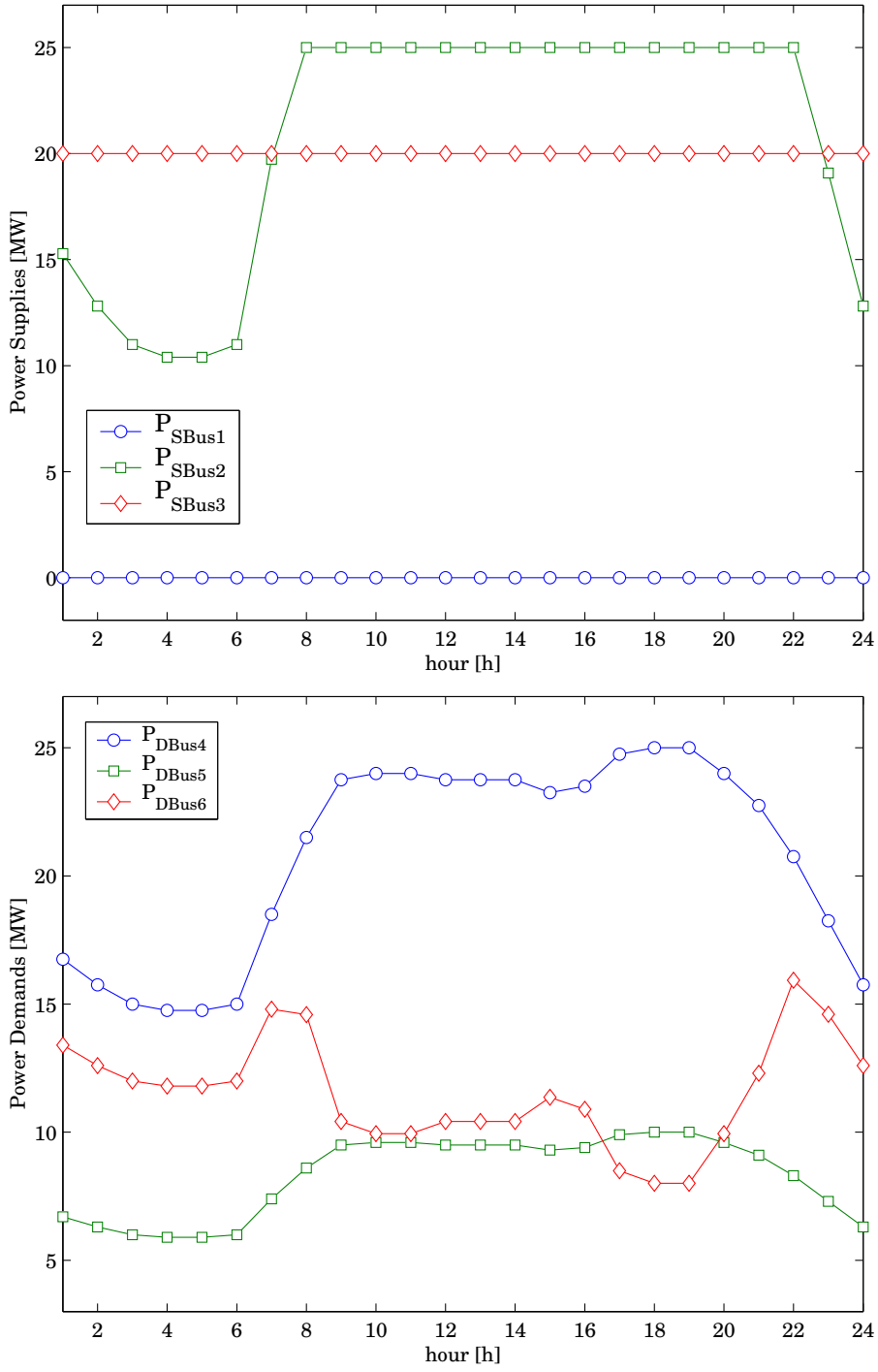

Figure 8.6: Daily-ahead power supplies P_S and demands P_D for the six-bus test system obtained with the VSC-OPF.

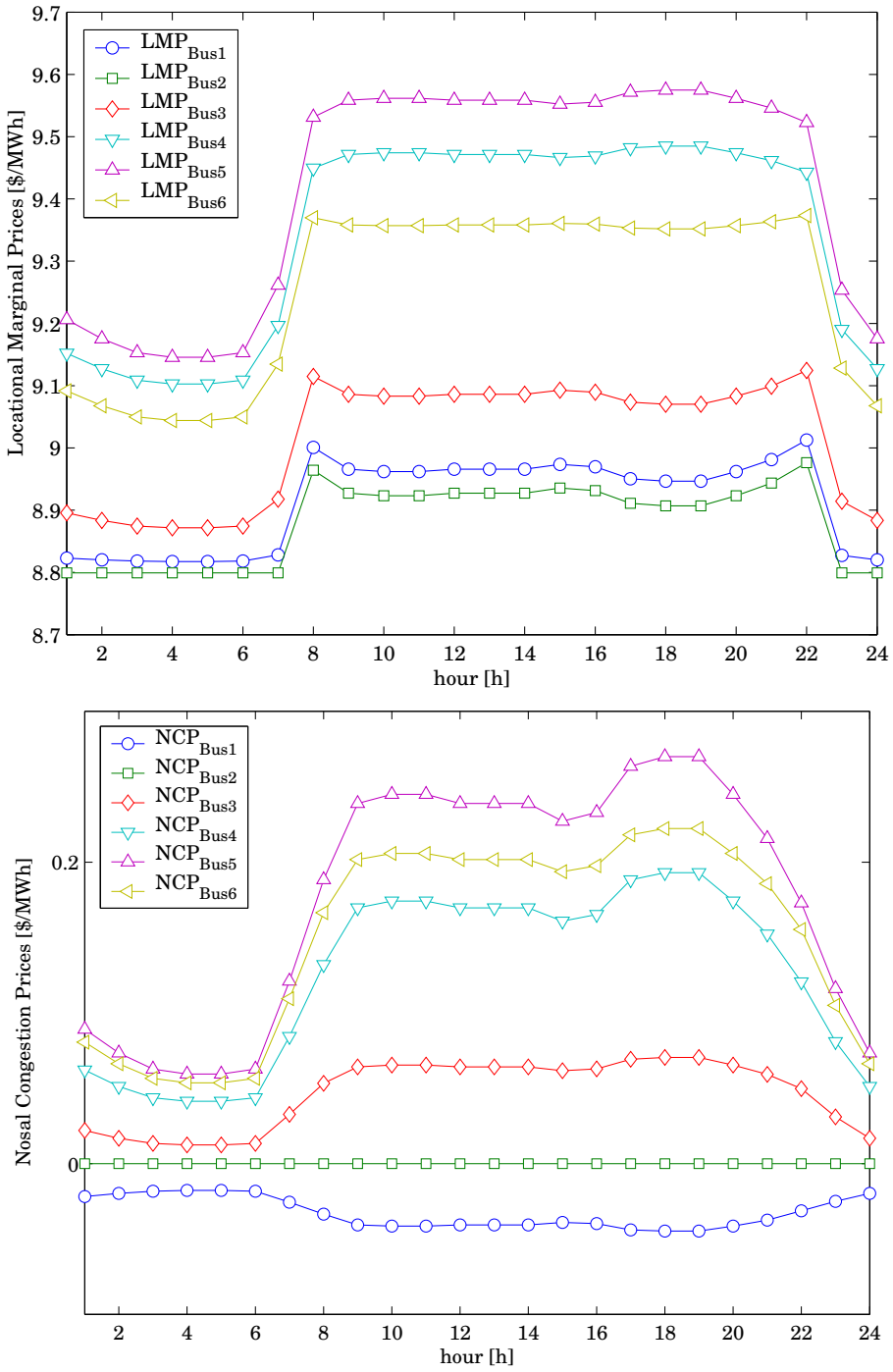

Figure 8.7: Daily-ahead LMPs and NCPs for the six-bus test system obtained with the VSC-OPF.

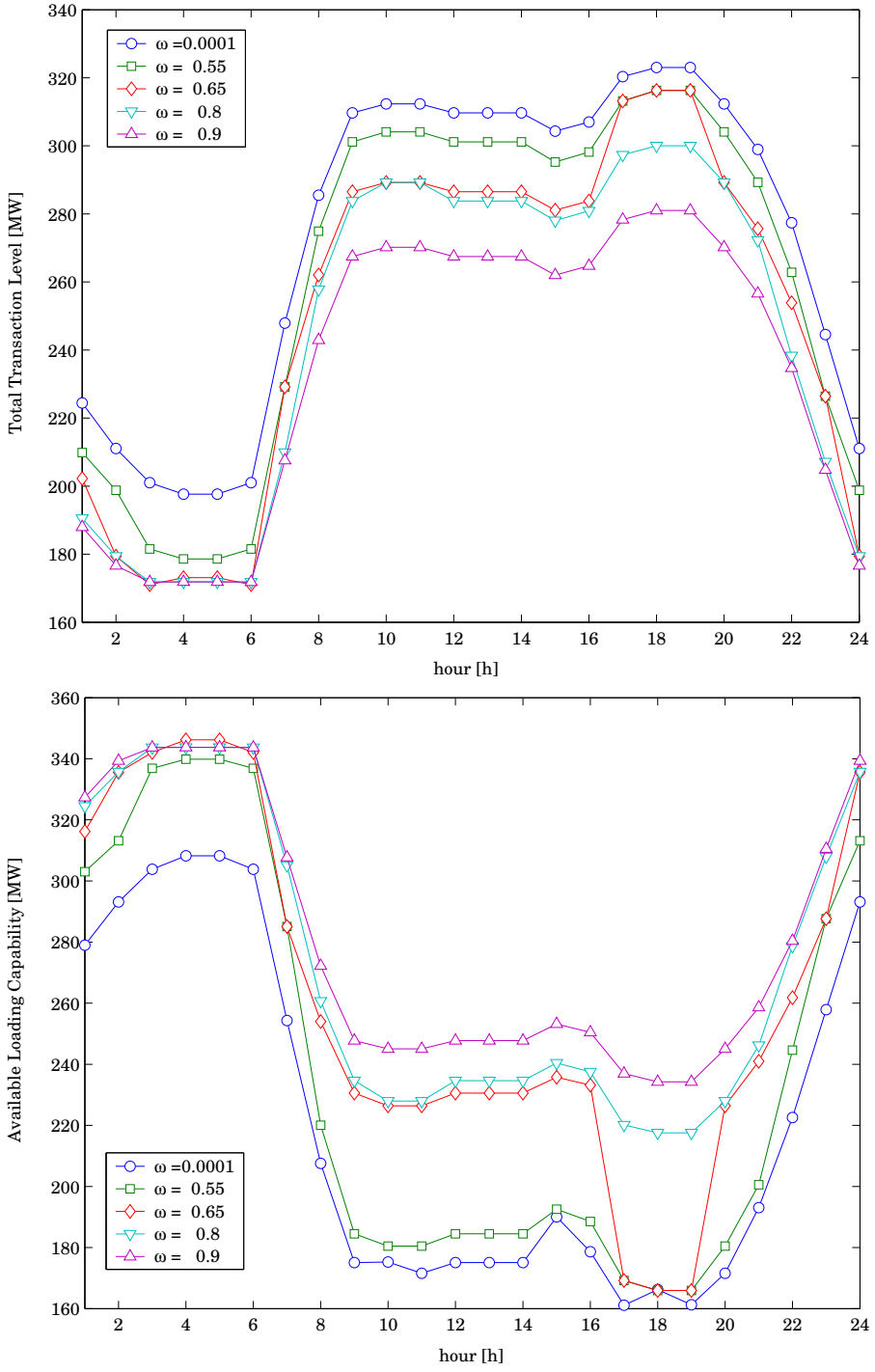

Figure 8.8: TTL and ALC for different weighting factors ω and with elastic demand model for the six-bus test system.

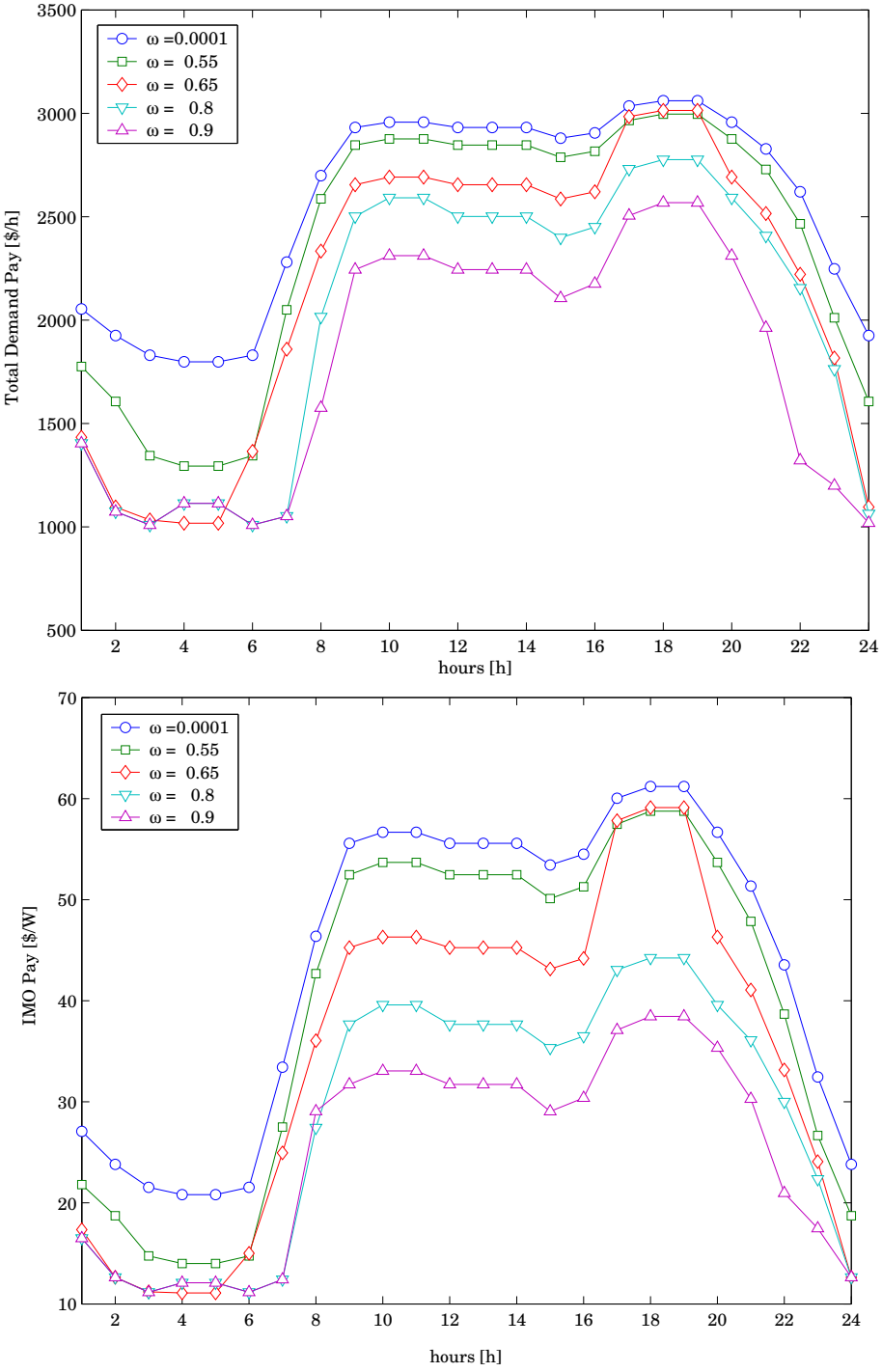

Figure 8.9: Total demand and IMO pay for different weighting factors ω and with elastic demand model for the six-bus test system.

the multi-period VSC-OPF for different values of the weighting factor ω. As expected, as the level of the desired security increases, i.e. as the weighting factor increases, TTL value and electricity (TDP) and congestion (IMO pay) costs decrease while ALC value increases. These results are consistent with what obtained for the single period VSC-OPF and are due to the elastic demand model used for the demand side bids.

Figures 8.10 and 8.11 illustrate the same quantities, i.e. TTL, ALC, TDP and IMO pay, but for the inelastic demand model. In this case, the TTL is forced to be a constant value for each scheduled hour (the values used in the example are the same as those obtained for the elastic demand model with $\omega = 0.0001$, to allow for a fair comparison). The fixed power demand level leads to a cost increase as the security increases, as it might be expected and in accordance with results obtained for the single-period VSC-OPF problem.

Multi-period VSC-OPF with Inclusion of N-1 Contingency Criterion

The inclusion of an N-1 contingency criterion has been realized using results of sensitivity analysis presented in Chapter 7, i.e. five multi-period VSC-OPF have been computed including in the "critical" power flow equations (8.3) contingencies on the five lines which presents the highest sensitivity factors (see Table 7.3).

Figure 8.12 depicts the TTL and the ALC and were obtained using a weighting factor $\omega = 0.0001$, which allows maximizing mostly the social benefit and $\lambda_{c_{\min}} = 0.0001$, to better illustrate effects of line outages on system security and stability margins. Observe that all line outages leads to practically the same TTL (as it might be expected the TTL of Fig. 8.12 is lower than the ones depicted in Fig. 8.2 since the inclusion of a first class contingency criterion significantly reduces the stability margin), while provide quite different ALC values. In accordance with results discussed in Chapter 7, the outage of line 2-4 is confirmed to be the most

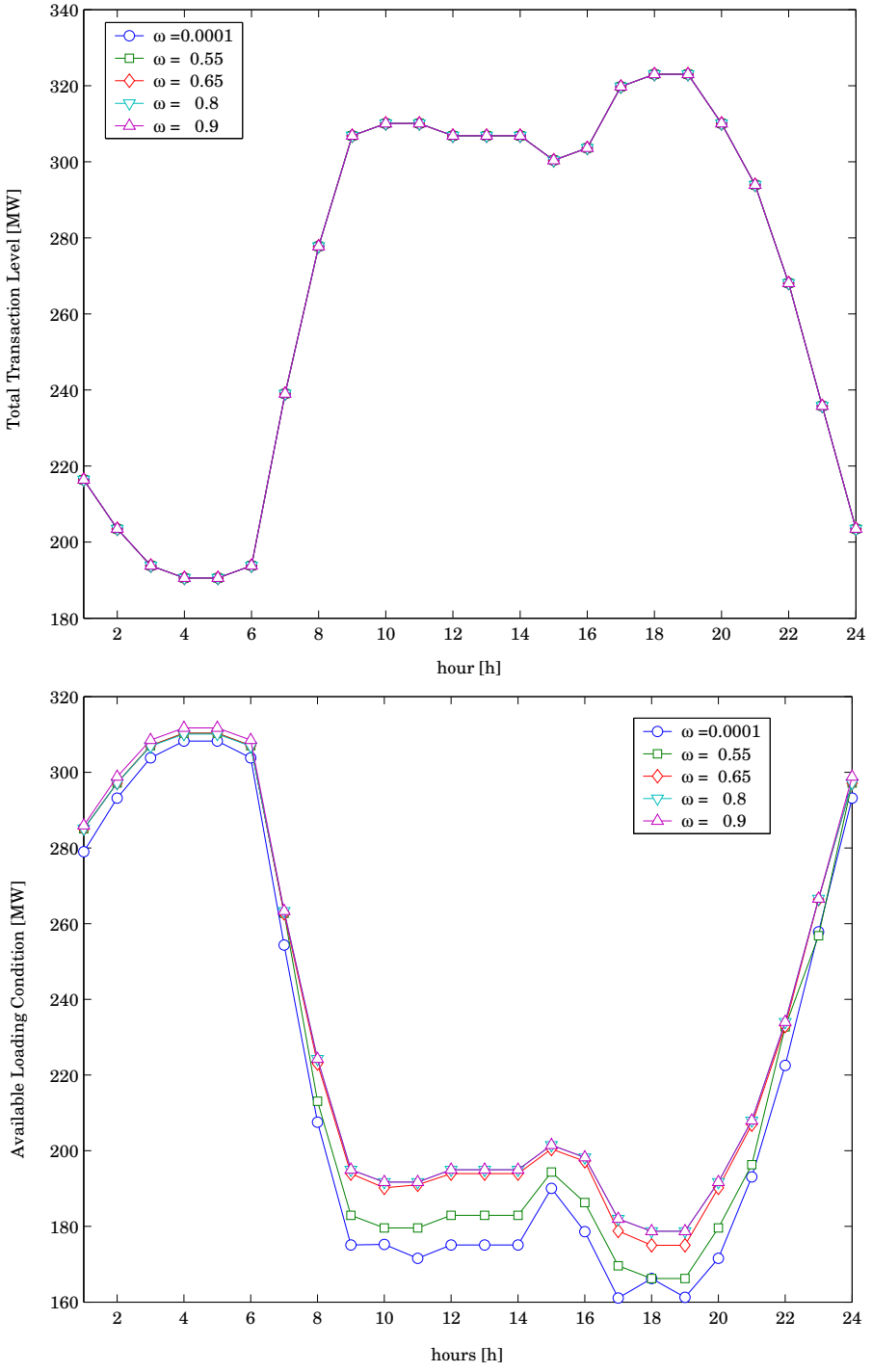

Figure 8.10: TTL and ALC for different weighting factors ω and with inelastic demand model for the six-bus test system.

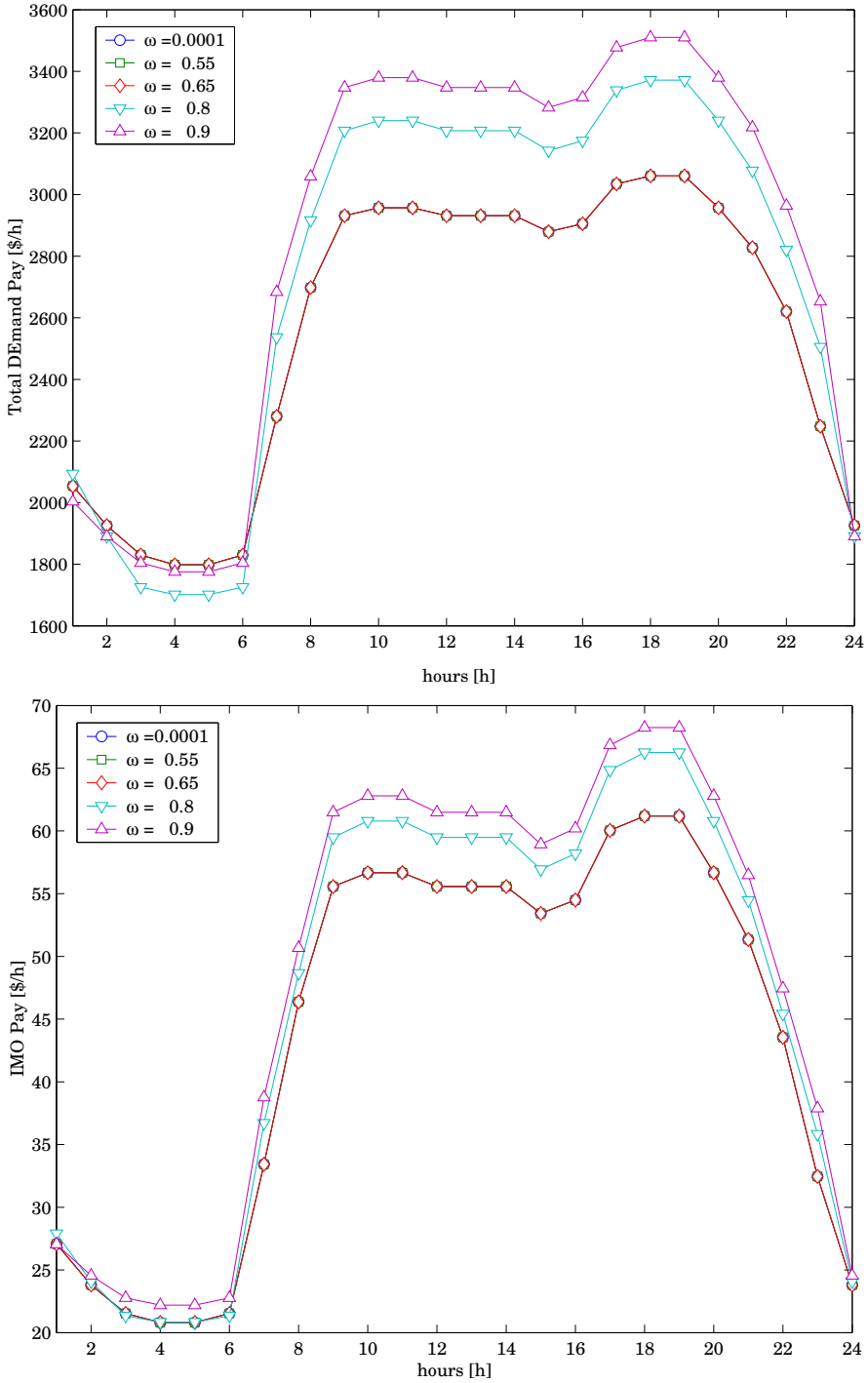

Figure 8.11: Total demand pay and IMO pay for different weighting factors ω and with inelastic demand model for the six-bus test system.

critical one, since it leads to the lowest ALC.

8.3.2 129-bus Italian HV Transmission System

A multi-period VSC-OPF for the 129-bus model of the HV Italian transmission system is illustrated in this section to prove reliability of the proposed technique in case of realistic size examples. However, due to GAMS limits (the complete multi-period VSC-OPF model for the Italian system exceeds the maximum allowed number of system equations), only a relaxed mixed integer nonlinear programming problem has been solved. Results for the multi-period VSC-OPF have been obtained assuming $\omega = 0.0001$, $\lambda_{c_{\min}} = 0.1$ and $\lambda_{c_{\max}} = 0.8$ for the weighting factor and the minimum and maximum loading parameter limits respectively.

Figure 8.13 depicts the scheduled total transaction level for the daily-market, which is compared with the total transaction level obtained by means of the standard security constrained OPF. Observe that the proposed technique provides a higher TTL for all time horizon (not only at heavy-load hours). It is interesting to note that the solution of the multi-period VSC-OPF proved to be numerically more stable than the standard security constrained OPF. This fact is likely due to the difficulties in finding a good initial guess and to the maximum number of iterations associated when imposing power flow limits computed off-line.

Figure 8.14 depicts the available loading capability as determined by the VSC-OPF method. Minimum ALC values correspond to heavy-load hours, which are characterized by higher transmission costs (i.e. the pay to the Italian Independent Market Operator GRTN), as illustrated in Fig. 8.15.

Finally, Figs. 8.16, 8.17 and 8.18 show power bids, LMPs and NCPs for some significant suppliers (Trino, Tavazzano, Turbigo, and Fusina) and consumers (S. Sofia, Galatina, Colunga, and Roma Ovest). For the sake of comparison, market participants depicted here are the same as those illustrated in Figs. 6.18, 6.19 and

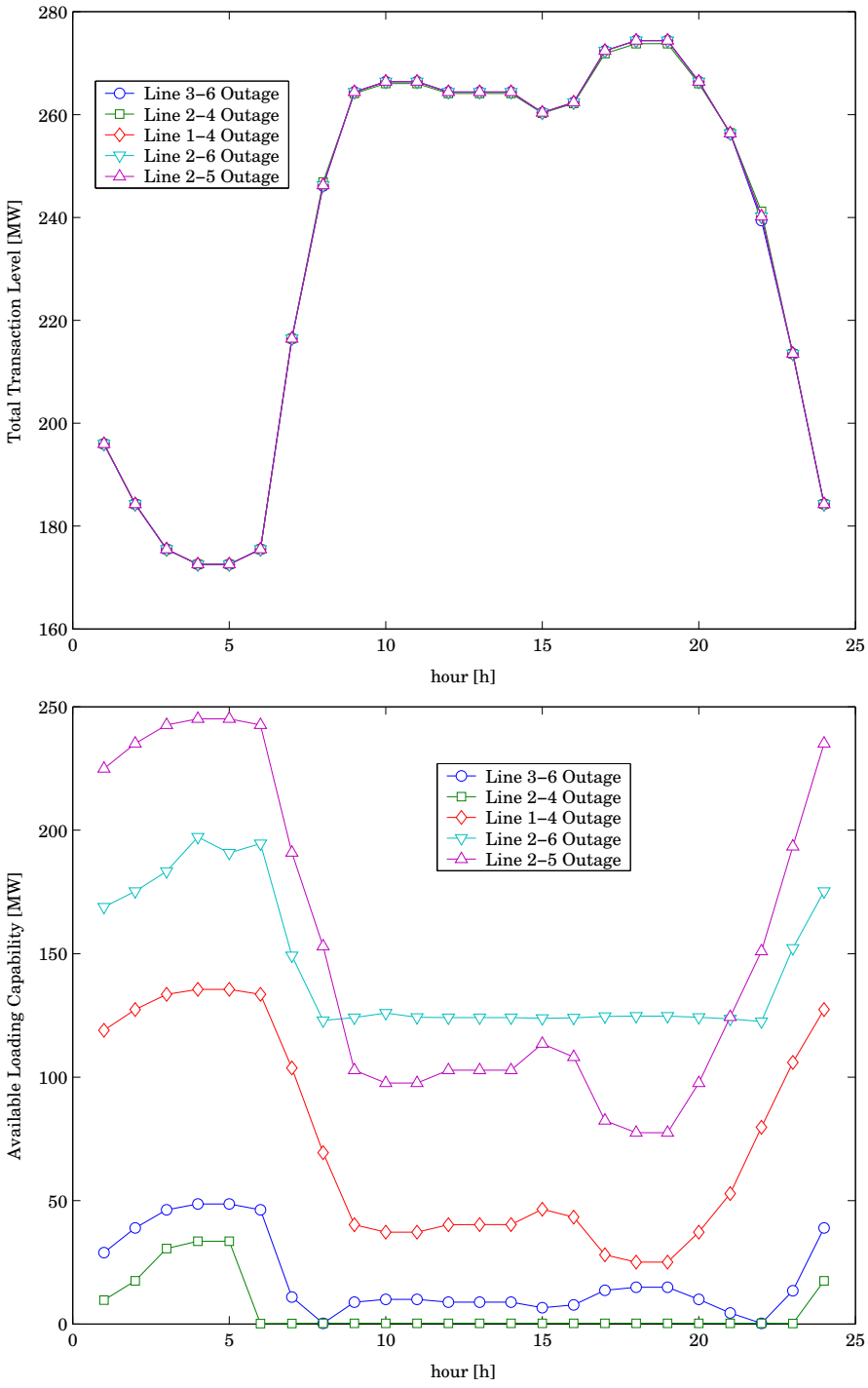

Figure 8.12: TTL and ALC for different line outages and with elastic demand model for the six-bus test system.

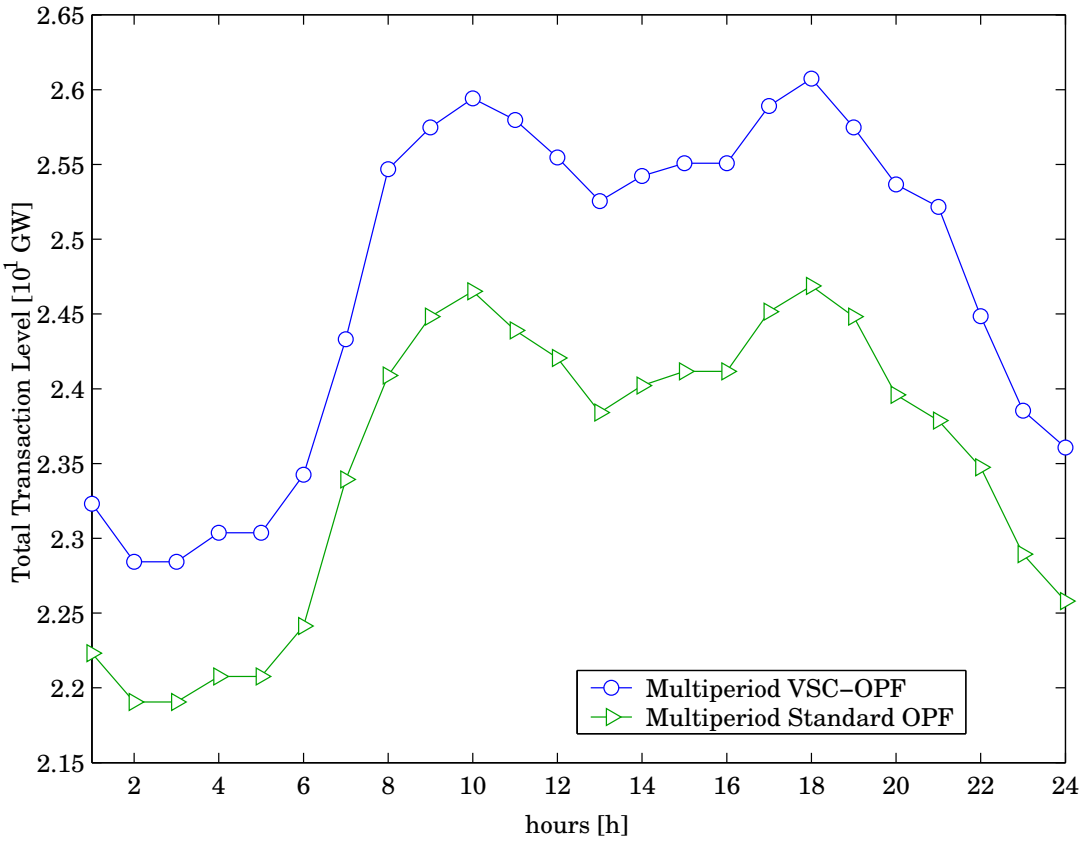

Figure 8.13: Comparison of TTLs for the 129-bus model of the HV Italian system, obtained by means of the multi-period VSC-OPF and the standard security constrained OPF.

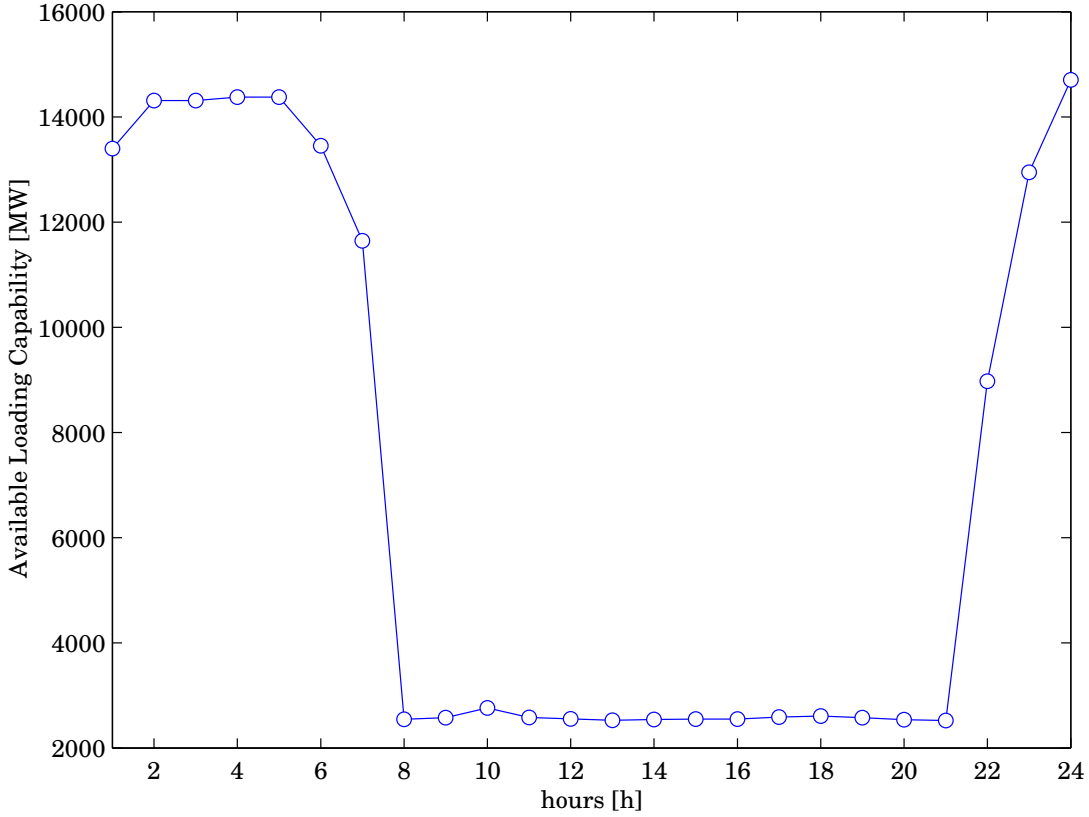

Figure 8.14: ALC for the 129-bus model of the HV Italian system, obtained by means of the multi-period VSC-OPF.

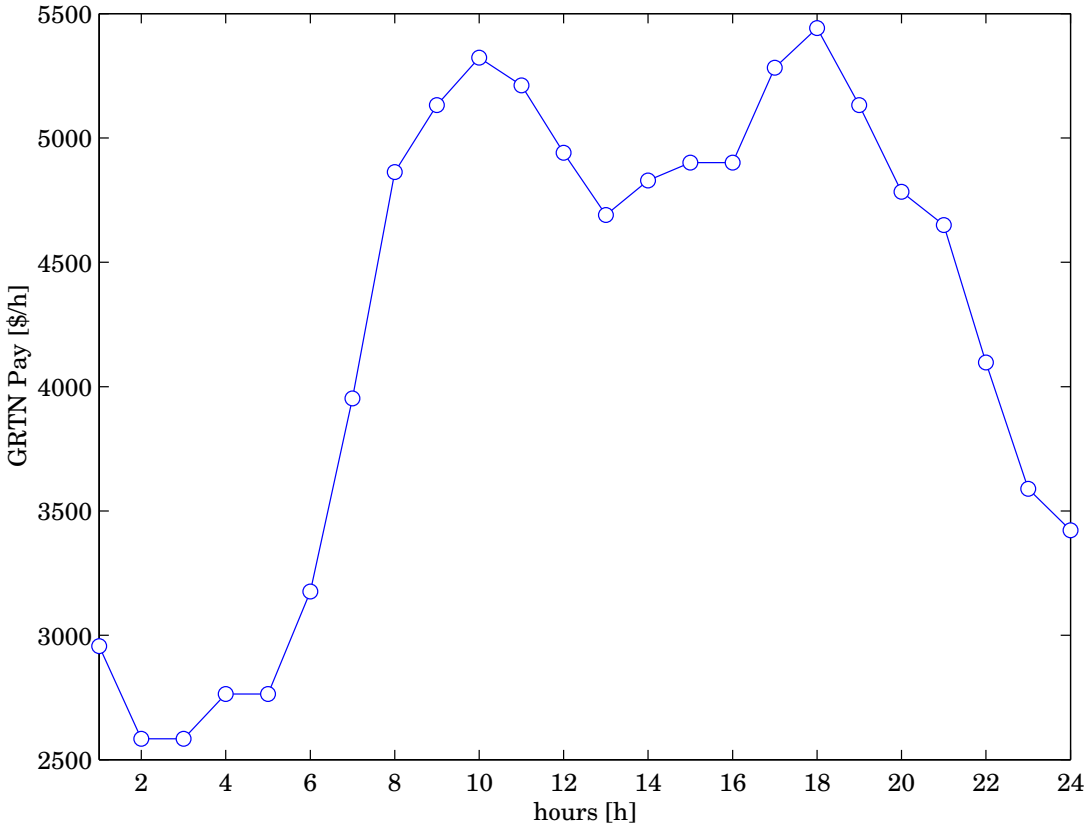

Figure 8.15: GRTN pay for the 129-bus model of the HV Italian system, obtained by means of the multi-period VSC-OPF.

6.20. Observe that both supplier and demand LMPs correctly increase for heavy-loaded hours, although, NCPs corresponding to generation buses may decrease, which basically explains the higher pay to GRTN.

8.4 Summary

This chapter has presented a multi-period voltage stability constrained OPF which allows computing the daily-ahead market taking in account both security and time constraints, such as unit commitment, ramp-up and ramp-down limits, minimum up and minimum down times and start-up and shut-down ramp rates of thermal plants. The proposed technique is compared to a standard multi-period OPF where security is modeled using real power congestions computed off-line. Several simulations for a six-bus test system has been discussed to explore a variety of scenarios: multi-objective multi-period VSC-OPF with elastic and inelastic demand and multi-period VSC-OPF with inclusion of N-1 contingency criteria. Test cases confirm the ability of the VSC-OPF-based market model to provide an accurate estimation of system security and price signals. Finally a 129-bus example has been used to test the reliability of the method for realistic size systems.

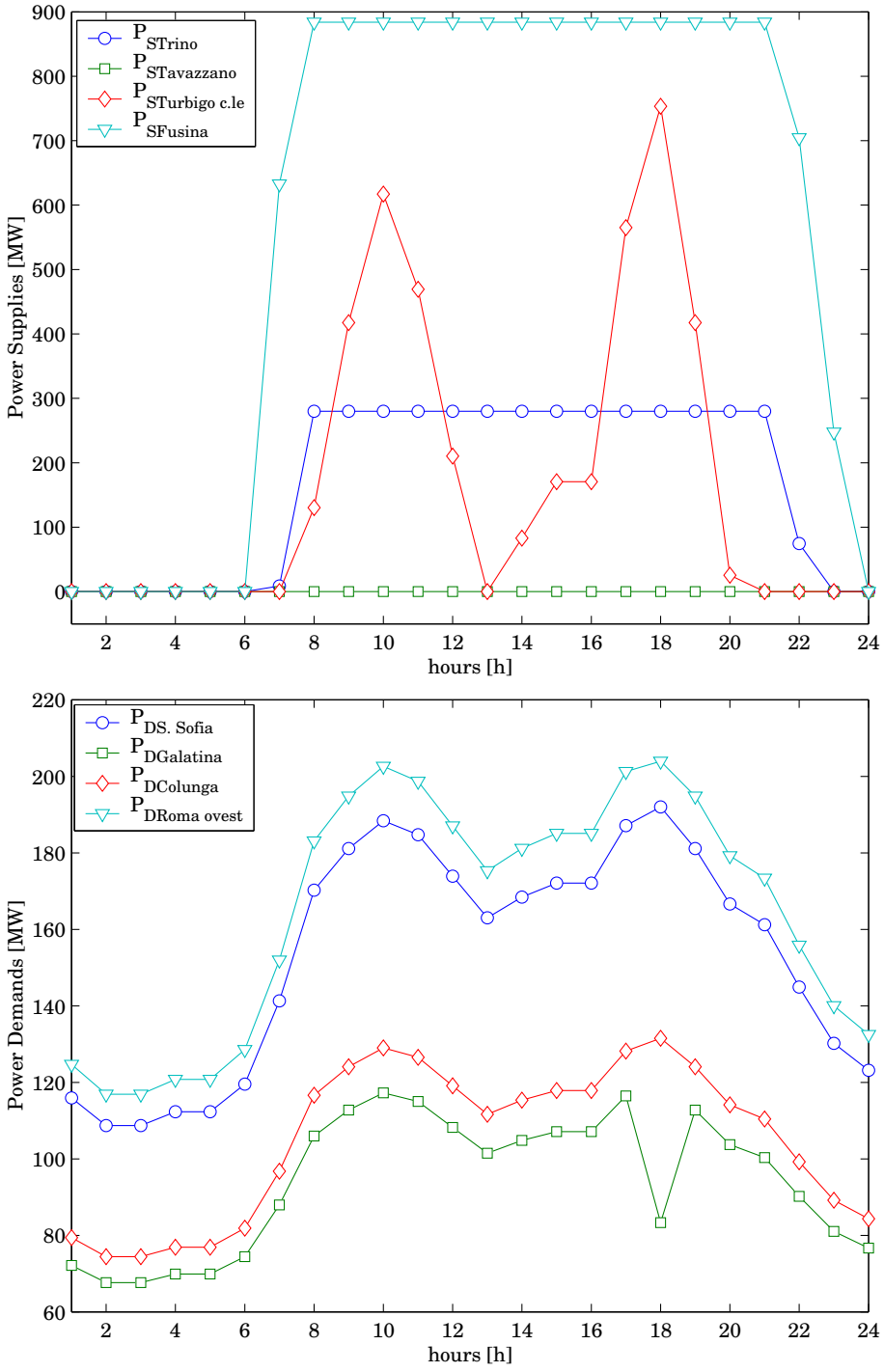

Figure 8.16: Power bids for the most significant buses of the 129-bus model of the HV Italian system, obtained by means of the multi-period VSC-OPF.

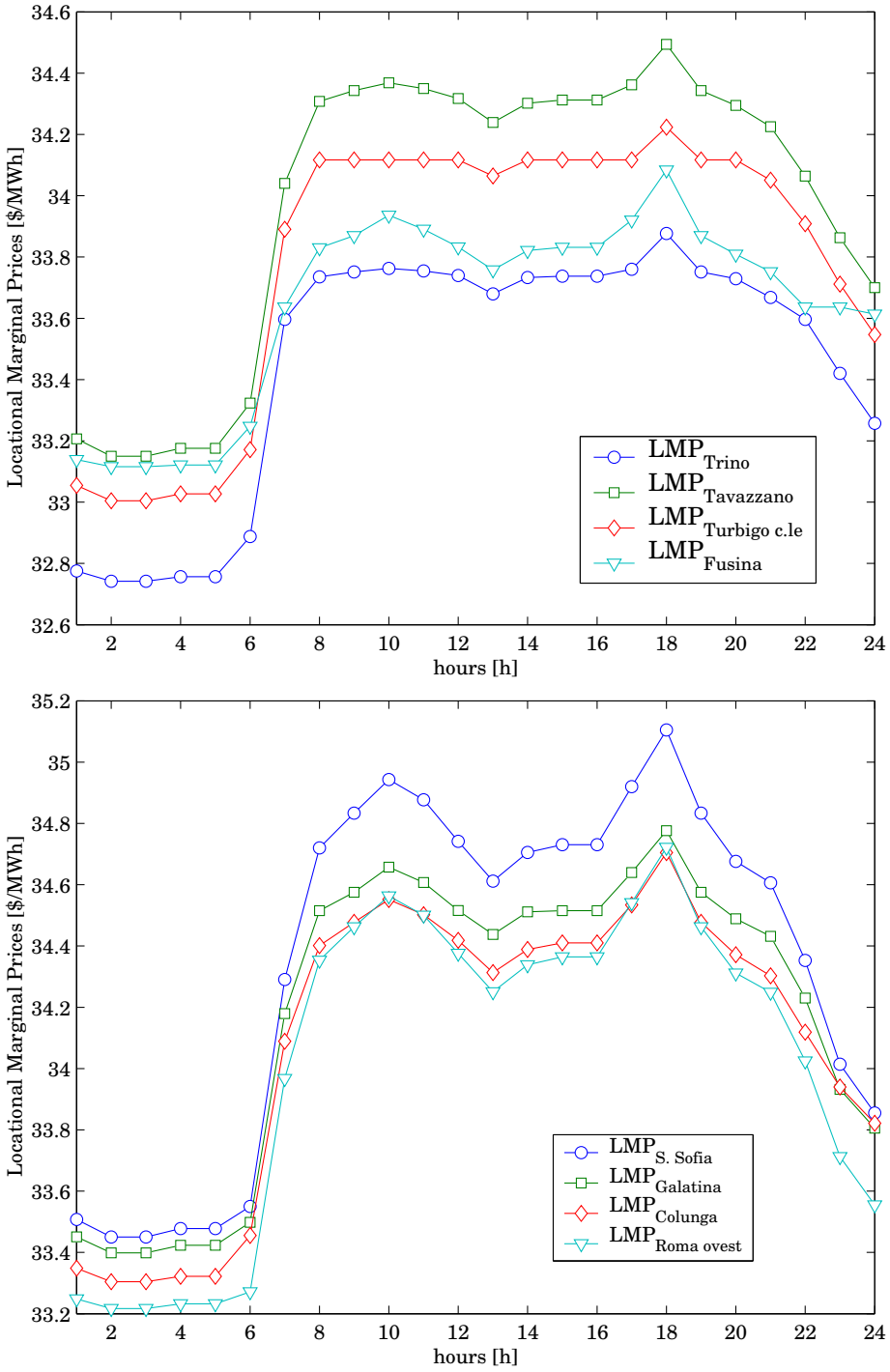

Figure 8.17: LMPs for the most significant buses of the 129-bus model of the HV Italian system, obtained by means of the multi-period VSC-OPF.

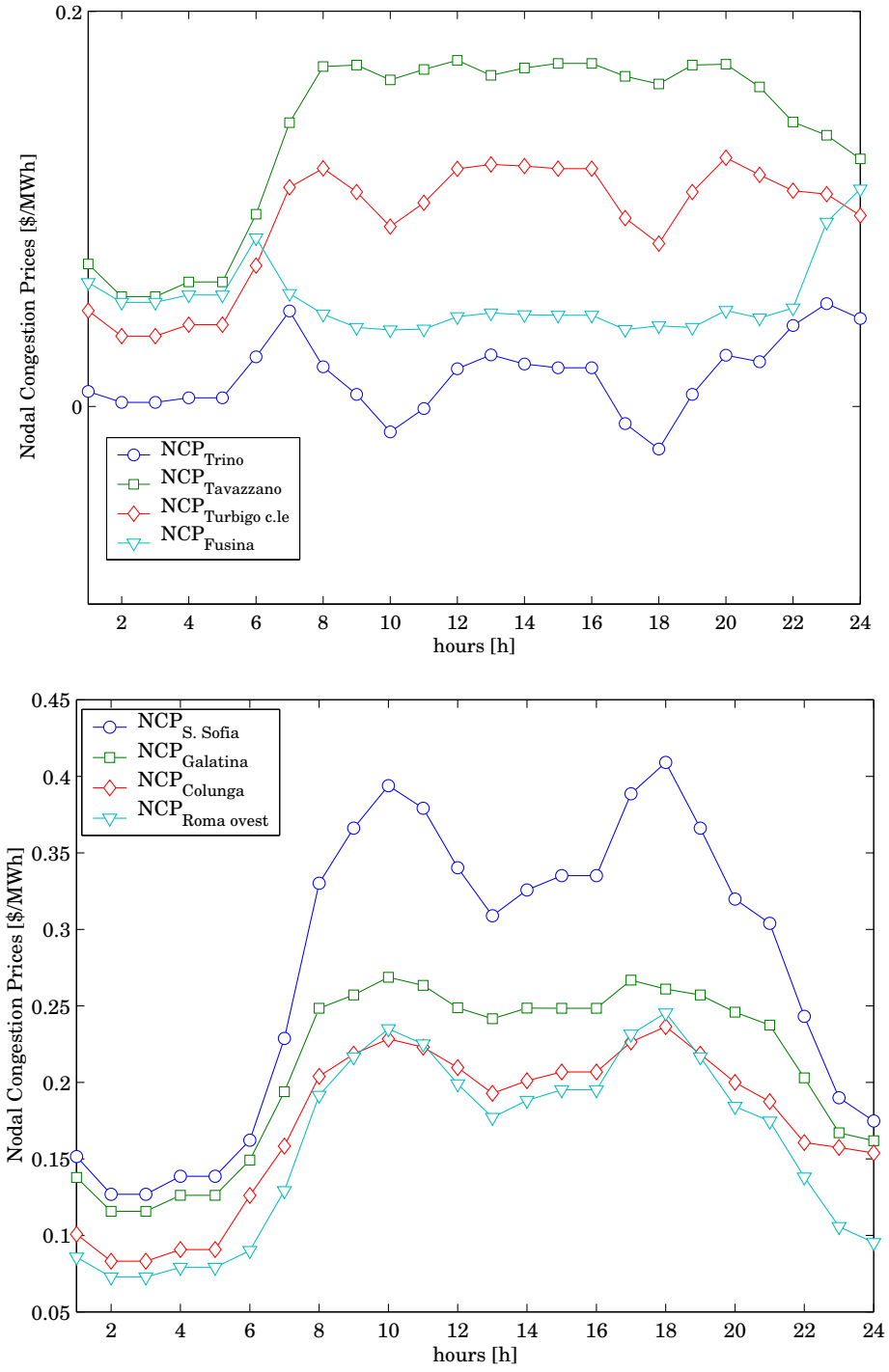

Figure 8.18: NCPs for the most significant buses of the 129-bus model of the HV Italian system, obtained by means of the multi-period VSC-OPF.

Chapter 9

Conclusions

9.1 Concluding Observations

THIS thesis has presented the study of OPF-based electricity markets with inclusion of voltage stability constraints and discussed how these constraints affect locational marginal prices and nodal congestion prices. Inclusion of N-1 contingency criteria and the extension from a single-period solution to a multi-period horizon with commitment logics and ramping constraints has also been presented and discussed. The following conclusions can be stated:

(i) The aim of the proposed Voltage Stability Constrained OPF-based electricity market model is twofold. Firstly, accurately evaluating the effect of voltage stability limits (i.e. saddle-node bifurcations, limit-induced bifurcations) and security limits (i.e. voltage boundaries, generator reactive power limits and thermal constraints) on the market clearing mechanism. Secondly, demonstrating that the current technique of including power transfer limits computed off-line to account for stability limits is not precise and may lead to both low transaction levels and erroneous price indications.

(ii) The proposed multi-objective VSC-OPF-based market model provides a set of solutions which range from a quasi maximization of the social benefit to a quasi maximization of the system loading margin. Thus practitioners can chose the best compromise between total transaction level and stability margin.

(iii) Increasing the security level (weighting factor) when using an inelastic demand models leads to a higher price of the electricity, as expected, whereas demand side bidding model may lead to cheaper transaction for higher values of the desired security. This may induce market participants to accept a lower transaction level if this is associated with higher security (voltage stability margin) and lower costs.

(iv) Nodal congestion prices shown by the proposed techniques are generally lower than the ones obtained by means of standard security constrained OPF computations, thus demonstrating that the inclusion of accurate security constraints help in getting better market solutions and fair prices.

(v) As a consequence of including the proposed voltage stability constraints, the solution of OPF-based electricity markets provides the available loading capability (ALC), which is a simple and direct index of the stability margin of the system current solution. Using an "all-in-one" optimization techniques, also avoids off-line stability computations, which are generally needed to validate security of standard simple auction-based market clearing mechanisms.

(vi) The proposed methods for including N-1 contingency criteria in the VSC-OPF define two different but complimentary approaches. The first approach combines iteratively VSC-OPF solutions to a standard N-1 contingency analysis obtained by means of a continuation power flow technique, while the

second method makes use of a sensitivity analysis to identify transmission lines which mostly affect the maximum loading condition.

(vii) Test cases proves that the techniques for including a N-1 contingency criterion in the VSC-OPF problem lead to identify a few "critical" areas of the network, i.e. whatever line outage within these areas causes similar effects on the resulting stability margin. Thus, the sensitivity analysis may be computed only once and multi-objective VSC-OPF can be computed assuming only few critical scenarios.

(viii) The proposed multi-period VSC-OPF-based electricity market is an accurate model which takes in account both temporal constraints (ramping rate, start-up/shut-down limits and unit-commitment logics) and voltage stability constraints. Test examples proves that an accurate modeling of security constraints may improve market transactions and lower prices. This conclusion is in accordance with results obtained for the single-period VSC-OPF.

(ix) Loading margins determined by means of an N-1 contingency analysis decrease as the loading level increase; this fact leads to the conclusion that the evaluation of the critical lines can be done only once, and the inclusion of N-1 contingency criterion in the multi-period VSC-OPF can be efficiently realized by means of a reduced set of simulations for the most critical line outages determined for the load peak.

(x) The presented test examples for a realistic size network demonstrate that the proposed techniques can be reasonably applied in practice, and can be used in on-line applications for single and multi-period market auctions and/or provide to system operators and market participants a tool to handle together electricity prices and stability issues.

9.2 Main Contributions

The main contributions of this thesis can be summarized as follows:

- **VSC-OPF-based market model:**

    1. Inclusion of concepts of static bifurcation (saddle-node bifurcations and limit-induced bifurcations) in the analysis of deregulated electricity markets with both supply and demand side bidding.
    2. Development of a multi-objective voltage stability constrained OPF for solving electricity market with the ability of tuning the desired security level.
    3. Definition of locational marginal prices and nodal congestion prices which take into account voltage stability constraints and properly price the congestion status of the current bid profile.

- **Inclusion of N-1 contingency criterion in VSC-OPF:**

    1. Development of two techniques for including N-1 contingency criteria in the voltage stability constrained OPF.
    2. Definition of a maximum loading condition which properly represents proximity to voltage collapse with respect to the current bid profile.

- **Multi-period VSC-OPF:**

    1. Extension of the voltage stability constrained OPF-based market to a multi-period centralized pool-auction which takes in account unit-commitment, generator ramping rates and start-up/shut-down logics.
    2. Inclusion of an N-1 contingency criterion in multi-period centralized pool-auctions, which allows to properly evaluates the stability margin of a daily-ahead market.

- **New Matlab-based Power System Analysis Toolbox:**

    1. Development of a new, complete and user-friendly Matlab-based software package for power system analysis (PSAT). The toolbox allows setting up networks in a CAD-like environment (Simulink) and then running advanced routines for power flow, continuation power flow, optimal power flow and time domain simulations.
    2. Development of a PSAT/GAMS interface to solve a variety of OPF-based market models. The interface merges the sophisticated optimization solvers provided by GAMS with the advanced graphic tools of Matlab.

9.3 Future Directions

The proposed techniques for including voltage stability constraints in electricity market computations can be enhanced by means of more detailed models, such as logics of reservoirs and regulated hydro plants, inter-tie constraints and area exchange limits. The latter would also help in extending the concept of Available Loading Capability and loading margin to the Available Transfer Capability concept, which is commonly in use. A more accurate study of the effects of a N-2 contingency criterion to market solutions and electricity prices appears also interesting.

An area of interest beyond the scope of this thesis is the inclusion in the market model of ancillary services, such as reserve and capacity bids and other unbundled services aimed to system control (voltage regulation, frequency regulation, etc.). The latter would imply including in the OPF equations also dynamic models of generators and control systems and could in turn be useful for extending the analysis to dynamic phenomena like transient instability, Hopf bifurcations, etc.

Finally, the proposed VSC-OPF models appears to be much more complicated than the techniques commonly in use by practitioners and market participants to determine electricity costs. This could in turn be considered a drawback, since the computation of electricity prices has to be as transparent and as simple as possible. A solution could be splitting the market clearing mechanism and the stability computations into two different yet linked processes, repeated iteratively until a satisfactory solution is found.

Appendix A

Three-bus Test System

A.1 Network and Market Data

The system data and price-quantity bids for the three-area electricity market example are depicted in Tables A.1, A.2 and A.3.

Table A.1: Bus Data for the Three-Bus Test System

Area	V_b [kV]	V [p.u.]	P_{G_0} [MW]	P_{L_0} [MW]	Q_{L_0} [MVar]	Shunt [MVar]	$Q_{G_{\text{lim}}}$ [MVar]
Bus 1	138	1.2	150	150	80	0	±150
Bus 2	138	1.0	100	150	70	80	±150
Bus 3	138	1.0	100	50	30	50	±150

Table A.2: Line Data for the Three-Bus Test System

Line i-j	R_{hk} [p.u.]	X_{hk} [p.u.]	$B_h/2$ [p.u.]	$P_{\max}$ [MW]	$I_{\max}$ [A]
1-2	0.01	0.12	0.0	-	-
1-3	0.01	0.12	0.0	-	-
2-3	0.01	0.12	0.0	-	-

Table A.3: Price-Quantity Bids for the Three-Bus Test System

Bus i	Participant	C [$/MWh]	$P_{\max}$ [MW]
1	$GENCO_1$	25	150
2	$GENCO_2$	33	100
3	$GENCO_3$	32	100
2	$ESCO_2$	30	100
3	$ESCO_3$	35	100

Appendix B

Six-bus Test System

B.1 Network and Market Data

This appendix depicts the complete data set for the six-bus test system of Fig. 2.2. Tables B.1 and B.2 show supply and demand bids and the bus data for the market participants (the latter table refers to data used for the VSC-OPF with N-1 contingency criteria), whereas Table B.3 depicts data for the multi-period daily-ahead market and Table B.4 shows the line data. Maximum active power flow limits were computed off-line using a continuation power flow with generation and load directions based on the corresponding power bids, whereas thermal limits were assumed to be twice the values of the line currents at base load conditions for a 400 kV voltage rating. In Table B.4, it is assumed that $I_{hk_{\max}} = I_{kh_{\max}} = I_{\max}$ and $P_{hk_{\max}} = P_{kh_{\max}} = P_{\max}$. Maximum and minimum voltage limits are considered to be 1.1 p.u. and 0.9 p.u.

Table B.1: GENCO and ESCO Bids and Bus Data for the six-Bus Test System

Participant	C [\$/MWh]	$P_{\max}^{\text{bid}}$ [MW]	P_{L_0} [MW]	Q_{L_0} [MVar]	P_{G_0} [MW]	$Q_{G_{\lim}}$ [MVar]
GENCO 1	9.7	20	0	0	90	±150
GENCO 2	8.8	25	0	0	140	±150
GENCO 3	7.0	20	0	0	60	±150
ESCO 1	12.0	25	90	60	0	0
ESCO 2	10.5	10	100	70	0	0
ESCO 3	9.5	20	90	60	0	0

Table B.2: GENCO and ESCO Bids and Bus Data for the Six-Bus Test System used for the VSC-OPF with N-1 contingency criteria

Participant	C [\$/MWh]	$P_{\max}^{\text{bid}(N-1)}$ [MW]	$P_{L_0}^{(N-1)}$ [MW]	$Q_{L_0}^{(N-1)}$ [MVar]	$P_{G_0}^{(N-1)}$ [MW]	$Q_{G_{\lim}}$ [MVar]
GENCO 1	9.7	30	0	0	67.5	±150
GENCO 2	8.8	37.5	0	0	103	±150
GENCO 3	7.0	30	0	0	45	±150
ESCO 1	12.0	37.5	67.5	45	0	0
ESCO 2	10.5	15	75	52.5	0	0
ESCO 3	9.5	30	67.5	45	0	0

Table B.3: Daily-Ahead Market Data for the Six-Bus Test System

Supplier	SD [MW/h]	SU [MW/h]	DT [h]	UT [h]	α_0 [h]	β_0 [h]
GENCO 1	50	50	1	1	1	0
GENCO 2	50	50	1	1	1	0
GENCO 3	50	50	1	1	0	1

Table B.4: Line Data for the Six-Bus Test System

Line h-k	R_{hk} [p.u.]	X_{hk} [p.u.]	$B_h/2$ [p.u.]	$P_{\max}$ [MW]	$P_{\max}^{(N-1)}$ [MW]	$I_{\max}$ [A]
1-2	0.1	0.2	0.02	15.4	11.7	37
1-4	0.05	0.2	0.02	50.1	39.8	133
1-5	0.08	0.3	0.03	42.9	50.4	122
2-3	0.05	0.25	0.03	21.6	18.3	46
2-4	0.05	0.1	0.01	68.2	57.7	200
2-5	0.1	0.3	0.02	33.6	33.1	103
2-6	0.07	0.2	0.025	52.1	43.3	132
3-5	0.12	0.26	0.025	26.1	23.0	95
3-6	0.02	0.1	0.01	65.0	47.5	200
4-5	0.2	0.4	0.04	9.8	7.7	26
5-6	0.1	0.3	0.03	2.2	2.2	29

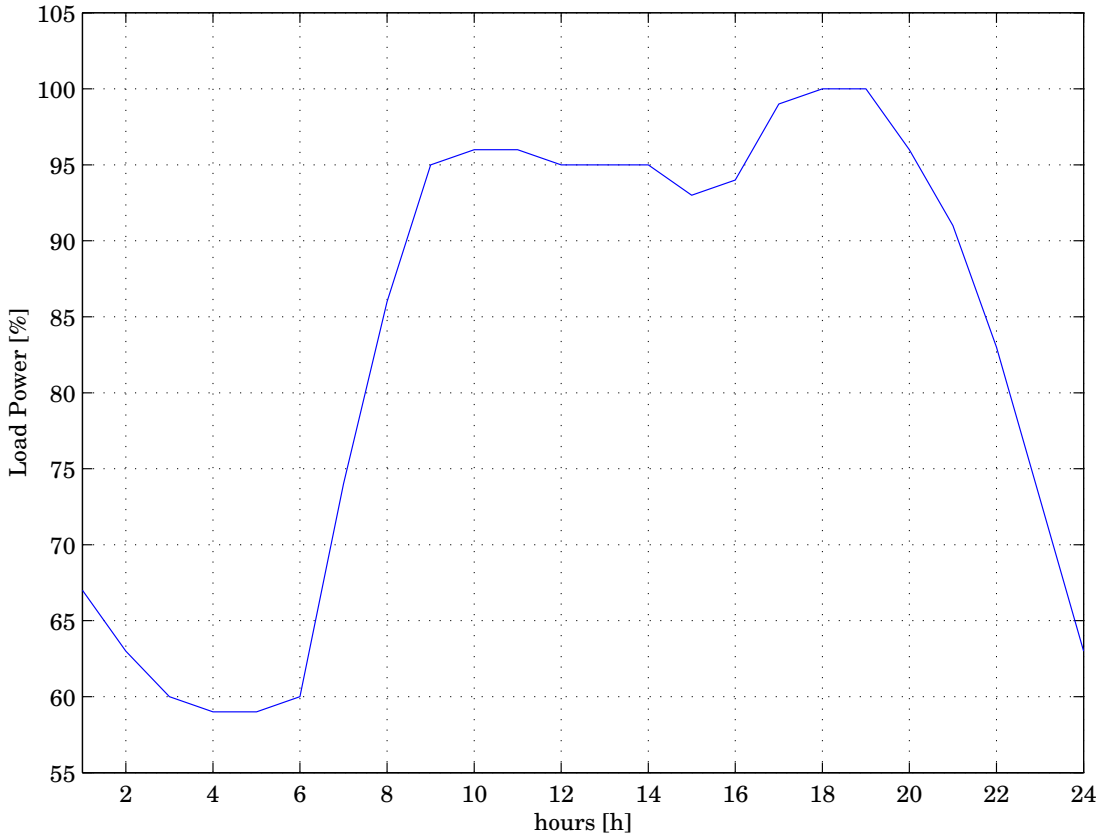

Figure B.1: Daily-ahead load power demand in % for the six-bus system.

Appendix C

HV Italian System

C.1 Network and Market Data

The 129-bus data which models the HV Italian transmission grid follows. The power flow data and limits are in the IEEE-CDF [82], whereas the market data for loads and generators are in PSAT format. Power flow data and security limits reported below have been provided by CESI, and are realistic values able to model accurately the HV Italian system. Price-quantity bids are depicted in Tables C.1, C.2, C.3, C.4, C.5 and C.6. Observe that the market data have been assumed here as "reasonable", and taking in account the market conditions and prices in other European countries (e.g. Spain), but cannot be considered as real bid values. Finally, for the multi-period VSC-OPF proposed in Chapter 8, base case powers P_{G_0} and P_{L_0} and demand bids $P_{D_{\max}}$ have been scaled using the daily-ahead power profile depicted in Fig. C.1.

```
 13/09/02 F. Milano           100.00 2002 S 129-Bus 167-Line System
BUS DATA FOLLOW                        129 ITEMS
  1  Entracque    1  0  2 1.0526  0.000   0.0000    0.0000 517.628   0.000  380.00 1.0526 1311.00 -986.00  0.0000  0.0000    1
  2  La Spezia    1  0  2 1.0405  0.000 144.0000  102.4000 374.381   0.000  380.00 1.0405 1372.00-1318.00  0.0000  0.0000    2
  3  Trino        1  0  2 1.0433  0.000   0.0000    0.0000 265.608   0.000  380.00 1.0433  490.00 -375.00  0.0000  0.0000    3
  4  Vado         1  0  2 1.0466  0.000 160.0000   56.0000 511.962   0.000  380.00 1.0466 1176.00 -824.00  0.0000  0.0000    4
  5  Edolo c.le   1  0  2 1.0647  0.000   0.0000    0.0000 393.626   0.000  380.00 1.0647 1152.00 -832.00  0.0000  0.0000    5
  6  La Casella   1  0  2 1.0530  0.000   0.0000    0.0000 241.654   0.000  380.00 1.0530 1176.00 -360.00  0.0000  0.0000    6
  7  Roncoval. c  1  0  2 1.0432  0.000   0.0000    0.0000 183.232   0.000  380.00 1.0432 1008.00 -728.00  0.0000  0.0000    7
  8  Ostiglia     1  0  2 1.0802  0.000-112.8000    9.6000 256.810   0.000  380.00 1.0802 1174.00 -550.00  0.0000  0.0000    8
```

9	S. Fiorano	1	0	2	1.0617	0.000	0.0000	0.0000	308.016	0.000	380.00	1.0617	560.00	-404.00	0.0000	0.0000	9
10	Piacenza	1	0	2	1.0524	0.000	0.0000	0.0000	236.800	0.000	380.00	1.0524	596.00	-360.00	0.0000	0.0000	10
11	Sermide	1	0	2	1.0847	0.000	0.0000	0.0000	494.438	0.000	380.00	1.0847	1176.00	-360.00	0.0000	0.0000	11
12	Tavazzano	1	0	2	1.0530	0.000	164.8000	3.2000	879.238	0.000	380.00	1.0530	1176.00	-404.00	0.0000	0.0000	12
13	Turbigo c.l	1	0	2	1.0462	0.000	0.0000	0.0000	764.045	0.000	380.00	1.0462	1550.00	-692.00	0.0000	0.0000	13
14	Fusina	1	0	2	1.0813	0.000	0.0000	0.0000	76.820	0.000	380.00	1.0813	879.00	-194.00	0.0000	0.0000	14
15	Portotolle	1	0	2	1.0889	0.000	7.2000	4.0000	1383.120	0.000	380.00	1.0889	2460.00	-1412.00	0.0000	0.0000	15
16	Monfalcone	1	0	2	1.0816	0.000	0.0000	0.0000	254.412	0.000	380.00	1.0816	291.00	-18.00	0.0000	0.0000	16
17	Bargi c.le	1	0	2	1.0471	0.000	0.0000	0.0000	191.998	0.000	380.00	1.0471	294.00	-214.00	0.0000	0.0000	17
18	Piombino	1	0	2	1.0568	0.000	0.0000	0.0000	838.390	0.000	380.00	1.0568	1176.00	-836.00	0.0000	0.0000	18
19	Torre nord	1	0	2	1.0553	0.000	0.0000	0.0000	981.600	0.000	380.00	1.0553	2352.00	-1080.00	0.0000	0.0000	19
20	Montalto c.	1	0	3	1.0589	0.000	0.0000	0.0000	2173.712	0.000	380.00	1.0589	3272.00	-1432.00	0.0000	0.0000	20
21	Torre sud	1	0	2	1.0536	0.000	0.0000	0.0000	387.190	0.000	380.00	1.0536	1048.00	-496.00	0.0000	0.0000	21
22	Brindisi c.	1	0	2	1.0783	0.000	20.8000	16.8000	1640.880	0.000	380.00	1.0783	2352.00	-900.00	0.0000	0.0000	22
23	Presenzano	1	0	2	1.0526	0.000	0.0000	0.0000	471.168	0.000	380.00	1.0526	1080.00	-780.00	0.0000	0.0000	23
24	Rossano	1	0	2	1.0711	0.000	96.8000	33.6000	599.270	0.000	380.00	1.0711	1235.00	-1048.00	0.0000	0.0000	24
25	Isab Erg	1	0	2	1.0367	0.000	0.0000	0.0000	251.973	0.000	380.00	1.0367	556.00	-354.00	0.0000	0.0000	25
26	Casanova	1	0	1	1.0000	0.000	304.8000	58.4000	0.000	0.000	380.00	0.0000	0.00	0.00	0.0000	0.0000	26
27	Castelnuovo	1	0	1	1.0000	0.000	191.2000	52.8000	0.000	0.000	380.00	0.0000	0.00	0.00	0.0000	0.0000	27
28	Magliano	1	0	1	1.0000	0.000	236.8000	68.0000	0.000	0.000	380.00	0.0000	0.00	0.00	0.0000	0.0000	28
29	Piossasco	1	0	1	1.0000	0.000	280.0000	140.0000	0.000	0.000	380.00	0.0000	0.00	0.00	0.0000	0.0000	29
30	Rondissone	1	0	1	1.0000	0.000	242.4000	72.0000	0.000	0.000	380.00	0.0000	0.00	0.00	0.0000	0.0000	30
31	Leini	1	0	1	1.0000	0.000	131.2000	80.8000	0.000	0.000	380.00	0.0000	0.00	0.00	0.0000	0.0000	31
32	Albertville	1	0	2	1.0420	0.000	0.0000	0.0000	719.200	0.000	380.00	1.0420	9900.00	-9900.00	0.0000	0.0000	32
33	Venaus	1	0	1	1.0000	0.000	65.6000	-12.8000	0.000	0.000	380.00	0.0000	0.00	0.00	0.0000	0.0000	33
34	Villarodin	1	0	2	1.0518	0.000	0.0000	0.0000	540.800	0.000	380.00	1.0518	9900.00	-9900.00	0.0000	0.0000	34
35	Vignole	1	0	1	1.0000	0.000	170.4000	102.4000	0.000	0.000	380.00	0.0000	0.00	0.00	0.0000	0.0000	35
36	Baggio	1	0	1	1.0000	0.000	236.8000	68.8000	0.000	0.000	380.00	0.0000	0.00	0.00	0.0000	0.0000	36
37	Bovisio	1	0	1	1.0000	0.000	296.0000	16.0000	0.000	0.000	380.00	0.0000	0.00	0.00	0.0000	0.0000	37
38	Ospiate	1	0	1	1.0000	0.000	215.2000	68.0000	0.000	0.000	380.00	0.0000	0.00	0.00	0.0000	0.0000	38
39	Lachiarella	1	0	1	1.0000	0.000	179.2000	38.4000	0.000	0.000	380.00	0.0000	0.00	0.00	0.0000	0.0000	39
40	Caorso	1	0	0	1.0000	0.000	0.0000	0.0000	0.000	0.000	380.00	0.0000	0.00	0.00	0.0000	0.0000	40
41	Cremona	1	0	1	1.0000	0.000	194.4000	96.8000	0.000	0.000	380.00	0.0000	0.00	0.00	0.0000	0.0000	41
42	Ciserano	1	0	1	1.0000	0.000	268.0000	23.2000	0.000	0.000	380.00	0.0000	0.00	0.00	0.0000	0.0000	42
43	Edolo	1	0	0	1.0000	0.000	0.0000	0.0000	0.000	0.000	380.00	0.0000	0.00	0.00	0.0000	0.0000	43
44	Cavo 871M1	1	0	0	1.0000	0.000	0.0000	0.0000	0.000	0.000	380.00	0.0000	0.00	0.00	0.0000	0.0000	44
45	Cavo 875M1	1	0	0	1.0000	0.000	0.0000	0.0000	0.000	0.000	380.00	0.0000	0.00	0.00	0.0000	0.0000	45
46	Flero	1	0	1	1.0000	0.000	115.2000	65.6000	0.000	0.000	380.00	0.0000	0.00	0.00	0.0000	0.0000	46
47	Gorlago	1	0	1	1.0000	0.000	129.6000	52.0000	0.000	0.000	380.00	0.0000	0.00	0.00	0.0000	0.0000	47
48	Nave	1	0	1	1.0000	0.000	84.8000	44.8000	0.000	0.000	380.00	0.0000	0.00	0.00	0.0000	0.0000	48
49	S. Rocco	1	0	1	1.0000	0.000	266.4000	102.4000	0.000	0.000	380.00	0.0000	0.00	0.00	0.0000	0.0000	49
50	Turbigo	1	0	0	1.0000	0.000	0.0000	0.0000	0.000	0.000	380.00	0.0000	0.00	0.00	0.0000	0.0000	50
51	Verderio	1	0	1	1.0000	0.000	224.0000	26.4000	0.000	0.000	380.00	0.0000	0.00	0.00	0.0000	0.0000	51
52	Dolo	1	0	0	1.0000	0.000	0.0000	0.0000	0.000	0.000	380.00	0.0000	0.00	0.00	0.0000	0.0000	52
53	Dugale	1	0	1	1.0000	0.000	204.8000	62.4000	0.000	0.000	380.00	0.0000	0.00	0.00	0.0000	0.0000	53
54	Planais	1	0	1	1.0000	0.000	96.0000	3.2000	0.000	0.000	380.00	0.0000	0.00	0.00	0.0000	0.0000	54
55	Redipuglia	1	0	1	1.0000	0.000	-1.6000	3.2000	0.000	0.000	380.00	0.0000	0.00	0.00	0.0000	0.0000	55
56	Venezia	1	0	1	1.0000	0.000	196.8000	21.6000	0.000	0.000	380.00	0.0000	0.00	0.00	0.0000	0.0000	56
57	Bargi	1	0	0	1.0000	0.000	0.0000	0.0000	0.000	0.000	380.00	0.0000	0.00	0.00	0.0000	0.0000	57
58	Calenzano	1	0	1	1.0000	0.000	280.8000	70.4000	0.000	0.000	380.00	0.0000	0.00	0.00	0.0000	0.0000	58
59	Forli'	1	0	1	1.0000	0.000	199.2000	74.4000	0.000	0.000	380.00	0.0000	0.00	0.00	0.0000	0.0000	59
60	Marginone	1	0	1	1.0000	0.000	263.2000	75.2000	0.000	0.000	380.00	0.0000	0.00	0.00	0.0000	0.0000	60
61	Martignone	1	0	1	1.0000	0.000	364.8000	76.8000	0.000	0.000	380.00	0.0000	0.00	0.00	0.0000	0.0000	61
62	Parma	1	0	1	1.0000	0.000	380.8000	76.0000	0.000	0.000	380.00	0.0000	0.00	0.00	0.0000	0.0000	62
63	Poggio a Ca	1	0	1	1.0000	0.000	400.0000	222.4000	0.000	0.000	380.00	0.0000	0.00	0.00	0.0000	0.0000	63
64	Suvereto	1	0	1	1.0000	0.000	48.0000	51.2000	0.000	0.000	380.00	0.0000	0.00	0.00	0.0000	0.0000	64
65	S. Damaso	1	0	1	1.0000	0.000	231.2000	69.6000	0.000	0.000	380.00	0.0000	0.00	0.00	0.0000	0.0000	65
66	Aurelia	1	0	0	1.0000	0.000	0.0000	0.0000	0.000	0.000	380.00	0.0000	0.00	0.00	0.0000	0.0000	66
67	Fano	1	0	1	1.0000	0.000	0.8000	0.0400	0.000	0.000	380.00	0.0000	0.00	0.00	0.0000	0.0000	67
68	Latina	1	0	1	1.0000	0.000	188.0000	87.2000	0.000	0.000	380.00	0.0000	0.00	0.00	0.0000	0.0000	68
69	Montalto	1	0	1	1.0000	0.000	111.2000	19.2000	0.000	0.000	380.00	0.0000	0.00	0.00	0.0000	0.0000	69
70	Roma nord	1	0	1	1.0000	0.000	450.4000	117.6000	0.000	0.000	380.00	0.0000	0.00	0.00	0.0000	0.0000	70
71	Roma sud	1	0	1	1.0000	0.000	481.6000	83.2000	0.000	0.000	380.00	0.0000	0.00	0.00	0.0000	0.0000	71
72	S. Lucia	1	0	1	1.0000	0.000	389.6000	79.2000	0.000	0.000	380.00	0.0000	0.00	0.00	0.0000	0.0000	72
73	Brindisi 30	1	0	0	1.0000	0.000	0.0000	0.0000	0.000	0.000	380.00	0.0000	0.00	0.00	0.0000	0.0000	73
74	Brindisi 00	1	0	1	1.0000	0.000	155.2000	28.8000	0.000	0.000	380.00	0.0000	0.00	0.00	0.0000	0.0000	74
75	Brindisi 01	1	0	0	1.0000	0.000	0.0000	0.0000	0.000	0.000	380.00	0.0000	0.00	0.00	0.0000	0.0000	75
76	Valmontone	1	0	1	1.0000	0.000	219.2000	54.4000	0.000	0.000	380.00	0.0000	0.00	0.00	0.0000	0.0000	76
77	Villanova	1	0	1	1.0000	0.000	200.8000	64.0000	0.000	0.000	380.00	0.0000	0.00	0.00	0.0000	0.0000	77
78	Benevento	1	0	1	1.0000	0.000	158.4000	44.0000	0.000	0.000	380.00	0.0000	0.00	0.00	0.0000	0.0000	78
79	Foggia	1	0	1	1.0000	0.000	168.0000	49.6000	0.000	0.000	380.00	0.0000	0.00	0.00	0.0000	0.0000	79
80	Garigliano	1	0	1	1.0000	0.000	114.4000	10.4000	0.000	0.000	380.00	0.0000	0.00	0.00	0.0000	0.0000	80
81	Laino	1	0	1	1.0000	0.000	113.6000	135.2000	0.000	0.000	380.00	0.0000	0.00	0.00	0.0000	0.0000	81
82	Matera	1	0	0	1.0000	0.000	0.0000	0.0000	0.000	0.000	380.00	0.0000	0.00	0.00	0.0000	0.0000	82
83	Montecorvin	1	0	1	1.0000	0.000	470.4000	187.2000	0.000	0.000	380.00	0.0000	0.00	0.00	0.0000	0.0000	83
84	Rizziconi	1	0	1	1.0000	0.000	224.8000	77.6000	0.000	0.000	380.00	0.0000	0.00	0.00	0.0000	0.0000	84
85	S. Sofia	1	0	1	1.0000	0.000	307.2000	144.0000	0.000	0.000	380.00	0.0000	0.00	0.00	0.0000	0.0000	85
86	Taranto	1	0	1	1.0000	0.000	52.8000	99.2000	0.000	0.000	380.00	0.0000	0.00	0.00	0.0000	0.0000	86
87	Sorgente	1	0	2	1.0114	0.000	0.0000	0.0000	221.600	0.000	380.00	1.0114	400.00	-400.00	0.0000	0.0000	87
88	Galatina	1	0	1	1.0000	0.000	191.2000	20.0000	0.000	0.000	380.00	0.0000	0.00	0.00	0.0000	0.0000	88
89	Bari ovest	1	0	1	1.0000	0.000	287.2000	126.4000	0.000	0.000	380.00	0.0000	0.00	0.00	0.0000	0.0000	89
90	Larino	1	0	1	1.0000	0.000	88.8000	30.4000	0.000	0.000	380.00	0.0000	0.00	0.00	0.0000	0.0000	90
91	Rosara	1	0	1	1.0000	0.000	226.4000	76.8000	0.000	0.000	380.00	0.0000	0.00	0.00	0.0000	0.0000	91

```
  92  Candia       1  0  1 1.0000  0.000 264.0000   70.4000    0.000    0.000  380.00 0.0000     0.00     0.00  0.0000  0.0000   92
  93  S. Martino   1  0  1 1.0000  0.000 178.4000   75.2000    0.000    0.000  380.00 0.0000     0.00     0.00  0.0000  0.0000   93
  94  Ravenna      1  0  1 1.0000  0.000  40.0000   27.2000    0.000    0.000  380.00 0.0000     0.00     0.00  0.0000  0.0000   94
  95  Divaca       1  0  2 1.0778  0.000   0.0000    0.0000  217.600    0.000  380.00 1.0778  9900.00-9900.00  0.0000  0.0000   95
  96  Adria        1  0  1 1.0000  0.000  69.6000   46.4000    0.000    0.000  380.00 0.0000     0.00     0.00  0.0000  0.0000   96
  97  Camin        1  0  1 1.0000  0.000 227.2000  106.4000    0.000    0.000  380.00 0.0000     0.00     0.00  0.0000  0.0000   97
  98  Salgareda    1  0  1 1.0000  0.000  73.6000  124.8000    0.000    0.000  380.00 0.0000     0.00     0.00  0.0000  0.0000   98
  99  Udine ovest  1  0  1 1.0000  0.000 204.8000   19.2000    0.000    0.000  380.00 0.0000     0.00     0.00  0.0000  0.0000   99
 100  Lonato       1  0  1 1.0000  0.000 202.4000  111.2000    0.000    0.000  380.00 0.0000     0.00     0.00  0.0000  0.0000  100
 101  Nogarole     1  0  1 1.0000  0.000  90.4000   38.4000    0.000    0.000  380.00 0.0000     0.00     0.00  0.0000  0.0000  101
 102  Cordignano   1  0  1 1.0000  0.000  96.0000   64.8000    0.000    0.000  380.00 0.0000     0.00     0.00  0.0000  0.0000  102
 103  Sandrigo     1  0  1 1.0000  0.000 209.6000  127.2000    0.000    0.000  380.00 0.0000     0.00     0.00  0.0000  0.0000  103
 104  Ferrara      1  0  1 1.0000  0.000 203.2000  107.2000    0.000    0.000  380.00 0.0000     0.00     0.00  0.0000  0.0000  104
 105  Colunga      1  0  1 1.0000  0.000 210.4000   79.2000    0.000    0.000  380.00 0.0000     0.00     0.00  0.0000  0.0000  105
 106  Tavarnuzze   1  0  1 1.0000  0.000 174.4000   43.2000    0.000    0.000  380.00 0.0000     0.00     0.00  0.0000  0.0000  106
 107  Roma est     1  0  1 1.0000  0.000  88.8000   30.4000    0.000    0.000  380.00 0.0000     0.00     0.00  0.0000  0.0000  107
 108  Rosen        1  0  2 1.0440  0.000   0.0000    0.0000  150.400    0.000  380.00 1.0440   200.00 -200.00  0.0000  0.0000  108
 109  Acciaiolo    1  0  1 1.0000  0.000  91.2000   15.2000    0.000    0.000  380.00 0.0000     0.00     0.00  0.0000  0.0000  109
 110  Rubiera      1  0  1 1.0000  0.000 371.2000   72.8000    0.000    0.000  380.00 0.0000     0.00     0.00  0.0000  0.0000  110
 111  Roma ovest   1  0  1 1.0000  0.000 330.4000  131.2000    0.000    0.000  380.00 0.0000     0.00     0.00  0.0000  0.0000  111
 112  Ceprano      1  0  1 1.0000  0.000  76.8000   47.2000    0.000    0.000  380.00 0.0000     0.00     0.00  0.0000  0.0000  112
 113  S. Maria     1  0  1 1.0000  0.000 132.8000   41.6000    0.000    0.000  380.00 0.0000     0.00     0.00  0.0000  0.0000  113
 114  Patria       1  0  1 1.0000  0.000 336.0000  161.6000    0.000    0.000  380.00 0.0000     0.00     0.00  0.0000  0.0000  114
 115  Scandale     1  0  1 1.0000  0.000  44.0000    8.8000    0.000    0.000  380.00 0.0000     0.00     0.00  0.0000  0.0000  115
 116  Paterno'     1  0  0 1.0000  0.000   0.0000    0.0000    0.000    0.000  380.00 0.0000     0.00     0.00  0.0000  0.0000  116
 117  Chiaramo     1  0  1 1.0000  0.000  92.0000   86.4000    0.000    0.000  380.00 0.0000     0.00     0.00  0.0000  0.0000  117
 118  Andria       1  0  1 1.0000  0.000 190.4000    6.4000    0.000    0.000  380.00 0.0000     0.00     0.00  0.0000  0.0000  118
 119  Mercallo     1  0  1 1.0000  0.000 213.6000   60.8000    0.000    0.000  380.00 0.0000     0.00     0.00  0.0000  0.0000  119
 120  Lavorges     1  0  2 1.0427  0.000   0.0000    0.0000  451.200    0.000  380.00 1.0427  9900.00-9900.00  0.0000  0.0000  120
 121  Musignano    1  0  0 1.0000  0.000   0.0000    0.0000    0.000    0.000  380.00 0.0000     0.00     0.00  0.0000  0.0000  121
 122  Cagno        1  0  1 1.0000  0.000 172.0000   57.6000    0.000    0.000  380.00 0.0000     0.00     0.00  0.0000  0.0000  122
 123  Cislago      1  0  1 1.0000  0.000  84.0000   41.6000    0.000    0.000  380.00 0.0000     0.00     0.00  0.0000  0.0000  123
 124  Bulciago     1  0  1 1.0000  0.000 271.2000   73.6000    0.000    0.000  380.00 0.0000     0.00     0.00  0.0000  0.0000  124
 125  Brugherio    1  0  1 1.0000  0.000 284.8000   96.0000    0.000    0.000  380.00 0.0000     0.00     0.00  0.0000  0.0000  125
 126  Piancamuno   1  0  1 1.0000  0.000 108.0000   13.6000    0.000    0.000  380.00 0.0000     0.00     0.00  0.0000  0.0000  126
 127  Chiari       1  0  1 1.0000  0.000 167.2000   21.6000    0.000    0.000  380.00 0.0000     0.00     0.00  0.0000  0.0000  127
 128  Travagliato  1  0  1 1.0000  0.000 140.8000   21.6000    0.000    0.000  380.00 0.0000     0.00     0.00  0.0000  0.0000  128
 129  Soazza       1  0  2 1.0381  0.000   0.0000    0.0000    8.000    0.000  380.00 1.0381  9900.00-9900.00  0.0000  0.0000  129
-999
BRANCH DATA FOLLOW                      167 ITEMS
  26   28  1 1  1 0 0.0006063 0.00890000 0.1791360 1422     0      0     0 0  0.0000   0.000 0.0000 0.0000 0.0000  0.0000 0.0000
  26   29  1 1  1 0 0.0005125 0.00599375 0.0867680 1235     0      0     0 0  0.0000   0.000 0.0000 0.0000 0.0000  0.0000 0.0000
  26   30  1 1  1 0 0.0010625 0.00996250 0.1405280 1086     0      0     0 0  0.0000   0.000 0.0000 0.0000 0.0000  0.0000 0.0000
  27    3  1 1  1 0 0.0007500 0.01098120 0.2183680 1853     0      0     0 0  0.0000   0.000 0.0000 0.0000 0.0000  0.0000 0.0000
  27   35  1 1  1 0 0.0004375 0.00636250 0.1299440 1422     0      0     0 0  0.0000   0.000 0.0000 0.0000 0.0000  0.0000 0.0000
  27   36  1 1  1 0 0.0007062 0.01018750 0.2079200 1422     0      0     0 0  0.0000   0.000 0.0000 0.0000 0.0000  0.0000 0.0000
  28   29  1 1  1 0 0.0007500 0.01098750 0.2184800 1422     0      0     0 0  0.0000   0.000 0.0000 0.0000 0.0000  0.0000 0.0000
  28    4  1 1  1 0 0.0007250 0.01236870 0.1932640 1243     0      0     0 0  0.0000   0.000 0.0000 0.0000 0.0000  0.0000 0.0000
  29   31  1 1  1 0 0.0004281 0.00631563 0.1257600 1253     0      0     0 0  0.0000   0.000 0.0000 0.0000 0.0000  0.0000 0.0000
  29   33  1 1  1 0 0.0004281 0.00631563 0.1257600 1253     0      0     0 0  0.0000   0.000 0.0000 0.0000 0.0000  0.0000 0.0000
  33   34  1 1  1 0 0.0004281 0.00631563 0.1257600 1832     0      0     0 0  0.0000   0.000 0.0000 0.0000 0.0000  0.0000 0.0000
  31   30  1 1  1 0 0.0004281 0.00631563 0.1257600 1422     0      0     0 0  0.0000   0.000 0.0000 0.0000 0.0000  0.0000 0.0000
  30    3  1 1  1 0 0.0002563 0.00368125 0.0731200 1853     0      0     0 0  0.0000   0.000 0.0000 0.0000 0.0000  0.0000 0.0000
  30   32  1 1  1 0 0.0002563 0.00368125 0.0731200 2486     0      0     0 0  0.0000   0.000 0.0000 0.0000 0.0000  0.0000 0.0000
  30   50  1 1  1 0 0.0008625 0.01267500 0.2547200 1422     0      0     0 0  0.0000   0.000 0.0000 0.0000 0.0000  0.0000 0.0000
   2   35  1 1  1 0 0.0019875 0.02380630 0.3072000  957     0      0     0 0  0.0000   0.000 0.0000 0.0000 0.0000  0.0000 0.0000
   2   60  1 1  1 0 0.0010437 0.01488120 0.3016800 1414     0      0     0 0  0.0000   0.000 0.0000 0.0000 0.0000  0.0000 0.0000
   2   62  1 1  1 0 0.0010250 0.01755000 0.2674400 1414     0      0     0 0  0.0000   0.000 0.0000 0.0000 0.0000  0.0000 0.0000
   2  109  1 1  1 0 0.0010250 0.01755000 0.2674400 1414     0      0     0 0  0.0000   0.000 0.0000 0.0000 0.0000  0.0000 0.0000
 109  108  1 1  1 0 0.0003125 0.00453125 0.0928000 1134     0      0     0 0  0.0000   0.000 0.0000 0.0000 0.0000  0.0000 0.0000
 109   60  1 1  1 0 0.0003125 0.00453125 0.0928000 2828     0      0     0 0  0.0000   0.000 0.0000 0.0000 0.0000  0.0000 0.0000
   4   35  1 1  1 0 0.0007688 0.01360000 0.1942400 1243     0      0     0 0  0.0000   0.000 0.0000 0.0000 0.0000  0.0000 0.0000
  36   38  1 1  1 0 0.0001563 0.00226562 0.0464000 1422     0      0     0 0  0.0000   0.000 0.0000 0.0000 0.0000  0.0000 0.0000
  38   37  1 1  1 0 0.0001563 0.00226562 0.0464000 1706     0      0     0 0  0.0000   0.000 0.0000 0.0000 0.0000  0.0000 0.0000
  36   39  1 1  1 0 0.0003625 0.00525625 0.1066000 1422     0      0     0 0  0.0000   0.000 0.0000 0.0000 0.0000  0.0000 0.0000
  39    6  1 1  1 0 0.0003625 0.00525625 0.1066000 1422     0      0     0 0  0.0000   0.000 0.0000 0.0000 0.0000  0.0000 0.0000
  36   50  1 1  1 0 0.0003062 0.00450625 0.1696800 1853     0      0     0 0  0.0000   0.000 0.0000 0.0000 0.0000  0.0000 0.0000
  37  123  1 1  1 0 0.0002708 0.00397708 0.0797333 1853     0      0     0 0  0.0000   0.000 0.0000 0.0000 0.0000  0.0000 0.0000
 123  122  1 1  1 0 0.0002708 0.00397708 0.0797333 1365     0      0     0 0  0.0000   0.000 0.0000 0.0000 0.0000  0.0000 0.0000
 122  121  1 1  1 0 0.0002708 0.00397708 0.0797333 1365     0      0     0 0  0.0000   0.000 0.0000 0.0000 0.0000  0.0000 0.0000
  37  125  1 1  1 0 0.0002563 0.00372187 0.0756000 1422     0      0     0 0  0.0000   0.000 0.0000 0.0000 0.0000  0.0000 0.0000
 125   12  1 1  1 0 0.0002563 0.00372187 0.0756000 1853     0      0     0 0  0.0000   0.000 0.0000 0.0000 0.0000  0.0000 0.0000
  37   50  1 1  1 0 0.0002563 0.00364375 0.0762400 1365     0      0     0 0  0.0000   0.000 0.0000 0.0000 0.0000  0.0000 0.0000
  37   51  1 1  1 0 0.0003563 0.00478125 0.0752800 1389     0      0     0 0  0.0000   0.000 0.0000 0.0000 0.0000  0.0000 0.0000
  37  124  1 1  1 0 0.0003563 0.00478125 0.0752800  941     0      0     0 0  0.0000   0.000 0.0000 0.0000 0.0000  0.0000 0.0000
 124  129  1 1  1 0 0.0003563 0.00478125 0.0752800  957     0      0     0 0  0.0000   0.000 0.0000 0.0000 0.0000  0.0000 0.0000
  40   41  1 1  1 0 0.0004438 0.00659687 0.1279200 1243     0      0     0 0  0.0000   0.000 0.0000 0.0000 0.0000  0.0000 0.0000
  41   46  1 1  1 0 0.0004438 0.00659687 0.1279200 1853     0      0     0 0  0.0000   0.000 0.0000 0.0000 0.0000  0.0000 0.0000
  40   49  1 1  1 0 0.0002625 0.00403125 0.0754400 1243     0      0     0 0  0.0000   0.000 0.0000 0.0000 0.0000  0.0000 0.0000
  40   65  1 1  1 0 0.0014062 0.02061250 0.4132800 1414     0      0     0 0  0.0000   0.000 0.0000 0.0000 0.0000  0.0000 0.0000
  43    9  1 1  1 0 0.0000969 0.00127938 0.1864000 2843     0      0     0 0  0.0000   0.000 0.0000 0.0000 0.0000  0.0000 0.0000
  43   44  1 1  1 0 0.0000484 0.00063969 0.0932000  975     0      0     0 0  0.0000   0.000 0.0000 0.0000 0.0000  0.0000 0.0000
  43   45  1 1  1 0 0.0000484 0.00063969 0.0932000  975     0      0     0 0  0.0000   0.000 0.0000 0.0000 0.0000  0.0000 0.0000
```

```
 44    5  1 1  1 0 0.0000484 0.00063969 0.0932000 1422     0     0    0 0  0.0000   0.000 0.0000 0.0000 0.0000  0.0000 0.0000
 45    5  1 1  1 0 0.0000484 0.00063969 0.0932000 1422     0     0    0 0  0.0000   0.000 0.0000 0.0000 0.0000  0.0000 0.0000
 46  128  1 1  1 0 0.0001708 0.00253125 0.0507733 1422     0     0    0 0  0.0000   0.000 0.0000 0.0000 0.0000  0.0000 0.0000
128  127  1 1  1 0 0.0001708 0.00253125 0.0507733 1422     0     0    0 0  0.0000   0.000 0.0000 0.0000 0.0000  0.0000 0.0000
127   47  1 1  1 0 0.0001708 0.00253125 0.0507733 1422     0     0    0 0  0.0000   0.000 0.0000 0.0000 0.0000  0.0000 0.0000
 46   48  1 1  1 0 0.0003125 0.00357500 0.0520800 1235     0     0    0 0  0.0000   0.000 0.0000 0.0000 0.0000  0.0000 0.0000
 46    8  1 1  1 0 0.0011000 0.01610620 0.3228800 1422     0     0    0 0  0.0000   0.000 0.0000 0.0000 0.0000  0.0000 0.0000
 47  126  1 1  1 0 0.0002375 0.00360625 0.1786000 1422     0     0    0 0  0.0000   0.000 0.0000 0.0000 0.0000  0.0000 0.0000
126    9  1 1  1 0 0.0002375 0.00360625 0.1786000 1422     0     0    0 0  0.0000   0.000 0.0000 0.0000 0.0000  0.0000 0.0000
 47   51  1 1  1 0 0.0004375 0.00580000 0.0913600 1389     0     0    0 0  0.0000   0.000 0.0000 0.0000 0.0000  0.0000 0.0000
  6   49  1 1  1 0 0.0002875 0.00415000 0.0840000 1422     0     0    0 0  0.0000   0.000 0.0000 0.0000 0.0000  0.0000 0.0000
121  119  1 1  1 0 0.0004062 0.00589688 0.1196000 1422     0     0    0 0  0.0000   0.000 0.0000 0.0000 0.0000  0.0000 0.0000
119   50  1 1  1 0 0.0004062 0.00589688 0.1196000 1853     0     0    0 0  0.0000   0.000 0.0000 0.0000 0.0000  0.0000 0.0000
 48    9  1 1  1 0 0.0006375 0.01004380 0.1769600 1243     0     0    0 0  0.0000   0.000 0.0000 0.0000 0.0000  0.0000 0.0000
 48  100  1 1  1 0 0.0003792 0.00554375 0.1115730 1422     0     0    0 0  0.0000   0.000 0.0000 0.0000 0.0000  0.0000 0.0000
100  101  1 1  1 0 0.0003792 0.00554375 0.1115733 1853     0     0    0 0  0.0000   0.000 0.0000 0.0000 0.0000  0.0000 0.0000
101   53  1 1  1 0 0.0003792 0.00554375 0.1115733 1853     0     0    0 0  0.0000   0.000 0.0000 0.0000 0.0000  0.0000 0.0000
  8   11  1 1  1 0 0.0001500 0.00215625 0.0471200 1422     0     0    0 0  0.0000   0.000 0.0000 0.0000 0.0000  0.0000 0.0000
  8   53  1 1  1 0 0.0004625 0.00674375 0.1356800 1422     0     0    0 0  0.0000   0.000 0.0000 0.0000 0.0000  0.0000 0.0000
  8  104  1 1  1 0 0.0007531 0.01100625 0.2212000 1414     0     0    0 0  0.0000   0.000 0.0000 0.0000 0.0000  0.0000 0.0000
104   59  1 1  1 0 0.0007531 0.01100625 0.2212000 1414     0     0    0 0  0.0000   0.000 0.0000 0.0000 0.0000  0.0000 0.0000
 49   12  1 1  1 0 0.0004938 0.00713125 0.1450400 1853     0     0    0 0  0.0000   0.000 0.0000 0.0000 0.0000  0.0000 0.0000
 49   62  1 1  1 0 0.0007500 0.01075630 0.2185600 1414     0     0    0 0  0.0000   0.000 0.0000 0.0000 0.0000  0.0000 0.0000
 11   61  1 1  1 0 0.0007125 0.01044370 0.2096800 1414     0     0    0 0  0.0000   0.000 0.0000 0.0000 0.0000  0.0000 0.0000
 12   42  1 1  1 0 0.0004219 0.00617812 0.1218800 1853     0     0    0 0  0.0000   0.000 0.0000 0.0000 0.0000  0.0000 0.0000
 42   51  1 1  1 0 0.0004219 0.00617812 0.1218800 1137     0     0    0 0  0.0000   0.000 0.0000 0.0000 0.0000  0.0000 0.0000
 52   97  1 1  1 0 0.0004469 0.00650000 0.1304000 1853     0     0    0 0  0.0000   0.000 0.0000 0.0000 0.0000  0.0000 0.0000
 97   53  1 1  1 0 0.0004469 0.00650000 0.1304000 1853     0     0    0 0  0.0000   0.000 0.0000 0.0000 0.0000  0.0000 0.0000
 52   15  1 1  1 0 0.0004669 0.00693750 0.5196800 1422     0     0    0 0  0.0000   0.000 0.0000 0.0000 0.0000  0.0000 0.0000
 52   96  1 1  1 0 0.0002334 0.00346875 0.2598400 1853     0     0    0 0  0.0000   0.000 0.0000 0.0000 0.0000  0.0000 0.0000
 96   15  1 1  1 0 0.0002334 0.00346875 0.2598400 1422     0     0    0 0  0.0000   0.000 0.0000 0.0000 0.0000  0.0000 0.0000
 52   56  1 1  1 0 0.0001156 0.00168437 0.1280000 2843     0     0    0 0  0.0000   0.000 0.0000 0.0000 0.0000  0.0000 0.0000
 53  103  1 1  1 0 0.0006094 0.00891719 0.1765200 1422     0     0    0 0  0.0000   0.000 0.0000 0.0000 0.0000  0.0000 0.0000
103  102  1 1  1 0 0.0006094 0.00891719 0.1765200 1853     0     0    0 0  0.0000   0.000 0.0000 0.0000 0.0000  0.0000 0.0000
102   99  1 1  1 0 0.0006094 0.00891719 0.1765200 1853     0     0    0 0  0.0000   0.000 0.0000 0.0000 0.0000  0.0000 0.0000
 99   54  1 1  1 0 0.0006094 0.00891719 0.1765200 1422     0     0    0 0  0.0000   0.000 0.0000 0.0000 0.0000  0.0000 0.0000
 54   55  1 1  1 0 0.0003062 0.00451875 0.0884000 1422     0     0    0 0  0.0000   0.000 0.0000 0.0000 0.0000  0.0000 0.0000
 55   95  1 1  1 0 0.0003062 0.00451875 0.0884000 1706     0     0    0 0  0.0000   0.000 0.0000 0.0000 0.0000  0.0000 0.0000
 54   98  1 1  1 0 0.0003344 0.00491875 0.0975200 1422     0     0    0 0  0.0000   0.000 0.0000 0.0000 0.0000  0.0000 0.0000
 98   56  1 1  1 0 0.0003344 0.00491875 0.0975200 1422     0     0    0 0  0.0000   0.000 0.0000 0.0000 0.0000  0.0000 0.0000
 15   94  1 1  1 0 0.0003117 0.00461250 0.3531600 1414     0     0    0 0  0.0000   0.000 0.0000 0.0000 0.0000  0.0000 0.0000
 15   59  1 1  1 0 0.0006234 0.00922500 0.7063200 1414     0     0    0 0  0.0000   0.000 0.0000 0.0000 0.0000  0.0000 0.0000
 94   59  1 1  1 0 0.0003117 0.00461250 0.3531600 1414     0     0    0 0  0.0000   0.000 0.0000 0.0000 0.0000  0.0000 0.0000
 57   58  1 1  1 0 0.0004062 0.00654375 0.1062400 1135     0     0    0 0  0.0000   0.000 0.0000 0.0000 0.0000  0.0000 0.0000
 57   61  1 1  1 0 0.0005688 0.00825000 0.1657600 1414     0     0    0 0  0.0000   0.000 0.0000 0.0000 0.0000  0.0000 0.0000
 58   63  1 1  1 0 0.0001412 0.00212500 0.1886400 1414     0     0    0 0  0.0000   0.000 0.0000 0.0000 0.0000  0.0000 0.0000
 58  106  1 1  1 0 0.0000706 0.00106250 0.0943200 1414     0     0    0 0  0.0000   0.000 0.0000 0.0000 0.0000  0.0000 0.0000
106   63  1 1  1 0 0.0000706 0.00106250 0.0943200 1414     0     0    0 0  0.0000   0.000 0.0000 0.0000 0.0000  0.0000 0.0000
 58   64  1 1  1 0 0.0012438 0.01818750 0.3652000 1414     0     0    0 0  0.0000   0.000 0.0000 0.0000 0.0000  0.0000 0.0000
 59  105  1 1  1 0 0.0006719 0.00979063 0.1939200 1414     0     0    0 0  0.0000   0.000 0.0000 0.0000 0.0000  0.0000 0.0000
105   61  1 1  1 0 0.0006719 0.00979063 0.1939200 1414     0     0    0 0  0.0000   0.000 0.0000 0.0000 0.0000  0.0000 0.0000
 59   93  1 1  1 0 0.0002742 0.00402312 0.3237600 1414     0     0    0 0  0.0000   0.000 0.0000 0.0000 0.0000  0.0000 0.0000
 59   67  1 1  1 0 0.0005484 0.00804625 0.6475200 1414     0     0    0 0  0.0000   0.000 0.0000 0.0000 0.0000  0.0000 0.0000
 93   67  1 1  1 0 0.0002742 0.00402312 0.3237600 1414     0     0    0 0  0.0000   0.000 0.0000 0.0000 0.0000  0.0000 0.0000
 60   63  1 1  1 0 0.0001844 0.00269750 0.2164800 2828     0     0    0 0  0.0000   0.000 0.0000 0.0000 0.0000  0.0000 0.0000
 61   65  1 1  1 0 0.0002812 0.00415625 0.0828000 1414     0     0    0 0  0.0000   0.000 0.0000 0.0000 0.0000  0.0000 0.0000
 62  110  1 1  1 0 0.0003656 0.00522813 0.1099200 1414     0     0    0 0  0.0000   0.000 0.0000 0.0000 0.0000  0.0000 0.0000
110   65  1 1  1 0 0.0003656 0.00522813 0.1099200 1414     0     0    0 0  0.0000   0.000 0.0000 0.0000 0.0000  0.0000 0.0000
 63   64  1 1  1 0 0.0011000 0.01590000 0.3215200 1414     0     0    0 0  0.0000   0.000 0.0000 0.0000 0.0000  0.0000 0.0000
 63   70  1 1  1 0 0.0031688 0.04543750 0.9129600 1414     0     0    0 0  0.0000   0.000 0.0000 0.0000 0.0000  0.0000 0.0000
 64   69  1 1  1 0 0.0007031 0.01055440 0.7951200 2828     0     0    0 0  0.0000   0.000 0.0000 0.0000 0.0000  0.0000 0.0000
 66   69  1 1  1 0 0.0001719 0.00257813 0.1937600 3924     0     0    0 0  0.0000   0.000 0.0000 0.0000 0.0000  0.0000 0.0000
 66   71  1 1  1 0 0.0009750 0.01426870 0.2855200 1962     0     0    0 0  0.0000   0.000 0.0000 0.0000 0.0000  0.0000 0.0000
 66   72  1 1  1 0 0.0000219 0.00034375 0.0254400 3924     0     0    0 0  0.0000   0.000 0.0000 0.0000 0.0000  0.0000 0.0000
 67   92  1 1  1 0 0.0009146 0.01350620 0.2647470 1422     0     0    0 0  0.0000   0.000 0.0000 0.0000 0.0000  0.0000 0.0000
 92   91  1 1  1 0 0.0009146 0.01350620 0.2647470 1365     0     0    0 0  0.0000   0.000 0.0000 0.0000 0.0000  0.0000 0.0000
 91   77  1 1  1 0 0.0009146 0.01350620 0.2647470 1365     0     0    0 0  0.0000   0.000 0.0000 0.0000 0.0000  0.0000 0.0000
 68   71  1 1  1 0 0.0003006 0.00381000 0.2707360 3270     0     0    0 0  0.0000   0.000 0.0000 0.0000 0.0000  0.0000 0.0000
 68   76  1 1  1 0 0.0006750 0.00790000 0.1104000 1308     0     0    0 0  0.0000   0.000 0.0000 0.0000 0.0000  0.0000 0.0000
 68  112  1 1  1 0 0.0003950 0.00512500 0.3461520 1308     0     0    0 0  0.0000   0.000 0.0000 0.0000 0.0000  0.0000 0.0000
 68   80  1 1  1 0 0.0007900 0.01025000 0.6923040 1422     0     0    0 0  0.0000   0.000 0.0000 0.0000 0.0000  0.0000 0.0000
112   80  1 1  1 0 0.0003950 0.00512500 0.3461520 1134     0     0    0 0  0.0000   0.000 0.0000 0.0000 0.0000  0.0000 0.0000
 69   76  1 1  1 0 0.0008219 0.01239690 0.9364800 3327     0     0    0 0  0.0000   0.000 0.0000 0.0000 0.0000  0.0000 0.0000
 69   77  1 1  1 0 0.0026750 0.03920620 0.7835200 1962     0     0    0 0  0.0000   0.000 0.0000 0.0000 0.0000  0.0000 0.0000
 70   72  1 1  1 0 0.0011688 0.01298120 0.2033440 1308     0     0    0 0  0.0000   0.000 0.0000 0.0000 0.0000  0.0000 0.0000
 70  107  1 1  1 0 0.0000744 0.00087000 0.0121680 1308     0     0    0 0  0.0000   0.000 0.0000 0.0000 0.0000  0.0000 0.0000
107   76  1 1  1 0 0.0006694 0.00783000 0.1095120 1308     0     0    0 0  0.0000   0.000 0.0000 0.0000 0.0000  0.0000 0.0000
 71  111  1 1  1 0 0.0001375 0.00151250 0.0236368 1308     0     0    0 0  0.0000   0.000 0.0000 0.0000 0.0000  0.0000 0.0000
111   72  1 1  1 0 0.0012375 0.01361250 0.2127312 1308     0     0    0 0  0.0000   0.000 0.0000 0.0000 0.0000  0.0000 0.0000
 22   73  1 1  1 0 0.0000500 0.00055469 0.0395200 4537     0     0    0 0  0.0000   0.000 0.0000 0.0000 0.0000  0.0000 0.0000
 76   23  1 1  1 0 0.0014000 0.02048750 0.4094400 1702     0     0    0 0  0.0000   0.000 0.0000 0.0000 0.0000  0.0000 0.0000
 77   90  1 1  1 0 0.0009406 0.01377190 0.2742400 1663     0     0    0 0  0.0000   0.000 0.0000 0.0000 0.0000  0.0000 0.0000
 90   79  1 1  1 0 0.0009406 0.01377190 0.2742400 1422     0     0    0 0  0.0000   0.000 0.0000 0.0000 0.0000  0.0000 0.0000
```

```
  78   79  1 1  1 0 0.0014188 0.01606250 0.2540000 1134     0     0    0 0  0.0000   0.000 0.0000 0.0000 0.0000  0.0000 0.0000
  78   23  1 1  1 0 0.0007562 0.01112500 0.2236000 1702     0     0    0 0  0.0000   0.000 0.0000 0.0000 0.0000  0.0000 0.0000
  78   85  1 1  1 0 0.0003750 0.00538750 0.1089440 1365     0     0    0 0  0.0000   0.000 0.0000 0.0000 0.0000  0.0000 0.0000
  74   73  1 1  1 0 0.0000344 0.00045937 0.0484800 3404     0     0    0 0  0.0000   0.000 0.0000 0.0000 0.0000  0.0000 0.0000
  74   75  1 1  1 0 0.0002775 0.00403563 0.0813920 1134     0     0    0 0  0.0000   0.000 0.0000 0.0000 0.0000  0.0000 0.0000
  74   89  1 1  1 0 0.0013875 0.02017810 0.4069600 1066     0     0    0 0  0.0000   0.000 0.0000 0.0000 0.0000  0.0000 0.0000
  89   79  1 1  1 0 0.0013875 0.02017810 0.4069600 1365     0     0    0 0  0.0000   0.000 0.0000 0.0000 0.0000  0.0000 0.0000
  74   86  1 1  1 0 0.0006312 0.00916250 0.1845280 1365     0     0    0 0  0.0000   0.000 0.0000 0.0000 0.0000  0.0000 0.0000
  73  118  1 1  1 0 0.0014812 0.02119688 0.4292000 1702     0     0    0 0  0.0000   0.000 0.0000 0.0000 0.0000  0.0000 0.0000
 118   79  1 1  1 0 0.0014812 0.02119688 0.4292000 1702     0     0    0 0  0.0000   0.000 0.0000 0.0000 0.0000  0.0000 0.0000
  73   82  1 1  1 0 0.0013625 0.01931250 0.3872000 1702     0     0    0 0  0.0000   0.000 0.0000 0.0000 0.0000  0.0000 0.0000
  73   88  1 1  1 0 0.0007469 0.01101250 0.2217600 1702     0     0    0 0  0.0000   0.000 0.0000 0.0000 0.0000  0.0000 0.0000
  88   86  1 1  1 0 0.0007469 0.01101250 0.2217600 1702     0     0    0 0  0.0000   0.000 0.0000 0.0000 0.0000  0.0000 0.0000
  80   23  1 1  1 0 0.0003437 0.00498125 0.1010560 1702     0     0    0 0  0.0000   0.000 0.0000 0.0000 0.0000  0.0000 0.0000
  80  113  1 1  1 0 0.0002153 0.00292006 0.2224720 1414     0     0    0 0  0.0000   0.000 0.0000 0.0000 0.0000  0.0000 0.0000
 113   85  1 1  1 0 0.0002153 0.00292006 0.2224720 1365     0     0    0 0  0.0000   0.000 0.0000 0.0000 0.0000  0.0000 0.0000
  80  114  1 1  1 0 0.0002153 0.00292006 0.2224720 1134     0     0    0 0  0.0000   0.000 0.0000 0.0000 0.0000  0.0000 0.0000
 114   85  1 1  1 0 0.0002153 0.00292006 0.2224720 1365     0     0    0 0  0.0000   0.000 0.0000 0.0000 0.0000  0.0000 0.0000
  81   82  1 1  1 0 0.0013000 0.01906250 0.3825600 1702     0     0    0 0  0.0000   0.000 0.0000 0.0000 0.0000  0.0000 0.0000
  81   83  1 1  1 0 0.0007031 0.01022810 0.8224320 2843     0     0    0 0  0.0000   0.000 0.0000 0.0000 0.0000  0.0000 0.0000
  81   24  1 1  1 0 0.0004281 0.00620625 0.5002880 2843     0     0    0 0  0.0000   0.000 0.0000 0.0000 0.0000  0.0000 0.0000
  82   86  1 1  1 0 0.0007438 0.01095000 0.2197600 1702     0     0    0 0  0.0000   0.000 0.0000 0.0000 0.0000  0.0000 0.0000
  83   85  1 1  1 0 0.0008250 0.01201870 0.2420000 1422     0     0    0 0  0.0000   0.000 0.0000 0.0000 0.0000  0.0000 0.0000
  84  115  1 1  1 0 0.0011781 0.01702187 0.3413600 1702     0     0    0 0  0.0000   0.000 0.0000 0.0000 0.0000  0.0000 0.0000
 115   24  1 1  1 0 0.0011781 0.01702187 0.3413600 1702     0     0    0 0  0.0000   0.000 0.0000 0.0000 0.0000  0.0000 0.0000
  84   87  1 1  1 0 0.0015375 0.01275630 0.9529600  867     0     0    0 0  0.0000   0.000 0.0000 0.0000 0.0000  0.0000 0.0000
  25  117  1 1  1 0 0.0007958 0.01133750 0.2583360 1365     0     0    0 0  0.0000   0.000 0.0000 0.0000 0.0000  0.0000 0.0000
 117  116  1 1  1 0 0.0007958 0.01133750 0.2583360 1365     0     0    0 0  0.0000   0.000 0.0000 0.0000 0.0000  0.0000 0.0000
 116   87  1 1  1 0 0.0007958 0.01133750 0.2583360 1365     0     0    0 0  0.0000   0.000 0.0000 0.0000 0.0000  0.0000 0.0000
  28    1  1 1  1 0 0.0005750 0.01051870 0.1410880 2486     0     0    0 0  0.0000   0.000 0.0000 0.0000 0.0000  0.0000 0.0000
 121    7  1 1  1 0 0.0000375 0.00027500 0.0508800 2502     0     0    0 0  0.0000   0.000 0.0000 0.0000 0.0000  0.0000 0.0000
 121  120  1 1  1 0 0.0000375 0.00027500 0.0508800 1209     0     0    0 0  0.0000   0.000 0.0000 0.0000 0.0000  0.0000 0.0000
  49   10  1 1  1 0 0.0000750 0.00079375 0.0124000 1235     0     0    0 0  0.0000   0.000 0.0000 0.0000 0.0000  0.0000 0.0000
  50   13  1 1  1 0 0.0000078 0.00003906 0.0070400 3706     0     0    0 0  0.0000   0.000 0.0000 0.0000 0.0000  0.0000 0.0000
  52   14  1 1  1 0 0.0002563 0.00250625 0.0368800  975     0     0    0 0  0.0000   0.000 0.0000 0.0000 0.0000  0.0000 0.0000
  55   16  1 1  1 0 0.0002188 0.00230625 0.0407200 1235     0     0    0 0  0.0000   0.000 0.0000 0.0000 0.0000  0.0000 0.0000
  57   17  1 1  1 0 0.0000063 0.00011094 0.0048800 2268     0     0    0 0  0.0000   0.000 0.0000 0.0000 0.0000  0.0000 0.0000
  64   18  1 1  1 0 0.0001312 0.00146563 0.0912800 2268     0     0    0 0  0.0000   0.000 0.0000 0.0000 0.0000  0.0000 0.0000
  66   19  1 1  1 0 0.0000313 0.00035425 0.0836000 5232     0     0    0 0  0.0000   0.000 0.0000 0.0000 0.0000  0.0000 0.0000
  69   20  1 1  1 0 0.0000187 0.00027150 0.0815360 5459     0     0    0 0  0.0000   0.000 0.0000 0.0000 0.0000  0.0000 0.0000
  72   21  1 1  1 0 0.0000531 0.00059206 0.0370400 2275     0     0    0 0  0.0000   0.000 0.0000 0.0000 0.0000  0.0000 0.0000
-999
LOSS ZONES FOLLOW                      1 ITEMS
  1 129-Bus
-99
INTERCHANGE DATA FOLLOW                1 ITEMS
 1    1 Entracque       0.00 999.99  129Bus  129-Bus 167-Line System
-9
TIE LINES FOLLOW                       0 ITEMS
-999
END OF DATA
```

Table C.1: Supply Bids for the 129-Bus Test System (I)

Bus Name	Bus #	Quantity [100 MW]	Bid Price [$/MWh]	Type
Entracque	1	2.5167	30	Hydro
La Spezia	2	1.8500	34.16	Thermal
Trino	3	1.1667	33.6	Thermal
Vado	4	2.4667	32.52	Thermal
Edolo c.le	5	2.1333	30	Hydro
La Casella	6	1.2333	37.96	Thermal
Roncoval.	7	0.9333	34	Hydro
Ostiglia	8	1.2333	35.2	Thermal
S. Fiorano	9	0.5167	30	Hydro
Piacenza	10	1.2333	36.52	Thermal
Sermide	11	2.4667	35.04	Thermal
Tavazzano	12	1.2333	34.84	Thermal
Turbigo c.le	13	3.2833	34.12	Thermal
Fusina	14	3.6833	33.64	Thermal
Portotolle	15	5.0000	33.04	Thermal
Monfalcone	16	0.1542	39	Thermal

Table C.2: Supply Bids for the 129-Bus Test System (II)

Bus Name	Bus #	Quantity [100 MW]	Bid Price [$/MWh]	Type
Bargi c.le	17	0.2733	30	Hydro
Piombino	18	1.2333	37.76	Thermal
Torre Nord	19	5.0000	32.88	Thermal
Montalto c.le	20	3.4333	32.8	Thermal
Torre Sud	21	2.2167	35.52	Thermal
Brindisi c.le	22	2.5000	36.6	Thermal
Presenzano	23	2.0000	30	Hydro
Rossano	24	3.4000	39.12	Thermal
Isab Erg	25	1.1467	36.44	Thermal
Albertville	32	1.2361	32	Intertie
Villarodin	34	0.9295	32	Intertie
Sorgente	87	0.3809	34	Thermal
Divaca	95	0.3740	32	Intertie
Rosen	108	0.2585	34	Thermal
Lavorges	120	0.7755	32	Intertie
Soazza	129	0.0138	32	Intertie

Table C.3: Demand Bids for the 129-Bus Test System (I)

Bus Name	Bus #	Quantity [100 MW]	Bid Price [$/MWh]
Casanova	26	0.7937	34.8
Castelnuovo	27	0.4979	36
Magliano	28	0.6167	36.4
Piossasco	29	0.7292	34.8
Rondissone	30	0.6312	36.4
Leini	31	0.3417	37.2
Vignole	35	0.4437	35.2
Baggio	36	0.6167	34.8
Bovisio	37	0.7708	34.8
Ospiate	38	0.5604	36.4
Lachiarella	39	0.4667	35.2
Cremona	41	0.5062	36
Ciserano	42	0.6979	35.6
Flero	46	0.3000	36.4
Gorlago	47	0.3375	34.4
Nave	48	0.2208	36
S. Rocco	49	0.6937	35.2
Verderio	51	0.5833	34
Dugale	53	0.5333	35.2
Planais	54	0.2500	34
Venezia	56	0.5125	34

Table C.4: Demand Bids for the 129-Bus Test System (II)

Bus Name	Bus #	Quantity [100 MW]	Bid Price [$/MWh]
Calenzano	58	0.7312	37.6
Forlí	59	0.5188	35.2
Marginone	60	0.6854	36
Martignone	61	0.9500	36.4
Parma	62	0.9917	36.4
Poggio	63	1.0417	35.6
Suvereto	64	0.1250	36.8
S. Damaso	65	0.6021	36.4
Fano	67	0.0021	34
Latina	68	0.4896	34.4
Montalto	69	0.2896	36
Roma Nord	70	1.1729	35.2
Roma Sud	71	1.2542	35.2
S. Lucia	72	1.0146	34.8
Brindisi	74	0.4042	38
Valmontone	76	0.5708	36.8
Villanova	77	0.5229	35.6
Benevento	78	0.4125	36.4
Foggia	79	0.4375	34.8
Garigliano	80	0.2979	37.2
Laino	81	0.2958	34

Table C.5: Demand Bids for the 129-Bus Test System (III)

Bus Name	Bus #	Quantity [100 MW]	Bid Price [$/MWh]
Montecorvino	83	1.2250	35.6
Rizziconi	84	0.5854	34.4
S. Sofia	85	0.8000	35.2
Taranto	86	0.1375	34.4
Sorgente	88	0.4979	34.8
Bari Ovest	89	0.7479	37.2
Larino	90	0.2313	36.4
Rosara	91	0.5896	34
Candia	92	0.6875	36.4
S. Martino	93	0.4646	37.2
Ravenna	94	0.1042	34.8
Adria	96	0.1812	36.4
Camin	97	0.5917	38
Salgareda	98	0.1917	34.8
Udine Ovest	99	0.5333	36
Lonato	100	0.5271	36.8
Nogarole	101	0.2354	37.6
Cordignano	102	0.2500	34.4
Sandrigo	103	0.5458	35.6
Ferrara	104	0.5292	37.6
Colunga	105	0.5479	34.8
Tavarnuzze	106	0.4542	38

Table C.6: Demand Bids for the 129-Bus Test System (IV)

Bus Name	Bus #	Quantity [100 MW]	Bid Price [$/MWh]
Roma Est	107	0.2313	36.8
Acciaiolo	109	0.2375	34.4
Rubiera	110	0.9667	35.2
Roma Ovest	111	0.8604	34.8
Ceprano	112	0.2000	35.6
S. Maria	113	0.3458	36.8
Patria	114	0.8750	37.2
Scandale	115	0.1146	36.4
Chiaramo	117	0.2396	35.2
Andria	118	0.4958	36.8
Mercallo	119	0.5563	36
Cagno	122	0.4479	34.4
Cislago	123	0.2188	36.8
Bulciago	124	0.7063	34.8
Brugherio	125	0.7417	37.2
Piancamuno	126	0.2812	34
Chiari	127	0.4354	36
Travagliato	128	0.3667	37.6
Roma Est	107	0.2313	36.8
Acciaiolo	109	0.2375	34.4
Rubiera	110	0.9667	35.2
Roma Ovest	111	0.8604	34.8

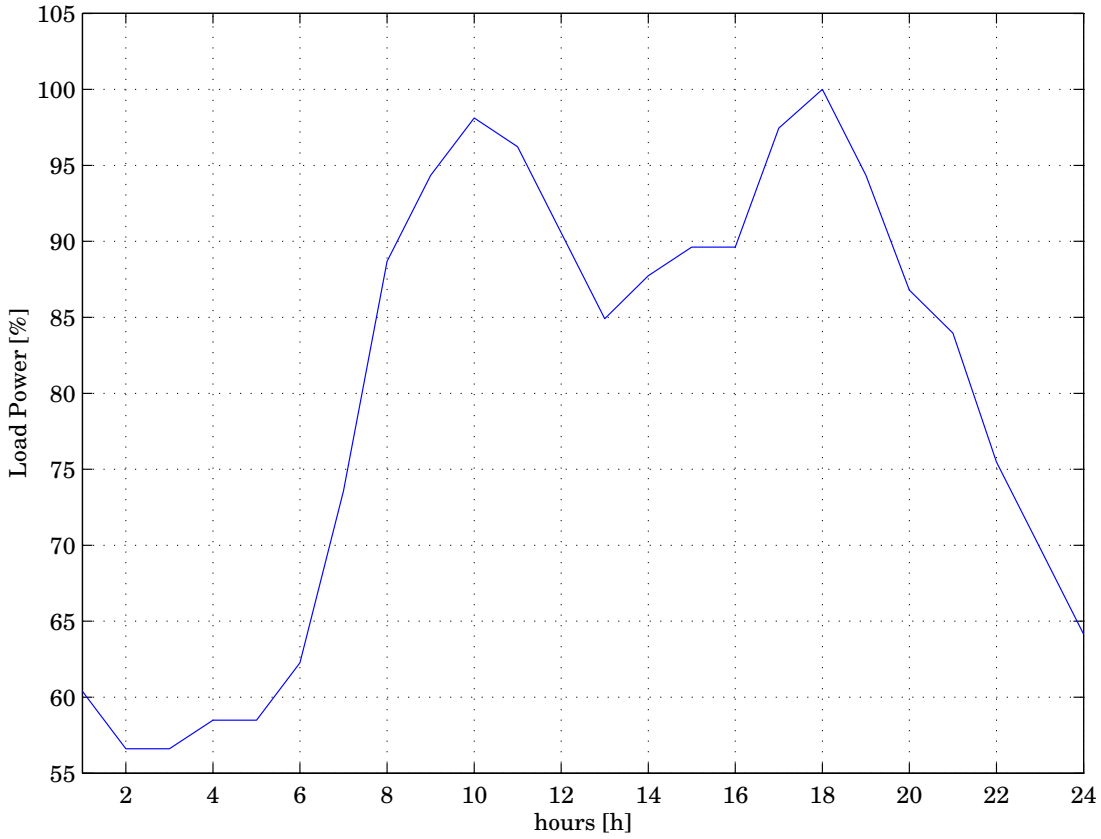

Figure C.1: Daily-ahead load power demand in % for the 129-bus model of the HV Italian network.

Bibliography

[1] G. B. Sheblé, *Computational Auction Mechanism for Restructured Power Industry Operation*, Kluwer Academic Publishers, Boston, 1998.

[2] M. Ilić and J. Zaborszky, *Dynamic and Control of Large Electric Power Systems*, Wiley-Interscience Publication, New York, 2000.

[3] S. Hunt and G. Shuttleworth, "Unlocking the Grid," *IEEE Spectrum*, pp. 20–25, July 1996.

[4] F. C. Schweppe, M. C. Caramanis, R. D. Tabor, and R. E. Bohn, *Spot Pricing of Electricity*, Kluwer Academic Publisher, Boston, MA, 1988.

[5] M. L. Baughman and S. N. Siddiqi, "Real Time Pricing of Reactive Power: Theory and Case Study Results," *IEEE Transactions on Power Systems*, vol. 6, no. 1, Feb. 1993.

[6] M. Einbom and R. Siddiqi, *Electricity Transmission Pricing and Technology*, Kluwer Academic Publisher, Boston, MA, 1996.

[7] R. Lugtu, "Security Constrained Dispatch," *IEEE Transactions on Power Apparatus and Systems*, , no. PAS-98, pp. 270–274, 1979.

[8] C-N. Yu and M. Ilić, "Congestion Cluster-based Markets for Transmission Management," in *IEEE PES Winter Meeting*, New York, NY, 1999.

[9] C. A. Cañizares, H. Chen, and W. Rosehart, "Pricing System Security in Electricity Markets," in *Proc. Bulk Power systems Dynamics and Control-V*, Onomichi, Japan, Sept. 2001.

[10] H. Chen, C. A. Cañizares, and A. Singh, "Transaction Security Cost Analysis by Take-risk Strategy," *Power System Computation Conference*, June 2002, Spain.

[11] H. Chen, *Security Cost Analysis in Electricity Markets Based on Voltage Security Criteria and Web-based Implementation*, Ph.D. thesis, University of Waterloo, Waterloo, ON, Canada, 2002.

[12] B. Stott, J. L. Marino, and O. Alsac, "Review of Linear Programming Applied to Power System Rescheduling," in *Proc. PICA IEEE International Conference*, 1979, pp. 142–154.

[13] O. Alsac, J. Bright, M. Prais, and B. Stott, "Further Developments in LP-based Optimal Power Flow," *IEEE Transactions on Power Systems*, vol. 5, no. 3, pp. 697–711, Aug. 1990.

[14] J. Momoh et al., "Challenges to Optimal Power Flow," *IEEE Transactions on Power Systems*, vol. 12, no. 1, pp. 444–455, Feb. 1997.

[15] M. Huneault and F. D. Galiana, "A Survey of the Optimal Power Flow Literature," *IEEE Transactions on Power Systems*, vol. 6, no. 2, pp. 762–770, May 1991.

[16] C. N. Lu and M. R. Unum, "Network Constrained Security Control using an Interior Point Algorithm," *IEEE Transactions on Power Systems*, vol. 8, no. 3, pp. 1068–1076, Aug. 1993.

[17] S. Granville, "Optimal Reactive Dispatch through Interior Point Methods," *IEEE Transactions on Power Systems*, vol. 9, no. 1, pp. 136–146, Feb. 1994.

[18] J. A. Monmoh, S. X. Guo, E. C. Ogbuobiri, and R. Adapa, "The Quadratic Interior Point Method solving Power System Optimization Problems," *IEEE Transactions on Power Systems*, vol. 9, no. 3, pp. 1327–1336, Aug. 1994.

[19] V. H. Quintana and G. L. Torres, "Nonlinear Optimal Power Flow in Rectangular Form via Primal-Dual Logarithmic Barrier Interior Point Method," Tech. Rep., University of Waterloo, 1996, Technical Report 96-08.

[20] G. L. Torres and V. H. Quintana, "Introduction to Interior-Point Methods," in *IEEE PICA*, Santa Clara, CA, May 1999.

[21] G. D. Irisarri, X. Wang, J. Tong, and S. Mokhtari, "Maximum Loadability of Power Systems using Interior Point Nonlinear Optimization Method," *IEEE Transactions on Power Systems*, vol. 12, no. 1, pp. 162–172, Feb. 1997.

[22] C. A. Cañizares, "Applications of Optimization to Voltage Collapse Analysis," in *IEEE-PES Summer Meeting*, San Diego, USA, July 1998.

[23] W. Rosehart, C. A. Cañizares, and V. H. Quintana, "Optimal Power Flow Incorporating Voltage Collapse Constraints," in *Proc. 1999 IEEE-PES Summer Meeting*, Edmonton, Alberta, July 1999.

[24] C. A. Cañizares, W. Rosehart, and V. Quintana, "Costs of Voltage Security in Electricity Markets," in *Proc. 2001 IEEE-PES Summer Meeting*, Seattle, WA, USA, July 2000.

[25] C. A. Cañizares, W. Rosehart, A. Berizzi, and C. Bovo, "Comparison of Voltage Security Constrained Optimal Power flow Techniques," in *Proc. 2001 IEEE-PES Summer Meeting*, Vancouver, BC, Canada, July 2001.

[26] M. Madrigal and V. H. Quintana, "Optimal Day-ahead Network-constrained Power System's Market Operations Planning using an Interior Point Method," in *IEEE Canadian Conference on Electrical and Computer Eng.*, May 1998, vol. 1, pp. 388–401.

[27] M. Madrigal, *Optimization Model and Techiniques for Implementation and Pricing of Electricity Markets*, Ph.D. thesis, University of Waterloo, Waterloo, ON, Canada, 2000.

[28] J. Abadie and J. Carpentier, "Generalization of the Wolfe Reduced Gradient Method to the case of Nonlinear Constraints," in *Optimization*, R. Fletcher, Ed., New York, 1969, pp. 37–47.

[29] F. Milano, C. A. Cañizares, and M. Invernizzi, "Multi-objective Optimization for Pricing System Security in Electricity Markets," *IEEE Transactions on Power Systems*, vol. 18, no. 2, May 2003.

[30] M. Rivier and I. Perez-Ariaga, "Computation and Decomposition of Spot Price for Transmission Pricing," in *11 PSCC Conference*, 1991.

[31] A. A. El-Keib and X. Ma, "Calculating of Short-run Marginal Costs of Active and Reactive Power Production," *IEEE Transactions on Power Systems*, vol. 12, no. 1, May 1997.

[32] J. D. Finney, H. A. Othman, and W. L. Rutz, "Evaluating Transmission Congestion Constraints in System Planning," *IEEE Transactions on Power Systems*, vol. 12, no. 3, pp. 1143–1150, Aug. 1997.

[33] K. Xie, Y.-H. Song, J. Stonham, E. Yu, and G. Liu, "Decomposition Model and Interior Point Methods for Optimal Spot Pricing of Electricity in Deregulation Environments," *IEEE Transactions on Power Systems*, vol. 15, no. 1, pp. 39–50, Feb. 2000.

[34] O. Alsaç and B. Stott, "Optimal Load Flow with Steady-State Security," *IEEE Trans. Power App. Syst.*, vol. PAS-93, no. 3, pp. 745–751, May/June 1974.

[35] W. C. Merritt, C. H. Saylor, R. C. Burchett, and H. H. Happ, "Security Constrained Optimization - A Case Study," *IEEE Transactions on Power Systems*, vol. 3, no. 3, pp. 970–977, Aug. 1988.

[36] M Rodrigues, O. R. Saavedra, and A. Monticelli, "Asynchronous Programming Model for the Concurrent Solution of the Security Constrined Optimal Power Flow Problem," *IEEE Transactions on Power Systems*, vol. 9, no. 4, pp. 2021–2027, Nov. 1994.

[37] F. Xia and A. P. Sakis Meliopoulos, "A Methodology for Probabilistic Transfer Capability Analysis," *IEEE Transactions on Power Systems*, vol. 11, no. 3, pp. 1269–1278, Aug. 1996.

[38] V. C. Ramesh and X. Li, "A Fuzzy Multiobjective Approach to Contingency Constrained OPF," *IEEE Transactions on Power Systems*, vol. 12, no. 3, pp. 1348–1354, Aug. 1997.

[39] F. Capitanescu and T. Van Cutsem, "Preventive Control of Voltage Security Margins: A Multicontingency Sensitivity-based Approach," *IEEE Transactions on Power Systems*, vol. 17, no. 2, pp. 358–364, May 2002.

[40] E. E. El-Araby, N. Yorino, H. Sasaki, and H. Sugihara, "A Hybrid genetic Algorithm/SLP for Voltage Stability Constrained VAR Planning Problem," in *Proc. Bulk Power systems Dynamics and Control-V*, Onomichi, Japan, Sept. 2001.

[41] F. Milano, C. A. Cañizares, and M. Invernizzi, "Voltage Stability Constrained OPF Market Models Considering N-1 Contingency Criteria," *submitted to*

International Journal of Electrical Power & Energy Systems, Dec. 2002, 20 pages.

[42] F. Zhuang and F. D. Galiana, "Towards a more Rigorous and Practical Unit Commitment by Lagrangian Relaxation," *IEEE Transactions on Power Systems*, vol. 3, no. 2, pp. 763–773, May 1988.

[43] F. N. Lee, "Short-term Thermal Unit Commitment - A New Approach," *IEEE Transactions on Power Systems*, vol. 3, no. 2, pp. 421–428, May 1988.

[44] C. Li, R. B. Johnson, and A. J. Svoboda, "A New Unit Commitment Method," *IEEE Transactions on Power Systems*, vol. 12, no. 1, pp. 113–118, Feb. 1997.

[45] C. Murillo-Sanchez and R. J. Thomas, "Thermal Unit Commitment with Nonlinear Power Flow Constraints," in *PES IEEE Winter Meeting*, New York, NY, 1999, vol. 1.

[46] C. Wang and S. M. Shahidehpour, "Ramp-rate limits in unit commitment and economic dispatch incorporating roto fatigue effect," *IEEE Transactions on Power Systems*, vol. 9, pp. 1539–1545, Aug. 1994.

[47] A. J. Conejo and J. M. Arroyo, "Multiperiod Auction for a Pool-based electricity market," *IEEE Transactions on Power Systems*, vol. 17, no. 4, pp. 1225–1231, Nov. 2002.

[48] A. L. Motto, F. D. Galiana, A. J. Conejo, and J. M. Arroyo, "Network-constrained multiperiod auction for a pool-based electricity market," *IEEE Transactions on Power Systems*, vol. 17, no. 3, pp. 646–653, Aug. 2002.

[49] W. R. Barcelo and W. W. Lemmon, "Standardized Sensitivity Coefficients for Power System Networks," *IEEE Transactions on Power Systems*, vol. 3, no. 4, pp. 1591–1599, Nov. 1988.

[50] editor C. A. Cañizares, "Voltage Stability Assessment: Concepts, Practices and Tools," Tech. Rep., IEEE/PES Power System Stability Subcommittee, Final Document, Aug. 2002, available at http://www.power.uwaterloo.ca.

[51] R. Seydel, *Practical Bifurcation and Stability Analysis: From Equilibrium to Chaos*, Second Edition, Springer-Verlag, New York, 1994.

[52] P. Kundur, *Power System Stability and Control*, McGraw Hill, New York, 1994.

[53] A. C. Z. Souza, C. A. Cañizares, and V. H. Quintana, "New Technique to Speed Up Voltage Collapse Computations Using Tangent Vector," *IEEE Transactions on Power Systems*, vol. 12, no. 3, pp. 1380–1387, Aug. 1997.

[54] C. A. Cañizares and F .L. Alvarado, "Point of Collapse and Continuation Methods for Large AC/DC Systems," *IEEE Transactions on Power Systems*, vol. 8, no. 1, pp. 1–8, Feb. 1993.

[55] V. Ajjarapu and C. Christy, "The continuation power flow: a tool for steady state voltage stability analysis," *IEEE Transactions on Power Systems*, vol. 7, pp. 416–423, 1992.

[56] NERC, "Available Transfer Capability Definition and Determination," Tech. Rep., NERC, USA, 1996.

[57] P. W. Sauer, "Technical Challenges of Computing Available Transfer Capability (ATC) in Electric Power Systems," in *Proc. Thirtieth Hawaii International Conference on System Sciences*, 1997, vol. 5, pp. 589–593.

[58] G. C. Ejebe, J. Tong, J. G. Waight, J. G. Frame, X. Wang, and W. F. Tinney, "Available Transfer Capability Calculations," *IEEE Transactions on Power Systems*, vol. 13, no. 4, pp. 1521–1527, Nov. 1998.

[59] S. Greene, I. Dobson, and F. L. Alvarado, "Sensitivity of the Loading Margin to Voltage Collapse with Respect to Arbitrary Paramters," in *Proc. of IEEE/PES Winter Meeting*, 1996.

[60] C. A. Cañizares and Z. T. Faur, "Analysis of SVC and TCSC Controllers in Voltage Collapse," *IEEE Transactions on Power Systems*, vol. 14, no. 1, pp. 158–165, Feb. 1999.

[61] A. J. Conejo and J. M. Arroyo, "Optimal response of a thermal unit to an electricity spot market," *IEEE Transactions on Power Systems*, vol. 15, pp. 1098–1104, Aug. 2000.

[62] B. S. Gisin, M. V. Obessis, and J. V. Mitsche, "Practical Methods for Transfer Limit Analysis in the Power Industry Deregulated Environment," in *Proc. PICA IEEE International Conference*, 1999, pp. 261–266.

[63] A. S. Drud, "A GRG Code for Large Sparse Dynamic Nonlinear Optimization Problems," *Mathematical Programming*, , no. 31, pp. 153–191, 1985.

[64] D. Bertsimas and J. N. Tsitsiklis, *Introduction to Linear Optimization*, Athena Scientific, Belmont, USA, 1997.

[65] R. Fuentes-Loyola, *Hydro-Thermal Coordination Problem Using Improved Direct and Indirect Methods*, Ph.D. thesis, University of Waterloo, Waterloo, ON, Canada, 2002.

[66] I. E. Grossmann, J. Viswanathan, A. Vecchietti, R. Raman, and E. Kalvelagen, *GAMS/DICOPT: A Discrete Continous Optimization Package*, Engi-

neering Research Design Center, Carnegie Mellon University, Pittsburg, PA, 2002, available at http://www.gams.com/.

[67] M. A. Duran and I. E. Grossmann, "An Outer-Approximation Algorithm for a Class of Mixed-Integer Nonlinear Programs," *Mathematical Programming*, vol. 36, pp. 307–339, 1986.

[68] R. Marconato, *Electric Power Systems*, vol. 2, CEI, Italian Electrotechnical Committee, Milano, Italy, 2002.

[69] F. Milano, "PSAT, Matlab-based Power System Analysis Toolbox," available at http://thundebox.uwaterloo.ca/∼fmilano, 2002.

[70] A. Brooke, D. Kendrick, A. Meeraus, R. Raman, and R. E. Rosenthal, *GAMS, a User's Guide*, GAMS Development Corporation, 1217 Potomac Street, NW, Washington, DC 20007, USA, Dec. 1998, available at http://www.gams.com/.

[71] M. C. Ferris, *MATLAB and GAMS: Interfacing Optimization and Visualization Software*, Computer Sciences Department, Wisconsin-Madison, Aug. 1999, available at http://www.cs.wisc.edu/math-prog/matlab.html.

[72] D. J. Hill, "Nonlinear Dyanmic Load Models with Recovery for Voltage Stability Studies," *IEEE Transactions on Power Systems*, vol. 8, no. 1, pp. 166–176, Feb. 1993.

[73] *Extended Transient-Midterm Stability Program (ETMSP) Ver. 3.1: User's Manual*, EPRI, TR-102004-V2R1, May 1994.

[74] R. D. Zimmerman and D. Gan, *Matpower, Documentation for version 2*, Power System Engineering Research Center, 1997, available at http://www.pserc.cornell.edu/matpower/matpower.html.

[75] *Power System Toolbox Version 2.0: Load Flow Tutorial and Functions*, Cherry Tree Scientific Software, RR-5 Colborne, Ontario K0K 1S0, 1991-1999.

[76] *Power System Toolbox Version 2.0: Dynamic Tutorial and Functions*, Cherry Tree Scientific Software, RR-5 Colborne, Ontario K0K 1S0, 1991-1997.

[77] A. H. L. Chen, C. O. Nwankpa, H. G. Kawatny, and Xiao ming Yu, "Voltage Stability Toolbox: An Introduction and Implementation," in *Proc. NAPS'96*, MIT, Nov. 1996.

[78] *Voltage Stability Toolbox, version 2*, Center for Electric Power Engineering, Drexel University, 2002, available at http://power.ece.drexel.edu/-research/VST/vst.htm.

[79] A. S. Drud, *GAMS/CONOPT*, ARKI Consulting and Development, Bagsvaerdvej 246A, DK-2880 Bagsvaerd, Denmark, 1996, available at http://www.gams.com/.

[80] H. A. Eiselt, G. Pederzoli, and C.-L. Sandblom, *Continuous Optimization Models*, de Grueter, New York, 1987.

[81] C. A. Cañizares and M. Pozzi, "FACTS Controllers Performance and Influence on Voltage Control in the Presence of Secondary Voltage Regulation," Tech. Rep., CESI, RETE-A0/021456, Milan, Italy, June 2000, 66 pages.

[82] Working Group on a Common Format for the Exchange of Solved Load Flow Data, "Common Data Format for the Exchange of Solved Load Flow Data," *IEEE Transactions on Power Apparatus and Systems*, vol. 92, no. 6, pp. 1916–1925, Nov./Dec. 1973.